

CONTROL THEORY APPROACH TO THE STUDY OF  
CIRCADIAN LEAF MOVEMENT IN TRIFOLIUM REPENS

by

G.R. Robinson, B. Sc.(Hons.)

submitted in fulfilment of the requirements  
for the degree of Doctor of Philosophy.

UNIVERSITY OF TASMANIA

HOBART

JANUARY, 1979

This thesis contains no material which has been accepted for the award of any other degree or diploma in any university.

To the best of my knowledge and belief, the thesis contains no material previously published or written by another person except where due reference is made in the text.

G. R. Robinson

G.R. Robinson

## CONTENTS

	Page
SUMMARY	<i>i</i>
ACKNOWLEDGEMENTS	<i>iv</i>
CHAPTER ONE : GENERAL INTRODUCTION	1
CHAPTER TWO : CIRCADIAN RHYTHMS IN BIOLOGICAL SYSTEMS	
2.1 Introduction	5
2.2 Occurrence	6
2.3 Characteristics of circadian systems	8
(a) Light effects	8
(b) Temperature effects	10
(c) Chemical effects	12
2.4 Models	14
CHAPTER THREE : CONTROL THEORY AND ITS APPLICATION TO BIOLOGICAL SYSTEMS	
3.1 Introduction	18
3.2 Basic concepts	18
3.3 Linear systems	21
3.4 The Laplace transform and system transfer function	23
3.5 System frequency response	25
3.6 Relationship between frequency response and impulse response	25
3.7 Determination of frequency response	27
(1) Transient inputs	27
(2) Continuous inputs	
3.8 Matching a transfer function to the frequency response	28

	Page
3.9 Frequency response for a biological system	31
3.10 Examples of application to biological systems	34
3.11 Pulse-phase response curves	36

#### CHAPTER FOUR : ANALYTICAL METHODS

4.1 Introduction	44
4.2 The discrete Fourier transform	45
4.3 Spectral analysis from a least squares viewpoint	47
4.3.1 Estimating amplitude and phase	48
4.3.2 Estimation of frequency	50
4.3.3 Several periodic terms	51
4.4 Properties of the DFT	51
4.4.1 Leakage	52
4.4.2 Aliasing	58
4.5 Reliability of spectral estimates	64
4.5.1 Presence of frequency components	64
4.5.2 Reliability of frequency, amplitude and phase estimates	66
4.5.3 Combination of estimates	69
4.6 Oscillations with nonstationary parameters	71
4.7 Future developments	72

#### CHAPTER FIVE : EXPERIMENTAL METHOD

5.1 Introduction	77
5.2 Measurement and recording of leaf angle	78
5.3 Measurement and recording errors	84
5.3.1 Absolute leaf angle	84
5.3.2 Leaf angle changes	85
5.4 Control of plant environment	87



	Page
5.5 Preparation of material	90
5.6 Analysis of leaf records	93

## CHAPTER SIX : EXPERIMENTAL RESULTS. A : LIGHT TREATMENTS

6.1 Introduction	96
6.2 Response to continuous light	96
6.3 Responses to periodic light variations	105
6.3.1 Rectangular wave light changes	105
6.3.2 Entrainment by sinusoidal log-light variations	108
6.4 Frequency response of leaf movement	113
6.5 Discussion of models	120
6.6 Response to transients	128
6.6.1 Off-on switching of a 10 c/d variation	128
6.6.2 System pulse-phase response curve	130
6.7 Examination of some nonlinear features	133
6.7.1 Dependence of response on background light intensity	133
6.7.2 Dependence of response on leaf position	135

## CHAPTER SEVEN : EXPERIMENTAL RESULTS. B: CHEMICAL TREATMENTS

7.1 Introduction	142
7.2 Effect of excision	143
7.3 Treatment with sucrose	146
7.4 Varying pH	147
7.5 Treatments with KCl and NaCl	150
7.6 Effect of ethanol	151
7.7 Azide	154

## CHAPTER EIGHT : EXPERIMENTAL RESULTS. C: PULVINULE CELL

## POTENTIAL CHANGES

8.1	Introduction	158
8.2	Method	160
8.2.1	Electrode preparation & potential recording system	160
8.2.2	Preparation and mounting of specimens	163
8.2.3	Observation of potential changes	164
8.3	Results	164
8.4	Discussion	165

## CHAPTER NINE : DISCUSSION OF RESULTS

9.1	Introduction	169
9.2	Linearity of the system	169
9.3	The secondary loop	172
9.4	Interpretation of the model	175

## CHAPTER TEN : CONCLUDING REMARKS

182

## APPENDICES

Appendix 1	: Residual variance for least squares estimates	185
Appendix 2	: Variance of a function dependent on several variables	187
Appendix 3	: Spectral estimation of frequency, amplitude and phase in the presence of a second component	189

	Page
Appendix 4 : Leaf anglemeters and cabinet controls	196
Appendix 5 : Influence of thorium ions on micro-electrode tip potentials.	203
REFERENCES	206

---

## SUMMARY

This thesis describes a study of natural and forced leaf oscillations in white clover (*Trifolium repens* L.). Apparatus was constructed which permitted the accurate control and programmed variation of environmental conditions surrounding clover plants and also the automatic recording of changes in clover leaf angle. Records of leaf movement were examined and interpreted by applying the techniques of Fourier analysis and of control theory.

Problems associated with the analysis of short oscillatory data records are discussed and the advantages and limitations of Fourier analysis are described. Particular attention is given to possible errors in spectral estimates.

Experiments are described in which clover leaves were treated with constant intensity light, single light pulses, rectangular wave light changes and sinusoidal log-light variations; i.e. light oscillations for which the logarithm of light intensity varied sinusoidally with time. For continuous light treatment the characteristics of the natural (circadian) leaf oscillation (e.g. frequency, damping rate, harmonic content) are considered for different light intensities. Experiments with sinusoidal log-light oscillations of various amplitude indicate that entrainment is not an all-or-none response but that frequency components due to both the natural and forcing oscillation may contribute to the leaf movement.

As part of a control theory approach to analysing the clover leaf oscillator plants were treated with sinusoidal log-light oscillations ranging in frequency from  $2/3$  c/d (cycle per day) to 20 c/d. The amplitude and phase of the component in the leaf movement at the frequency of the forcing oscillation were determined for each case. These frequency response data are graphed as separate amplitude and phase plots (Bode plots). A feedback model having a transfer function which is consistent with these data is developed. Some nonlinear features of this system relating light changes to leaf movement are also described.

A characteristic of a circadian system considered to be important by many investigators is its *light-pulse phase response*. This is shown graphically by plotting the change in phase of a circadian oscillator caused by a light pulse applied at different times during the natural cycle. Pulse phase response studies are considered and the relationship between these and a frequency response analysis is examined. Results for 2 hour light pulses are given and are shown to be consistent with the mathematical model developed from the frequency response data.

A phase response curve for 2.5 mM 2 hour azide pulses is also presented and is shown to have a form similar to the light phase response curve. Repeated KCl and NaCl pulses do not entrain the clover leaf oscillator but do have some effect on leaf movement.

Frequency changes caused by the presence of ethanol are reported. Finally circadian rhythm for excised leaves in continuous light is shown to be markedly less heavily damped if the leaves are supplied with sucrose.

Attempts were made to continuously monitor pulvinule transmembrane potential. Although such monitoring proved unsuccessful it is shown that the potential for both adaxial and abaxial pulvinule cortical cells varies in a circadian fashion.

These results and in particular the mathematical model developed are discussed in terms of possible physiological models for the circadian oscillator.

---

## ACKNOWLEDGEMENTS

The author wishes to express his gratitude to Dr. B.I.H. Scott for his constant support and guidance throughout this project. Frequent discussions with Dr. I.A. Newman were also of considerable assistance.

The practical help of Mr. D.F. Dainton in the construction of the controlled cabinets and other equipment used in these studies is also acknowledged, as is the advice of Miss H. Gulline on matters relating to the chemical treatment of clover plants.

The author was supported by a Commonwealth Post-Graduate Research award during much of this project.

## CHAPTER ONE

### GENERAL INTRODUCTION

It is well established that living organisms undergo cyclic physiological changes with day and night. In a wide range of organisms these changes have been observed to continue for many cycles even under apparently constant environmental conditions, though generally with a period somewhat different from 24 hours. Originally referred to as diurnal, this rhythmic behaviour has since been renamed circadian (circa dies - about a day), following a suggestion by Halberg (1959), the term diurnal being reserved as the complement to nocturnal. During recent years a large quantity of literature has accumulated concerning the occurrence and properties of circadian rhythms. However, although general mathematical and physical models have been proposed for the endogenous oscillators (biological clocks) responsible for such rhythms, their nature and the manner in which they interact with environmental changes such as light and temperature is still far from being fully understood. By way of introduction to circadian rhythm research much of the literature concerning circadian rhythmicity is surveyed in the following chapter.

A circadian system controlling rhythmic metabolic or physiological changes may be regarded as a regulatory system. Furthermore it is a system which not only assists an organism in its



adjustment to day-night environmental changes, but also permits some predictive behaviour; e.g. the metabolism of an organism may prepare in advance for daybreak or nightfall, guided by its internal timing system, perhaps hoarding energy reserves during some parts of each cycle in preparation for their requirement in others. Internal timing permits the temporal organisation of physiological processes.

Since World War II a branch of physical science has developed which concerns itself with the theory of operation of man-made regulatory systems. This branch is commonly known as control systems theory and it is finding an increasing number of applications in the study of biological regulatory systems.

The purpose of the studies undertaken for this thesis was to apply the approaches of control systems theory to a particular circadian system with the intention of arriving at a mathematical model describing much of the behaviour of the system. The material chosen for study was white clover (*Trifolium repens* L.) due to its ready availability and to the known circadian behaviour of its leaf movement (see Scott & Gulline, 1972).

Circadian studies have in the past been hampered by the shortcomings of the experimental techniques available for accurately recording particular physiological oscillations and for maintaining and controlling the artificial environment around the organism under investigation. In order to obtain sufficient data for a detailed analysis of circadian behaviour it is necessary to make observations

of the oscillatory changes at frequent intervals over long periods. This is tedious, to say the least, to do manually and it is clearly preferable to find ways of obtaining and recording the data automatically.

It is also obvious that the larger the number of cycles that can be studied, the more precisely can the oscillatory system be characterized. However, a circadian system can seldom be studied conveniently for more than five or ten cycles and even during this time the properties of the organism (including those of its clock) may change significantly due, for example, to growth or ageing. Direct estimation of period and phase from a small number of quasi-periodic cycles tends to be subjective and prone to error. Thus techniques are required to maximize the extraction of spectral information from circadian data records.

With the advent of inexpensive computing facilities and modern control technology the above difficulties can largely be overcome, as is described in this thesis. The environmental control and data recording and storage requirements led to considerable work in these areas. This resulted in the construction of the control and recording systems described in chapter 5. A minicomputer was also constructed (see chapter 5) as a flexible means of directing and monitoring the control systems and for processing recorded data.

Data analysis requirements led to extensive study in the areas of control theory and of spectral analysis. A brief summary of the concepts of control theory is included in chapter 3, along with some discussion of a tool commonly used in the investigation

of circadian systems, namely the pulse-phase response curve. Information that might be obtained from pulse phase response studies yet which is not available in the control theory approach is also considered. The topic of spectral analysis is treated in chapter 4. Emphasis is placed on the techniques of spectral analysis, and on its advantages and limitations in circadian studies.

Data resulting from the application of these experimental and analytical techniques are presented in three chapters. Chapter 6 deals with the light interaction of the clover leaf oscillator and leads to the mathematical model considered in chapter 9. Chapter 7 concerns changes in the leaf movement resulting from various chemical treatments, while chapter 8 deals with the application of micro-electrode techniques to determine the variation in the transmembrane potential of clover leaf pulvinule cells during a circadian leaf cycle. These results are considered in each chapter and further developed in chapter 9.

---

## CHAPTER TWO

### CIRCADIAN RHYTHMS IN BIOLOGICAL SYSTEMS

#### 2.1 INTRODUCTION

The current chapter is intended as an introduction to circadian rhythm research and to the characteristics of circadian systems in general. Organisms whose rhythms have been studied in detail are also listed. Finally, various models that have been proposed to explain the behaviour of this apparently commonplace oscillatory system are presented and their merits considered.

For further information on circadian oscillators and biological clocks in general a large selection of monographs and review articles is available. The topic is treated generally by Bunning (1964), Palmer (1976) and Sollberger (1965), while rhythms in particular sections of the living world (mammals, plants etc.) are examined in monographs by Cloudsley-Thompson (1961), Conroy (1970), Luce (1971), Saunders (1976) and Sweeney (1969). Aschoff's symposium (1965) and the Cold Spring Harbour symposium (1960) bring together a number of articles covering a wide area of research and a number of important research techniques.

Circadian rhythms are also treated in reviews by Aschoff (1963), Halberg (1969), Harker (1958) and Kleitman (1948). Perhaps the last comprehensive survey of circadian rhythms in the plant kingdom was published by Cumming and Wagner (1968). The body of knowledge on circadian rhythms is now large and is expanding at an increasing rate, so later reviews restrict themselves to selected topics, such as physiological timing (Hillman, 1976) and circadian metabolic patterns (Queiroz, 1974).

## 2.2 OCCURRENCE

Many organisms exhibiting circadian rhythms have been studied, ranging from single celled flagellates and algae to more complex organisms such as higher plants, birds and mammals, including man. Circadian rhythmicity is remarkable in its ubiquity among living systems, with the notable exception of prokaryotic organisms such as bacteria and the blue-green algae (Sweeney, 1969, P. 18).

Historically the first circadian phenomena to be documented was leaf movement. In 1729 de Mairan recorded that plant leaf movements continued in constant darkness. Zinn (1759), working with *Mimosa vergata*, made a similar observation and concluded that some innate factor in the plant was responsible for this phenomena. The literature is interspersed with observations of apparently endogeneous circadian leaf movements through the nineteenth century, as indicated in the review by Cumming and Wagner (1968).

In this century the circadian leaf movements of a number of plants have been studied in detail and changes in these movements in response to light and temperature variations and chemical treatments examined. The plants, chosen for their obvious rhythmic behaviour and the ease with which this may be monitored under laboratory conditions, include the common bean *Phaseolus multiflorus* (Bunning and Tazawa, 1957), the Pinto bean, *P. vulgaris* (Hoshizaki and Hamner, 1964), and the legumes *Samanea saman* (Palmer and Asprey, 1958; Satter et al, 1974) and *Albizia julibrissin* (Hillman and Koukhari, 1967; Jaffe and Galston, 1967). Circadian petal movement in the succulent plant *Kalanchoe blossfeldiana* has also been studied by Bunsow (1960), Engelman (1960), and Zimmer (1962) and more recently by Engelman et al (1974). Other plant rhythms, such as CO<sub>2</sub>

production by another succulent leaved plant, *Bryophyllum fedtschenkoi* (Wilkins, 1960) and root exudation from excised *Helianthus* plants (Vaadia, 1960; MacDowall, 1964) have also come under scrutiny.

In the animal kingdom considerable attention has been given to circadian rhythms in man, for obvious reasons. Rhythms studied include activity (Aschoff & Wever, 1962) and hormonal and other biochemical rhythms (Gordon et al, 1968). Studies of circadian activity rhythms in rodents (de Coursey, 1960; Swade & Pittendrigh, 1967) in birds (Hoffman, 1960) in cockroaches (Harker, 1956), reptiles (Hoffman, 1957) and in crustacea (Brown & Webb, 1948) have also appeared in the literature.

Circadian rhythmicity in the common fruitfly *Drosophila pseudoobscura* has been closely studied and much has been written concerning the circadian eclosion rhythm of a *Drosophila* population (Bruce et al, 1960; Pittendrigh & Minis, 1964; Winfree, 1970). *Drosophila* will emerge from their larval stage with a regular, circadian rhythm if left in constant darkness or dim light.

Circadian rhythmicity is not restricted to multi-cellular organisms. At the unicellular level rhythms in phototactic movement of the protistan *Euglena gracilis* (Bruce and Pittendrigh, 1956) and photosynthetic rates in the dinoflagellate *Gonyaulax polyedra* (Hastings et al, 1960) and the green alga *Acetabularia* (Sweeney and Haxo, 1961) have been studied. *Gonyaulax* is of particular interest as in addition to photosynthetic rate, rhythms in luminescent glow, luminescent flash and cell division are also observed.

It appears from these studies and from others (e.g. Strumwasser, 1965) that the circadian oscillator does not require the interaction of several cells: i.e. each cell may contain its own individual oscillator.

However, examination of the properties of such oscillators functioning in unison, as in a multicelled organism, can lead to a deeper understanding of the behaviour of individual oscillators.

### 2.3 CHARACTERISTICS OF CIRCADIAN SYSTEMS

The organisms referred to in the previous section have in common the property that within a certain range of constant environmental conditions they will exhibit a periodic variation in some physical or physiological quantity, the period of the variation being in the vicinity of 24 hours. Under constant conditions the variation may continue undamped for 40 or more cycles as with the leaf movement of *Phaseolus vulgaris* (Hoshizaki and Hamner, 1964), or the oscillation may vanish after just 2 or 3 cycles. Under natural day-night conditions these oscillations have a period of one day, but under experimentally constant conditions the period usually changes slightly and stabilizes at a value generally within the range 22-28 hours.

There is still some argument as to whether the oscillations might be a response to some subtle geophysical variation (Brown et al, 1970) but it is currently commonly accepted that the observed rhythms are due to an endogenous oscillator. The effects of light, temperature and chemical treatments on the frequency, phase, damping rate and waveform of the observed variations have been examined and reported in the literature. These effects will be summarised in turn under subheadings of light, temperature and chemical effects.

#### 2.3 (a) Light Effects

For organisms in continuous light the frequency of the circadian rhythm is marginally dependent on the level of illumination, varying approximately linearly with the logarithm of light intensity (Aschoff, 1960).

In gathering the evidence concerning the effect of light intensity on animal rhythms Aschoff observed that in diurnally active animals the frequency increases as light intensity is raised, while the reverse held for nocturnally active creatures. This has come to be known as 'Aschoff's rule' (Sweeney, 1969, P.38). The observed waveform was also found to be light dependent, the ratio of activity to inactivity increasing with light intensity in diurnal and vice versa in nocturnal creatures. Similar changes have also been observed with plant leaf movement, the frequency of oscillation and the proportion of each cycle a leaf passes in the open position changing with light intensity (see section 6.2).

Damping rate is also affected by light intensity, either bright light or darkness accelerating the fade out of the observed rhythm. For example, the rhythm is stimulated luminescence in *Gonyaulax* will continue for some time in continuous light, but damps very rapidly in darkness (Sweeney and Hastings, 1958). In contrast the leaf movement of *Samanea* damps more rapidly in bright light (Simon et al, 1976).

While the frequency of each circadian oscillator is relatively stable its phase can be readily adjusted merely by the application of a single brief light pulse. Much attention has been given to the phase changes evoked from circadian systems by this treatment. The phase changes are generally plotted against the phase of the oscillation at which the pulse was applied. The resulting graph is referred to as a 'phase response curve' or PRC (Pavlidis, 1973, P. 54). Although different circadian systems are more or less sensitive to the intensity and duration of the light pulse the appearances of the PRC's for a wide variety of plants and animals are remarkably similar (Winfree, 1970) but the question as to whether this reflects an underlying similarity between the basic oscillators still remains unanswered.



Repetitive light pulses, or any repetitive light variation of sufficient magnitude will entrain the circadian oscillator, provided the applied frequency is in the vicinity of the natural frequency of the system. If the amplitude of the light variation is small the system may go through a transitory phase before establishing a rhythm at the applied frequency. Larger amplitude input variations will cause more rapid entrainment. The range of frequencies over which the system may be entrained varies from species to species. Bunning (1964, P. 64) suggests typical limits for entrainment as light cycles of 18 hours (lower limit) and 30 hours (upper limit) period. Under some circumstances a circadian oscillator may oscillate with a period which is some multiple of the applied period. For example, an organism may be entrained to a 24 hour period by a 12 hour light variation. This is known as frequency demultiplication (Bunning 1964, P.65).

It is often implied that entrainment is an all or none process, that the biological system either oscillates at the frequency of the entraining signal or it continues to oscillate at its own natural frequency (Bunning, 1964, P. 63). Observations presented in this thesis show that in the case of the clover leaf oscillation the transition from one state to the other is a gradual process as the amplitude of the entraining signal is altered.

### 2.3 (b) Temperature effects

In some respects the effect of temperature is quite similar to that of light. Again there is some interaction with the natural frequency, the frequency increasing or decreasing with increasing temperature. This temperature dependence is usually quoted as a  $Q_{10}$  value, or ratio of frequency at one temperature to that at a temperature  $10^{\circ}\text{C}$  less. These

values lie within the range 0.85 to 1.1 for most studied circadian systems. Notable exceptions are the sporulation rhythms in the green alga *Oedogonium cardiacum* ( $Q_{10} = 0.8$ , Bunneman, 1955) and the fungus *Pilobolus sphaerosporus* ( $Q_{10} = 1.3$ , Schmidle, 1951). Even so, the  $Q_{10}$  values for most biochemical reactions are of the order of 2. The small  $Q_{10}$ 's for circadian systems appear to indicate the presence of some temperature compensation mechanism. Published results also seem to show a temperature dependence of the waveform of observed oscillations (e.g. Hastings & Sweeney, 1957).

Temperature pulses applied at different phases of each natural cycle can cause phase shifts, and temperature PRC's may be plotted. These are generally similar in appearance to the light PRC's. Similarly, circadian systems may be entrained by temperature cycles, entraining over a range of frequencies comparable with that for light entrainment.

Temperatures below those required for normal metabolic processes ( $< 5^{\circ}\text{C}$ ) do not always have the effect of fixing the oscillation at its current phase. Rather, evidence seems to indicate that the system approaches a final resting state (Bunning, 1964, P. 51). Returning the organism to a more congenial temperature results in the rhythm continuing from that final state. At temperatures in the range  $5^{\circ}\text{C}$  to  $10^{\circ}\text{C}$  oscillations of smaller amplitude and at a much higher frequency may be observed in place of the circadian rhythm (7-14 hour period in *Phaseolus* at  $10^{\circ}\text{C}$ , Bunning & Tazawa, 1957). Bunning (1964) proposed that these low temperature features suggest that the circadian clock may be akin to a relaxation oscillator.

### 2.3 (c) Chemical Effects

In the case of chemical treatment it is important to distinguish between the observed rhythmically changing quantity and the oscillation presumably driving it. Inhibition of the observed oscillation does not imply inhibition of the underlying timer, which may be functioning unaffected. This is particularly noticeable in organisms where more than one oscillating quantity can be observed. For example, DCMU will suppress the photosynthetic rhythm in *Gonyaulax*, but it leaves the rhythm in carbon assimilation unaffected (Sweeney, 1969, P. 124). Nor do changes in amplitude or transient changes in phase imply an effect on the clock itself. These may also be due to changes in the driven system rather than in the driving oscillation. Furthermore, the continuous application of a chemical may result in a phase change due to modification of the behaviour of a secondary system. Thus modification of the basic oscillation through a brief chemical treatment would be indicated only by a steady state phase change and modification through a continuous treatment by a frequency change. With these restrictions remarkably few chemicals have shown positive results.

Buhemann (1955b) observed the effects of respiratory inhibitors in the sporulation rhythm of *Oedogonium*. These depressed sporulation markedly but did not change the period of the rhythm. A large number of substances which stimulate or inhibit cellular processes (e.g. photosynthesis, respiration, protein synthesis, cell division) have been applied to various organisms (Bunning and Baltes, 1963; Hastings, 1960, Hastings and Bode, 1962). Bunning (1964) observed that it was necessary to take care in interpreting experimental results as in many cases the chemical first caused a period increase followed by a period decrease. The implication was that the chemical only affected the coupling between driving and driven rhythm, not the driving rhythm itself. In general, with some notable exceptions, chemical treatments have proved ineffective in changing the period of the circadian oscillator.

Exceptions are as follows. Ethanol has been shown to produce an increase in period of oscillation in *Phaseolus* (Bunning and Baltes, 1962), in *Euglena* (Brinkmann, 1976) and in the isopod *Excirolana* (Enright, 1971). Heavy water ( $D_2O$ ) has a similar effect on unicells (Bruce & Pittendrigh, 1960), plants (Bunning & Baltes, 1963) and animals (Suter & Rawson (1968). Lithium ions have been reported as lengthening the circadian period of the *Kalanchoe* petal rhythm (Engelmann, 1972) and the activity of the small mammal *Meriones* (Engelmann, 1973). Finally, Feldman (1967) showed that cycloheximide, an inhibitor of protein synthesis, lengthens the period of the phototactic rhythm in *Euglena*.

Attempts to produce a phase shift by chemical pulsing have met with marginally greater success. Steady state phase shifts have been produced by the abovementioned chemicals, by potassium ion pulses (Eskin, 1972; Bunning & Moser, 1972), by valinomycin (Bunning & Moser, 1972), a substance known to complex potassium ions, and by actomycin D (Karakashian and Hastings, 1962; Strumwasser, 1965), a specific inhibitor of mRNA synthesis. Arsenite and PCMB produce variable amounts of phase change in *Gonyaulax* which may be caused by a reduction in the accuracy of the timing system in their presence (Hastings, 1960).

Circadian oscillators have in common the property that their frequencies and, to a lesser extent, their phases are surprisingly insensitive to chemical treatments. Metabolic inhibitors are often applied in concentrations that are almost lethal to the organism before all trace of rhythmicity disappears, and even then such a concentration does not cause a change in period. A physiological model for the circadian oscillator should include this insensitivity as one of its features.

## 2.4 MODELS

Models may be divided into 2 categories. Firstly, there are those of a mathematical nature which describe oscillatory systems having similar properties to circadian oscillators. These may allow predictions as to the behaviour of a circadian system under certain conditions and offer suggestions as to the oscillatory mechanism. They make little reference to the physical or biochemical detail of the system. Secondly, there are physical models, which describe a physical or biochemical system which may correspond to the circadian oscillator. Examples of each are given below.

Wever (1965) proposed a mathematical model based on a modified Van der Pol equation (see section 6.2) and demonstrated that such a differential equation described an oscillatory system possessing many of the properties of a circadian oscillator. The equation included a forcing term corresponding to a light input.

Pavlidis (1967a, 1967b) suggested that choosing a Van der Pol equation was placing an unnecessary restriction on the class of differential equations describing oscillatory systems. Pavlidis considered a general expression for an oscillatory system and proceeded to apply restrictions to this using the known properties of circadian systems. The resulting mathematical equations include a light dependent term, and in a later modified form, a temperature dependent element (Pavlidis et al, 1968).

Johnsson and Karlsson (1972) constructed a model by linking discrete elements in a feedback loop, an approach derived from control theory. With this model they were able to duplicate the light-phase response curves for the *Kalanchoe* petal rhythm (Karlsson & Johnsson, 1972; Engelman et al, 1973).

In recent years a number of physical models have been proposed. These may be broadly grouped into biochemical, transcriptional and membrane model categories.

An oscillator consisting of a biochemical network with oscillations arising from feedback within the biochemical system was considered by Pavlidis (1969) and Pye (1969). Cumming (1975) suggested the enzymes and substrates which might form this feedback system. Oscillatory biochemical systems have been reviewed elsewhere (Hess & Boiteux, 1971). These oscillations generally have periods of seconds or minutes rather than hours, and it is difficult to perceive how biochemical oscillations could possess a period of the required magnitude.

Pavlidis (1971) has suggested that coupled oscillators oscillating as a group may result in much longer periods than those of the individual components. This effect has been observed in work on the circadian rhythm in the compound action potential of the isolated eye of the sea hare *Aplysia* (Jacklet & Geronimo, 1971). Surgical reduction of the number of neuronal cells caused a decrease in the circadian period. Furthermore, there was a critical cell number below which much shorter periods, though still of several hours, were observed. Nonetheless, it is doubtful that a 'group frequency', which should be very dependent on coupling constants, could possess the required stability. Pavlidis and Kauzman (1969) also suggested that the required temperature compensation could be provided by a reduction in the enzyme levels at higher temperatures.

Ehret and Trucco (1967) proposed a transcriptional or chronon model for the circadian clock. The model involves the transcription of template RNA from consecutive polycistronic blocks of DNA, or chronons. The completion of transcription from one block initiates transcription from the

next until the last in the chain is reached. A chronon recycling component resulting from the final transcription evokes a repetition of the cycle. The process is rate limited by diffusion processes between each transcription. This allows for both the long period of oscillation and the relative insensitivity of the frequency to temperature. It does not, however, account for the negative temperature coefficients of some organisms (e.g. *Oedogonium* and *Gonyaulax*). Furthermore, it would be expected that inhibitors of RNA synthesis would have a greater influence on such a system. Apart from the effects of cycloheximide in *Euglena* and actinomycin D in *Gonyaulax* and *Aplysia* (Section 2.3c) this is not observed.

A membrane model has been proposed by Njus et al (1974) and extended by Njus et al (1976). The model involves lateral diffusion of proteins in cell membranes resulting in the assembly or dispersion of ion transport channels, the protein distribution being regulated by oscillating ion concentrations. The resulting transport changes then regulate the ion concentrations themselves to drive the oscillation. The relative temperature independence of this system might be accounted for in terms of the known temperature compensation properties of membrane lipids (Nozawa et al, 1974).

A further point concerns some intriguing data derived for *Acetabularia*. The *Acetabularia* photosynthesis rhythm continues in enucleated cells, but if the nucleus of a cell in one phase is transplanted into an enucleated cell of different phase, the phase of the receiver cell adjusts to that of the donor (Schweiger et al, 1964). The implication is that both the nucleus and the cytoplasm contain some kind of circadian clock. Furthermore, while actinomycin D will suppress rhythmicity in intact *Acetabularia* cells, it has little effect on enucleated cells (Vanden Driessche, 1966). Sweeney (1974) has suggested an explanation of

these data in terms of a membrane model similar to that of Njus et al (1974).

The effect of heavy water on circadian rhythms suggests that the biological clock is rate limited by diffusion processes (Enright, 1971b), while the ethanol effect is generally interpreted as due to action on membranes (Hillman, 1976). This interpretation is questioned by Brinkmann(1976) on the basis of experiments in which a variety of alcohols were applied to *Euglena*. The results seem to suggest that ethanol changes the period by influencing metabolic processes rather than by affecting membranes. Notwithstanding, the evidence seems to indicate membrane involvement in the biological clock and hopefully the nature of the clock will become clearer as our understanding of membrane properties develops.

---



### CHAPTER THREE

## CONTROL THEORY AND ITS APPLICATION TO BIOLOGICAL SYSTEMS

### 3.1 INTRODUCTION

In this thesis a model for the system relating light variation to leaf movement in white clover is developed. The information used was derived primarily through an approach based on the theory of control systems. For this reason an outline of the terms and concepts of control theory are presented, along with a brief review of the literature concerning the application of control theory to biological systems. For a more detailed examination of this topic review papers by Clynes (1960), Machin (1962) and Stark (1964) are available, as are monographs by Basar (1976), Kalmus (1966), Milhorn (1966), Milsum (1966) and Riggs (1970).

A common approach used in the study of circadian systems has been to examine the changes in phase of the natural oscillation produced by, for example, light or temperature pulses. Such pulse-phase response curves (PRC's) were discussed briefly in section 2.3. This approach is also considered in the current chapter and its relationship to a control systems analysis approach is evaluated.

### 3.2 BASIC CONCEPTS

A control system may be defined as an arrangement of physical components connected or related in such a manner as to control or regulate itself or another system. This controlling or regulating feature is often effected through the use of negative feedback (Sollberger, 1962). A feedback control system is one in which the output is compared with the input so that the control action is a function of both these quantities.

Advantages of a feedback control system are:

- (a) increased accuracy or precision,
- (b) reduced sensitivity to disturbances and to system characteristics,
- (c) reduced effects of nonlinearities,
- (d) increased range of frequencies (bandwidth) over which the system will respond satisfactorily.

Some of these are illustrated in the following elementary example.

Consider a circuit involving a signal  $x$  subject to some disturbance  $d$ .

The output is  $y = x + d$  (fig. 3.1a). If an amplifier of gain  $G$  is included in the circuit, with a feedback loop encompassing both amplifier and source of disturbance, the output becomes (fig. 3.1b):

$$\begin{aligned} y &= (Gx + d)/(1 + G) \\ &= x + d/G \text{ for } G \gg 1 \end{aligned}$$

Thus inclusion of a feedback loop has reduced the disturbance by a factor of  $G$ .

Suppose the loop also contains an element  $H$ , such that  $H$  is some function of  $x$  (fig. 3.1c). The output is now:

$$y = (GHx + d)/(1 + GH),$$

and for  $GH$  large,

$$y = x + d/GH$$

Thus provided  $G$  is such that  $GH$  is large, the variation of  $H$  with  $x$  may be ignored. In this example  $H$  is a nonlinear element and the system of fig. 3.1c is therefore nonlinear.

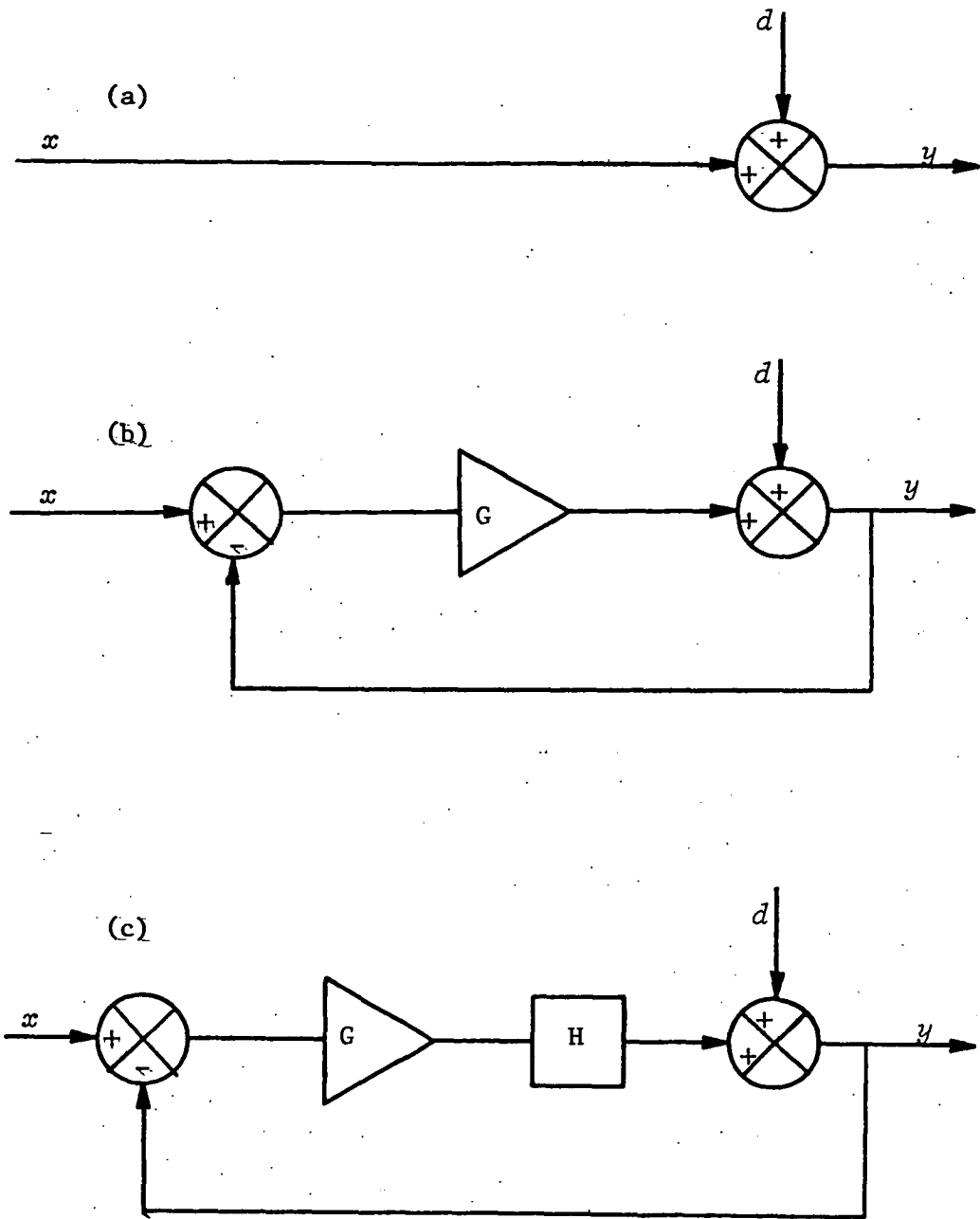


Fig. 3.1 (a) Signal ( $x$ ) subject to a disturbance ( $d$ ) resulting in an output  $y = x + d$ . The influence of the disturbance has been reduced in (b) by the inclusion of an amplifier of gain  $G$  and a feedback loop. In (c) a nonlinear element of gain  $H(x)$  is also present. See text for description.

### 3.3 LINEAR SYSTEMS

Two definitions for a linear system appear in the literature.

These are given below.

(1) A linear system is a system that can be described by a constant coefficient linear differential equation (Murdock, 1970, P.246).

(2) A linear system is a system such that its response to several inputs acting simultaneously is equal to the sum of the responses to each input acting alone (Kinariwala et al, 1973, P. 36).

The characteristic described in (2) is also known as the property of superposition (West, 1960, P.25). Definition (2) is broader than (1) and encompasses the systems defined by (1). It is the definition adopted in this thesis.

The input-output relationship for a linear system is often described by the superposition or convolution integral:

$$y(t) = \int_{-\infty}^{\infty} I(\tau)x(t-\tau)d\tau$$

- where  $I(t)$  is a function which describes the characteristics of the system, commonly known as the system weighting function or impulse response (West, 1960, P.30). One of the aims of the analysis of a system is the determination of this function.

To analyse a system its description must first be put into a form amenable to evaluation. Three representations of systems and their components are commonly employed.

(1) Block diagrams and signal flow graphs. These are shorthand representations of either a schematic of a physical system, or of the set of mathematical equations describing its parts.

(2) Graphical representation of the response of the system or of sections of the system to various inputs.

(3) Differential equations and other mathematical relationships. These give a detailed account of the system behaviour and may also explicitly describe subsections of the system.

Any system may theoretically be characterised by mathematical equations, the solutions of which represent the system's behaviour. This solution is often difficult to find and it can be necessary to make simplifying assumptions in the mathematical description. In a large number of cases these lead to a linear approximation to the system, which may be (but is not always) describable in terms of linear differential equations. A linear differential equation is one in which each term is first degree in the dependent variables and their derivatives. For example, a linear equation has terms such as  $y(t)$  and  $d^2y/dt^2$ , while a nonlinear one might contain  $\cos y$  or  $y d^2y/dt^2$ .

A general linear differential equation describing a system with input  $x = x(t)$  and output  $y = y(t)$  is:-

$$a_n d^n y/dt^n + a_{n-1} d^{n-1} y/dt^{n-1} + \dots + a_1 dy/dt + a_0 y$$

$$= b_m d^m x/dt^m + \dots + b_1 dx/dt + b_0 x$$

$$\text{i.e. } \sum_{i=0}^n a_i d^i y/dt^i = \sum_{i=0}^m b_i d^i x/dt^i$$

- where  $a_i$  and  $b_i$  are constants.

In reality systems cannot be described exactly for all possible inputs by such linear differential equations. However, many systems may be adequately represented over a limited operating range, or approximated to by such equations.

### 3.4 THE LAPLACE TRANSFORM AND SYSTEM TRANSFER FUNCTION

A useful approach to solving such differential equations as were described in the last section is by means of the Laplace transform:

$$L\{x(t)\} = X(s) = \int_0^{\infty} x(t)e^{-st} dt$$

- where  $s = \sigma + j\omega$ ;  $\sigma$  and  $\omega$  real numbers and  $j = \sqrt{-1}$

Two useful properties of this transform are as follows:-

(1) The transform of the convolution of two functions is simply the product of their respective transforms,

$$\text{i.e. } L\left\{\int_{-\infty}^{\infty} x(t-\tau)y(\tau)d\tau\right\} = X(s)Y(s)$$

(2) The transform of the derivative  $dx/dt$  of a function  $x(t)$  is given by:

$$L\{dx/dt\} = sX(s) - x(0)$$

Applying property (2) to the general linear differential equation of the previous section gives:

$$\sum_{i=0}^n \{a_i (s^i Y(s) - \sum_{k=0}^{i-1} s^{i-1-k} y_0^k)\} = \sum_{i=0}^m \{b_i (s^i X(s) - \sum_{k=0}^{i-1} s^{i-1-k} x_0^k)\}$$

- where  $y_0^k = d^k y/dt^k$  and  $x_0^k = d^k x/dt^k$  at time  $t = 0$ .

i.e. the initial conditions at both input and output.

On rearranging:

$$Y(s) = \left\{ \sum_{i=0}^m b_i s^i / \sum_{i=0}^n a_i s^i \right\} X(s) + \text{initial condition terms.}$$

The system transfer function  $G(s)$  may be defined as:

$$G(s) = \sum_{i=0}^m b_i s^i / \sum_{i=0}^n a_i s^i$$

If the system output and all its derivatives are zero prior to application of the input the initial condition terms are identically zero and so:

$$G(s) = Y(s)/X(s).$$

Thus the system transfer function is that function which describes the behaviour of the system or the manner in which the system operates on an input signal to produce the observed output. Knowledge of  $G(s)$  allows the prediction of the output transform  $Y(s)$  for any input whose transform is  $X(s)$ . The time course of this output may then be determined by evaluating the inverse transform of  $Y(s)$ .

Transfer functions have the following useful properties -

(1) The transfer function of a system is the Laplace transform of its weighting function or impulse response; i.e. if the input to a system with transfer function  $G(s)$  is a unit area impulse (a Dirac delta function) and all initial values are zero, the transform of the output is  $G(s)$ .

(2) The transfer function can be determined from the system differential equations by taking the Laplace transform and ignoring all terms arising from initial conditions.

(3) The transfer function of systems or elements in series is merely the product of their respective transfer functions.

It may be noted that the Laplace transform method yields a solution which includes both the transient and steady state parts of a system's response. This is because the Laplace integral in effect assumes that all signals are initiated at time zero. Switching effects are an intrinsic part of the method and no separate account need be taken of them.

### 3.5 SYSTEM FREQUENCY RESPONSE

Suppose a system is subject to a steady sinusoidal input of frequency  $\omega = 2\pi \nu$  and amplitude  $R$ ; i.e.  $x(t) = Re^{j\omega t}$ .

Its derivative is:  $dx/dt = j\omega Re^{j\omega t}$ .

It can be seen that the differential (or integral) of  $x(t)$  is still sinusoidal, only its amplitude and phase are altered. Thus if the input to a linear system is sinusoidal then so is the steady-state output. This leads to the result that the response of a system to a steady sinusoidal input may be determined simply by replacing the complex variable  $s$  in the transfer function with the imaginary term  $j\omega$ . Thus once the transfer function of a system is known its steady state frequency response, or variation of the amplitude and relative phase of the output with the frequency of a sinusoidal input can readily be calculated. Alternatively, if the system frequency response is known it is in principle possible to fit a transfer function to the phase and relative amplitude data.

### 3.6 RELATIONSHIP BETWEEN FREQUENCY RESPONSE AND IMPULSE RESPONSE

Both the frequency response and impulse response may be derived from the transfer function. These can be related as follows. Consider the sinusoidal input:

$$x(t) = R_i e^{j\omega t}.$$

The output (for a linear system) may be shifted in phase and altered in amplitude.



$$\text{i.e. } y(t) = R_o e^{j(\omega t + \phi)}$$

$$= R_o' e^{j\omega t}, \text{ where } R_o' = R_o e^{j\phi}$$

$$\text{Now } y(t) = R_i \int_{-\infty}^{\infty} I(\tau) e^{j\omega(t-\tau)} d\tau$$

i.e. the input convolved with the impulse response (see section 3.3).

$$\therefore y(t) = R_i e^{j\omega t} \int_{-\infty}^{\infty} I(\tau) e^{-j\omega\tau} d\tau$$

$$\therefore y(t)/x(t) = R_o'/R_i = \int_{-\infty}^{\infty} I(\tau) e^{-j\omega\tau} d\tau$$

Replacing the dummy variable  $\tau$  with  $t$  gives:

$$(R_o/R_i) e^{j\phi} = \int_{-\infty}^{\infty} I(t) e^{-j\omega t} dt$$

The integral expression is the Fourier transform of the impulse response (see section 4.2) while the opposite side of the equation contains the relative amplitude and phase of the output for an input of angular frequency  $\omega$ . Thus the system frequency response may be determined by applying a Fourier transformation to the system impulse response. The Fourier transform may be regarded as a special case of the Laplace transform, with the complex variable  $s$  replaced by  $j\omega$  and the integration range extended to  $-\infty$ .

The system frequency response is usually plotted as a polar diagram of phase shift ( $\phi$ ) against gain ( $|G|$  or  $R_o/R_i$ ) for each frequency (a Nyquist plot), or as separate phase and log gain against log of frequency graphs (Bode plots). The Nyquist plot is a useful summary of the properties of a known system, but for moving in the other direction, to infer the system transfer function from its frequency response, the Bode plots have some

advantages. Firstly, transfer functions which are merely powers of  $s$  appear as straight lines in the log gain bode plot. Secondly, if the plots for two systems or elements are known, the computation for the two in cascade merely involves the addition of two pairs of curves.

### 3.7 DETERMINATION OF FREQUENCY RESPONSE

In principle a frequency response may be determined by applying an arbitrary input and observing the resulting output, but in practice the difficulty of the analysis is greatly reduced if the inputs used are restricted to the following:

#### (1) Transient Inputs

In the previous section it was shown that a system's frequency response is simply the Fourier transform of its impulse response. Thus applying a pulse input seems a convenient means for determining a frequency response. The pulse width need only be small compared with the time scale of the response to appear as an impulse to the system. If a pulse is unsuitable, an alternative is a step input, the integral of an impulse. The frequency response is then obtained by Fourier transforming the derivative of the step response.

#### (2) Continuous inputs

Suppose a white noise input  $x(t)$  of variance  $\sigma_x^2$  is applied to a system with impulse response  $I(t)$ . The output is then:

$$y(t) = \int_{-\infty}^{\infty} I(\tau)x(t-\tau) d\tau$$

A cross-correlation function of  $y(t)$  with  $x(t)$  may be defined by:

$$R_{xy}(t') = \lim_{T \rightarrow \infty} 1/T \int_{-T/2}^{T/2} y(t)x(t-t') dt \quad (\text{Bracewell, 1965, P.46}).$$

Substituting for  $y(t)$  gives:

$$R_{xy}(t') = \int_{-\infty}^{\infty} I(\tau) R_{xx}(\tau - t') d\tau;$$

- where  $R_{xx}(t)$  is the cross-correlation of  $x(t)$  with itself, commonly known as the auto-correlation function of  $x(t)$  (Bracewell, 1965). If  $x(t)$  is a random process this can be shown to be an impulse of amplitude  $\sigma_x^2$  centred on  $t = 0$ . Therefore  $R_{xy}(t') = \sigma_x^2 I(t')$ .

Thus the system frequency response may be determined by treating the system with white noise, cross-correlating the output with the noise, and Fourier transforming the resultant. This method is useful when large or abrupt perturbations, such as occur with impulse or step treatments, might have a detrimental effect on the system.

An obvious means for determining a frequency response is to apply sinusoids of different frequencies, measuring the relative amplitude and phase of the output in each case. This method has the advantage that the maximum resolution is obtained for each frequency. The disadvantage is its time-consuming nature. The system must be treated with each frequency in turn, rather than with all frequencies in the one treatment as is the case with the other methods.

There are problems associated with each of the above methods when they are applied to biological systems. These problems are discussed in section 3.9.

### 3.8 MATCHING A TRANSFER FUNCTION TO THE FREQUENCY RESPONSE

Determining the frequency response for a system from its transfer function is a straightforward process. Frequency values are substituted

into the transfer function expression and each calculated gain and phase change is plotted. There is not, however, a corresponding direct means for deriving the transfer function of a system from its frequency response. The methods available are essentially graphical and largely intuitive. Furthermore, there may be several quite different transfer functions which will, within the accuracy of the experimental results, and over the particular frequency range examined, duplicate the data. Under these circumstances it is necessary to know something more about the system under investigation. For example, it may be possible to restrict the form of the transfer function by considering only those which represent physiologically realizable systems.

An approach often used to derive a transfer function from a frequency response is to have at hand a compilation of the plots for common elements and to proceed by successive approximation to match the plots for a combination of these to the experimental data (Machin, 1962; Milhorn, 1966). Some examples of common elements and their Bode plots are shown in figure 3.2.

The analysis of a feedback control system is difficult in that the very advantage of such a system is that it is relatively insensitive to the properties of most of its components (see section 3.2). The analysis is greatly simplified if the feedback loop can be opened, as is illustrated in figure 3.3.

In this figure the open loop transfer function is  $G_f(s)$ , or  $G_f(s)G_b(s)$  if the signal  $y_2(t)$  is accessible. The corresponding closed loop transfer function is:

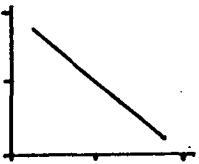
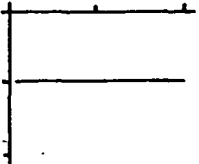
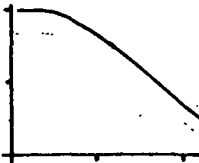
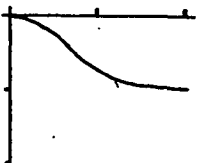
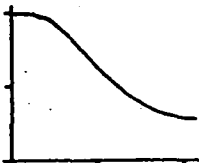
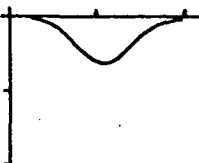
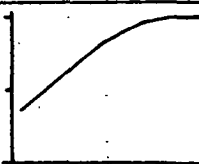

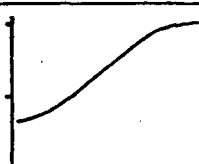
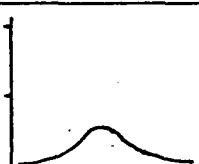
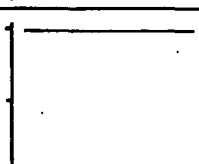
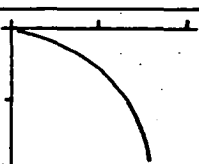
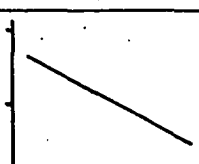
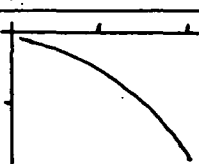
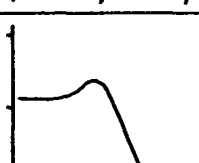

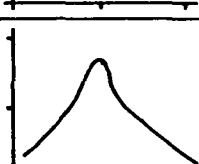
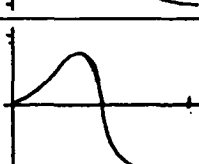
Element	Transfer Function	Bode Plot	
		Gain	Phase
Integration	$\frac{1}{s}$		
Exponential Lag	$\frac{1}{\tau s + 1}$		
Phase Delay	$\frac{\tau s + 1}{k\tau s + 1}$ $k > 1$		
Exponential lead	$\frac{\tau s}{\tau s + 1}$		
Phase advance	$\frac{\tau s + 1}{\tau s + k}$ $k > 1$		
Finite Delay	$e^{-\tau s}$		
Distributed delay	$e^{-\sqrt{\tau} s}$		
Resonant System	$\frac{k}{(\tau_1 s + 1)(\tau_2 s + 1 + k)}$		
Resonant System	$\frac{k(\tau_1 s + 1)}{(\tau_1 s + 1)(\tau_2 s + 1) + k}$		

Fig. 3.2 Transfer functions and Bode plots ( $\log |G| \sim \log \nu$  and  $\Delta\phi \sim \log \nu$ ) for some common elements. Divisions on log scales represent 10-fold changes in these quantities while phase scale divisions represent  $90^\circ$  intervals.

$$G(s) = G_f(s) / \{1 + G_f(s)G_b(s)\};$$

- i.e. if the loop can be opened the forward transfer function  $G_f(s)$  and the back transfer function  $G_b(s)$  might be deducted separately, rather than endeavouring to estimate each from the closed loop response.

The usefulness of this approach has been amply demonstrated by Stark and Sherman (1957) in an investigation of the pupillary light reflex. The area of a normal eye pupil is a function of light intensity, the pupil contracting to diminish the amount of light reaching the retina as the light intensity increases.

A light beam may be focussed so that its diameter in passing through the pupil is less than the smallest diameter of the pupil itself. Changes in pupil size will then have no effect on the amount of light reaching the retina, and the feedback loop is effectively open. By applying a focussed, sinusoidally varying light beam Stark and Sherman were able to deduce an open loop transfer function of the form:

$$0.16e^{-0.18s} / (1 + 0.1s)^3;$$

i.e. a finite delay or 'dead time' and three exponential lags (see figures 3.4 and 3.2). The corresponding closed loop transfer function was:

$$0.16e^{-0.18s} / \{(1 + 0.1s)^3 + 0.16e^{-0.18s}\}$$

This closed loop transfer function would obviously be more difficult to deduce from the closed loop system frequency response.

### 3.9 FREQUENCY RESPONSE FOR A BIOLOGICAL SYSTEM

The usefulness of transient inputs for determining the frequency response of a biological system is limited by the following considerations:

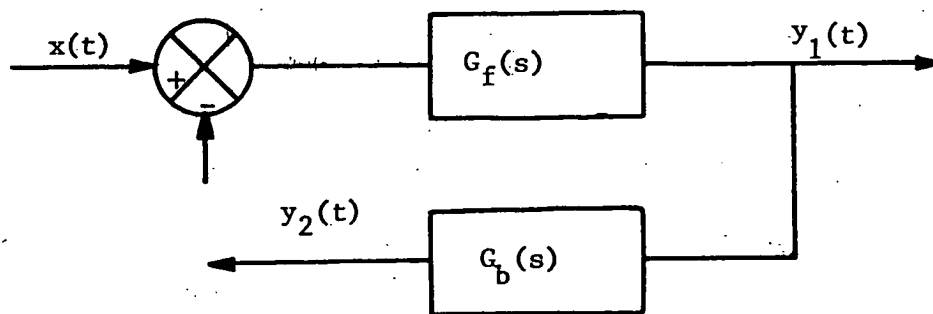


Fig. 3.3 Opened feedback loop.  $G_f(s)$  or  $G_f(s) G_b(s)$  might be determined by opening the loop in this fashion.

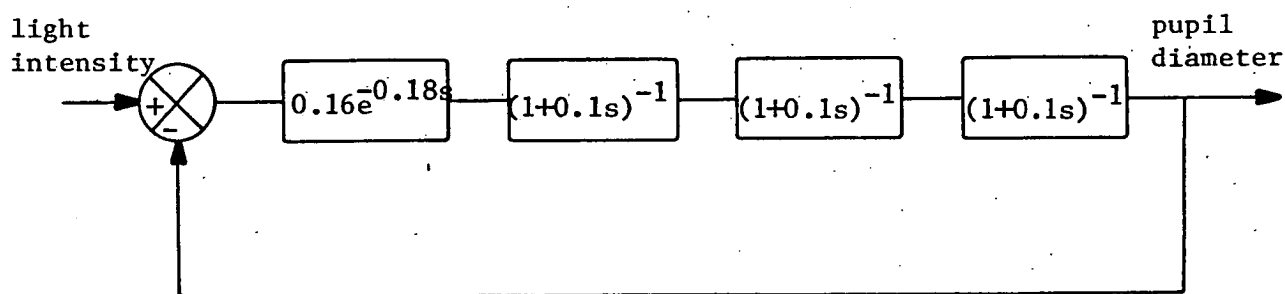


Fig. 3.4 Feedback loop controlling the pupillary light reflex deduced from the open-loop frequency response (Stark and Sherman, 1957).

(1) Most biological systems have pronounced nonlinear characteristics and these may behave in an approximately linear fashion only if the excursion of the input variable from its mean position is kept small.

(2) Changes in the output often occur when there is no apparent input. These changes may be random variations or there may be spontaneous components present, as is the case in circadian systems.

These points place upper and lower bounds on the amplitude of a transient input. It is required that the transient be sufficiently small so that nonlinear behaviour is minimized, yet sufficiently large so as to elicit a response that is well above the background level. In many cases it is not possible to meet both of these requirements.

White noise and sinusoid treatments overcome the above limitations, but in these cases a further problem is encountered. The parameters of a biological system may slowly change with time (due to ageing, for example). The white noise treatment only provides a true frequency response if it is applied for a time that is long compared with the period of the lowest frequency of interest. If the signal generated by the system itself is of comparatively large amplitude the treatment time required is even greater, due to spurious correlation. However, any change in the system parameters during the treatment will lead to errors in the estimation of the frequency response. Similarly, it may not be possible to treat the system with a sufficient range of sinusoid frequencies to determine its frequency response over the time interval in which the system parameters may be considered constant.



The above points require consideration whenever the frequency response for a biological system is desired. If the system is merely one of a population of similar biological systems it may be possible to determine the response for a 'typical' system by treating a sample from the population to a sinusoidal input of a particular frequency, a second sample with a different frequency, and so on until a satisfactory frequency response plot is obtained.

### 3.10 EXAMPLES OF APPLICATION TO BIOLOGICAL SYSTEMS

One application of control theory to the human pupillary response (Stark and Sherman, 1957) was described in section 3.8. Three other examples of such treatments are as follows:-

#### (1) Cockroach mechanoreceptor

Sinusoidal and pulse inputs have been applied to the mechanoreceptor of the large tactile spine on the femur of the cockroach *Periplaneta americana* by both Pringle and Wilson (1952) and Chapman and Smith (1963). In this system the input is mechanical stimulation and the output nerve impulse frequency. Pringle and Wilson derived the transfer function:

$$G(s) = (351s^3 + 789s^2 + 486s + 57)/(s^3 + 13.3s^2 + 15.5s + 2.3)$$

Chapman and Smith applied a greater range of input frequencies and concluded that their results suggested a transfer function of the form:

$$G(s) = b\Gamma(1-k)s^k;$$

- where  $b$  and  $k$  are constants and  $\Gamma$  represents the gamma function. The authors refer to the  $s^k$  factor as 'fractional differentiation' of the input with respect to time. This factor results in a phase difference between input and output which is independent of frequency.

## (2) Cerebral Ischemic Pressor Response

Ischemia (deprivation of blood flow) of the brain usually induces a pressor response which causes an increase in the systemic blood pressure to compensate for the decreased cerebral blood flow. This is a feedback control system and was studied extensively by Sagawa et al (1961a, 1961b, 1962).

Sagawa et al (1961a) opened the feedback loop by cutting the vessels connecting the brain of a dog with the rest of its body. The brain was then perfused by means of a donor dog and a servo system was incorporated to permit the setting of the cerebral perfusion pressure to the desired level.

Sinusoidal variations in pressure were then applied (Sagawa et al, 1961b). The amplitude of these variations was kept small so that a near linear response was evoked. The open loop system transfer function was deduced as:

$$G_o(s) = k_1 e^{-ls} / (t_1 s + 1);$$

- where  $k_1$ ,  $l$  and  $t_1$  are constants, i.e. a finite delay and an exponential lag (see fig. 3.2). It was also noted that some of the animals exhibited second order characteristics. The transfer function in these cases was:

$$G_o(s) = k_2 e^{-ms} / (s^2 + k_3 s + k_4);$$

where  $k_2$ ,  $k_3$ ,  $k_4$  and  $m$  are constants. The reason for the difference in the two cases was not known.

### (3) Single photoreceptor

Herman and Stark (1963) studied the response of the photoreceptor organ of the crawfish to small amplitude sinusoidal light variations about a mean level. The resulting transfer function relating light intensity to nerve impulse rate was:

$$G(s) = 12 \times 10^3 e^{-s} / (1.3s + 1)^2 \text{ (pulses/sec)/(lumens/m}^2\text{)}$$

A general review of control in biological systems with emphasis on a control theory approach to their analysis has been published by Iberall and Cardon (1964). Examples of later work on the analysis of smooth muscle response, the circulatory autoregulation and brain activity are given by Basar (1976), while a variety of human physiological systems are treated by Riggs (1970).

#### 3.11 PULSE - PHASE RESPONSE CURVES

Frequency response analyses for circadian systems are not apparent in the literature. As was indicated in section 3.1, circadian systems are more commonly studied through their pulse-phase response curves, or PRC's. Little information is available concerning the relationship between these two analytical techniques. It is therefore considered worthwhile to determine whether information can be obtained from a PRC that is not available in the system frequency response data. It would also be useful to determine the relationship between phase change and pulse height and duration for a simple oscillatory system.

Consider the linear differential equation:

$$\ddot{y} + \omega^2 y = x;$$

where  $\omega$  is a constant,  $x$  and  $y$  are functions of time and  $\ddot{y} = d^2y/dt^2$ .

The Laplace transform of this equation is:

$$L\{y\} (s^2 + \omega^2) = sy(0) + \dot{y}(0) + L\{x\}$$

- where  $y(0)$  and  $\dot{y}(0)$  are the values of  $y$  and  $dy/dt$  respectively at time  $t = 0$ .

The equivalent feedback system is shown in figure 3.5.

When  $x = 0$  the equation becomes:

$$L\{y\} = sy(0)/(s^2 + \omega^2) + \dot{y}(0)/(s^2 + \omega^2);$$

- which has the inverse Laplace transform:

$$\begin{aligned} y &= y(0)\cos \omega t + (\dot{y}(0)\sin \omega t)/\omega \\ &= R\sin(\omega t + \phi) \end{aligned}$$

where  $y(0) = R\sin \phi$  and  $\dot{y}(0) = \omega R\cos \phi$ .

Thus when  $x = 0$  the system produces sinusoidal oscillations of

frequency  $\omega/2\pi$  and amplitude and phase determined by the initial conditions.

In fact, the system of figure 3.5 represents a simple harmonic or pendulum oscillator.

Suppose a pulse of height  $h$  and duration  $\tau$  is applied immediately following  $t = 0$ . The Laplace transform of  $x$  is then given by:

$$L\{x\} = h(1 - e^{-\tau s})/s,$$

$$\begin{aligned} \text{and } L\{y\} &= h(1 - e^{-\tau s})/s(s^2 + \omega^2) + sy(0)/(s^2 + \omega^2) + \dot{y}(0)/(s^2 + \omega^2) \\ &= h \{1/s - s/(s^2 + \omega^2)\} (1 - e^{-\tau s})/\omega^2 + sy(0)/(s^2 + \omega^2) + \\ &\quad \dot{y}(0)/(s^2 + \omega^2) \end{aligned}$$

This has the inverse transform:

$$y = h \{ \cos \omega(t - \tau) - \cos \omega t \} / \omega^2 + R\sin(\omega t + \phi);$$

- for times  $t > \tau$ .

Let  $y = R'(\omega t + \phi')$ , where  $R'$  and  $\phi'$  are the amplitude and phase for the oscillation after the pulse.

$$\text{Then } R' \sin \phi' = R \sin \phi + h(\cos \omega\tau - 1)/\omega^2$$

$$\text{and } R' \cos \phi' = R \cos \phi + h(\sin \omega\tau)/\omega^2$$

and therefore:

$$\tan \phi' = \{ R\omega^2 \sin \phi + h(\cos \omega\tau - 1) \} / (R\omega^2 \cos \phi + h \sin \omega\tau)$$

Thus the new phase measured with respect to the phase of the unperturbed oscillation is given by the above equation.

Pittendrigh (1960) observed that the *Drosophila* eclosion rhythm showed two distinct types of resetting curve (i.e. plots of  $\phi'$  against  $\phi$ ), depending on the magnitude and duration of the applied light pulse. These Winfree (1970) refers to as type 1 (average slope of unity) and type 0 (average slope of zero) resetting curves according to their average slopes. It is shown below that resetting curves with these distinct average slopes are also a characteristic of a simple harmonic oscillator.

From the above equation it is obvious that for very small values of  $h$  and  $\tau$  a plot of  $\phi' \sim \phi$  would result in a line of approximately unit slope (i.e.  $\tan \phi' \approx \tan \phi$ ). At the other extreme, for very large values of  $h$  the equation becomes:

$$\tan \phi' \approx (\cos \omega\tau - 1)/\sin \omega\tau = -\tan \omega\tau/2$$

- i.e. a line with average slope of zero.

The change from type 1 to type 0 occurs when  $h$  and  $\tau$  are such that:

$$h \sin \omega\tau - R\omega^2 = 0$$

$$\text{i.e. when } \tan \phi' = (\sin \phi - \tan \omega\tau/2)/(\cos \phi + 1)$$

For smaller values of  $h$  and  $\tau$  both numerator and denominator in the expression for  $\tan \phi'$  can adopt positive and negative values and thus

the range for  $\phi'$  is unrestricted. For larger  $h$  and  $\tau$  values the denominator remains positive so that  $\phi'$  is limited to the range  $-90^\circ$  to  $+90^\circ$ .

An expression for the change in phase ( $\phi' - \phi$ ) can be determined from the equation for  $\tan \phi'$ . It is:

$$\tan (\phi' - \phi) = \{ \cos(\omega\tau + \phi) - \cos \phi \} / \{ R\omega^2/h + \sin(\omega\tau + \phi) - \sin \phi \}$$

The above equation permits the calculation of the phase *change* produced in a simple harmonic oscillator by a pulse of height  $h$  and duration  $\tau$ . By solving this equation for different values of  $\phi$  a Phase Response Curve may be constructed. Families of PRC's for a range of pulse heights and pulse durations were computed using an HP 97 calculator. These are shown in figures 3.6 and 3.7 respectively.

The PRC's are very nearly sinusoidal for small values of  $h$  and  $\omega\tau$ . As these quantities become larger the slope of the PRC through zero phase increases in magnitude, until for the range of combinations of  $h$  and  $\omega\tau$  which result in the condition:

$$h \sin \omega\tau - R\omega^2 = 0;$$

- the PRC passes vertically through phase zero and the phase change becomes indeterminate (see Fig. 3.6). This corresponds to the state where the pulse reduces the amplitude of the natural oscillation to zero.

Relationships between ( $\phi' - \phi$ ) and  $h$  and  $\tau$  were also calculated for signals taken from immediately following and immediately preceding the first integrating element in figure 3.5 (i.e.  $\dot{y}$  and  $\dot{y}'$ ). The corresponding expressions are:

$$\tan (\phi' - \phi) = \{\sin(\omega\tau + \phi) - \sin \phi\} / \{R\omega / h + \cos \phi - \cos (\omega\tau + \phi)\}$$

and:

$$\tan (\phi' - \phi) = \{\cos \phi - \cos(\omega\tau + \phi)\} / \{R/h + \sin \phi - \sin(\omega\tau + \phi)\}$$

The PRC's for these are of the same form as those for  $y$ , but are translated by  $+90^\circ$  (i.e. moved to the right) and  $+180^\circ$  respectively. Thus each integrator between comparator and output produces a  $90^\circ$  displacement of the PRC.

The oscillatory feedback system considered in figure 3.5 has the transfer function:  $1/(s^2 + \omega^2)$ . If the system was to be preceded or followed by, for example, an exponential lead element the transfer function would become  $Ts/(Ts + 1)(s^2 + \omega^2)$ , where  $T$  is the time constant for the lead element. The frequency responses for the two possible locations of the lead element are identical. A frequency response analysis might yield the above transfer function, but this does not contain information as to whether the lead element precedes or follows the loop.

Consider the PRC for this system. The passage of a pulse into the system would not be significantly affected by a preceeding lead element, provided  $T > \tau$ . Thus the PRC would be unchanged. However, if the lead element followed the loop the observed oscillation would actually lead  $y$  in phase, the phase advance given by  $\arctan 1/\omega T$ , and thus the PRC would be displaced along the phase axis by this amount when compared with the PRC's of figs. 3.6 and 3.7. The PRC's for the two cases are therefore not identical.

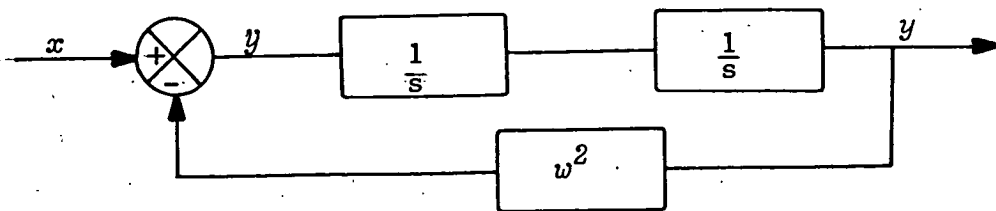


Fig. 3.5 Feedback system with differential equation:  $y + w^2 y = x$ .

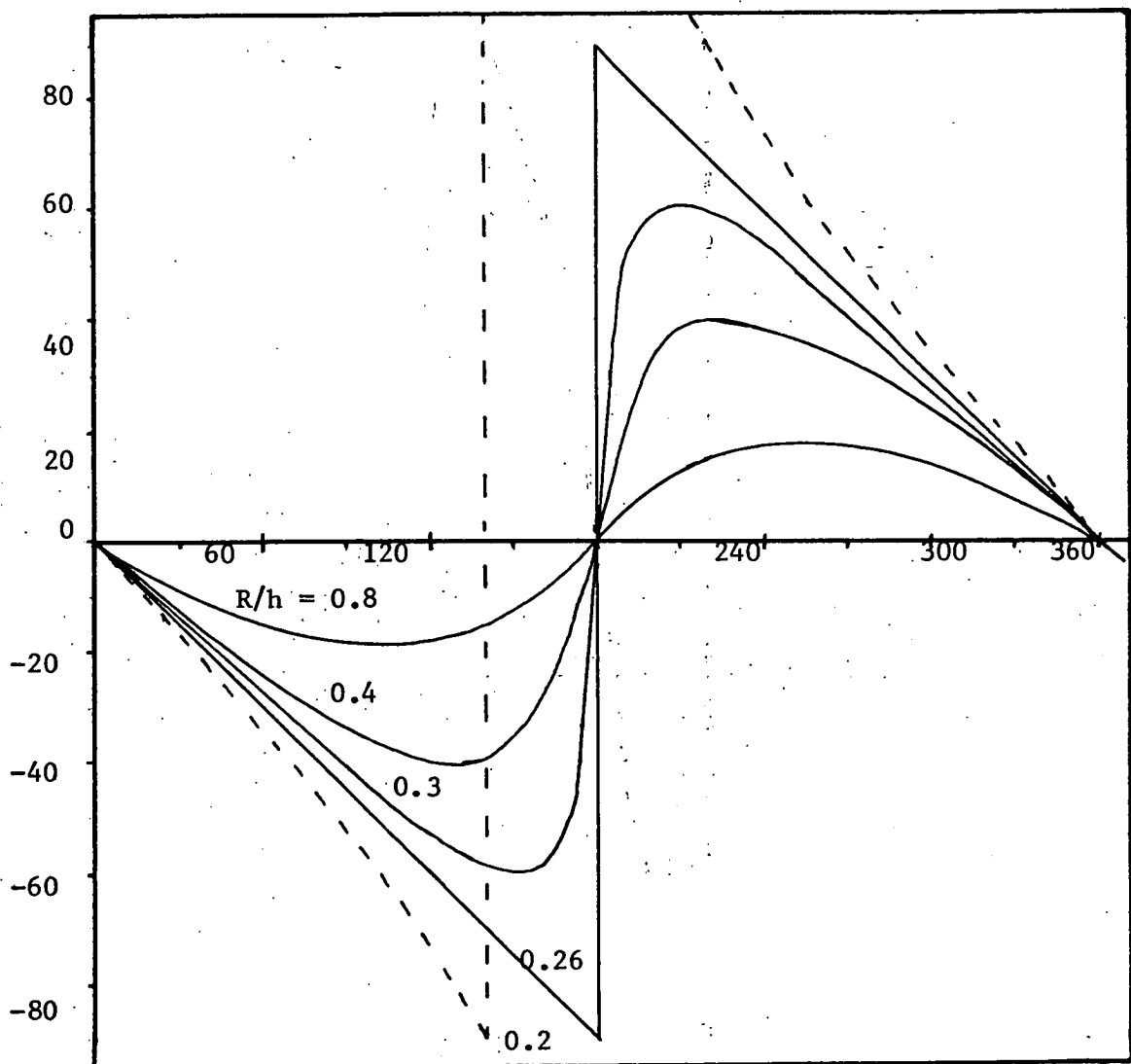


Fig. 3.6 PRC's for a range of  $R/h$  values ( $\omega = 1$  for simplicity). Pulse duration,  $\tau$  is  $1/24$ th of cycle period. Phase shift  $(\phi' - \phi)^\circ$  is plotted against  $(\phi + \omega\tau/2)^\circ$ . Discontinuities (vertical lines) appear in the PRC's where the pulse causes the oscillation to vanish. -  $h \sin \omega\tau - R\omega^2 = 0$  for  $R\omega^2/h = 0.26$  (see text).



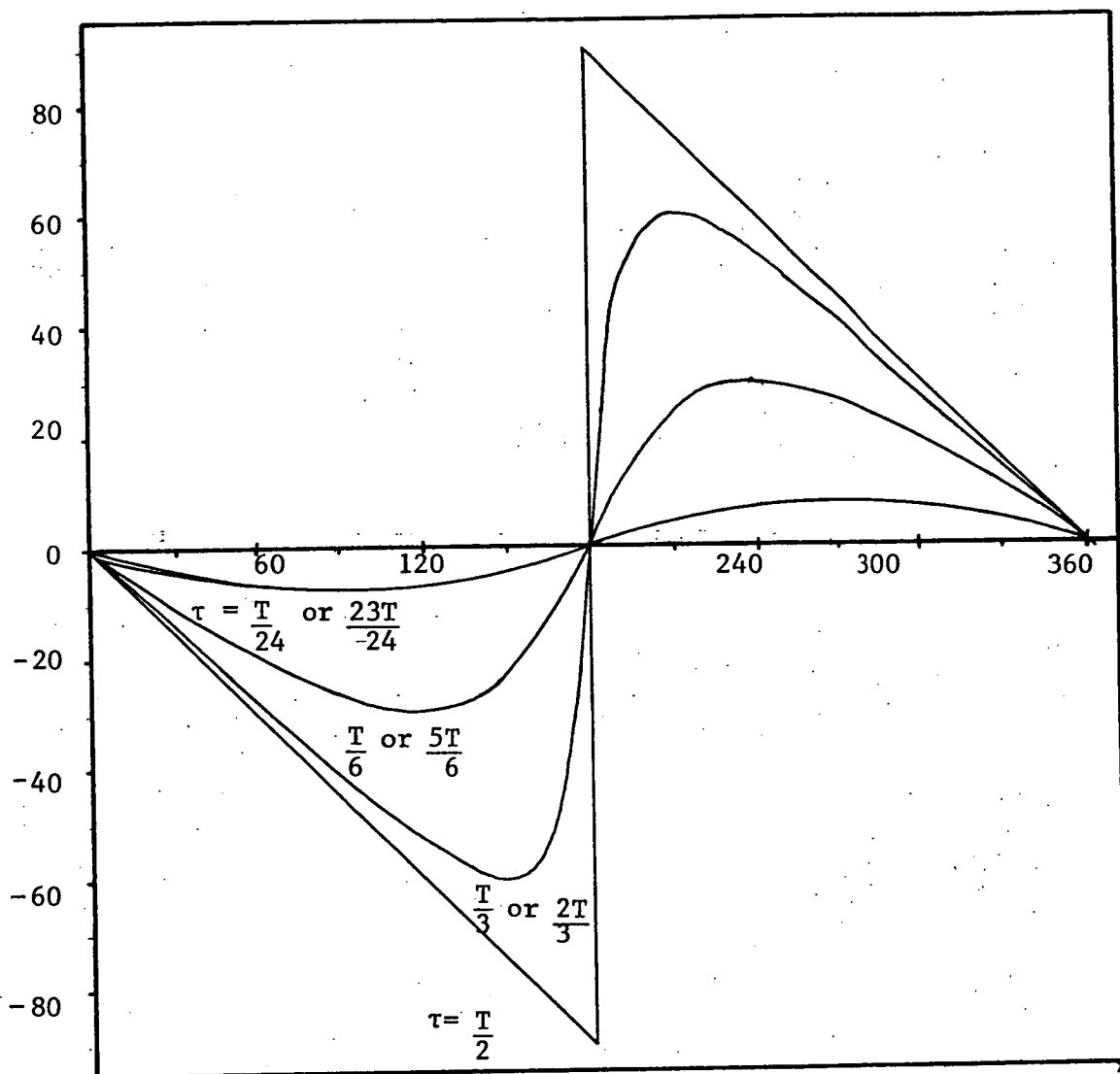


Fig. 3.7 PRC's for various pulse durations ( $\tau$ ).  $T$  is the period of the oscillation.  $R/h = 2$ .  $(\phi' - \phi)^\circ$  is plotted against  $(\phi + \omega\tau/2)^\circ$ ; i.e. the phase of the oscillation at the centre of each pulse.

It can thus be seen that PRC's contain information that cannot be determined through a frequency response analysis, information pertaining to the difference in phase between the oscillation at the output and the oscillation immediately following the comparator in the feedback loop. Pulse-phase response studies may thus compliment frequency response studies in the analysis of oscillatory systems.

This section on PRC's will be terminated by considering the case of a damped simple harmonic oscillator. The oscillator described by figure 3.5 can be modified to produce damped oscillations by replacing one or both integrators with exponential lag elements. If an exponential lag element with time constant  $T$  and gain  $k$  has the transfer function  $k/(Ts + 1)$ , replacing one integrator with such a lag results in an oscillatory system with transfer function:

$$k/(Ts^2 + s + k\omega^2) ;$$

- and the corresponding differential equation is:

$$T \ddot{y} + \dot{y} + k\omega^2 y = kx$$

In this case, for  $x = 0$  the amplitude  $R$  in the solution  $y = R\sin(\omega t + \phi)$  is an exponentially decreasing function of time and thus a pulse applied at a later time will cause a greater phase change than a pulse of identical height and duration applied in the same phase of an earlier cycle. Otherwise, provided the damping is not severe (i.e.  $k/T > \omega/2\pi$ ) the PRC's for this damped oscillation would be approximately the same as those for the undamped case.

---

## CHAPTER FOUR

### ANALYTICAL METHODS

#### 4.1 INTRODUCTION

In the studies described in this thesis the frequencies, amplitudes and phases of periodic components in the leaf movement of clover were estimated by spectral analysis. Some relevant aspects of spectral analysis, which are not readily available in the literature, are described in this chapter. The relationship between spectral analysis and the method of least squares is developed and the properties and pitfalls associated with the discrete Fourier transform method used are described. The statistical reliability of spectral estimates is also considered.

The title spectral analysis may, in a general sense, be applied to any analytical procedure that describes or measures the fluctuations in a time series (i.e. a collection of observations made sequentially in time) in terms of its frequency content. This frequency content is usually determined by comparing the time series (or a series derived from it) with sinusoids of different frequencies. The analysis is commonly performed either by applying a Fourier transformation to the time series, or by obtaining its power spectrum via the autocorrelation function (Blackman and Tukey, 1958). The name spectral analysis is sometimes restricted to this second approach (e.g. Chadfield, 1975). Some analysis of circadian rhythms have been shown in the form of power spectra (Hoshisaki and Hammer, 1969, Simon et al, 1976), but the power spectral analysis approach has the disadvantage that phase information is not retained. This is a limitation because in studies of oscillatory systems knowledge of phase may be as important as frequency and amplitude.

Fourier transformations are commonly implemented on a computer by way of the fast Fourier transform algorithm, or FFT (Cooley and Tukey, 1965; Higgins, 1976). Both conventional discrete Fourier transform and FFT methods were used in the studies reported in this thesis for the reasons given in section 5.6.

#### 4.2 THE DISCRETE FOURIER TRANSFORM

For some time it has been recognised that the frequency content  $F(\nu)$  of a time varying function  $f(t)$  can be related to that function by the Fourier transform:

$$F(\nu) = \int_{-\infty}^{\infty} f(t) e^{-j\omega t} dt$$

- where  $j = \sqrt{-1}$  and  $\omega = 2\pi\nu$

The properties of this transform and of the inverse transform:

$$f(t) = \int_{-\infty}^{\infty} F(\nu) e^{j\omega t} d\nu$$

- are well defined in the literature (Bracewell, 1965; Brigham, 1974).

However, real data are usually obtained by recording observations at discrete intervals for a finite period of time. Thus the continuous transform  $F(\nu)$  cannot be determined from the data, and instead an approximation to it, the discrete Fourier transform, or DFT is used. If there are  $n$  observations recorded at intervals of  $\tau$  during a total time of  $T = n\tau$ , the DFT:

$$F_{\nu} = 1/n \sum_{t/\tau=0}^{n-1} f_t e^{-j\omega t}$$

is determined for  $\nu = 0, 1/T, 2/T \dots (n-1)/T$  (Cooley et al, 1969).

Thus the DFT of  $n$  observations is an  $n$ -point frequency series with resolution equal to the reciprocal of the total time of observation, or 'data window'. This series of  $n$  complex numbers completely represents the data, which can be reproduced from it by the reverse transformation:

$$f_t = 1/n \sum_{v/T=0}^{n-1} F_v e^{j\omega t}$$

The complex series  $F_v$  can be written as:

$$F_v = (a_v - jb_v)/2, \text{ where}$$

$$a_v = 2/n \sum_{t/T=0}^{n-1} f_t \cos \omega t$$

$$\text{and } b_v = 2/n \sum_{t/T=0}^{n-1} f_t \sin \omega t$$

It will be shown in section 4.3 that  $a_v$  and  $b_v$  give the amplitudes of the cosine and sine of best fit to the data at frequency  $v$  by the principle of least squares. The amplitude spectrum of  $f_t$  is the set of values:

$$r_v = (a_v^2 + b_v^2)^{1/2}$$

and the power spectrum is given by the square of this. The corresponding values of phase,  $\phi$  can be determined from:

$$\tan \phi = b_v/a_v,$$

though care must be taken in interpreting the sign of the angle (Bloomfield, 1974, P.12). Generally it is assumed that a large peak in the amplitude spectrum indicates the presence of a periodicity in the same series, the frequency of the periodicity being approximately that of the peak value. Criteria for establishing this shall be developed in section 4.5.

A practical consideration is that the spectrum is being represented by a set of points at frequency intervals of  $1/T$ . The

frequencies of these points are therefore determined by the total period of observation and not by any characteristic of the data. Thus the parameter of spectral components with frequencies lying between these points cannot be accurately estimated. This is known as the 'picket fence effect' because it is as if a continuous spectrum is being viewed through the gaps in a picket fence (Bergland, 1969). There exist methods for interpolating between the spectral points, but these are not straightforward and require some computational effort (Jenkins and Watts, 1968, P.51).

A convenient alternative is to use the DFT procedure itself to estimate the spectral content of the time series at frequencies between these values. In these cases a non-integral number of cycles at these frequencies occupy the data window (i.e. the time  $T$ ) and  $a_v$  and  $b_v$  are then only approximate estimations for the sinusoids of best fit. However, the departures from their correct values is negligible provided a sufficient number of cycles is included in the data window. For example, the error in peak position is no more than 1.5% if at least 3 cycles are included. This is discussed further in section 4.5 and in Appendix 3.

#### 4.3 SPECTRAL ANALYSIS FROM A LEAST SQUARES VIEWPOINT

The method of least squares is an approach commonly used when it is required that a function be fitted to a series of observations. The relationship between spectral analysis and least squares fitting is outlined in this section. The first subject, least squares estimation of amplitude and phase for a known or assumed frequency is particularly relevant to circadian studies in that such estimations form an integral part of the 'cosinor' method for quantifying biological rhythms (Halberg et al, 1967; Koukhari et al, 1973).

#### 4.3.1 Estimating amplitude and phase by least squares

Suppose that  $n$  observations  $f_t$ , recorded at times  $t = i\tau$ ,  $i = 0, 1, \dots, n-1$ , are believed to be values of a periodic function of the form:

$$\begin{aligned} f(t) &= R \cos(\omega_0 t - \phi) + u(t) \\ &= A \cos \omega_0 t + B \sin \omega_0 t + u(t) \end{aligned}$$

where  $\nu_0 = \omega_0 / 2\pi$  is the frequency of the periodicity and  $u(t)$  represents normally distributed random (white) noise of variance  $\sigma^2$ .

It is required to estimate the amplitude  $R$  and phase  $\phi$  and to determine the variances of these estimates due to the presence of the noise. The least squares approach to this problem is to minimize the quantity  $V(\hat{A}, \hat{B})$  where:

$$V(\hat{A}, \hat{B}) = (1/n) \sum_{t/\tau=0}^{n-1} (f_t - \hat{A} \cos \omega_0 t - \hat{B} \sin \omega_0 t)^2 \quad \dots\dots\dots(1)$$

i.e.  $V(\hat{A}, \hat{B})$  is the sum of squares of the difference between actual and fitted data points, scaled by a factor of  $1/n$ . The values of  $\hat{A}$  and  $\hat{B}$  determined thereby are least squares estimates of  $A$  and  $B$ , and can be used to calculate estimates for  $R$  and  $\phi$ .

The function  $V(\hat{A}, \hat{B})$  is minimized when the partial derivatives  $\partial V / \partial A$  and  $\partial V / \partial B$  are both zero. Taking partial derivatives of equation (1) and equating each to zero gives:

$$\hat{A} = p(\sum f_t \cos \omega_0 t \sum (\sin \omega_0 t)^2 - \sum f_t \sin \omega_0 t \sum \cos \omega_0 t \sin \omega_0 t) \dots\dots(2), \text{ and}$$

$$\hat{B} = p(\sum f_t \sin \omega_0 t \sum (\cos \omega_0 t)^2 - \sum f_t \cos \omega_0 t \sum \cos \omega_0 t \sin \omega_0 t) \dots\dots\dots(3),$$

- where  $1/p = \sum (\cos \omega_0 t)^2 \sum (\sin \omega_0 t)^2 - (\sum \cos \omega_0 t \sum \sin \omega_0 t)^2$ , and the summation limits are as in equation (1).

Now:

$$\Sigma(\cos \omega_0 t)^2 = (n/2) \{1 + (\sin \omega_0 T \cos \omega_0 T(n-1)/n) / (n \sin \omega_0 T/n)\},$$

$$\Sigma(\sin \omega_0 t)^2 = (n/2) \{1 - (\sin \omega_0 T \cos \omega_0 T(n-1)/n) / (n \sin \omega_0 T/n)\}$$

and:

(Bloomfield, 1976, P12).

$$\Sigma(\sin \omega_0 t \cos \omega_0 t) = (n/2) \{ \sin \omega_0 T \sin (\omega_0 T(n-1)/n) \} / (n \sin \omega_0 T/n).$$

Provided  $n \gg \omega_0 T$ ; i.e. provided the number of observations is much greater than the number of cycles in the time series the above equations simplify to:

$$\Sigma(\cos \omega_0 t)^2 = (n/2) \{1 + (\sin 2\omega_0 T)/2\omega_0 T\}, \quad \dots(4),$$

$$\Sigma(\sin \omega_0 t)^2 = (n/2) \{1 - (\sin 2\omega_0 T)/2\omega_0 T\} \quad \dots(5),$$

$$\text{and } \Sigma(\sin \omega_0 t \cos \omega_0 t) = (n/2) (\sin \omega_0 T)^2 / \omega_0 T \quad \dots(6).$$

The above condition shall be reconsidered in section 4.4.2.

Substituting (4), (5) and (6) into equations (2) and (3) and

putting:  $a = (2/n) \Sigma f_t \cos \omega_0 t,$

and  $b = (2/n) \Sigma f_t \sin \omega_0 t,$

gives:

$$\hat{A} = p \{a \{1 - (\sin 2\omega_0 T)/2\omega_0 T\} - b (\sin \omega_0 T)^2 / \omega_0 T\}$$

$$\text{and } \hat{B} = p \{b \{1 + (\sin 2\omega_0 T)/2\omega_0 T\} - a (\sin \omega_0 T)^2 / \omega_0 T\},$$

where  $1/p$  has become:

$$1 - \{(\sin 2\omega_0 T)/2\omega_0 T\}^2 - \{(\sin \omega_0 T)^2 / \omega_0 T\}^2.$$

Provided there are several cycles of frequency  $\nu_0$  in the data window (i.e.  $\omega_0 T \gg 1$ ) the equations reduce to:

$$\hat{A} \approx a,$$

and  $\hat{B} \approx b,$

- and if the number of cycles is integral or half integral these



relationships become exact. The quantities  $a$  and  $b$  are those which are evaluated in the DFT (section 4.2). Furthermore the variances of the estimates  $a$  and  $b$  due to the white noise may be shown to be:

$$\text{var } a = \text{var } b = 2\sigma^2/n$$

$$\text{Also cov } (a,b) = 0$$

(Kendall, 1946, P.433; Bliss, 1970, P.268)

Combining these give:

$$\text{var } r = 2\sigma^2/n$$

$$\text{and } \text{var } \bar{\phi} = \sigma^2/nR^2,$$

where  $r$  and  $\bar{\phi}$  ( $\bar{\phi}$  in radians) are the estimates for  $R$  and  $\phi$  respectively (see Appendix 2). The above relationships may be used to assess the confidence that might be placed in least square estimates of amplitude and phase determined in the presence of white noise of variance  $\sigma^2$ .

#### 4.3.2 Estimation of Frequency

The estimates  $\hat{A}$  and  $\hat{B}$  are those values which minimize  $V(\hat{A}, \hat{B})$  for a particular value of  $\omega$ . Usually however,  $\omega$  is not known and must also be estimated. Suppose  $V(\hat{A}, \hat{B})$  is evaluated for each  $\omega$ .  $V(\hat{A}, \hat{B})$  will vary with  $\omega$  and it may be shown that (Appendix 1):

$$V(\hat{A}, \hat{B}, \omega) = (1/n) \sum (f_t)^2 - ((\hat{R}(\omega))^2/2)(1 + \{\sin \omega T \cos (\omega T - 2\hat{\phi}(\omega))\}/\omega T) \dots\dots\dots(7),$$

$$\text{where } \{\hat{R}(\omega)\}^2 = \{\hat{A}(\omega)\}^2 + \{\hat{B}(\omega)\}^2$$

$$\text{and } \tan \hat{\phi}(\omega) = \hat{B}(\omega)/\hat{A}(\omega).$$

The summation limits are as in equation (1).

The second term on the right in equation (7) is the variance of a sinusoid of angular frequency  $\omega$  observed for a time  $T$ . Thus the above equation may be written:

$$\text{Residual variance} = \text{total variance of data} - \text{variance of fitted sinusoid.}$$

The corresponding Fourier transform approximation is:

$$V(\hat{A}, \hat{B}, \omega) = (1/n) \sum (f_t)^2 - (\{r(\omega)\}^2/2)(1 - \{\sin \omega T \cos (\omega T - 2\bar{\phi}(\omega) / \omega T)\},$$

where  $\{r(\omega)\}^2 = \{a(\omega)\}^2 + \{b(\omega)\}^2$ ,

and  $\tan \bar{\phi}(\omega) = b(\omega)/a(\omega)$ .

This reduces to:

$$V(\hat{A}, \hat{B}, \omega) = (1/n) \sum (f_t)^2 - \{r(\omega)\}^2/2$$

- for integral or half integral numbers of cycles and is approximately correct for large non-integral numbers of cycles. A plot of  $r$  against frequency constitutes the amplitude spectrum for  $f_t$ , and it may be observed that a maximum in  $r$  will correspond to a minimum in  $V(\hat{A}, \hat{B}, \omega)$  provided the conditions:  $\omega T \gg 1$  and  $n \gg \omega T$  are true.

#### 4.3.3 Several Periodic Terms

The equations for the estimates  $a$  and  $b$  were derived on the assumption that the data were obtained from a single sinusoidal variation plus white noise. When several frequency components are present there will under most circumstances be minima in  $V(\hat{A}, \hat{B}, \omega)$  associated with each, and corresponding maxima in  $r(\omega)$ . The estimation of  $v$ ,  $R$  and  $\phi$  for each will be influenced by both the background noise and the presence of other spectral components. This interaction between spectral terms is known as leakage (Bergland, 1969) and shall be discussed in section 4.4.1. The effect of background noise on the estimates for each peak will be described in section 4.5.2.

#### 4.4 PROPERTIES OF THE DFT

The properties of the DFT described in this section arise due to the discrete, finite nature of the data that are transformed. The finite period over which  $f(t)$  is observed leads to *leakage*, and the discrete character of the observations may result in an effect known as *aliasing* (Blackman & Tukey, 1958, P.31). These features and means of

minimizing their corrupting influence, shall be discussed.

#### 4.4.1 Leakage

Leakage is best described by returning to the Fourier integral (section 4.2). This is defined for the full range of possible  $t$  values in the time domain. Thus applying this integral to a function  $f(t)$  that has been recorded for only a finite interval is equivalent to obtaining the transform of the product of  $f(t)$  with a function that is unity inside and zero outside that interval.

$$\text{i.e. } F(v) = \int_0^T f(t)e^{-j\omega t} dt = \int_{-\infty}^{\infty} w(t) f(t)e^{-j\omega t} dt,$$

where the 'window function'.  $w(t) = 1$  for  $0 \leq t \leq T$ ,

$$w(t) = 0 \text{ elsewhere.}$$

Now the Fourier transform of the product of two functions is equal to the convolution of their respective transforms (Bracewell, 1965, P.170).

Convolution is defined in section 3.2. The Fourier transform of a window function as defined above was calculated and plotted using a minicomputer and chart recorder (see chapter 5) and is shown in figure 4.1. Its amplitude spectrum is the modulus of a 'sinc function',  $(\sin \pi v T)/\pi v T$  (Bracewell, 1965, p. 65). The effect of this convolution is to broaden the sharp spectral peak corresponding to each frequency component into the form of the sinc function - i.e. a broad central peak (main lobe) located at the frequency of the component and flanked by a series of smaller peaks, or side lobes.

The main lobe and side lobes corresponding to each spectral component can cause the corruption of neighbouring spectral peaks, particularly if they represent much weaker components. Corruption may cause the frequency, amplitude and phase of a component to be wrongly estimated, and in some cases a component may go undetected.

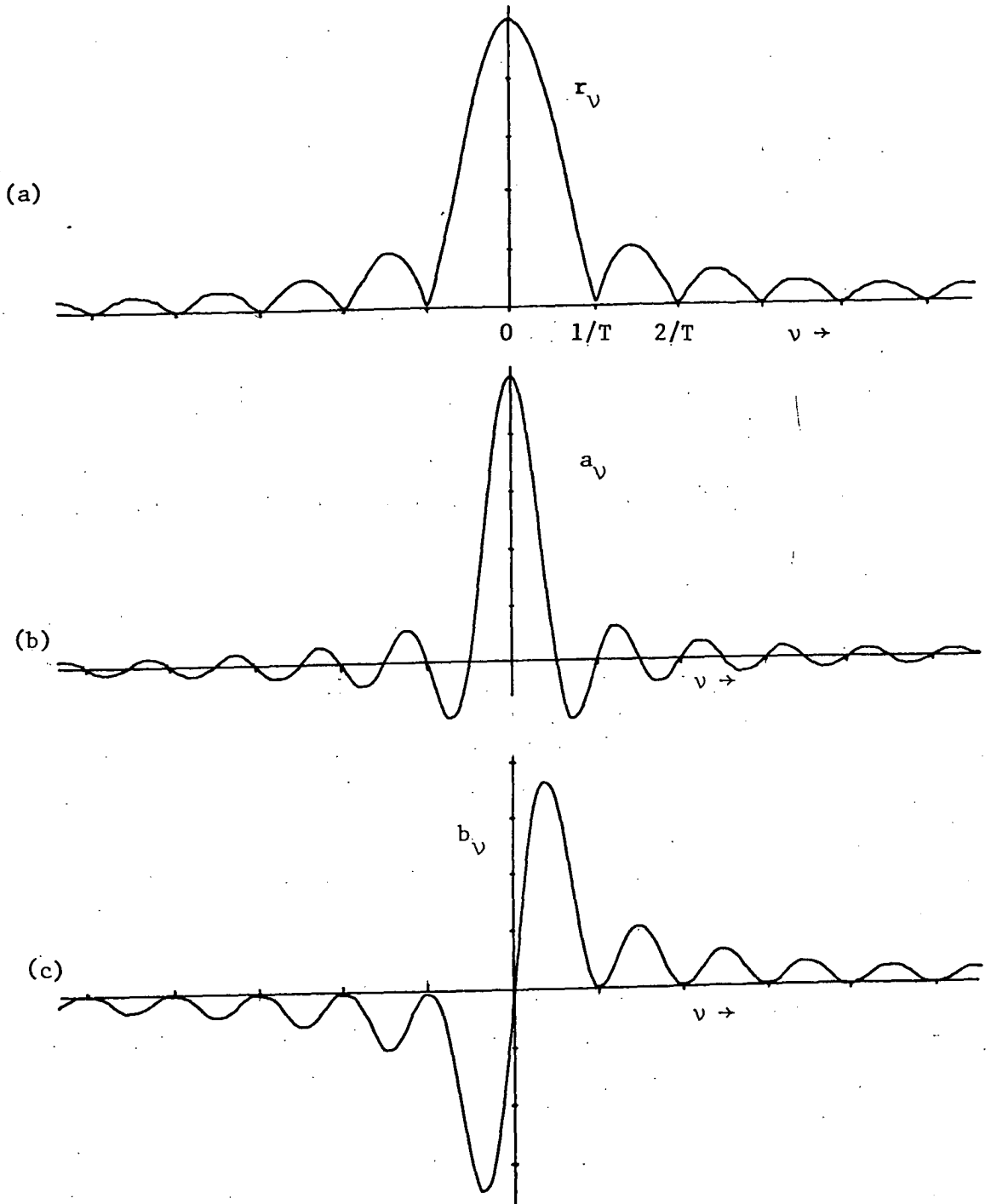


Fig. 4.1 Real (b) and Imaginary (c) parts of the transform for a rectangular data window of duration  $T$ . The resulting amplitude spectrum (a) is the modulus of a sinc function; i.e.  $\left| \frac{\sin \pi v T}{\pi v T} \right|$ . This consists of a broad central peak, or main lobe, flanked by a series of smaller peaks, or side lobes, at frequency intervals of  $1/T$ .

A common approach to this problem is to tailor the shape of the window function so that its transform has some form other than the sinc function. In practice this can be done by weighing the data most strongly in the middle of the period of observation and tapering towards zero at the beginning and end (Blackman and Tukey, 1958, Jenkins and Watts, 1968). Its effect is to decrease the size of the side lobes in the resulting spectrum at the expense of broadening the main lobe. This is illustrated in figure 4.2 where rectangular, extended cosine bell, cosine bell (Hanning) and triangular (Bartlett) windows were applied to a sinusoidal oscillation.

Some objections to windowing can be raised. Firstly, tampering with the data in this fashion is of questionable validity as it introduces a subjective step into the analysis. Secondly, if two spectral components have very similar frequencies the decreased resolution or broadening of peaks caused by windowing may prevent their separate identification (fig. 4.3).

The procedure adopted in the experiments described in this thesis for overcoming most of the effects of leakage is that due to Gray and Desikachary (1973) and is illustrated in figure 4.4. The mean of the data (fig. 4.4a) was set to zero, its Fourier transform was computed (fig. 4.4b) and the frequency, amplitude and phase of the largest peak in the amplitude spectrum were recorded (table 4.1). The transform of the corresponding sinusoid was then calculated using the expression given in Appendix 3, and this was subtracted from the data transform (fig. 4.4c).

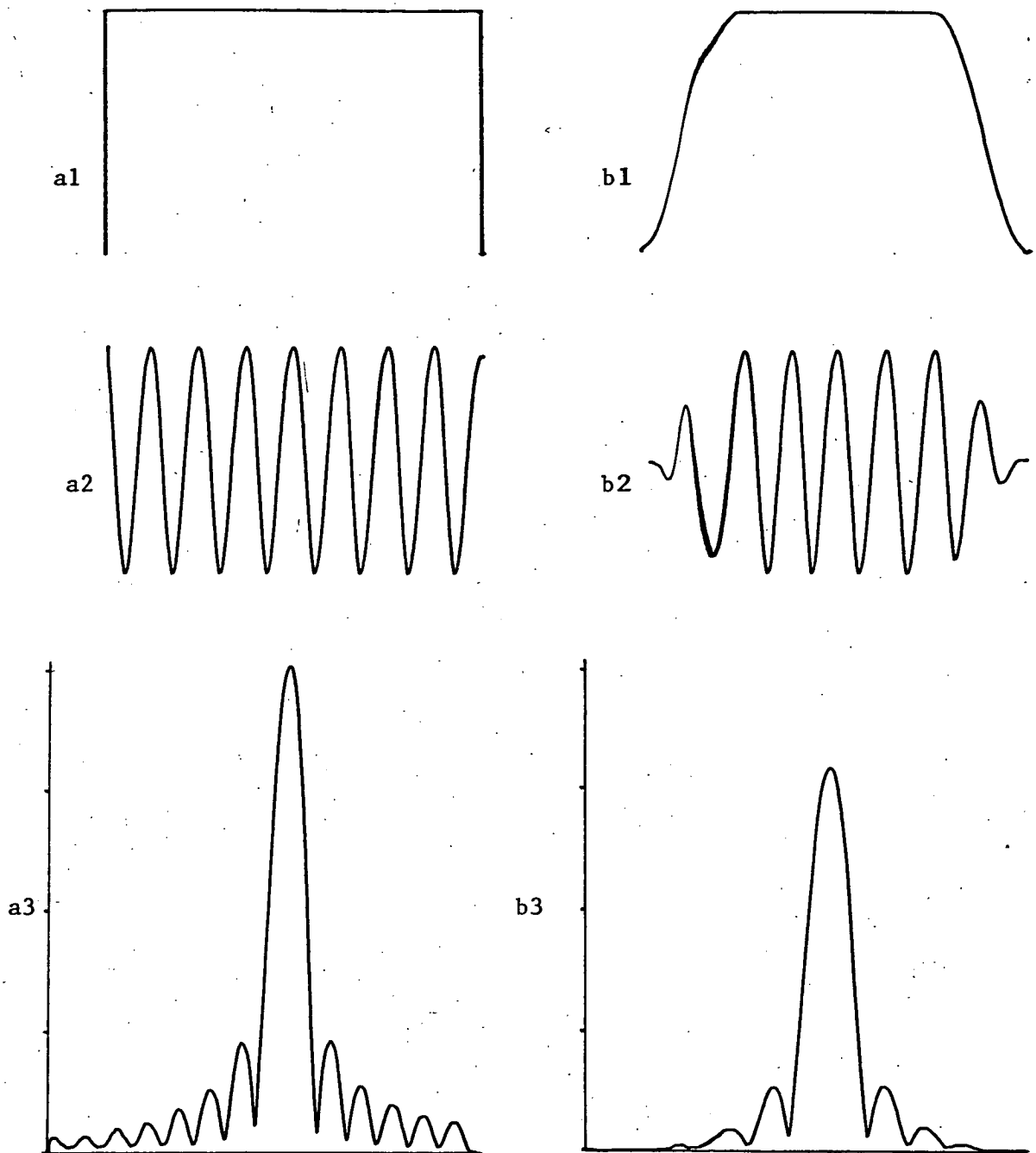


Fig. 4.2 (a) Sinusoid (a2) viewed through a rectangular data window (a1) and its amplitude spectrum (a3).

(b) Sinusoid (b2) viewed through an extended cosine bell window (b1) and its spectrum (b3). In this case the first and last 20% of the data have been tapered to zero by multiplication with segments of the function  $(1 - \cos \omega t)/2$ .

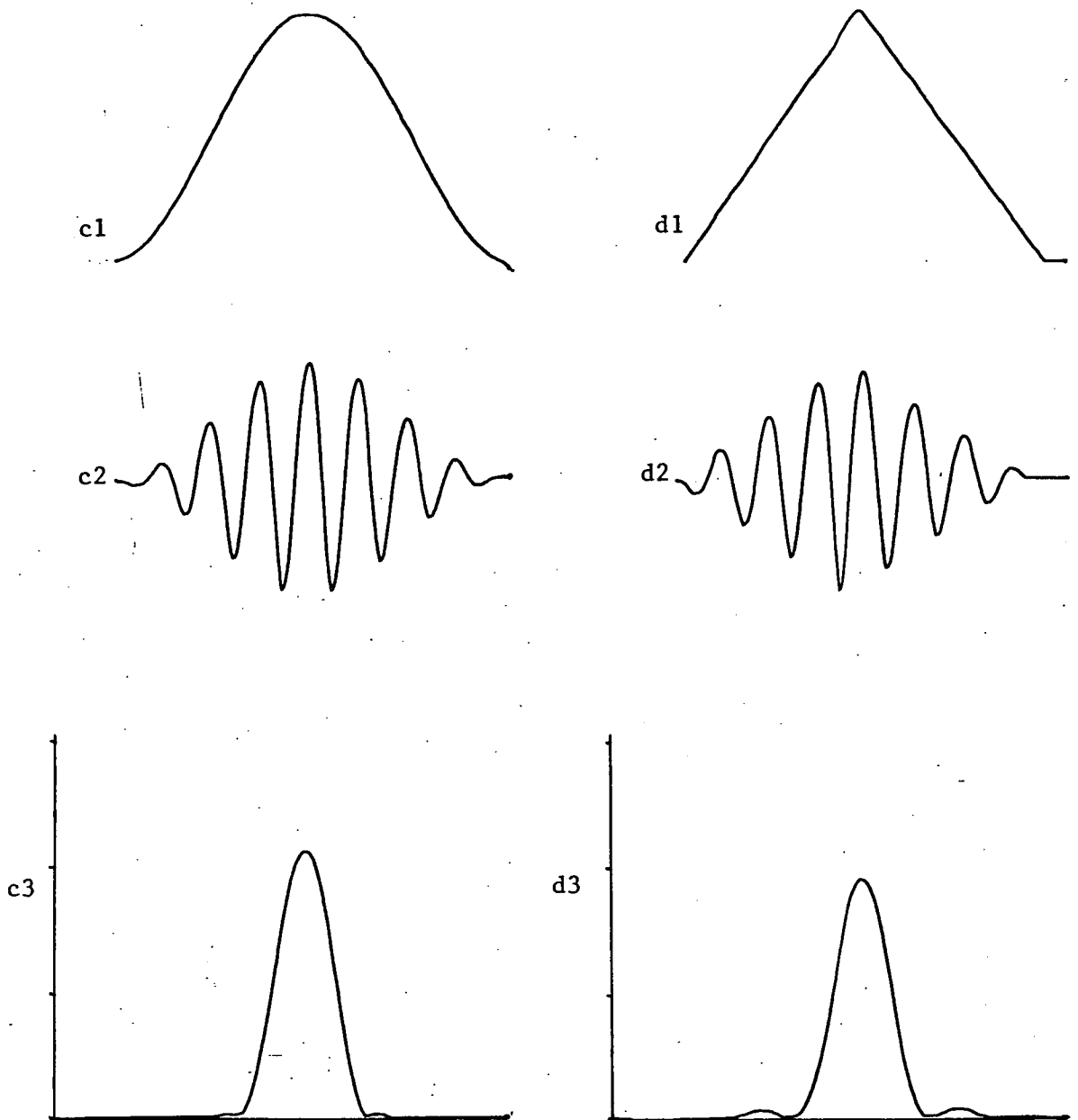


Fig. 4.2 (c) Cosine bell or Hanning window (c1) through which a sinusoid is viewed (c2), and the resulting spectrum (c3). Data has been multiplied by the function:  $(1 - \cos \omega t)/2$ .

(d) Triangular or Bartlett window (d1) through which a sinusoid is viewed (d2), and the resulting spectrum (d3). The triangular window is more readily effected than the cosine bell, but it does not reduce side lobes to the same degree, and results in a slightly wider main lobe.

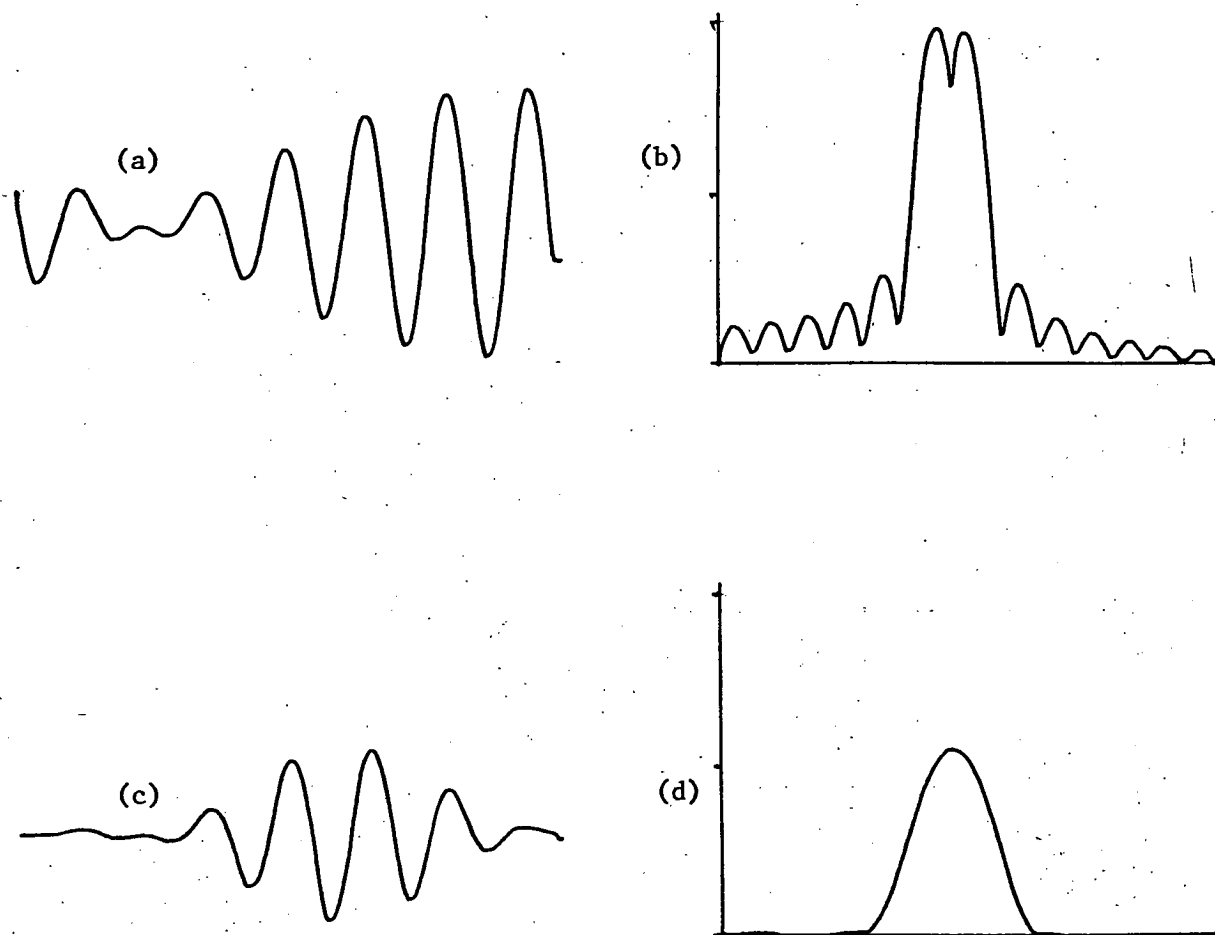


Fig. 4.3 A time series (a) and its amplitude spectrum using a rectangular data window (b). The same time series viewed through a cosine bell window (c) results in the spectrum shown in (d). Fig. 4.3 (b) indicates that the time series consists of two sinusoids of similar frequencies. The separate spectral peaks corresponding to these are not resolved in (d).



This removed the peak and associated side lobes from the transform and therefore any effect they may have had on adjacent spectral terms. The procedure was repeated automatically by computer for the next largest peak (fig. 4.4d) and so on until no significant peak remained (fig. 4.4e). The test used for significance is given in section 4.5. The data used to illustrate the analytical method was derived from an experiment described in section 6.3.2. The significance of the results in table 4.1 will be developed at a later stage.

The procedure is not completely satisfactory as each peak that is extracted is to some extent corrupted by the remaining smaller peaks adjacent to it. That is, there may be some error in the estimation of the parameters of each component to be extracted. These errors are discussed in section 4.5. As a useful check on the validity of the procedure a time domain signal can be constructed in which the extracted components are recombined (fig. 4.4f). This may then be compared with the original time series.

#### 4.4.2 Aliasing

For a time series  $f_t$  to correctly portray a function  $f(t)$  it must have sufficiently closely spaced points to represent the highest frequency component present in  $f(t)$ . For a frequency component to be identifiable there must be at least two observations taken in each of its cycles, so if observations are made at intervals of  $\tau$ , the highest frequency determinable is  $(2\tau)^{-1}$ . If this restriction is complied with the function  $f(t)$  is completely represented by the series  $f_t$  and may be derived from it (Jenkins and Watts, 1968, p. 51). This is known as the

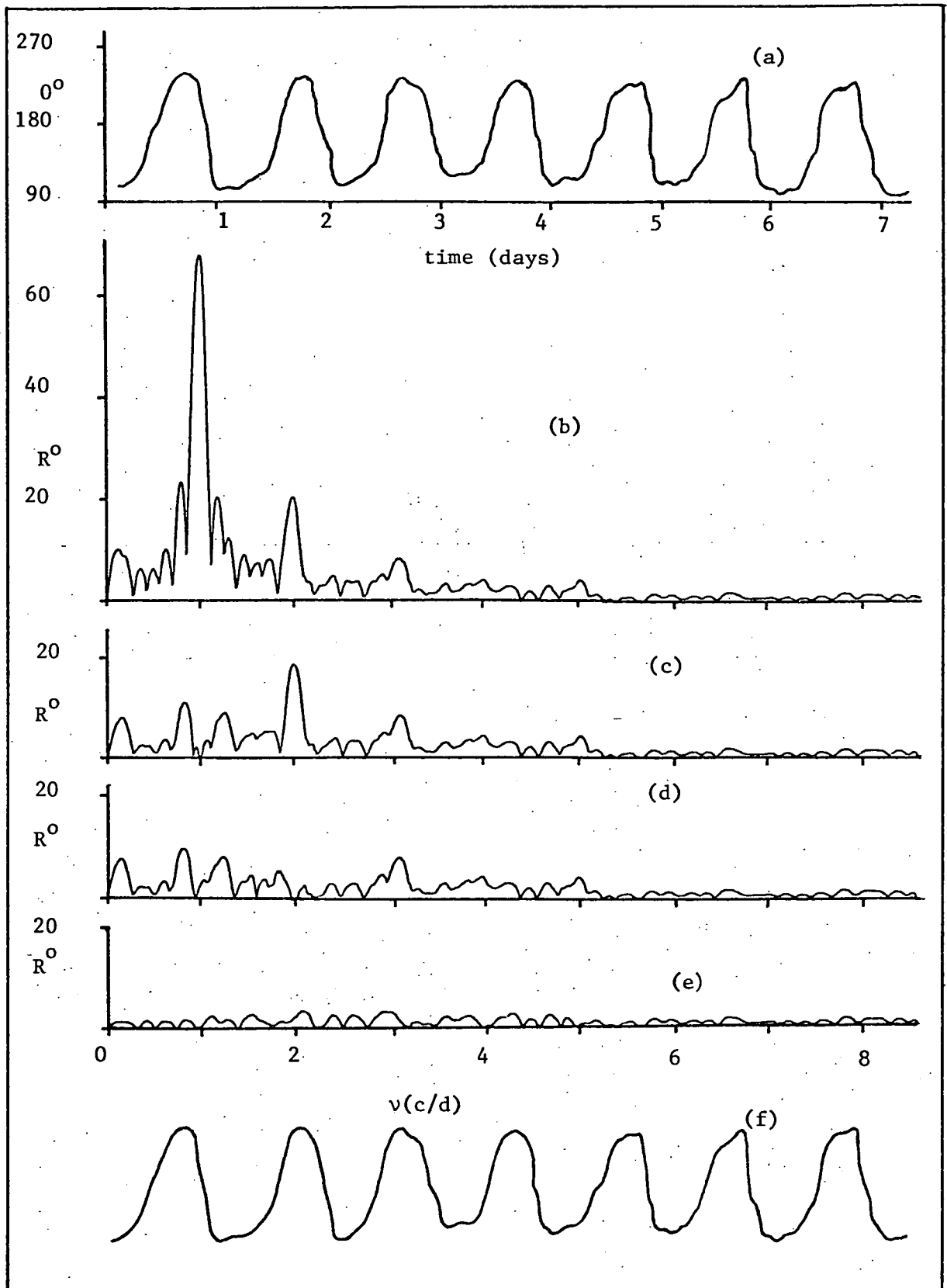


Fig. 4.4. (a) Movement of a leaf subject to a 1c/d sinusoidal log-light variation between 400 and 3700 lux. (b) is its amplitude spectrum and (c), (d) and (e) are spectra with 1, 2 and 9 components extracted, leaving only a background in the case of (e). (f) is the reconstructed signal.

No.	$v(c/d)$	$r(^{\circ})$	$\phi(^{\circ})$	Interpretation
1	$1.00 \pm .001$	$68.1 \pm 1.0$	$12 \pm 2$	$f_1$
2	$1.99 \pm .004$	$18.7 \pm "$	$-172 \pm 6$	$f_2$
3	$0.86 \pm .007$	$10.7 \pm "$	$-18 \pm 10$	$c_1$
4	$0.14 \pm .008$	$9.4 \pm "$	$-25 \pm 12$	$f_1 - c_1$
5	$2.99 \pm .009$	$8.5 \pm "$	$115 \pm 13$	$f_3$
6	$1.27 \pm .010$	$8.0 \pm "$	$164 \pm 14$	
7	$1.71 \pm .011$	$6.6 \pm "$	$161 \pm 17$	$c_2$
8	$3.97 \pm .018$	$4.3 \pm "$	$152 \pm 26$	$f_4$
9	$4.95 \pm .019$	$4.0 \pm "$	$29 \pm 28$	$f_5$

Table 4.1. Parameters of components extracted from the transform in figure 4.4. ( $\pm$ ) values are standard errors due to the noise background (section 4.5).  $c_1$  and  $f_1$  are the fundamental circadian and forced oscillations, and  $c_2$ ,  $f_2 - f_5$  are higher harmonics of these.

sampling theorem, and the frequency  $(2\tau)^{-1}$  as the Nyquist frequency (Blackman & Tukey, 1958, P.32). The Nyquist frequency will be denoted by  $\nu_N$ .

Now suppose  $f(t)$  consists of an oscillation with frequency  $\nu$ , which exceeds  $\nu_N$  by some amount  $\Delta\nu$ ,

$$\text{i.e. } \nu = \nu_N + \Delta\nu$$

$$\text{Let } f(t) = \cos 2 \pi \nu t$$

$$\text{Then } f_t = \cos 2 \pi t(\nu_N + \Delta\nu) \dots\dots(a)$$

$$\text{-- where } t = i\tau = i(2\nu_N)^{-1}, i \text{ an integer;}$$

$$\therefore f_t = \cos (\pi i + 2 \pi \Delta\nu t)$$

$$= \cos (\pi i - 2 \pi \Delta\nu t)$$

$$= \cos 2 \pi t(\nu_N - \Delta\nu) \dots\dots(b);$$

i.e. the time series defined by (a) derived from an oscillation of frequency  $\nu = \nu_N + \Delta\nu$ , is identical to the time series defined by (b) with frequency  $\nu = \nu_N - \Delta\nu$ .

This leads to the result that if there is a frequency component in the sampled quantity which exceeds  $\nu_N$  by some amount it will appear in the DFT as a component of frequency less than  $\nu_N$  by the same amount. The frequency spectrum will therefore appear to be folded back about  $\nu_N$ . Frequency components above  $\nu_N$  are said to alias below  $\nu_N$  (Blackman and Tukey, 1958, p.32) and care must be taken to establish whether peaks in a spectrum represent genuine frequency components or are due to aliasing.

It is also observed that if a spectral peak is close to  $\nu_N$  its own side lobes may be higher in frequency than  $\nu_N$  and these will therefore fold

back. Thus a spectral peak may be corrupted by its own side lobes. Under these circumstances the condition  $n \gg \omega T$  (section 4.3.1) required for the DFT to give approximately equivalent results to a least squares fitting is not true. The possible errors in determining the parameters of a spectral component in the vicinity of  $\nu_N$  therefore logically follow from the approximations made in relating the DFT to the method of least squares.

Aliasing may be minimized by employing a sufficiently high sampling rate so that  $\nu_N$  is well beyond the spectral range of interest. For example, figure 4.5a is a record of the movement of a clover leaf subject to a 24 hour light variation, obtained from experiments described in section 6.3.2. Figure 4.5b is the corresponding amplitude spectrum using all of the data points (10 minute intervals,  $\nu_N = 72$  c/d) and figure 4.5c using only data points obtained at 2 hour intervals (i.e.  $\nu_N = 6$  c/d). It is clearly seen that the component at approximately 8 c/d (cycles per day) in figure 4.5b appears in fig. 4.5c as a spurious peak at 4 c/d due to aliasing.

Finally, in section 4.2 it was stated that the DFT in its usual form produces from the time series a series of  $n$  complex numbers at frequencies:  $\nu = 0, 1/T, 2/T, \dots, (n-1)/T$ . However,  $\nu = \nu_N$  when  $\nu = n/2T$ . That is, the last half of the frequency series is above the Nyquist frequency and there is actually no further information contained in it. The time series is fully described by the first  $n/2$  complex numbers.

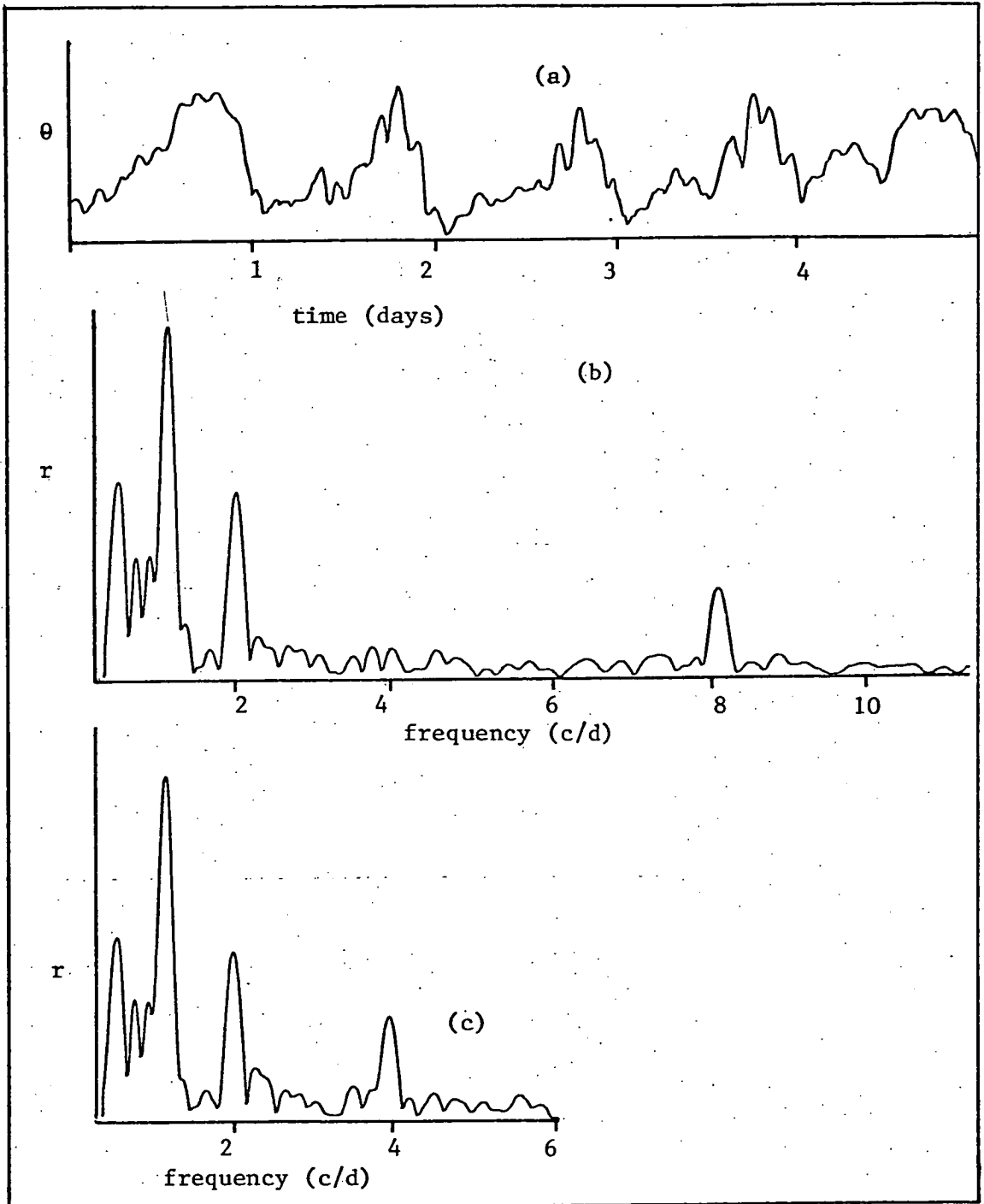


Fig. 4.5 Illustrating the effect of aliasing as described in the text.  
Vertical scales are arbitrary.

#### 4.5 RELIABILITY OF SPECTRAL ESTIMATES

Spectral analysis of a time series should not only indicate (1) which frequency components are present, but also (2) the confidence that may be placed in the estimates of amplitude, frequency and phase for these components. In relation to (1) criteria have been established for determining whether peaks in the spectrum represent true periodicities (Walker, 1914; Fisher, 1929; Jenkins and Priestly, 1957). Very little attention has been given to (2), so that frequencies, for example, of spectral components are often quoted with no indication of the reliability of these estimates. Both aspects are considered below.

##### 4.5.1 Presence of Frequency Components

The spectrum of a time series may contain peaks that represent frequency components truly present in the observed variation. Alternatively peaks may arise due to the interaction of side lobes associated with periodicities truly present (leakage), or due to random fluctuations in the spectrum resulting from the presence of background noise.

The tests for significance of spectral peaks are in general based on an hypothesis of random normal variation in the original series. If a particular peak is not shown, on this hypothesis, to have a maximum value significantly greater than the mean spectral value then it may be assumed that it does not represent a true periodicity (Kendall 1946, p.434). However, if one spectral value is shown to be significant then the test cannot reasonably be applied to other values, since the presence of a periodicity negates the hypothesis on which the test is based. This

criticism has been overcome in part by later work on periodogram analysis (Hartly, 1949; Jenkins and Priestly, 1957).

It has also been suggested (Kendall, 1946, p.434) that the criticism may be countered by subtracting the significant component from the time series and then testing the remainder for the presence of periodicities. This is essentially the procedure that is described in section 4.1, with the modification that the subtraction is performed in the frequency domain.

The procedure applied to test for the presence of frequency components and used in conjunction with the component extraction technique was that suggested by Schuster (1898) and modified by Walker (1914). The test assumes as a null hypothesis that the time series  $f_t$  consists of random elements from a normal population. By the Central Limits theorem the DFT coefficients,  $a_v$  and  $b_v$ , for this time series will also be normally distributed (Kendall, 1948) and the elements of the power spectrum:

$$r_v^2 = a_v^2 + b_v^2$$

- will therefore have a Chi-squared distribution with two degrees of freedom. This is an exponential distribution, and if the original series has a variance of  $\sigma^2$ , the probability that an  $r^2$  value chosen at random exceeds some value  $k$  is immediately obtainable as  $e^{-k/c}$ , where  $c = 4\sigma^2/n$ . The probability that  $m$  independent estimates of  $r^2$  do not exceed  $k$  is therefore:

$$(1 - e^{-k/c})^m,$$

and so the probability that at least one exceeds this amount is:

$$1 - (1 - e^{-k/c})^m.$$



The quantity  $c$  is approximately the mean of the  $m$  independent power spectrum elements, and therefore may be calculated from the spectral values.

The above equation gives the probability that at least one peak in the spectrum derived from a random time series exceeds the value  $k$ . Thus when the spectrum of actual data contains a peak of height  $k$  the probability for which in random data is very small, it can be assumed to represent a true periodicity. In the work described in this thesis the highest peak was assumed to represent a true periodicity if this probability was less than 0.05. The component was then subtracted from the spectrum and the next highest peak tested, a new  $c$  value being calculated for this modified spectrum. The procedure was repeated until remaining peaks had greater probabilities than 0.05. It was then assumed that this residue represented a noise background. The variance of this noise was estimated and used to place confidence limits on the parameters of the extracted components.

#### 4.5.2 Reliability of Frequency, Amplitude and Phase Estimates

Two sources of error in estimating the parameters of spectral components are leakage, or interaction between spectral terms, and background noise in the original time series. Analytical errors resulting from these shall be considered in turn.

The interaction between spectral terms is complex and depends on the relative amplitudes of the terms, the difference in their frequencies and phases, and the duration of the data record. A procedure for assessing the extent of corruption by neighbouring peaks is given in

Appendix 3. Using this procedure it may, for example, be shown that the first component in table 4.1 is corrupted by component 2 (the second harmonic) as follows :  $\delta v = 0.002c/d$ ,  $\delta R = 0.01^\circ$  and  $\delta\phi = 2.3^\circ$ . That is, the values for component 1 in table 4.1 are displaced from their true values by these amounts due to the presence of component 2. It is further corrupted by component 3 (the circadian component) by the following amounts:  $\delta v = 0.005 c/d$ ,  $\delta R = 0.5^\circ$  and  $\delta\phi = 6.3^\circ$ .

Unlike errors due to background noise, these are systematic errors which would be unlikely to average to zero if the experiment was repeated many times. However, the component extraction procedure will detect the residue of a component wrongly extracted if the residue is significantly greater than the noise level. Thus extracted terms that are seriously in error due to corruption by neighbouring peaks may be corrected at a later stage in the procedure.

It is now necessary to consider errors due to a noise background. In section 3.1 the variances of amplitude and phase estimates due to a white noise background for least squares fitting to a periodicity of known frequency were given. The variances of the estimates when the frequency is not known but is also estimated from the time series are difficult to derive. The problem was studied by Whittle (1952) and later by Walker (1971).

Walker considered a single periodicity plus white noise of variance  $\sigma^2$ .

$$\text{i.e. } f_t = R \cos(\omega_0 t - \phi) + u_t$$

$$= A \cos \omega_0 t + B \sin \omega_0 t + u_t \quad (\text{see section 4.3.1}).$$

His conclusions were essentially:

$$\text{var } a = (2\sigma^2/n) (1 + 3B^2/R^2),$$

$$\text{var } b = (2\sigma^2/n) (1 + 3A^2/R^2),$$

$$\text{var } \omega = 24\sigma^2/n R^2 T^2,$$

$$\text{cov } (a, b) = (-6\sigma^2/n) (AB/R^2),$$

$$\text{cov } (a, \omega) = (12\sigma^2/n) (B^2/R^2),$$

$$\text{and cov } (b, \omega) = (-12\sigma^2/n) (A^2/R^2)$$

The above relationships may be combined (see Appendix 2) to produce the results:

$$\text{var } r = 2\sigma^2/n,$$

$$\text{var } \phi = 8\sigma^2/n R^2 \quad (\phi \text{ in radians}),$$

$$\text{and var } v = 6\sigma^2/n \pi^2 R^2 T^2;$$

- and since generally when  $n \gg \omega T \gg 1$  (see section 4.3)  $r$  is an unbiased estimator for  $R$  (i.e.  $r$  tends to  $R$  as  $n$  tends to infinity), it seems reasonable to replace  $R$  with  $r$  in these estimated variances.

When a number of sinusoids have been extracted from the data leaving a noise residue, the error in the estimation of the parameters of each due to the background noise may be assessed using the above equations.

In practice a problem arises because the background noise is rarely white. For example, in the case of clover the sluggishness of the leaf movement precludes the presence of high frequency components.

This feature is readily seen in each amplitude spectrum residue which generally tapers to very nearly zero for frequencies above about 10 c/d. Thus data points in the noise background more frequent than 20/day cannot be regarded as independent for the purpose of estimating variances using the above equations. For this reason the estimates of standard errors due to background noise in the 7-day record analysed in table 4.1 used a value of  $n = 20 \times 7 = 140$ , rather than the full number of data points, which was approximately 1000.

#### 4.5.3 Combination of Estimates

The analysis of a time series representing a biological process might result in, for example, a frequency estimate plus a variance for this estimate arising from a noise background. This noise may be caused by the variability of the biological source itself, or it may be due to (or be contributed to by) the recording system and the actual analytical technique used. It is now necessary to consider how the estimates and associated variances for a number of similarly treated biological systems should be combined to produce a variance that accounts for these sources of error and also for dissimilarities between systems (i.e. biological scatter).

Suppose these are  $n$  samples, each the mean estimate arising from  $m$  repetitions of an experiment with the same source material: i.e. each sample  $\bar{x}_j$  is the mean of  $m$  values  $x_{jk}$ . The variance of these  $n$  by  $m$  estimates is:

$$(1/mn) \sum_{j=1}^n \sum_{k=1}^m (x_{jk} - \bar{x})^2, \text{ where } \bar{x} \text{ is the mean of the samples.}$$

The difference term may be written as:

$$\bar{x}_j + d_{jk} - \bar{x}, \text{ where } d_{jk} = x_{jk} - \bar{x}_j.$$

Squaring gives:

$$\bar{x}_j^2 + \bar{x}^2 - 2\bar{x}\bar{x}_j + d_{jk}^2 + 2\bar{x}_j d_{jk} - 2\bar{x}d_{jk}$$

Thus:

$$(1/m) \sum_{k=1}^m (x_{jk} - \bar{x})^2 = \bar{x}_j^2 + \bar{x}^2 - 2\bar{x}\bar{x}_j + \sigma_j^2,$$

where  $\sigma_j^2$  is the variance of the  $j$ th sample

$$\begin{aligned} \therefore (1/mn) \sum_{j=1}^n \sum_{k=1}^m (x_{jk} - \bar{x})^2 &= (1/n) \bar{x}^2 + \bar{x}^2 - 2\bar{x}^2 + (1/n) \sigma_j^2 \\ &= (1/n) \sum (\bar{x}_j - \bar{x})^2 + (1/n) \sigma_j^2. \end{aligned}$$

In practice there is only one observation in each sample, i.e.

$m = 1$ , so:

$$(1/n) \sum_{j=1}^n (x_{j1} - \bar{x})^2 = (1/n) \sum_{j=1}^n (\bar{x}_j - \bar{x})^2 + (1/n) \sum_{j=1}^n \sigma_j^2$$

The terms on the right are the variance of the  $n$  samples and the mean of the variances of each sample (i.e. due to the noise background) respectively. Thus the variance calculated for the combination of individual estimates from each of the time series incorporates terms arising due to both biological scatter and the uncertainty in each estimate. For this reason errors due to background noise in the spectrum of each leaf record in each sample are not treated separately in most of the studies described in this thesis.

A final point concerns the accuracy with which spectral frequencies are determined. The DFT represents the frequency content of a time series by values at discrete frequencies. A large value in the spectrum may correspond to the tested frequency that is closest to that of a periodicity actually present in the time series. Thus frequency estimates are quantized, and if the tested frequencies are well spaced a variance calculated for a set of frequency estimates will appear smaller than is actually the case. To minimize this effect it may be necessary to interpolate between points in the vicinity of a spectral peak if the necessary frequency resolution is not obtainable.

#### 4.6 OSCILLATIONS WITH NONSTATIONARY PARAMETERS

Biological oscillations frequently exhibit gradual changes in amplitude and frequency and may also show abrupt changes in phase due to some stimulus received. For this reason it is relevant to examine how these changes affect the information derived from the corresponding Fourier transforms. Figure 4.6 shows exponentially damped oscillations and their amplitude spectra. Spectral values were determined at intervals of 0.01 of the undamped oscillation frequency. Deviations from the correct values for both frequency and phase could not be detected within the resolution of the analysis. Each amplitude, however, represents approximately the geometric mean for the oscillation.

Figure 4.7 shows oscillations decreasing in frequency and their amplitude spectra. In these cases each spectral peak is centred on the average frequency for the oscillation, with amplitude somewhat below the correct value. There are also obvious difficulties in interpreting phase information for variations of this kind.

Oscillations subject to phase jumps or discontinuities are shown in figure 4.8. The discontinuity causes a double peaked structure in the spectrum, and in the case of a  $180^\circ$  phase change the transform may show zero frequency content at the actual frequency of oscillation (fig. 4.8e). Thus it is possible for such abrupt phase changes to lead to severe errors in the estimation of the parameters for an oscillation. However, these examples show the phase change as occurring in the centre of each time series. The effect is far less marked if this change is displaced from the centre. In this respect the examples are extreme cases.

Some of the variations depicted in figure 4.6, 4.7 and 4.8 are quite severe and would rarely be encountered in circadian studies. Even so the transform still provides information about the average properties of the oscillation. Furthermore the presence of such variations may be tested by dividing the time series into segments and analysing these separately. Nonstationary behaviour of component parameters will appear as differences in the amplitude, frequency or phase estimates for these components between earlier and later segments of the data record.

#### 4.7 FUTURE DEVELOPMENTS

Two spectral analysis techniques have recently been developed which in general give superior resolution in analyses of very limited amounts of cyclic data. These are the Maximum Likelihood Method, or MLM (Capon, 1969; Burg, 1972) and the Maximum Entropy Method, or MEM (Burg, 1967). The techniques are finding favour in some geophysical

studies where the available data may cover only one or two oscillations (Lacoss, 1971; Ulrych, 1972; Ables, 1974; Chen and Stegen, 1974).

The new techniques have the advantage that they are not necessarily subject to the leakage effects inherent in the conventional approach. However, they are more difficult to use than the conventional transform. Furthermore, the conventional spectrum is obtained from the time series by a definite, easy to visualize procedure. The process by which the MLM and MEM spectra are derived is abstruse and complex (Ball, 1975). At this stage their use may not be warranted for most circadian studies, particularly since they do not provide phase information.

A development of MEM, The Maximum Entropy Prediction Method (Ulrych et al, 1973) overcomes this last limitation and its usefulness in circadian studies may be worthy of examination in the future.

---



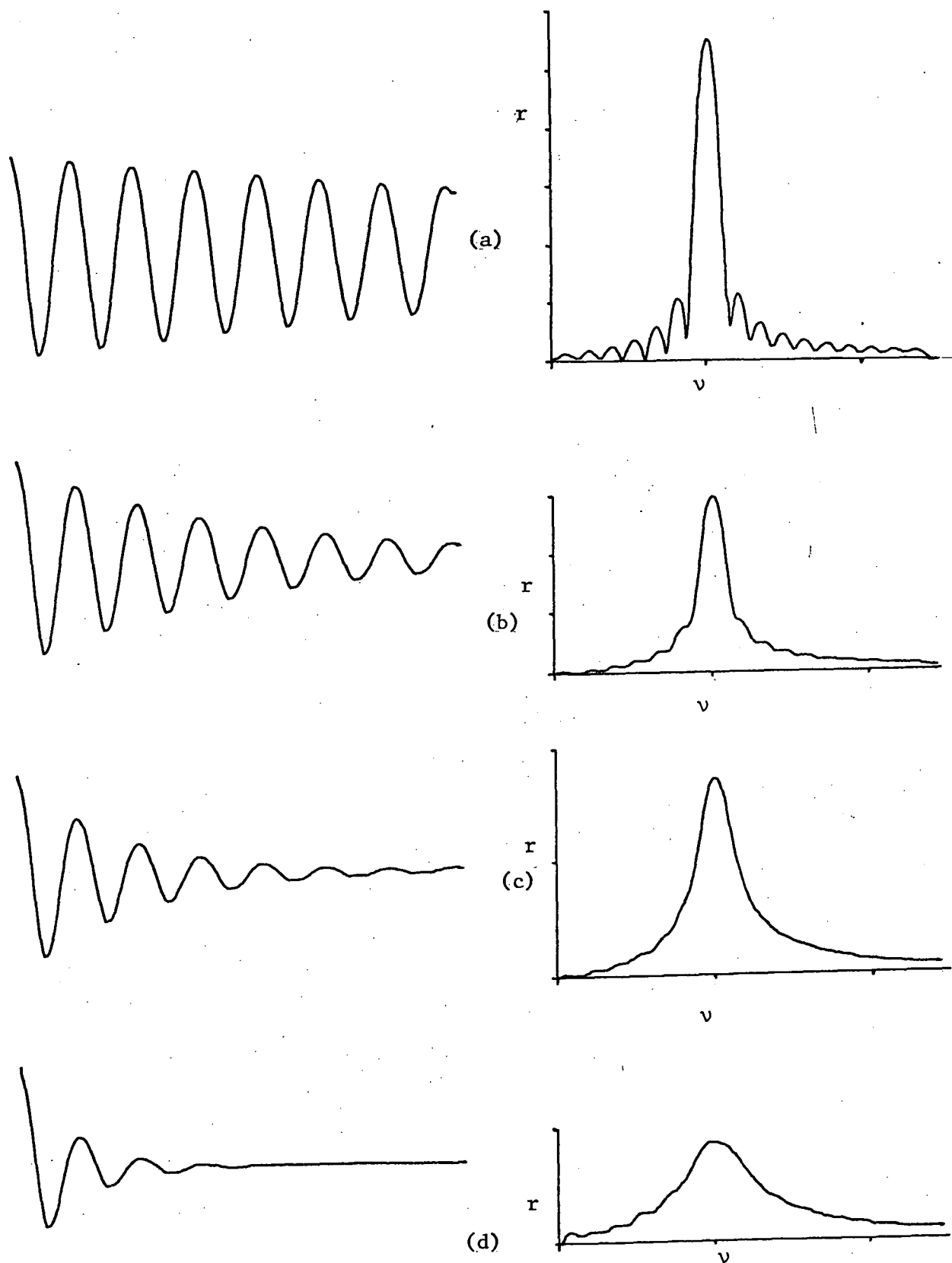


Fig. 4.6 Damped sinusoids and their amplitude spectra.

Cosines (a) - (d) decrease in amplitude by factors of 0.6, 0.15, 0.03 and 0.005 over 7 cycles. Each spectral peak is at the correct frequency, and the corresponding transform gives the correct phase value.

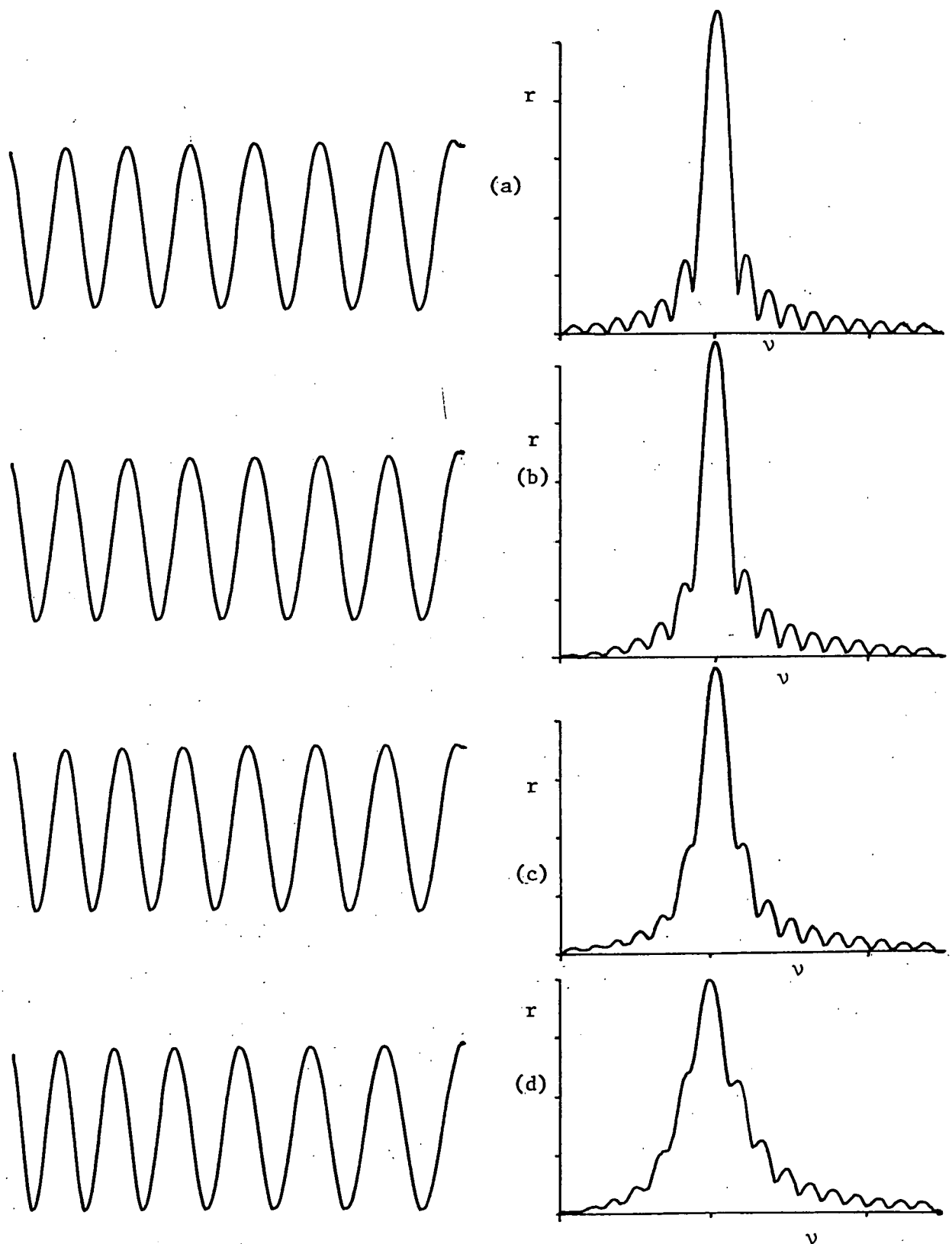


Fig. 4.7. Sinusoids decreasing linearly in frequency and their amplitude spectra. Frequencies in (a) - (d) change by factors of 1.15, 1.30, 1.45 and 1.60 over 7 cycles. Spectral peaks are at the average frequency for the oscillation.

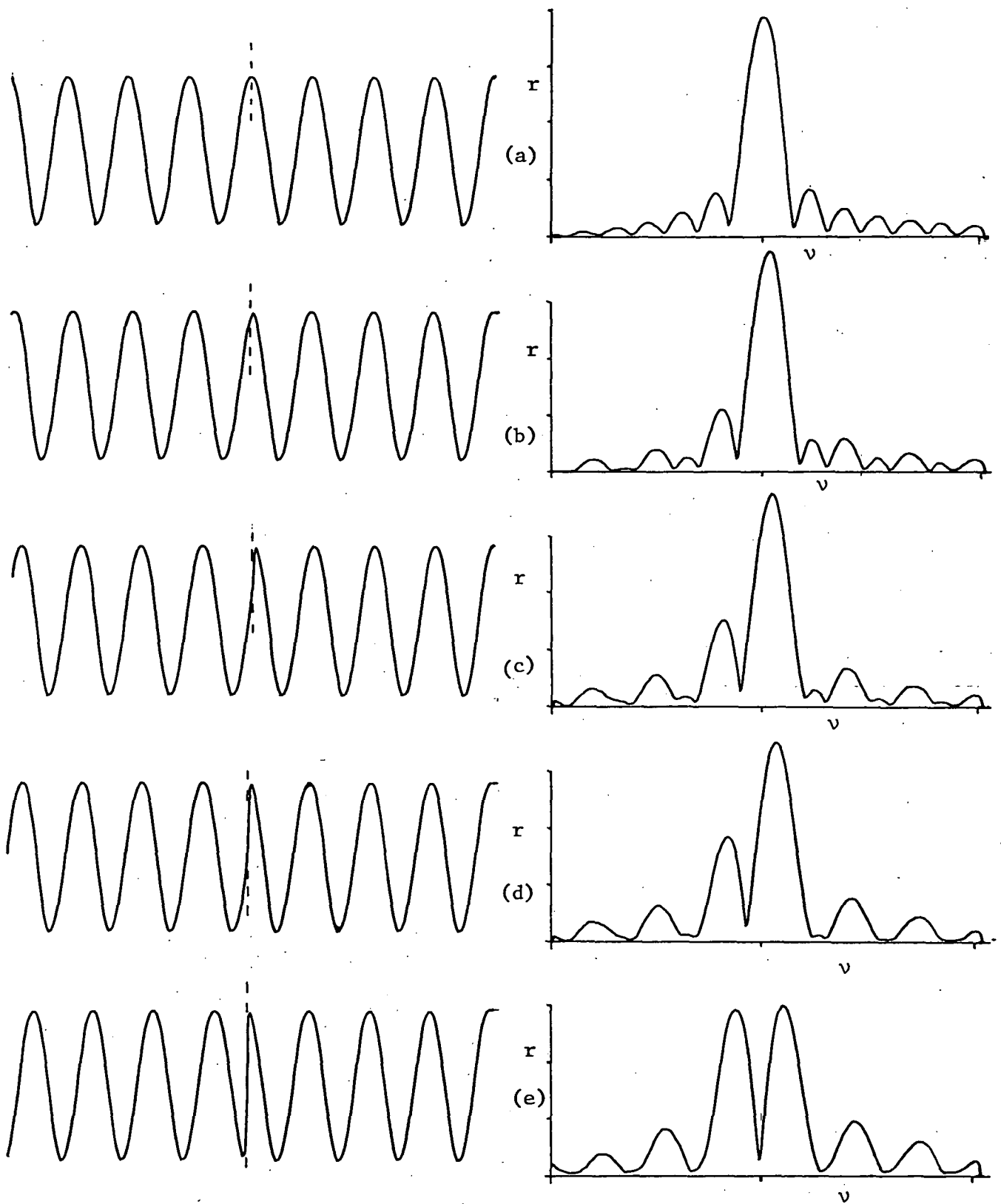


Fig. 4.8. Sinusoids undergo phase jumps and their amplitude spectra. Phase changes for (a) - (e) are  $0^\circ$ ,  $22\frac{1}{2}^\circ$ ,  $45^\circ$ ,  $90^\circ$  and  $180^\circ$  respectively.

## CHAPTER FIVE

### EXPERIMENTAL METHOD

#### 5.1 INTRODUCTION

Most of the experiments listed in this thesis involve the application of a stimulus or treatment, periodic or otherwise, to white clover (*Trifolium repens* L.) and the recording of the leaf movement during and after that treatment. The experiments have some aspects in common. The same means were used for measuring and recording leaf angle in each case. Experiments were performed with whole plants or excised leaves in one of two controlled cabinets. Thirdly records of leaf movements were in general processed in a similar fashion. Such general features of experimental method shall be described in this chapter. Techniques or approaches unique to particular experiments will be described at a later stage, in association with the actual description of these experiments and the presentation of the results thereof.

The leaf of *T. repens* consists of one terminal and two lateral leaflets, each attached to a common petiole by a short pulvinate stalk. The terminal leaflet was chosen for study as its movements are simpler and more easily monitored than those of the lateral leaflets. Under normal day-night conditions the three leaflets rotate back and forth with a 24 hour period, the terminal leaflet moving through an angle of about  $180^{\circ}$ . As the three leaflets perform these movements simultaneously the state of the terminal leaflet and its pulvinule were taken as indicative of the leaf as a whole.

## 5.2 MEASUREMENT AND RECORDING OF LEAF ANGLE

In the past a number of techniques have been employed for recording leaf and petal movements. A frequent approach has been the use of time lapse photography. The leaf angle is measured manually on each frame and the values recorded (Hoshizaki and Hammer, 1964; Koukhari et al, 1973; Scott and Gulline, 1972). A means of automatically and continuously recording leaf angle in *Phaseolus multiflorus* was used by Bunning (1931) and Bunning and Tazawa (1957). A leaf was attached to a lever arm by a light thread, so that movement of the leaf caused corresponding movements of the lever, which traced a line on a Kymograph drum. Engelman et al (1975) devised a convenient means for recording petal movement in *Kalanchoe blossfeldiana*. A photo-sensitive element was placed under the petals to measure the length of the petal shadows. These measurements were digitalized and recorded on paper tape.

It is obviously desirable to have a means for recording leaf angle that is both automatic and in a form suitable for computer analysis. The devices used in the studies described in this thesis possessed both attributes. The principle of operation of these devices, or 'anglemeters', is shown schematically in figure 5.1 and a single leaflet mounted in an anglemeter appears in figure 5.2.

A fine, semirigid wire (25  $\mu\text{m}$  diameter molybdenum) was attached to the centre leaflet of each clover petiole with low melting point wax so that it extended axially beyond the leaf tip by about 15 mm. The lateral leaflets were excised and the centre leaflet

clamped just below the pulvinule to minimize movement of its axis of rotation. A thicker, rigid gold plated wire loop in the form of an arc of a circle (radius 3 cm) centred on the pulvinule was mounted so that it rotated at one revolution per minute about an axis which was aligned with the axis of rotation of the leaf. At some time during each revolution the wire loop briefly made contact with the fine wire. The curvature of the loop allowed some sideways twisting of the leaf to occur without causing a significant change in the time at which contact was made. Contact between the wires caused some stimulus to the leaf, producing a small, transient displacement of one or two degrees. However, comparison between the behaviour of these leaves and others which were unstimulated showed no modifications to the leaf movements that could be attributed to these stimuli.

The motor rotating the wire loop was synchronised with an 8-bit binary counter, the value of which, at the moment of contact between fine wire and rotating loop, was automatically loaded into a storage register. Further changes to the contents of this register were inhibited for a 10 second interval after each loading so that only the counter value at the initial instant of contact was recorded.

This 8-bit number was a measure of the angular position of the leaf at the time of contact. The counter advanced from 0 to 255 while the wire loop rotated through  $300^{\circ}$  (the maximum range of movement of a leaf), allowing leaf angle changes to be measured to an accuracy of  $\pm 0.6^{\circ}$ . At regular intervals, which could be set manually within the range 1 minute to 10 minutes, the contents of the register were

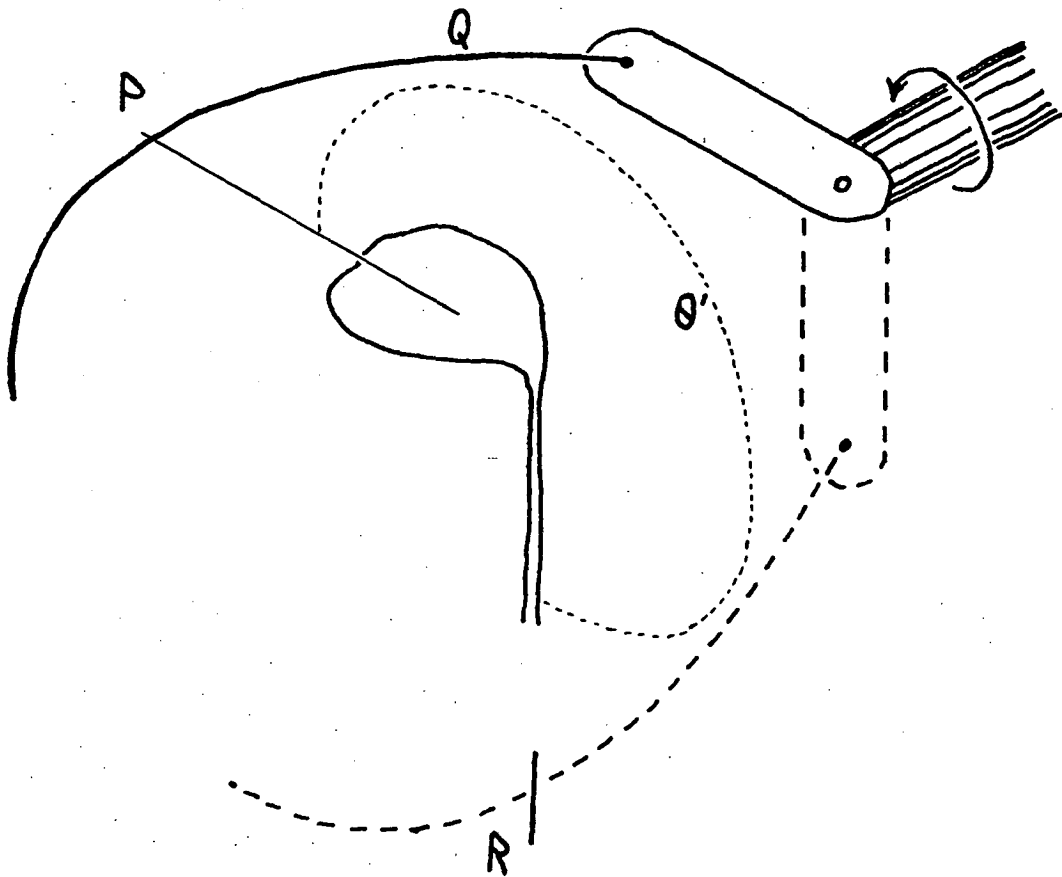


Fig. 5.1. Measurement of leaf angle. The arm Q rotates about the leaf (shown in the open position) at a uniform rate of 1 revolution per minute. The time taken for the arm to move from the reference position R to P, where it makes contact with a fine wire attached to the leaf, is recorded. This time is proportional to the angle  $\theta'$ . Since the convention used is that the leaf angle is small for the open leaf and large for the closed leaf, the leaf angle is defined as  $(360^\circ - \theta')$ .



*Fig. 5.2.* A single clover leaf mounted in an anglemeter is shown. Lateral leaflets have been excised. The rotating arm and the fine wire waxed to the centre leaflet (see fig. 5.1) are clearly visible.



recorded on cassette (Hitachi C90 Ultradynamic or Sony C90), by the method of Robinson (1976). A Teac A160 cassette deck, modified to provide a remote electronic pause control, was used for this purpose.

This method involved transferring the contents of the storage register in serial fashion to the cassette deck via a voltage to frequency converter. Data were thereby recorded as brief bursts of 10 KHz oscillations or as blank sections on the cassette tape. Timing information was similarly recorded on the second channel of the stereo cassette. On playback each set of oscillations were combined to form a rising voltage staircase, each data bit being accepted as a binary one if the staircase reached a certain voltage within a set interval, a binary zero otherwise. The method provided a high noise immunity and an insensitivity to imperfections in the cassette tape recording medium.

Cassettes were a convenient and efficient means for recording and storing leaf angle data. However, to some extent their portability and common use was a disadvantage in that on one occasion a number were stolen from the laboratory, resulting in the loss of data records obtained over approximately a one year period. After this event data records were duplicated and the duplicate cassettes safely stored.

Leaf anglemeters were constructed to record leaf angle data from groups of up to 6 leaves simultaneously, with a common 8-bit counter and motor drive, but separate rotating loop and register for each leaf (see Fig. 5.3). The circuitry used in each anglemeter is shown in Appendix 4. Data derived from all leaf anglemeters were recorded through a common cassette recording system.

Unless otherwise stated leaf angles in experiments described in this thesis were recorded on cassette at 10 minute intervals. Environmental condition data (light, temperature and humidity) were also recorded by transforming the output of each sensor (see section 5.4) to binary form using an 8-bit analog to digital (A/D) converter. At the end of an experiment, typically of a week's duration, the data on the cassette were transferred to a minicomputer for examination and analysis.

At the time of commencement of this project the funds available did not permit the purchase of a minicomputer, which was required for control and analysis purposes (sections 5.4 and 5.6). One was therefore constructed, using a National Semiconductor IMP-16C microprocessor board as the central processor. Construction had some advantages in that the ultimate use for both control and computation could be taken into account in its design.

Leaf anglemeters were initially used by Rust (1974), but were modified and improved in these studies to provide digital output. Rust also examined the possibility of using glues rather than wax to attach the fine wires to the leaflets. These experiments proved unsuccessful as the glues would not adhere to the leaflets for more than 2 or 3 days. The 25  $\mu\text{m}$  diameter molybdenum wire was chosen because it was sufficiently rigid so that a 15 mm length could be held horizontally without curving significantly (see section 5.3.2), yet the wire would bend when pressed by the rotating loop without noticeably affecting the angle of the leaf to which it was attached.

### 5.3 MEASUREMENTS AND RECORDING ERRORS

Errors in the estimation of both absolute leaf angle and leaf angle changes arise from a number of causes. These shall be considered in turn. Since leaf angle changes were considered of greater relevance than knowledge of absolute leaf angle, the measurement technique is orientated toward measuring the former with the greater accuracy.

#### 5.3.1 Absolute leaf angle

Where absolute leaf angle was required this was measured for each leaf at the commencement and also at the completion of each experiment. Angles between stem and leaf base (i.e. the pulvinule angle) and stem and fine wire were determined with the aid of a protractor. The resolutions of each stem - leaf and stem - wire measurement were approximately  $\pm 5^\circ$  and  $\pm 1^\circ$  respectively. Differences between the two measurements were due to the following:-

(a) Curvature of the leaf between pulvinule and point of attachment of the wire. In many cases this was observed to increase marginally during the course of an experiment.

(b) Curvature of the fine wire. The wire was usually deformed to some extent due to the handling required to attach it to the leaf. Further deformation of the wire during the course of the experiment due to repeated contact with the rotating loop was not observed.

(c) Angle of attachment of wire to leaf. Waxing a fine wire onto the centre rib of each leaf was a delicate process and usually resulted in the wire adhering at some small angle to the leaf.

The measurements described permitted the above differences to be taken into consideration so that absolute leaf angles could be estimated from leaf angle records to an accuracy of approximately  $\pm 5^\circ$ . Differences between measurements taken at the commencement and completion of an experiment were noted, and were usually attributed to conformational changes in the leaf itself. Such differences were rarely greater than  $10^\circ$  and were, within the accuracy of the measurements, always such as to suggest that the leaf angle was smaller than was actually the case - i.e. leaf curvature had increased. Such conformational changes were slow (i.e. typically less than  $10^\circ$  per week) and did not affect the study of the oscillatory changes in leaf position, other than to add a slow drift in mean position.

### 5.3.2 Leaf angle changes

Errors in measurements of leaf angle changes may be attributed to the following occurrences:-

(a) Change in curvature of the fine wire with leaf position. The fine wire used was semirigid and would bend due to its own weight if held horizontally. However, for a 3 cm unsupported length the wire sag was no greater than  $1^\circ$ . Thus for large changes in leaf angle ( $90^\circ$  to  $270^\circ$ ) the maximum resulting error was  $2^\circ$ . Since leaf movements were generally through much smaller angles ( $< 100^\circ$ ) the errors due to wire sag were correspondingly less.

(b) Imperfect contact between fine wire and rotating loop. Poor conduction between wire and loop occasionally resulted in a delay after initial contact before the counter value was loaded into the

corresponding register. This was an intermittent source of error which could usually be detected if present in leaf records. In addition the high sampling rate (1 per 10 min.) allowed for the adjustment of individual points that were obviously not in sequence with adjacent points. Thus errors due to poor electrical contact could, to a large extent, be corrected.

(c) Quantization error. The conversion of a signal varying continuously with time into digital form has two aspects. These are sampling and quantization. Problems arising due to sampling concern aliasing and were discussed in the previous chapter. The quantization of a signal, i.e. the subdividing of the signal into discrete intervals or values, contributes a small amount of noise to the original input. Quantization increases the variance of the signal by  $q^2/12$ , where  $q$  is the quantization interval (Otness and Enochson, 1972, p.52). This places a lower limit on the size of small amplitude variations which may be detected. The quantization step in these measurements was  $1.2^{\circ}$  and thus the contribution of quantization noise to each digitized signal was in general negligibly small.

The quantization interval is of particular importance when the statistical properties of a signal are required (e.g. probability distribution, variance, skewness). Just as there is a sampling theorem which describes the relationship between the frequency properties of the signal and the sampling period, so there is a quantization theorem describing the relationship between the signal's amplitude properties and the quantization step (Soucek, 1970, pp 341-345). However, since these studies concern the frequency content of leaf

records rather than their statistical properties, the  $1.2^{\circ}$  quantization interval used was considered adequate.

(d) Recording errors. Leaf angle and cabinet condition data were occasionally incorrectly recorded due to imperfections in the cassette tape recording medium. This again was an intermittent source of error which on average might result in one 8-bit word in one thousand appearing corrupt on playback. Regular cleaning of the cassette deck recording head assisted in minimizing this source of error. In addition since these were usually obviously not in sequence with adjacent data values they could be adjusted before the data were analysed (see section 5.6).

#### 5.4 CONTROL OF PLANT ENVIRONMENT

Leaf anglemeters and clover plants were placed in cabinets of size 4.5' x 1.5' x 1.5' (fig. 5.3). Cool air (typically at  $10^{\circ}\text{C}$ ) was supplied to each cabinet by an external cooling system. This entered across heating elements and was circulated by a fan. The relative proportion of recirculating air to cool air entering each cabinet was manually adjustable. The cabinets were each illuminated by 2 40W incandescent and 8 40W fluorescent tubes. Power supplied to the lights was controlled by silicon controlled rectifiers, using a circuit by Laletin and Erdman (1964). By this means the fraction of each AC cycle for which the fluorescent arcs were struck could be altered, allowing the light intensity to be varied continuously from approximately zero up to the maximum light output of the tubes. Dissipation from the heating elements was controlled in a similar fashion (see Appendix 4).

Cabinet conditions were monitored by light intensity, temperature and relative humidity sensors. These were mounted in each cabinet adjacent to each leaf anglemeter (fig. 5.3). The light and temperature sensors were incorporated as feedback elements in the light and temperature control systems to minimize any disturbance in these parameters, and to linearize the response of the controls to changes in the feedback loop reference levels (see chapter 3.2). A schematic diagram of the arrangement is shown in figure 5.3 and circuit diagrams for the control and sense circuitry in Appendix 4.

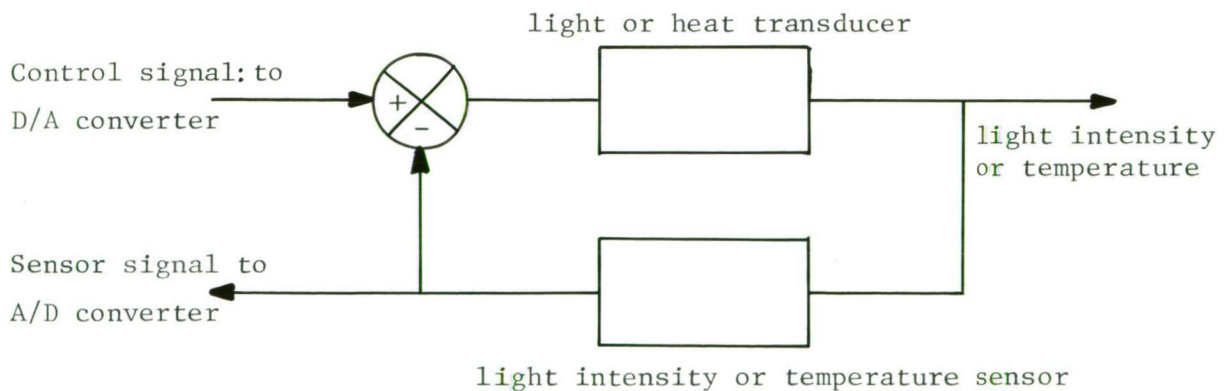
Light intensity and temperature were under minicomputer control and could be kept constant or varied as desired by program within ranges of 0 to 10,000 lux and 12°C to 32°C respectively. The reference voltages were effected by the minicomputer via 10 bit digital to analog (D/A) converters, permitting the reference levels to be varied over their full ranges in 1024 steps. The relationship between light intensity and reference voltage was determined using a 'lightmaster' photometer (Evans Electrochemical Ltd., Eng.) and was observed to be approximately logarithmic over a large part of the light intensity range. The calibration curves relating light intensity and temperature to the corresponding reference voltages are shown in Appendix 4.

Temperature was maintained at 20°C for all light and chemical treatments described in this thesis. The accuracy with which it could be controlled was affected to some extent by the thermal inertia of each cabinet. With the cabinet empty the mean temperature

(a)



(b)



Fib. 5.3 (a) Leaf anglemeter mounted in a controlled cabinet. Cabinet light, temperature and humidity sensors are fixed to a pivoted arm which is attached to the rear wall of the cabinet. The anglemeter is shown monitoring the angular positions of six leaves. (b) Schematic diagram of the feedback loops in each cabinet, installed to minimize disturbances in light intensity and temperature (see text).



varied slowly over the range  $20^{\circ}\text{C} \pm 0.2^{\circ}\text{C}$  and included a  $\pm 0.2^{\circ}\text{C}$  (15 minute period) ripple due to time delays in the feedback system. Under normal operating conditions (anglemeter and clover plants present) the temperature ripple increased to  $\pm 0.3^{\circ}\text{C}$  (20 min. period). Two factors affecting the  $\pm 0.2^{\circ}\text{C}$  variation in the mean level were day-night changes in the temperature of the cold air supply, and changes in the intensity of the light falling on the temperature sensor in each cabinet. The relative humidity was not controlled, but in general this remained within the range  $70\% \pm 5\%$ .

An interrupt signal was supplied to the minicomputer at one minute intervals, upon reception of which the minicomputer would examine the required light and temperature levels for the cabinets and adjust them if necessary. The cabinet conditions were also periodically sampled by the minicomputer through a 16 channel multiplexed 10-bit analog to digital converter. Failure or aberrant behaviour of the control circuitry could thereby be detected and a warning given to the experimenter. The sample values were also passed through a D/A converter to a dotting chart recorder, providing a record of the light, temperature and humidity variations during the course of an experiment. The control and recording apparatus is shown in figure 5.4 while a block diagram of the total system is given in figure 5.5.

## 5.5 PREPARATION OF MATERIAL

Clover plants were grown from cuttings in 10 cm plastic pots, the cuttings having originated from the same clone. The growth medium was either potting soil, with the addition of a complete fertilizer ('U.C. 1 mix') or dolerite gravel, watered with Hoagland's solution (see table 7.1). Plants were exposed to daylight until the

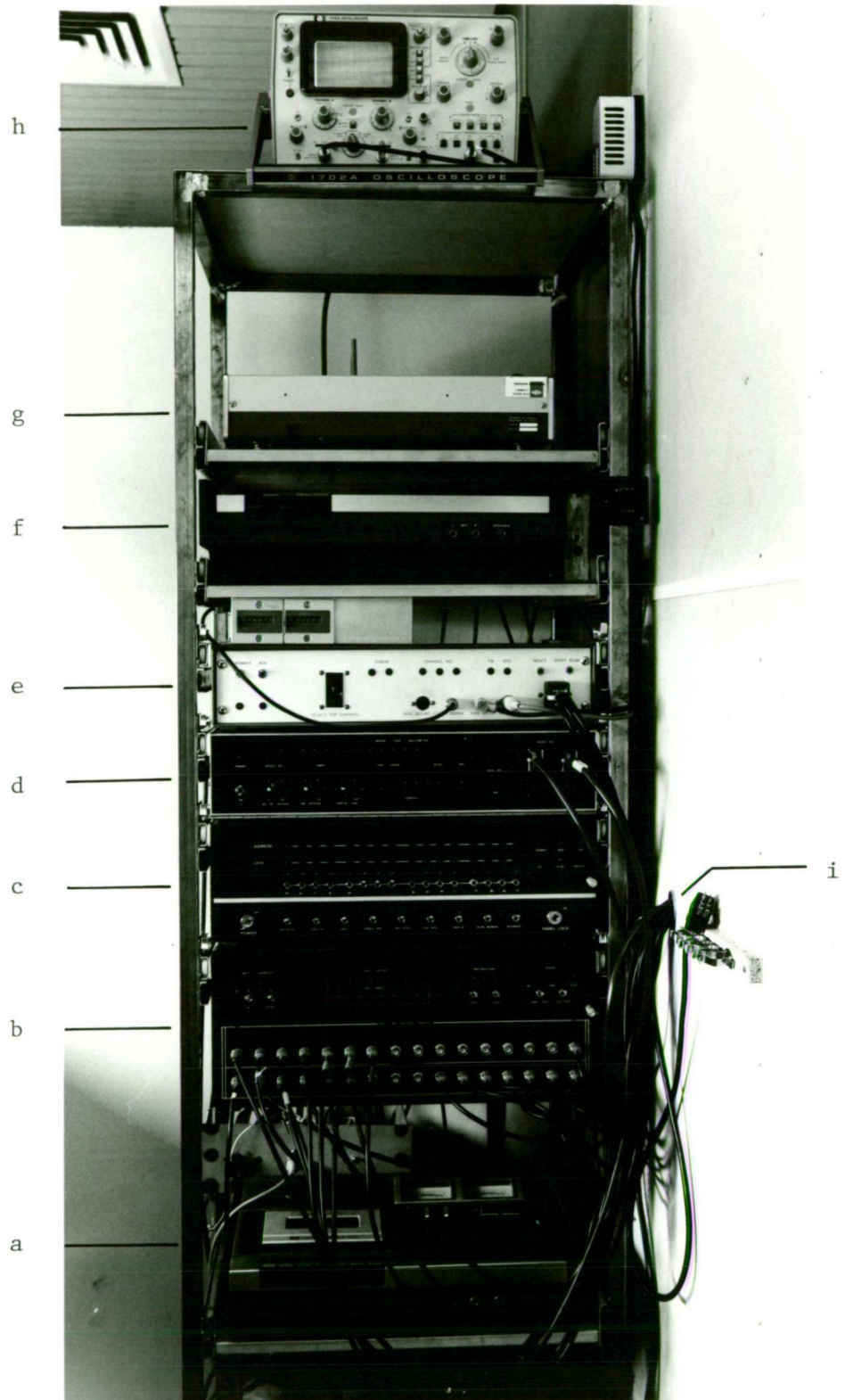


Fig. 5.4 Rack mounted equipment used in the studies described in this thesis.

(a) and (f) Cassette decks for recording and playback respectively.

(b) 16-channel A/D and D/A converter. (c) Minicomputer. (d) and (e) Apparatus for storing and recording leaf angle and cabinet condition data.

(g) Chart recorder. (h) C.R.O. display. (i) Connections through to cabinets and leaf anglemeters.



commencement of each treatment, at which time they were transferred to the controlled cabinets. For treatments involving periodic light variations the first cycle of the light change was synchronized with the day-night variation to which the plants had previously been exposed. A pretreatment period of up to 3 days was allowed before leaves were mounted in anglemeters. The central leaflet on the second fully open leaf on each shoot was used in most experiments. The lateral leaflets were excised so that they did not interfere with the movement of the central leaflet or with the operation of the anglemeter.

Leaves remained attached to the plants for light and temperature treatments while excised leaves were used in chemical treatments, chemicals being supplied to the leaf through the cut end of the petiole. In these cases each leaf stalk was passed through a small aperture in a one inch diameter perspex tube containing the solution required for the particular treatment. The perspex containers were connected by thin plastic tubing to several feeder flasks. The medium bathing the leaf stalks could thus be changed during the course of an experiment by adjusting Hoffman clamps attached to each plastic tube.

## 5.6 ANALYSIS OF LEAF RECORDS

Analysis of data was effected in two stages:-

(a) Preprocessing. The data for a particular experiment was transferred from cassette to minicomputer memory and sorted into leaf and environmental condition records. These were examined by displaying each on an oscilloscope screen, via a D/A converter.

Records relating to constant environmental parameters were discarded. Leaf records that were incomplete or disjointed due to electrical or mechanical failure (e.g. fracturing of the fine wire) were also rejected. Individual 'wild points' (Otness and Enochson, 1972, p.56) in leaf records, due to poor electrical contact or recording errors, were adjusted by program by averaging the preceeding and following values. Several such points in sequence were adjusted by manually altering the contents of the memory locations containing these values. The records were then transferred sequentially to magnetic cassette. Each record set constituted a file for a particular experiment. A chart record of the contents of each file was also made.

(b) Spectral analysis. Initial development of analytical techniques (Rust, 1974) and earlier analyses of records were performed in Algol on an Elliot 503 computer. Files were copied onto paper tape for input to this machine. Each leaf record was analysed separately using the methods given in chapter 4. A Fast Fourier Transform algorithm was used, each record being extrapolated with zeros to produce the required frequency resolution in the resulting spectrum (see Bergland, 1969).

Operation of the Elliot 503 was discontinued at a critical stage in the project while a new computer was being commissioned. It was therefore necessary to find other means for extracting the spectral information from the data records. The IMP-16C minicomputer, formerly used for control and preprocessing only, was adapted for this function. Later analytical work was therefore conducted in machine code on this minicomputer.

Due to the limited memory space available and little requirement for speed a conventional DFT program was found to be more convenient for these analyses (see Higgins, 1976). The minicomputer transform program produced sine and cosine coefficients plus an amplitude spectrum to whatever frequency resolution was required (typically 0.01 c/d). The amplitude spectrum was scanned either visually or by program to locate the highest peak in each case. The corresponding phase was then determined by examining the adjacent sine and cosine coefficient values.

---

## CHAPTER SIX

### EXPERIMENTAL RESULTS. A : LIGHT TREATMENTS

#### 6.1 INTRODUCTION

In the course of some 50 experiments continuous light, periodically varying light and transient light changes were applied to clover plants in order to determine the characteristics of the clover leaf response to light. The light treatments and results thereof are described in this chapter, along with some discussion. Implications as to the properties of the system controlling clover leaf movement are also briefly considered in each section.

#### 6.2 RESPONSE TO CONTINUOUS LIGHT

Whole plants were pretreated with continuous white light (see section 5.3) of one of the 7 intensities given in figure 6.2 for 2 days. Leaflets of healthy appearance were then positioned in leaf anglemeters (see section 5.2) and leaf angle changes recorded for a 7 day period. Typical records of leaf movements at 4 intensities are shown in figure 6.1.

Noteworthy features of the leaf records were as follows:-

- (1) The circadian frequency decreased with increasing light intensity.
- (2) At higher light intensities leaves seemed to pass a greater proportion of each cycle in the open position than at lower intensities.
- (3) The oscillation appeared more heavily damped at lower light intensities.

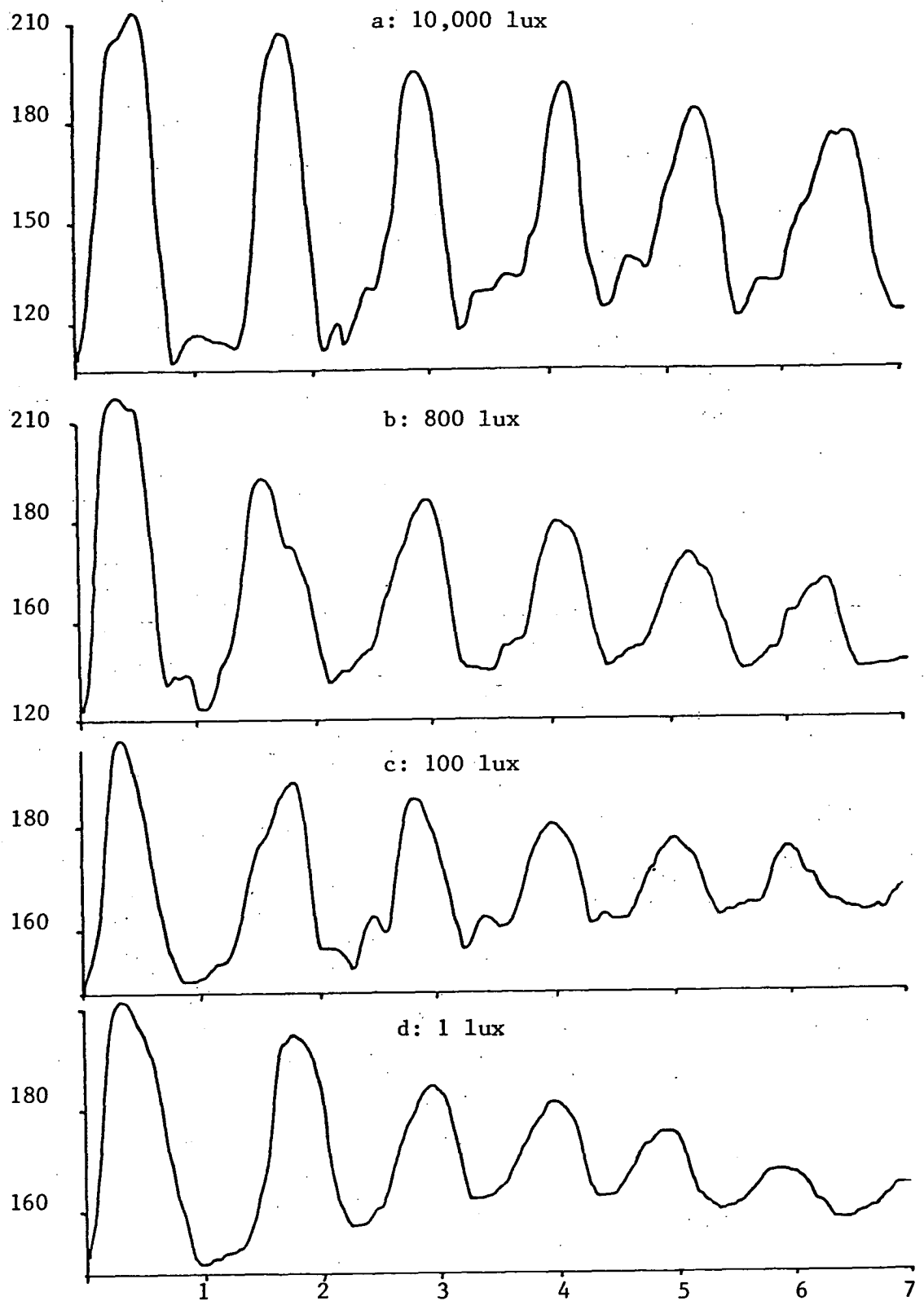


Fig. 6.1. Typical leaf records for the given light intensities. Vertical axis: leaf angle in degrees. Horizontal axis: time in days. See text for description.



These features seem to be associated with many circadian systems as was discussed in chapter 2.

The frequency of oscillation for each leaf was determined by spectral analysis, to a frequency resolution of 0.005 c/d. The means of these values are plotted against light intensity in figure 6.2. The circadian frequency appears to be linearly related to the logarithm of light intensity over a wide range of intensities. The results indicate a relationship approximately described by the equation:

$$v_c = 0.946 - 0.0242 \log_{10} (I + 5.70);$$

where the circadian frequency ( $v_c$ ) is in c/d and the light intensity (I) is in lux. It may be noted that the form of this response agrees with the Weber-Fechner law for biological receptors (Milsum, 1966, p.360), i.e. the outputs of receptors (y) can in general be related to the input stimulus (x) by an equation of the form:

$$y = A + B \log (x + C), \text{ where } A, B \text{ and } C \text{ are constants.}$$

The dependence of the circadian frequency on light intensity is further illustrated by the following experiment. The minicomputer was programmed to generate a light variation such that the logarithm of light intensity increased linearly with time (i.e. the light intensity increased by the same factor in equal intervals of time). The increase was from 1 to 10,000 lux over 8 days. Each leaf record was then divided into overlapping 83 hour (approximately 3 cycle) segments as illustrated in figure 6.3. The mean frequency of oscillation in each segment was estimated by spectral analysis, and the

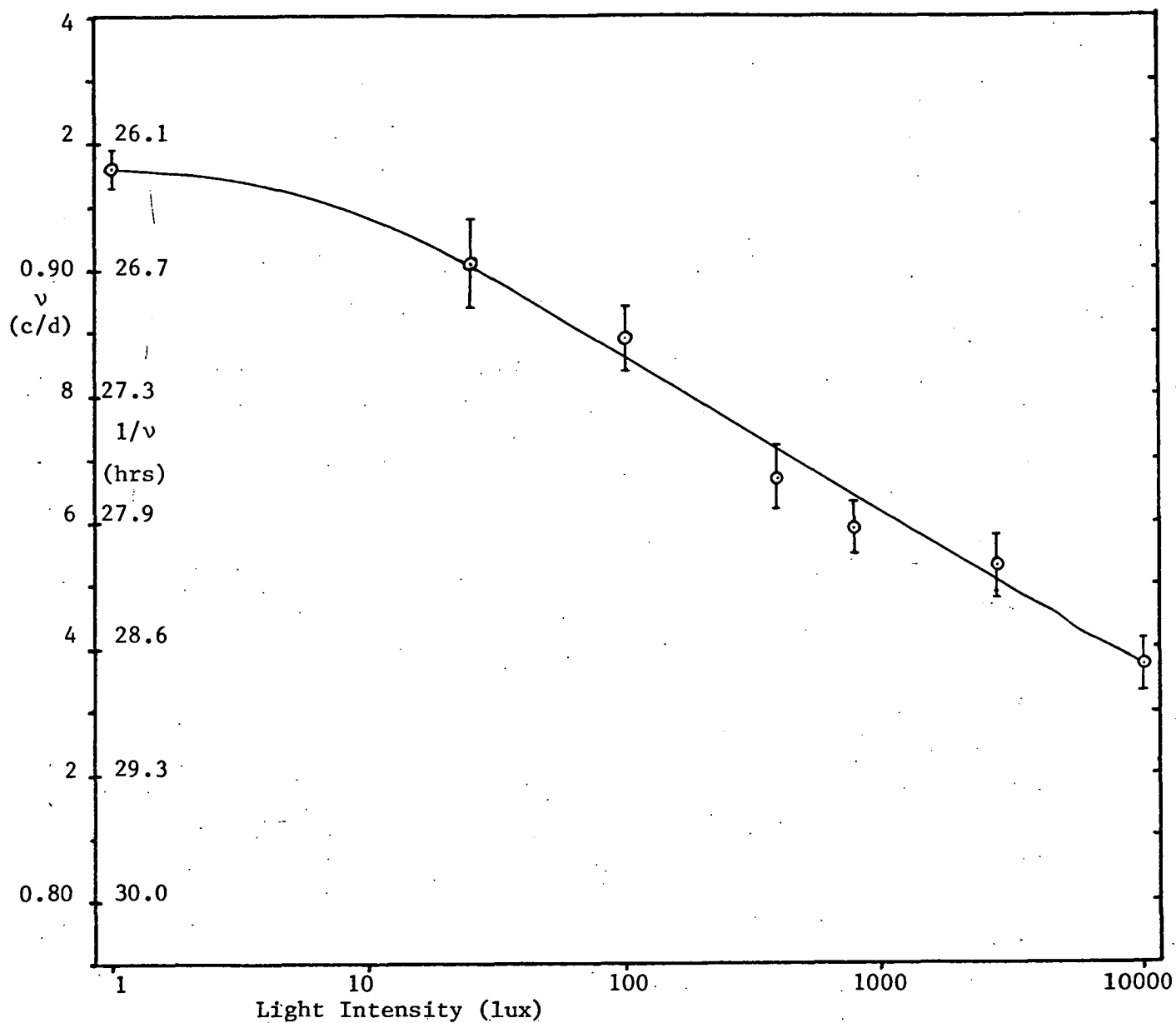


Fig. 6.2 Frequency of leaf oscillation plotted against light intensity.

Bars are standard error bars for from 5 to 8 leaves. Period ( $1/v$ ) in hours is also shown.

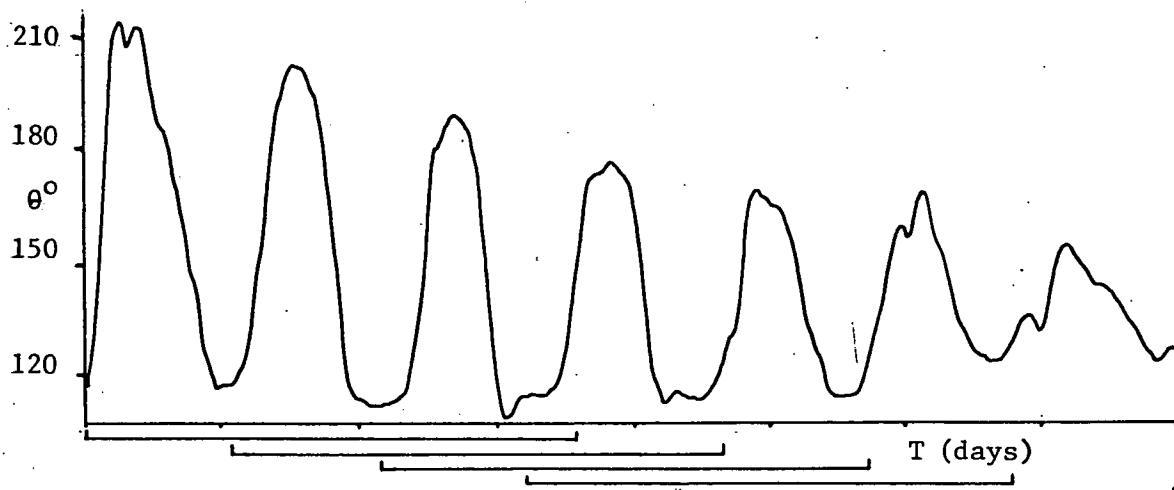


Fig. 6.3. Leaf record for a leaf treated with a light ramp. Each such record was divided into overlapping 83 hour segments as shown. The mean frequency of oscillation for each segment was determined by spectral analysis. See text for explanation.

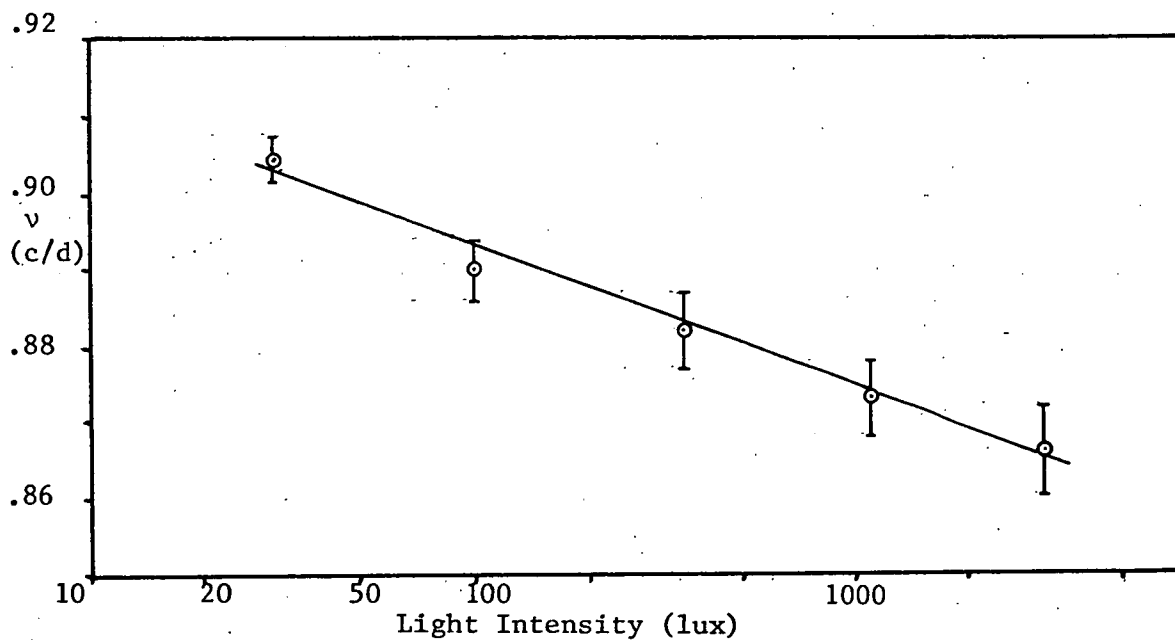


Fig. 6.4. Mean frequency plotted against mean light intensity for an upward sloping ramp change in light intensity (1 - 10,000 lux) over 8 days. Bars are standard error bars for 5 records.

frequencies of the corresponding record segments for each of the 5 leaf records in the experiment file were averaged. The geometric mean of the light intensity for each segment was also calculated. The results are shown in figure 6.4 and these clearly show a decrease in the mean frequency of oscillation during the course of the experiment. The slope of this graph is  $-0.0201$  ( $\pm 0.0040$  s.e.) compared with  $-0.0242$  ( $\pm 0.0045$  s.e.) for the graph from plants in constant light.

For control purposes a similar analysis was also performed on the records obtained from leaves under the constant light conditions of the previous experiment. These analyses did not reveal significant variations in frequency in these leaf records.

To illustrate the relationship between light intensity and the proportion of each cycle where the leaf is in the open position, the following procedure was applied. The mean of the second recorded cycle in each leaf record was determined. Time intervals above and below this mean were measured for the cycle and the ratio calculated. The ratios for each file were then averaged. These are plotted in figure 6.5a. An upward trend in the time open/time closed ratio with increasing light intensity is clearly evident. The averages for the mean leaf positions for each second cycle were also plotted (figure 6.5b). A downward trend in mean leaf position is apparent in these. That is, the mean position for the leaf oscillation moves toward the open state with increasing light intensity, while the proportion of each cycle passed on the open side of this mean increases. This may be observed as an increase in the asymmetry of the leaf oscillation with increasing light intensity (see fig. 6.1).

The variation in damping rate with light intensity was estimated by determining the amplitude of the sinusoid of best (least squares) fit to the second and fifth cycle of each record. Damping coefficients were then calculated on the assumption of an exponential decay. The mean damping coefficient is plotted against light intensity in figure 6.6. The coefficient decreases markedly with increasing light intensity. The results indicate that at 1 lux the natural oscillation will damp to one half of its initial value in 2.5 days, while at 10,000 lux a similar decrease in amplitude requires 6.5 days.

Simple mathematical models of oscillations with properties such as decreasing frequency and increasing asymmetry with increasing input-level are easily developed. Consider, for example, the simple harmonic oscillator shown in schematic diagram form in figure 3.5. If positive feedback is included around one integrating element the oscillation will increase in amplitude. The addition of an element which limits the maximum amplitude will result in a stable oscillation with clipped output (fig. 6.7a). Applying a constant input will move the mean of the observed oscillation toward one of the extremes. This will cause increased clipping on that side (i.e. increased asymmetry) and computer simulation indicates that in some models this can result in a decrease in frequency of oscillation.

In an electrical system clipping occurs when the oscillations grow to the limits imposed by the power supply voltage. Such clipping might also be exhibited by, for example, a chemical oscillator, since obviously chemical concentrations cannot become negative.

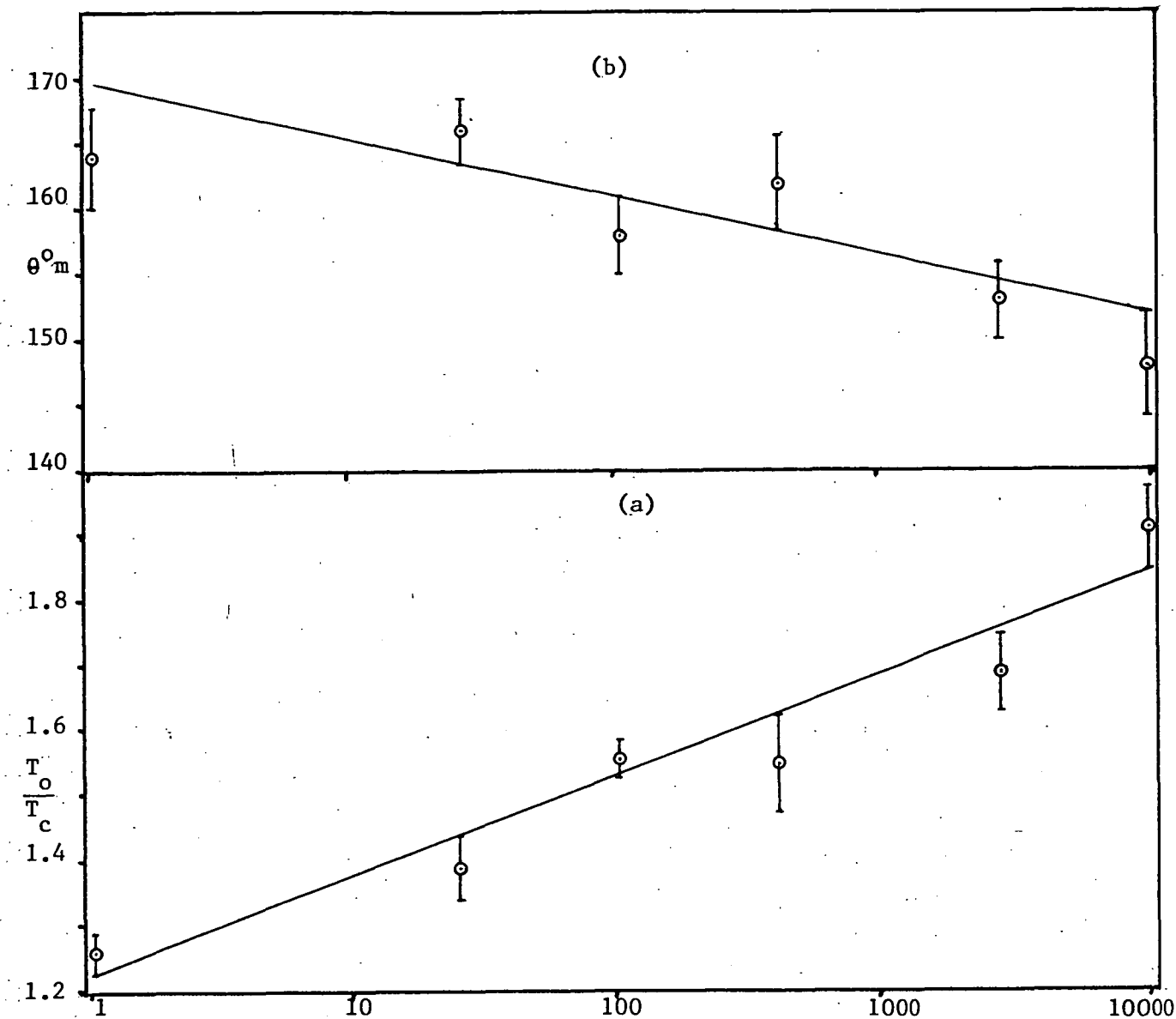


Fig. 6.5. Time open/time closed (a) and mean leaf angle (b) plotted against light intensity in lux. Bars are s.e. bars for from 5 to 8 leaves.

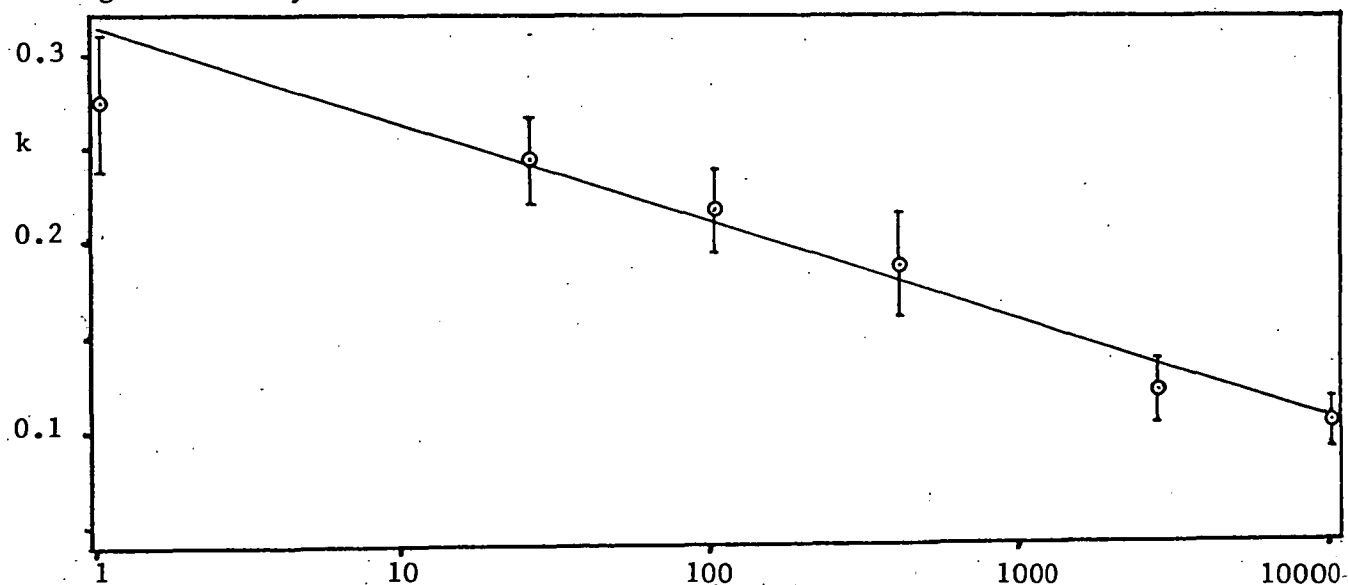


Fig. 6.6. Damping coefficient  $k$ , in  $(\text{days})^{-1}$  plotted against light intensity in lux. Bars are s.e. bars for from 5 to 8 leaves.

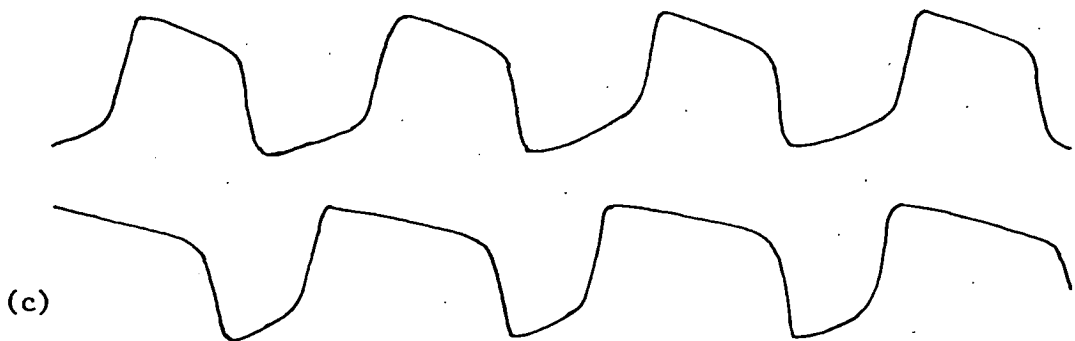
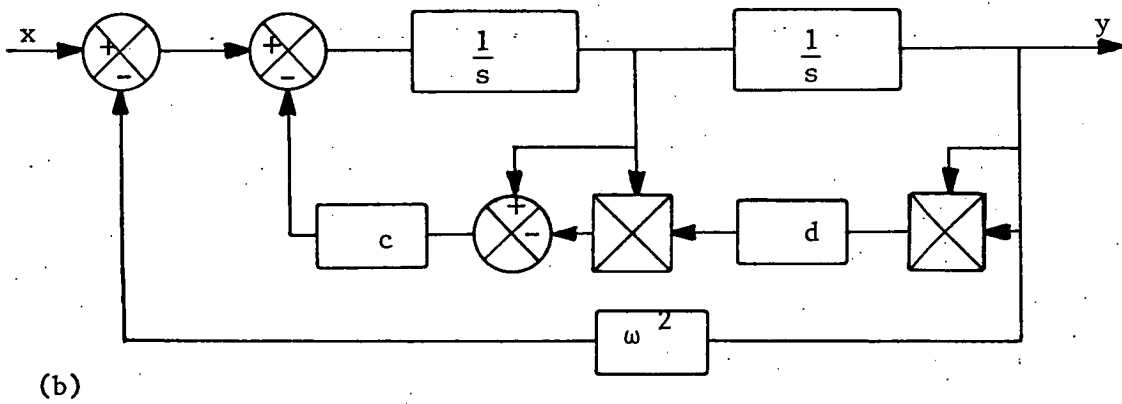
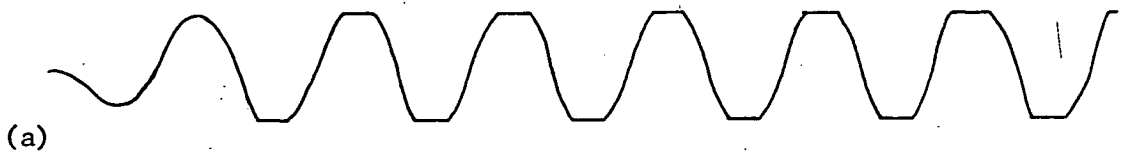
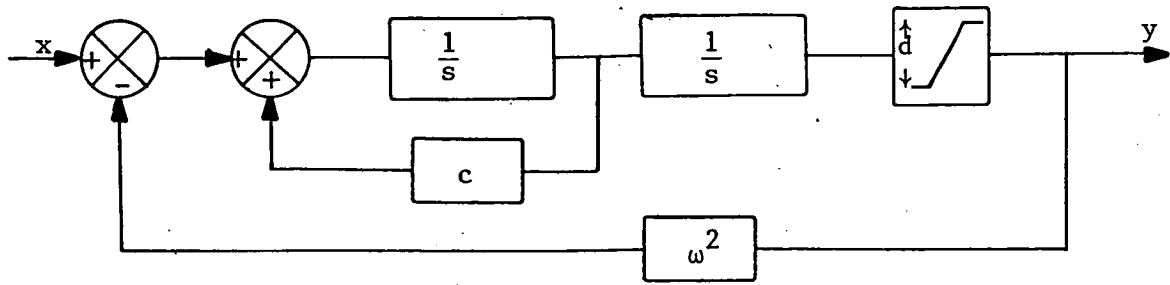


Fig. 6.7(a) Representation of an oscillator with positive feedback of gain  $c$  around one integrator, and with a nonlinear element which limits the amplitude of  $y$  to  $d/2$ . The output for  $x = 0$  is also given.

(b) Representation of a Van der Pol oscillator. Crossed squares represent multiplication. (c) Its output for zero input and for a constant positive input. Note the assymetry and decreased frequency (see text).

Another oscillatory system displaying the above properties is described by the differential equation:

$$\ddot{y} + c(dy^2 - 1) \dot{y} + \omega^2 y = x;$$

- where  $c$ ,  $d$  and  $\omega$  are constants. Such an equation describes a van der Pol oscillator, the properties of which are well documented in the literature (see section 2.4 and Wever, 1965). The equation includes a term which describes feedback around one integrating element, the sign and magnitude of which depends on the value of the output. The system is shown schematically in figure 6.7(b) and its output for zero input and for a constant positive input in 6.7(c).

The above systems exhibit 'limit cycle' behaviour. That is, each system has a set amplitude of oscillation which it will return to after receiving a stimulus which has altered this amplitude. The amplitude of oscillation for the systems in figures 6.7a and 6.7b are essentially determined by the constant  $d$ . It is thus difficult for these systems to simulate damping behaviour in that this requires the value of  $d$  to decrease with time. The characteristics of the circadian oscillator described in this section shall be discussed further in chapter 9.

### 6.3 RESPONSES TO PERIODIC LIGHT VARIATIONS

#### 6.3.1 Rectangular Wave Light Changes

Studies of the entrainment properties of circadian systems have commonly involved 'rectangular wave' light treatments, i.e. the light intensity is periodically switched from one level to another (Aschoff, 1960; Scott and Gulline, 1972). Although the studies



reported in this section primarily concern sinusoidal log-light variations (see section 6.3.2) some rectangular wave treatments were also carried out for the purpose of comparison.

Figure 6.8(b) shows a typical leaf response to a 1 c/d rectangular wave light variation over the range 1 lux to 10,000 lux (a). The light variation was initially of opposite phase to the leaf rhythm. The leaves adapted to the new light phase within 2 light cycles. The amplitude spectrum of the last 5 days of each leaf record contained a multitude of harmonic terms, as might be expected from the waveform depicted by the leaf movement. The first harmonic of each response was approximately in phase with the light variation (phase lag  $10^{\circ} \pm 6^{\circ}$  s.e. for 5 leaves). The mean amplitude of this first harmonic was  $88^{\circ} (+ 5^{\circ}$  s.e.).

Plants were also treated with a 1 c/d rectangular wave light variation over the range 800-2800 lux (figures 6.8(c) and (d). The leaf angle oscillations still had a 'rectangular' appearance as in the first case, but the range of angles through which each leaf moved was greatly reduced and rapid oscillations (frequency 8 to 10 c/d) were also frequently observed. Spectral analysis revealed a mean amplitude for the first harmonic of the 1 c/d rhythm of  $33^{\circ} (+ 3^{\circ}$  s.e.) and a phase lead of  $12^{\circ} (+ 5^{\circ}$  s.e.) for 5 leaves. These responses will be compared with responses for other light variations given later in this chapter (see table 6.3).

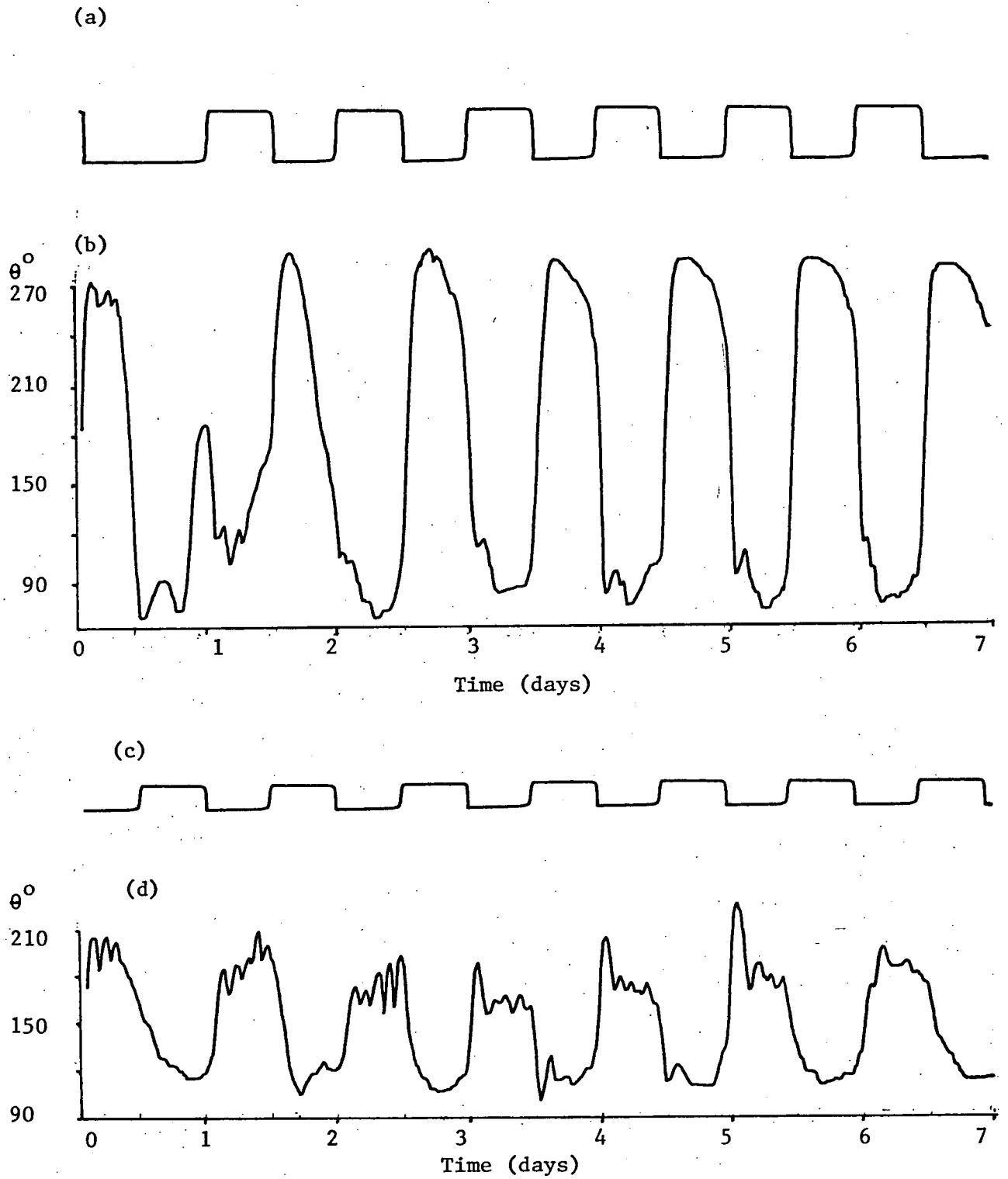


Fig. 6.8. Light variation from 1 to 10,000 lux (a) and an example of leaf movement (b) Light variation from 800 to 2800 lux (c) and leaf movement (d).

### 6.3.2 Entrainment by Sinusoidal Log-Light Variations

Before commencing experiments required for a frequency response analysis of the clover system (see section 3.7) it was necessary to examine the relationship between the amplitude of the input light variation and the leaf response. For this purpose the following experiments were performed.

The minicomputer was programmed to vary the light reference voltage so that the logarithm of light intensity changed in a sinusoidal fashion with a frequency of 1 c/d. A logarithmic variation was chosen because the logarithmic relationship between light intensity and the frequency of the natural oscillation had suggested that the leaves responded to proportional changes in light intensity rather than to absolute changes. This suggestion is supported by results described in section 6.7.

Plants received the above treatment for a total of 8 days, leaf angle changes being recorded for the final 7 days. Light variations over the 5 ranges given in table 6.1 were applied. Examples of recorded leaf movements are shown in figure 6.9 (a-e).

Direct examination of the leaf records showed that the leaves appeared to be fully entrained when the light intensity variations were large (a and b) whereas there was no apparent entrainment when the variation was small (e) and the leaves oscillated at the circadian frequency of about 1 cycle per 28 hours (0.85 c/d). These observations were confirmed in the corresponding spectra (fig. 6.10) where the 1 c/d peak was dominant in Fig. 6.10(a) and (b) and the 0.85 c/d peak

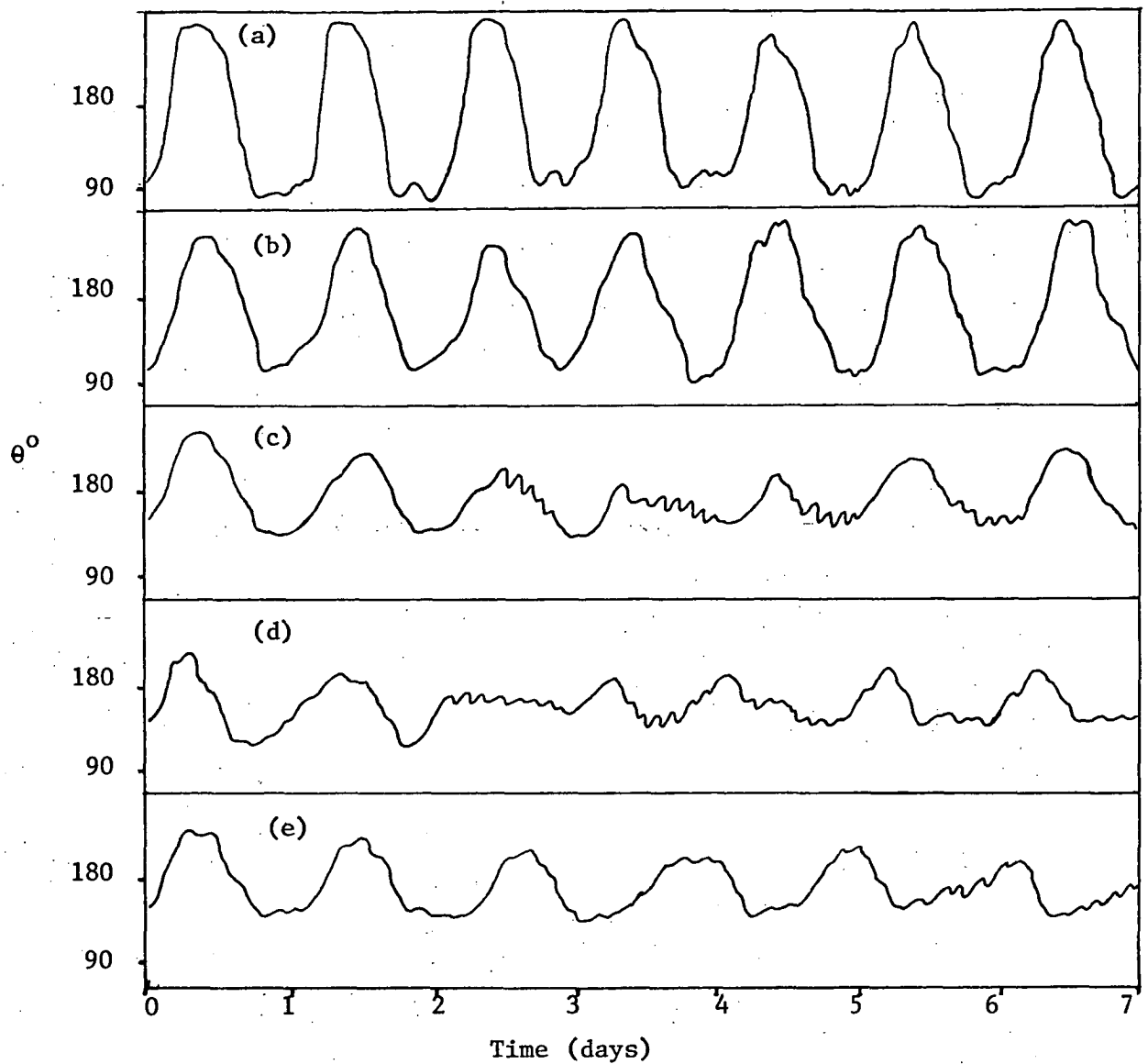


Fig. 6.9. Typical leaf movements for 1 c/d sinusoidal log-light variations over the following ranges: (a) 10-10,000 lux, (b) 400-3700 lux, (c) 800-2800 lux, (d) 1800-2800 lux, (e) 800-1200 lux.

was dominant in Fig. 6.10(e). Leaf movements were less easily interpreted for the intermediate ranges of light variations (Fig. 6.9(c) and (d) but the spectra showed that there were components at both the circadian and forcing frequencies in these cases. In fact it was the interaction between these two components which caused the leaf oscillations to fall in amplitude and then rise again. The frequency of the amplitude modulation cycle was the difference between the two frequencies, i.e.  $(1 - 0.85)$  c/d or approximately one cycle per 6.7 days.

In cases where one peak in a spectrum is dominant it is not possible to establish immediately whether small neighbouring peaks are genuine additional components, or side lobes of the main peak. However this may be clarified by the component extraction technique. By this means it was revealed that there was a significant circadian component in 6.9(b), but not in (a) and a small 1 c/d component in 6.9(e).

Details of the oscillatory components at the circadian and forcing frequencies for a number of leaves with various ranges of light oscillation are summarised in table 6.1. From this table it may be seen that an increase in the amplitude of the light oscillation increases the amplitude of the leaf oscillation at that frequency, with some corresponding fall in the amplitude of the circadian component. A large amplitude light oscillation appears to suppress the circadian component completely. In (d) and (e) of table 6.1 the frequency of the forced oscillation appears to differ significantly from 1 c/d, although in these cases the sample size was very small so the 95% confidence limits are large. If it is a genuine difference

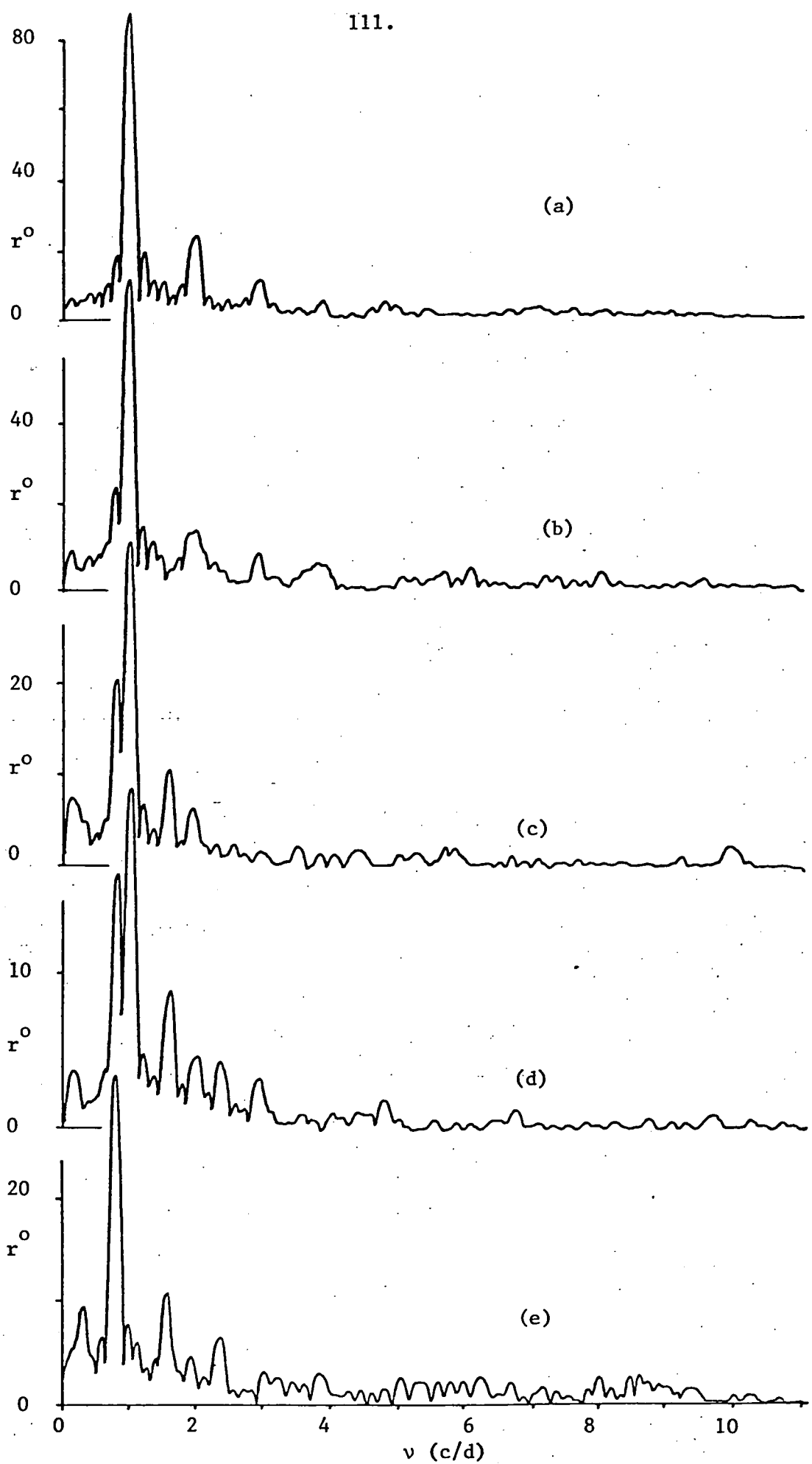


Fig. 6.10. Amplitude spectra corresponding to the leaf movements shown in figure 6.9.

	Light Range (lux)	$\nu$ (c/d)	$r(^{\circ})$	$\phi(^{\circ})$	No. of Records
(a)	1 - 10,000	$1.000 \pm .002$	$79 \pm 4$	$4 \pm 9$	4
		-	-	-	-
(b)	400 - 3,700	$1.002 \pm .004$	$68 \pm 5$	$12 \pm 7$	4
		$.850 \pm .004$	$13 \pm 2$	$-15 \pm 7$	(2)
(c)	800 - 2,800	$1.003 \pm .003$	$30 \pm 4$	$32 \pm 6$	8
		$.856 \pm .003$	$14 \pm 3$	$-3 \pm 6$	(6)
(d)	1800 - 2,800	$1.020 \pm .005$	$20 \pm 4$	$35 \pm 6$	3
		$.836 \pm .005$	$16 \pm 2$	$-14 \pm 3$	(3)
(e)	800 - 1,200	$.980 \pm .004$	$8 \pm 1$	$27 \pm 15$	(2)
		$.851 \pm .003$	$24 \pm 4$	$-17 \pm 13$	3
Continuous Light (10,000 lux)		$.847 \pm .004$	$38 \pm 3$	-	7

Table 6.1. Frequency, amplitude and phase for the fundamental circadian and forced components in the leaf oscillation. Numbers in brackets are the number of records containing both circadian and forced components. Results for continuous bright light are also given. Values are means  $\pm$  standard errors. Phases are relative to the phase of the light oscillation at the start of the record.

it may be due to the leaves not locking fully to the small amplitude light variation. Application of the technique for estimating the corruption influence of adjacent peaks (Chapter 4 and Appendix 3) indicates that these would not have caused departures from 1 c/d of these magnitudes.

The phase information indicates that the 1 c/d component of the leaf oscillation is closely in phase with light oscillations of large amplitude but leads by about  $30^{\circ}$  when the amplitude is small. Both the circadian and forced oscillations show higher harmonics whose amplitudes relative to the fundamental fall as the light variation is reduced. Mean ratios of second to first harmonics for both forcing and circadian frequencies are given in table 6.2. It appears that as the amplitude of the forcing signal is decreased, the leaf response more closely approximates that of a linear system. Higher frequency components in the range 8-10 c/d were also frequently found (e.g. 6.9(c) and (d)), particularly at times when the circadian and 1 c/d components were acting antagonistically so that the leaves spent more time in the half open state.

Table 6.3 lists the relative amplitudes of the harmonics in the leaf responses to sinusoidal log-light and rectangular wave light variations over the range 800-2800 lux. Since in the following studies information pertaining to only the fundamental is employed the lesser harmonic content shown for the sinusoidal log-light response is added justification for the use of this input rather than the rectangular wave light variation (see next section).

#### 6.4 FREQUENCY RESPONSE OF LEAF MOVEMENT

Some discussion of signals that may be used to determine the frequency response of a system was presented in chapter 3. It was necessary to consider which signal was most suited as an input to the clover system.



	$H_2^f/H_1^f$	$H_2^c/H_1^c$
a	$0.25 \pm 0.02$ (4)	-
b	$0.20 \pm 0.02$ (4)	$0.60 \pm 0.03$ (2)
c	$0.14 \pm 0.03$ (5)	$0.56 \pm 0.03$ (3)
d	$0.12 \pm 0.04$ (3)	$0.47 \pm 0.02$ (3)
e	-	$0.25 \pm 0.02$ (3)

Table 6.2. Relative amplitude of second harmonic ( $H_2$ ) in the leaf oscillation for both the circadian (c) and forced (f) rhythms for the five light treatments given in table 6.1. Values are means  $\pm$  standard errors. Numbers of leaf records examined are shown in brackets. The mean relative amplitude of the second harmonic for both circadian and forced rhythms decreases with decreasing amplitude of the forcing rhythm.

Harmonic	Relative amplitude	
	(a) sinusoidal	(b) rectangular
2	$0.14 \pm 0.03$	$0.32 \pm 0.03$
3	$0.07 \pm 0.03$	$0.18 \pm 0.03$
4	-	$0.08 \pm 0.02$
5	$0.05 \pm 0.01$	$0.11 \pm 0.02$
6	-	$0.05 \pm 0.02$
7	-	$0.04 \pm 0.01$

Table 6.3. Relative amplitudes of harmonics of the fundamental forcing oscillation for a 1 c/d sinusoidal log-light (a) and rectangular wave (b) input over the range 800-2800 lux. Values are means  $\pm$  standard errors for 5 records in each case. It is apparent that the harmonics in leaf records for (a) are far smaller in magnitude than for (b).

The system controlling leaf movement in clover possesses nonlinear features, as is indicated by the presence of harmonics in the leaf response. In addition, a relatively large proportion of the system output in this case is generated by the system itself, in the form of random and circadian leaf movements, for example. These features make the determination of the system response to a transient input difficult.

An attempt was made to obtain a clover leaf frequency response using a white noise input. This method was soon observed to have the following disadvantage. In order to separate the response to the noise input from the signal generated by the system itself it was found necessary to maintain such a treatment for several weeks (see section 3.9). Over such a period individual leaves will undoubtedly change their oscillatory properties, due for example to ageing.

Although sinusoidal treatments have the disadvantage that a single leaf cannot be studied at a range of frequencies due to its age varying properties, the method is relatively uncomplicated and does permit the maximum resolution of the leaf response to each frequency tested. It was therefore decided that a small amplitude sinusoidal log-light variation was the most suitable input for obtaining a clover frequency response. Accordingly, experiments were conducted in which clover leaves of similar ages (second fully open leaf on each shoot) were treated with a number of frequencies of light variation.

The intensity range 800-2800 lux was chosen for the following reasons. Firstly, the suitability of this range (i.e. forcing

component dominant in the leaf response, and harmonics relatively small) had been indicated by the results of the previous experiments. Secondly, the cabinet light intensity/reference voltage relationship was very closely logarithmic in this range (see Appendix 4).

Clover plants were pretreated with white light, varying with the required frequency, for one day before recording commenced. Leaf movements were then recorded for a 7 day period. Sixteen frequencies in the range  $2/3$  c/d to 20 c/d were applied in consecutive experiments and the movements of from 4 to 8 leaves recorded and analysed for each frequency. Examples of leaf movements are shown in figure 6.11 and the corresponding transforms in figure 6.12.

In general components at both forced and circadian frequencies were observable in the leaf records, the amplitude of the circadian component decreasing with time. This damping was more rapid for forced frequencies closer to the circadian frequency than for those further away. Spontaneous high frequency oscillations were also frequently observed (fig. 6.11(a) and (c)).

The corresponding spectra showed peaks at both the circadian and forced frequencies, with one exception. The spectra for leaves treated with a  $0.833$  c/d ( $5/6$  c/d) variation did not contain a separate, significant circadian component. The circadian component seemed to have been completely suppressed or altered in frequency by the presence of this forcing signal.

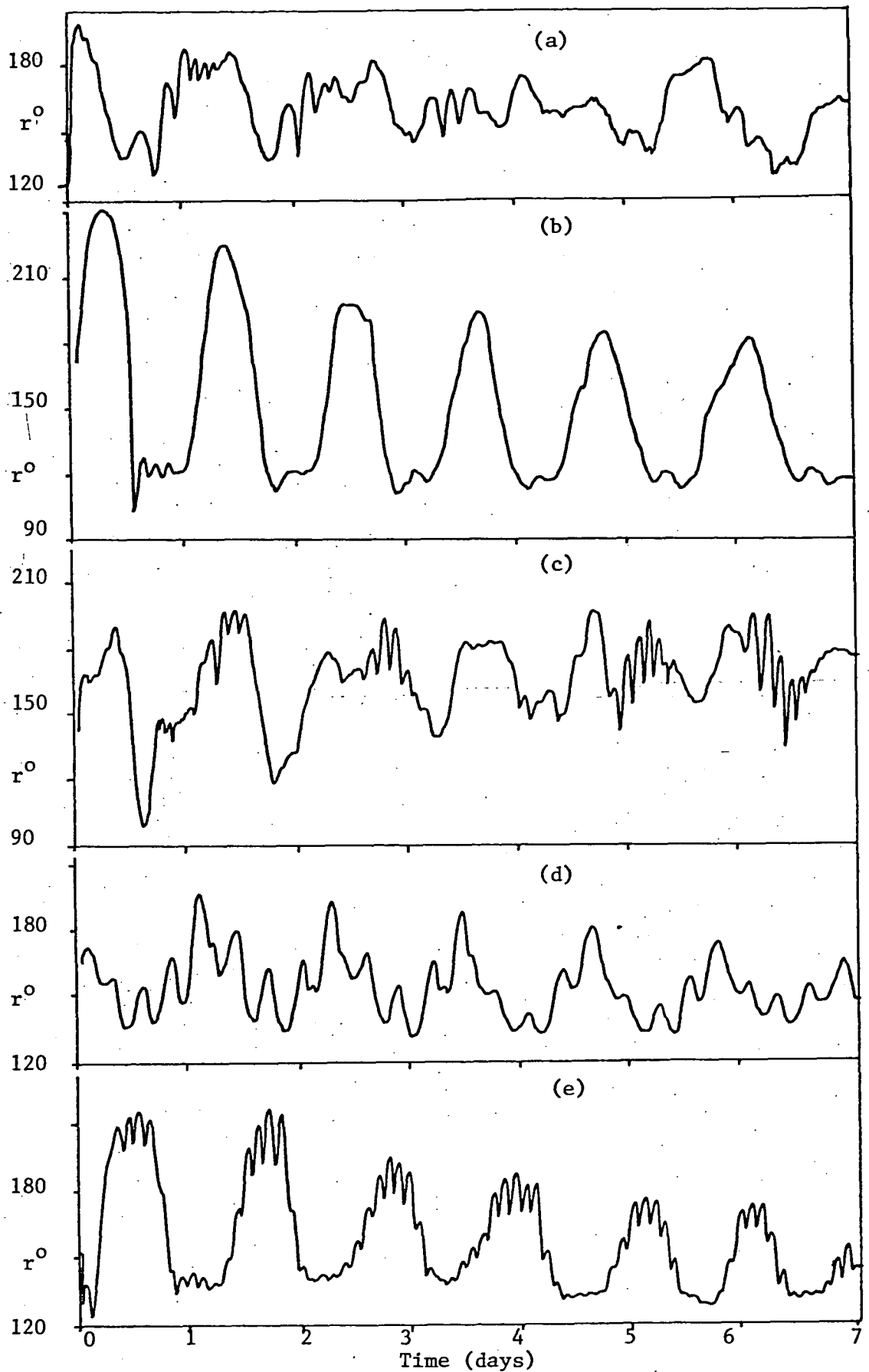


Fig. 6.11. Examples of leaf records for leaves treated with sinusoidal log-light variations over the range 800-2800 lux and at frequencies of 0.67 (a), 0.83 (b), 1.25 (c), 3.33 (d) and 10 c/d (e) respectively.

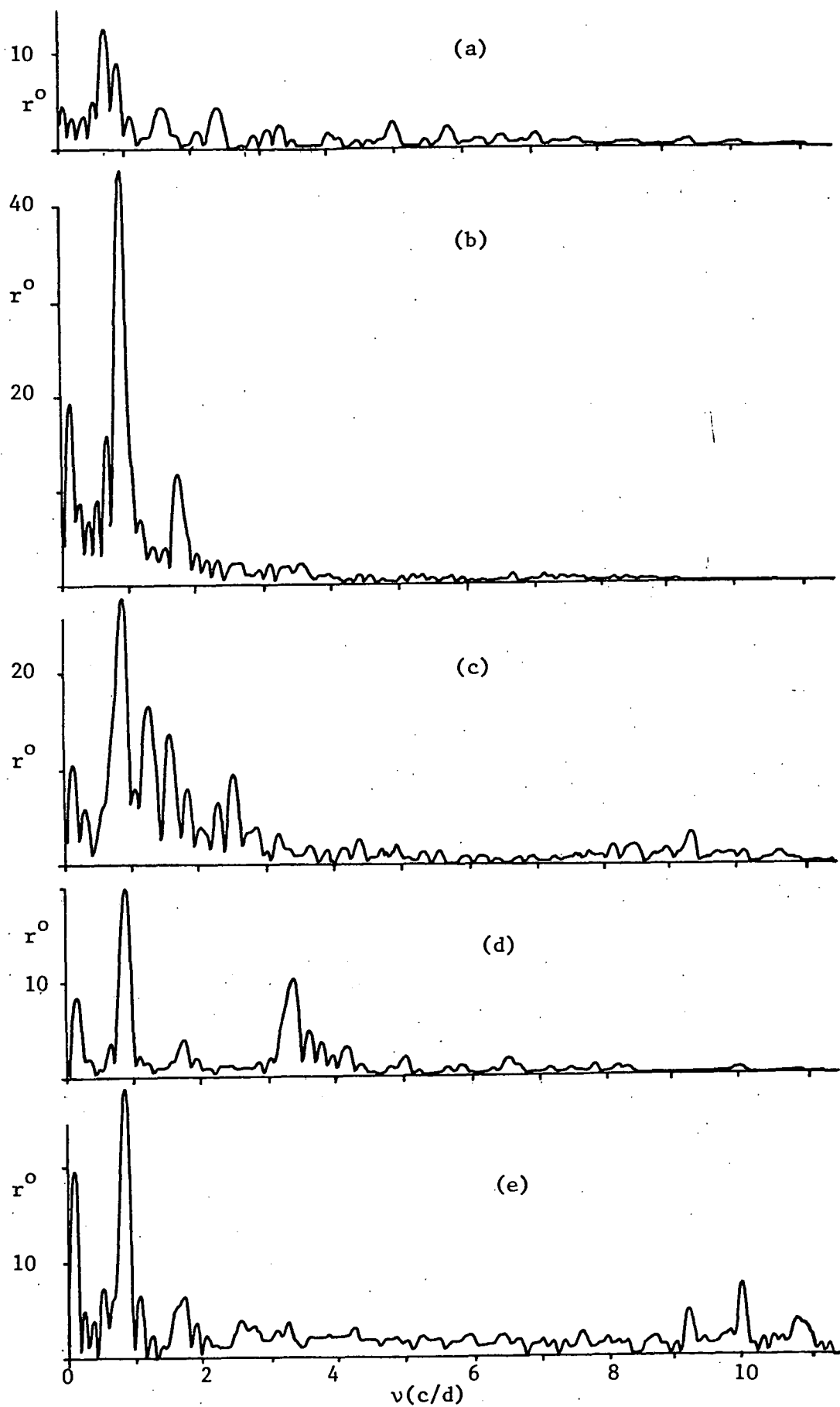


Fig. 6.12. Amplitude spectra for the leaf records given in figure 6.11.

The component extraction technique revealed the presence of spectral peaks at multiples of the circadian and forced frequencies (i.e. harmonics) and also peaks corresponding to the sum and difference of these in many cases (e.g. see table 4.1). Spontaneous high frequency oscillations (frequency 9-10 c/d) were also observed. The frequency of the circadian component was typically about 0.855 c/d (i.e. approximately  $1/28 \text{ hr}^{-1}$ ). The continuous light treatments (section 6.2) indicated a natural frequency in the interval : 0.868 to 0.855 c/d for light intensities within the range 800-2800 lux. For leaves treated with 1.67, 2.5 and 3.33 c/d variations the circadian peaks occurred at a sub-multiple of these frequencies, i.e. at 0.833 c/d (see table 6.3). This may be observed in fig. 6.11(d) where a complete number of cycles of the forced oscillation occupies each circadian cycle. This shift in the natural frequency to a value which is in this fashion commensurable with the forcing frequency is known as frequency demultiplication (see section 2.3) and is a property exhibited by a range of nonlinear oscillatory systems (Pavlidis, 1973, p.94).

The frequency, amplitude and phase of the spectral component corresponding to the forcing frequency in each case are listed in table 6.4. The results are the mean values for the given number of leaves (far right column). Frequencies of peaks in spectra were estimated to the nearest 0.005 c/d. The mean frequencies listed in table 6.4 are not regarded as significantly different from the frequency of the input signal in each case, in general being within one standard error of this value. In some cases (i.e. some records at

2/3, 18 and 20 c/d) the peaks at the forcing frequency were not significantly above the noise level in some spectra. These records were therefore not included in the analysis.

The results in table 6.4 were plotted as separate phase and amplitude graphs, or Bode plots (figures 6.13a and b). The following features may be noted in these response curves. A mean phase advance of  $119^\circ$  occurs at 0.67 c/d. This has decreased to about  $70^\circ$  by 0.86 c/d, which corresponds to a peak in the amplitude plot. Both phase and amplitude change rapidly with frequency in this region. A relatively constant section in the phase plot corresponding to a slowly changing yet still decreasing section in the amplitude response occurs between 3 and 10 c/d. This is followed by a rapid decrease in both amplitude and phase for higher frequencies. The maximum mean phase delay determined was about  $187^\circ$  at 20 c/d. At this frequency the slope of the phase curve is negative and still large in magnitude. The amplitude response curve has a slope of approximately -2 for frequencies greater than about 10 c/d.

## 6.5 DISCUSSION OF MODELS

At this stage the question arises as to whether the observed frequency characteristics may be duplicated by a simple linear model. Consider, for example, the damped simple harmonic oscillator briefly described in section 3.11. The output for this system may be taken from (a) immediately after the comparator ( $\ddot{y}$  in fig. 3.4) or after the first (b) or second (c) integrator ( $\dot{y}$  or  $y$ ). The amplitude response for each of these outputs contains a peak corresponding to a large

Applied $v$ (c/d)	$v_f$ (c/d)	s.e.	$r^0$	s.e.	$\phi^0$	s.e.	$v_c$ (c/d)	s.e.	no.
.667	.675	.006	13.9	1.8	119	17	0.861	.004	4
.769	.772	.004	15.9	1.5	111	16	0.858	.005	5
.833	.837	.003	48.1	1.4	86	10	0.833	.003	6
.909	.910	.003	39.3	1.9	44	6	0.850	.005	5
1.000	1.003	.003	29.9	4.1	32	6	0.855	.005	8
1.250	1.248	.004	17.8	1.9	-8	11	0.853	.003	5
1.667	1.670	.005	19.7	0.9	-33	11	0.833	.003	6
2.000	1.996	.006	15.4	1.1	-51	20	0.855	.005	5
2.500	2.500	.003	14.4	1.1	-66	8	0.834	.004	7
3.333	3.328	.006	11.0	0.9	-60	4	0.834	.004	5
5.000	4.998	.004	10.5	1.5	-52	12	0.850	.007	6
6.667	6.668	.005	9.5	0.7	-63	9	0.845	.008	4
10.000	10.004	.005	9.0	0.9	-79	13	0.856	.007	6
15.000	14.900	.008	3.4	0.4	-151	15	0.860	.006	5
18.000	17.998	.010	2.4	0.4	-178	16	0.855	.006	4
20.000	19.980	.013	1.9	0.5	-187	18	0.859	.005	4

Table 6.4. Frequency response data for clover plants treated with sinusoidal log-light oscillations over the range 800-2800 lux.

Both the applied frequency and the frequency of the leaf response ( $v_f$ ) determined from the amplitude spectrum are shown. The frequency of the spectral component corresponding to the circadian rhythm ( $v_c$ ) is also given.



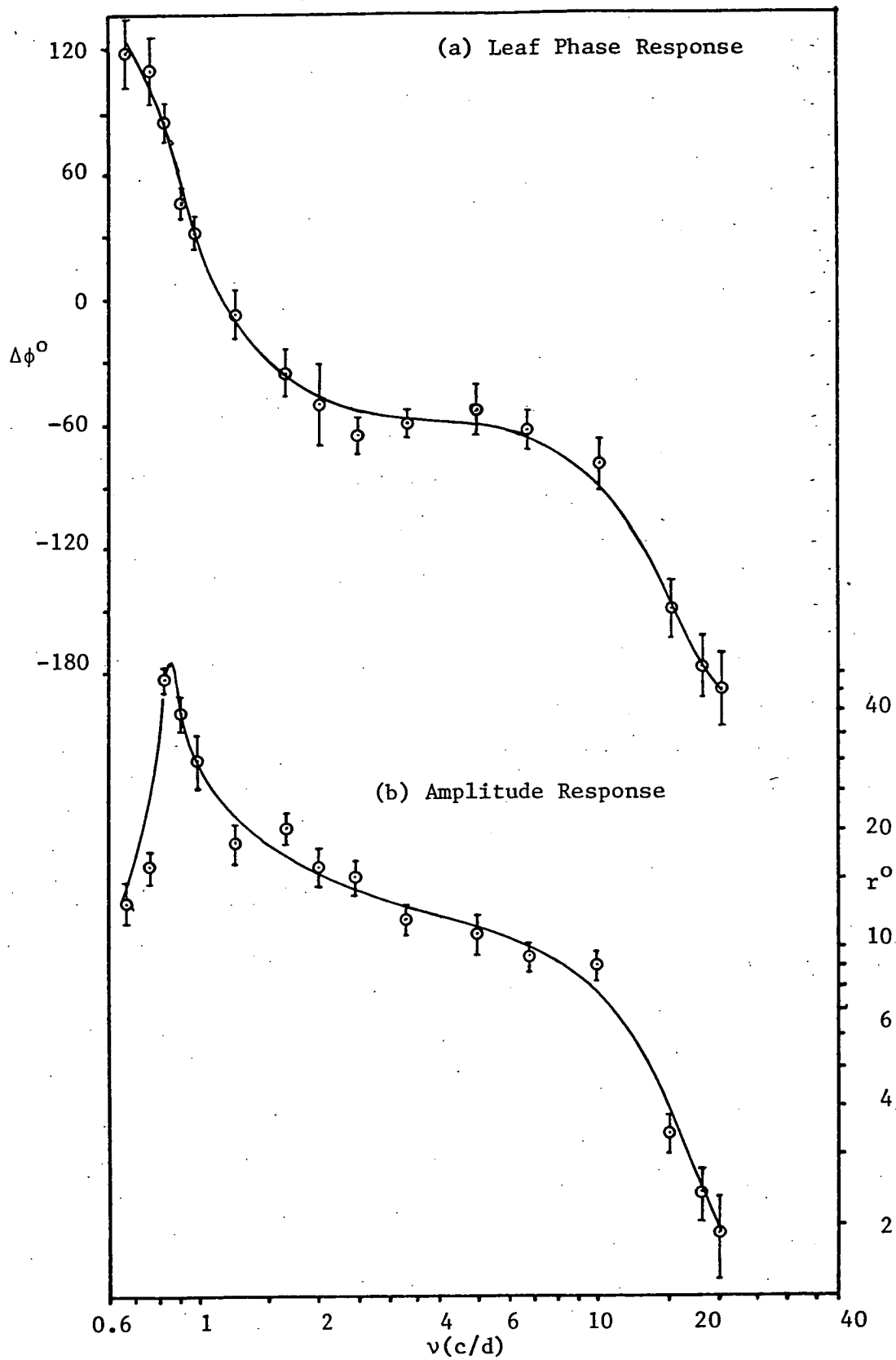


Fig. 6.13. Bode plots showing the clover leaf response to sinusoidal log-light variations of different frequencies. See text for description.

negative slope in the phase plot, and it may readily be shown from the transfer functions for these cases that amplitude response peaks occur at relative phases in the vicinity of  $+90^\circ$ ,  $0^\circ$  and  $-90^\circ$  respectively.

The relative phase in the third case (c) is quite different to the required phase at resonance ( $+70^\circ$ ) and so this system may be tentatively eliminated as the basis for a model. Also, although for case (a) the phase for the amplitude peak is in the proximity of that required, examination of the frequency response for such a system indicated that it would be difficult to match this to the experimental data. The second case (b) was therefore considered as the basis for a model.

The frequent presence of rapid oscillations (frequency 9-10 c/d) necessitates the inclusion in this model of some mechanism for their production. A second feedback loop arranged to produce damped oscillations at 9.5 c/d was therefore added after the first. The frequency response for a model consisting of two loops in series was determined for a range of gain and time constant values, using an HP 97 calculator. The best match between this model and the experimental data is shown in figure 6.14. The frequency response has a resonant peak at 0.86 c/d corresponding to a phase lead of  $10^\circ$ .

The required phase lead of  $70^\circ$  at resonance may be obtained by including a phase advance or exponential lead element in the model, although this tends to detract from the match at higher frequencies.

It was found that a much improved match could be obtained by including two (or even three) phase advance elements to supply the required phase lead.

The final model is shown schematically in figure 6.14(a). Bode plots for the model are shown in figures 6.14 (b) and (c). The actual leaf data is also given for comparison. Time constants and gain values for the model are listed in table 6.5.

Biological receptors often show adaptive behaviour, a step input producing an immediate, large response which subsequently decays to a steady value (Milsum, 1966, p.79). This behaviour may be represented by the *phase advance* element (Milsum, 1966, p.226). Hence the phase advance elements in the model are envisaged as possibly representing the photoreceptive system which relates the basic oscillator to light changes. Thus although their position does not affect the frequency response of the model these have been placed before the basic oscillation in the model. This is discussed further in chapter 9.

Complete adaptation, i.e. a return to the initial output value following a step input, may be represented by exponential lead elements. In this model the parameter values are such that replacing the phase advance elements with exponential leads with time constants of 6.6 hours and 8.0 hours respectively has little effect on its frequency response (for the range of frequencies examined). Phase advance elements were chosen because the constant light results

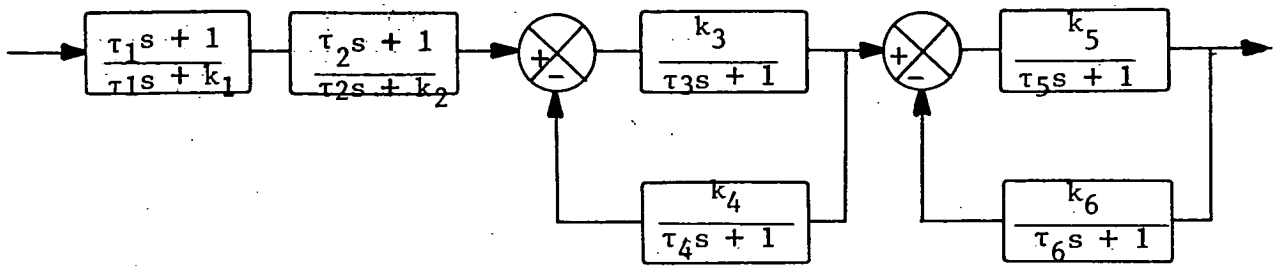


Fig. 6.14(a). Representation of the model for the system relating light charges to clover leaf movement. The model consists of two phase advance elements followed by a feedback loop representing the circadian oscillator. This in turn is followed by a second loop representing the system which produces the observed rapid oscillations.

	$\tau(\text{hours})$	$k$
1	32	4
2	33	5
3	36	8
4	36	8
5	1.2	3
6	1.2	3

Table 6.5. Time constants and  $k$  values for elements in the system represented by figure 6.14(a). Replacing the phase advance elements by exponential lead elements with time constants of 8 hours and 6.6 hours respectively does not significantly affect the frequency response, shown in fig. 6.14(b) and (c), of the above system.

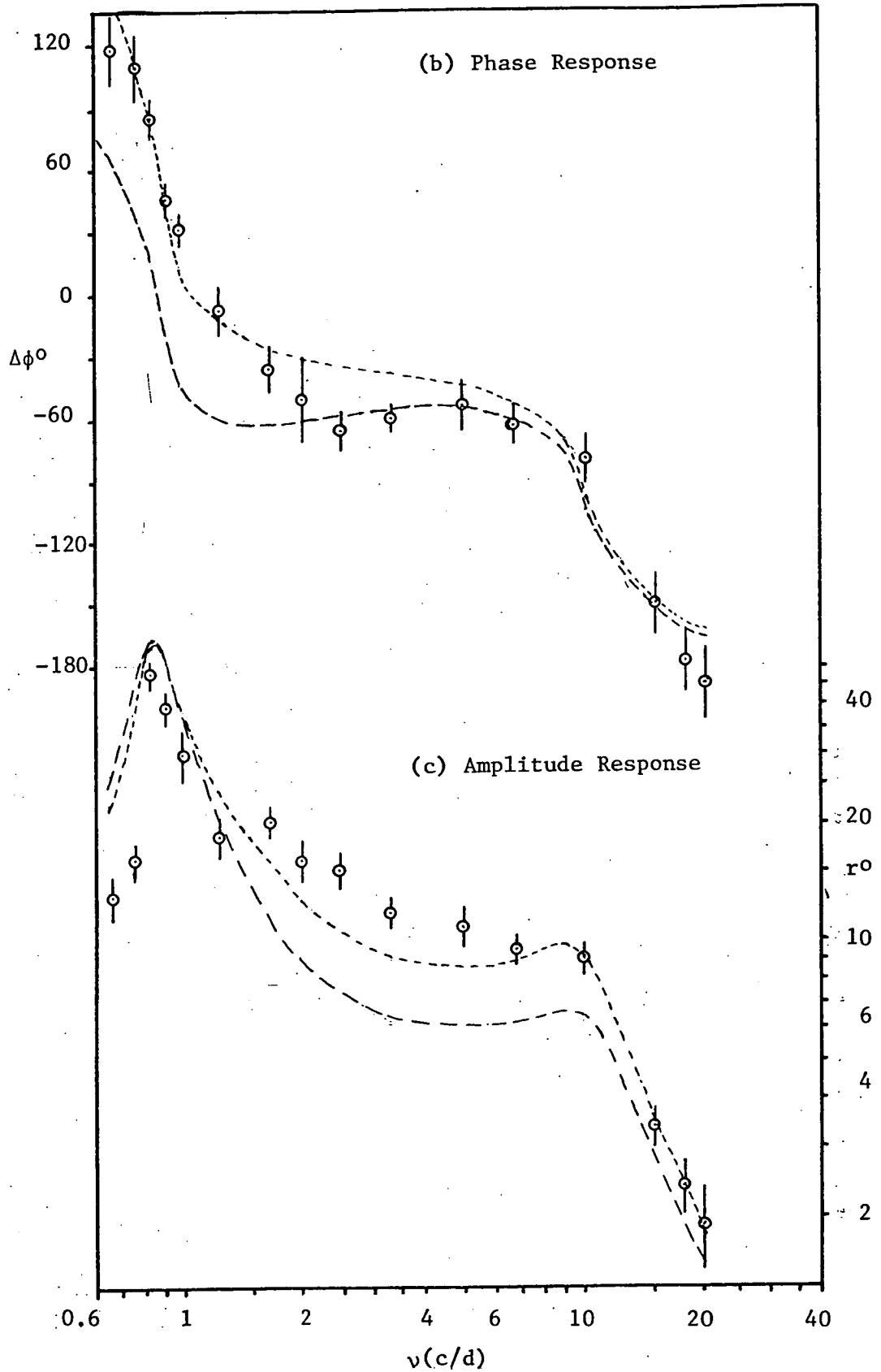


Fig. 6.14(b) Phase response and (c) amplitude response for the model shown in fig. 6.14(a). Short lines (---) represent the response of the model as shown while long lines (—) show the models response without the preceeding phase advance elements.

indicate that there is some relationship between the operating point or mean value for the oscillation and the absolute light intensity (see section 6.2). The implication is that adaptation cannot be complete, thus phase advance elements are suggested rather than exponential leads.

The transfer function for the first loop is:

$$k_3 (\tau_4 s + 1) / \{ (\tau_3 s + 1)(\tau_4 s + 1) + k_3 k_4 \} \text{ (see fig. 3.2)}$$

Factorizing the denominator of this expression reveals that such a loop will produce damped oscillations with frequency given by:

$$\{ 4\tau_3\tau_4 k_3 k_4 - (\tau_3 - \tau_4)^2 \}^{1/2} / 4 \pi \tau_3 \tau_4,$$

and damping coefficient by:

$$(\tau_3 + \tau_4) / 2\tau_3\tau_4$$

For  $\tau_3 = \tau_4$  and  $k_3 = k_4$  these expressions simplify to  $k_3/2 \pi \tau_3$  and  $1/\tau_3$  respectively. The second loop, identical in form to the first, will obviously also produce damped oscillations.

Gains and time constants for the forward path and feedback path element in each feedback loop are given identical values in table 6.5. In fact variations in these values by a factor of 1.5 can be tolerated with little deterioration of the frequency response match, provided the resonant frequency for each loop remains fixed.

The model described has a frequency response which is very similar to the observed frequency response for the clover leaf oscillator. It will also produce damped oscillations at 0.86 c/d (the circadian frequency) and at 9.5 c/d. The model is not the only arrangement of

linear elements which possesses the above characteristics, but it does so using a minimal number of elements. Extra lag elements could, for example, be incorporated into either feedback loop. However, examination of the frequency responses for such arrangements indicated that these did not provide an improved match to the experimental data. Further information supporting the basic form of the model is presented in the following sections while possible physical interpretations of the model are considered in chapter 9.

## 6.6 RESPONSE TO TRANSIENTS

### 6.6.1 Off-on Switching of a 10 c/d Variation

Six leaves were treated with a 10 c/d (800-2800 lux) sinusoidal log-light variation for 5 days, the leaves previously having been under a normal day-night light regime. After 5 days the variation ceased due to equipment failure and light intensity remained constant at 1500 lux for 13.2 hours (5.5 cycles). At this time the malfunction was discovered and the fault rectified. The variation was then reapplied for a further 2 days.

Although not achieving its original intent, this experiment does indicate the rapidity with which clover leaves respond to changes in the light conditions. A typical leaf record is shown in figure 6.15 along with the light variation. An expansion of part of the record in the region of the change in light regime is also included. On removal of the 10 c/d stimulus the response at this frequency vanished within 30 minutes (i.e. 3 samples) although in 3 records some indication of a damped 9-10 c/d oscillation existed, occurring immediately following the removal (see fig. 6.15). A response

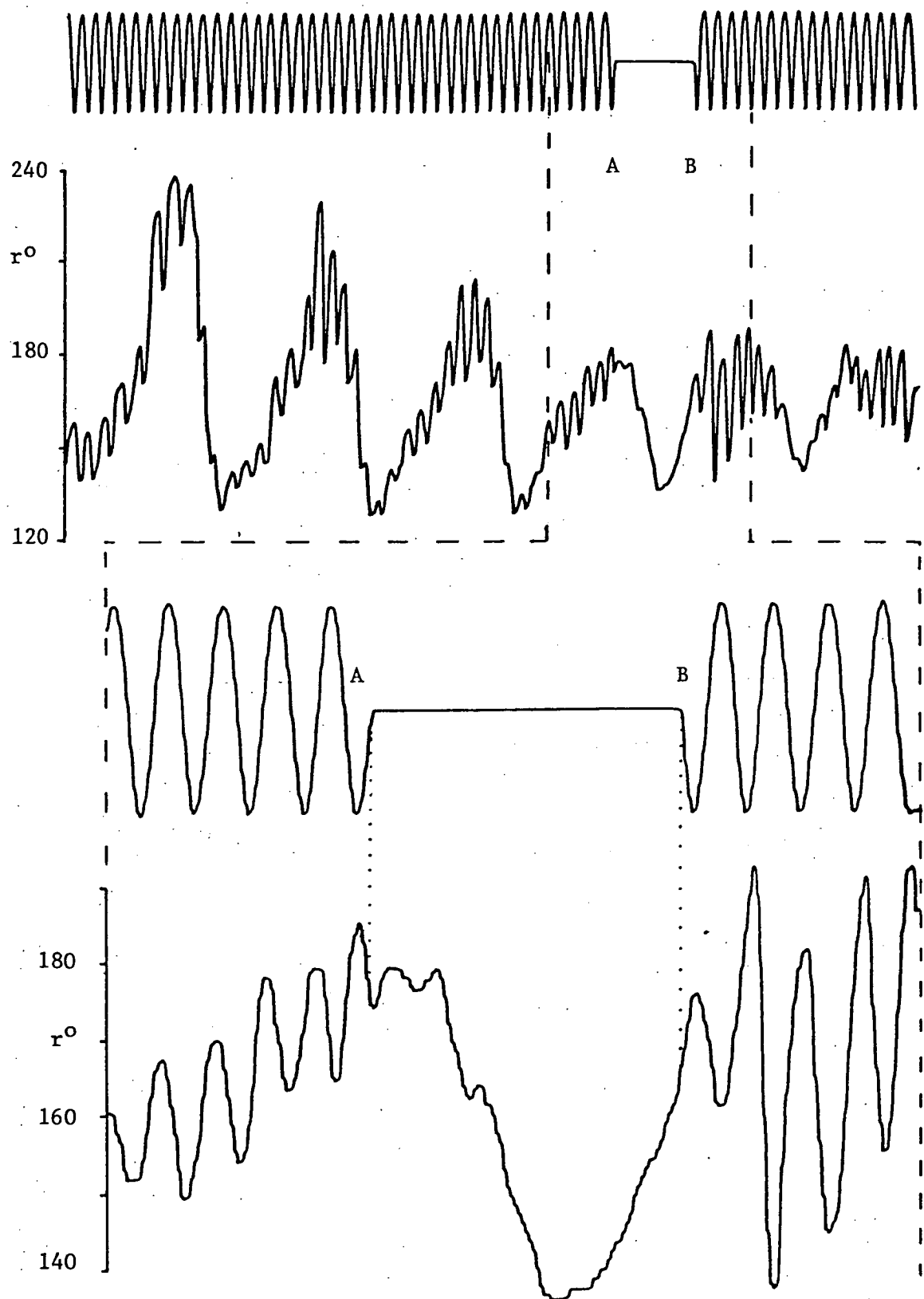


Fig. 6.15. Leaf record for a 10 c/d sinusoidal log-light variation (800–2800 lux). Treatment was discontinued at point A and recommenced at point B. A magnified section of the light and leaf records is also shown.



to reapplication of the light variation was observable by the third data sample after this time (i.e. within 30 minutes). These results place an upper limit of 30 minutes on the time constant of any finite delay element that might form part of the system's forward transfer function. A model such as the Karlsson-Johnsson model for the Kalanchoe petal rhythm (see section 2.4) would thus not serve for the clover leaf oscillator since this model contains a 6 hour finite delay separating input from output.

#### 6.6.2 System Pulse-Phase Response

The following experiments were performed in order to determine a pulse-phase response curve (PRC) for the clover leaf system (see section 3.11). Clover plants were treated with a 1 c/d rectangular wave light variation from 400 to 10,000 lux for 3 days. Leaves were mounted in anglemeters on the third day. After the fourth bright light to dim light transition the variation was discontinued and light intensity was maintained at 400 lux. At some later time the plants were subjected to a single 2 hour light pulse from 400 to 10000 lux, following which leaf movements were recorded for a further 6 days in 400 lux. The final 5 days of these records were analysed and the phase of the fundamental in each spectrum determined. These phases were averaged and compared with the mean phase determined for 6 control (i.e. non-pulsed leaves). The phase change produced by the light pulse was thereby estimated. Pulses were applied at 6 different times after the last light-dark transition in 6 consecutive experiments.

Phase shifts in PRC's are often plotted against circadian time (CT) or alternatively against subjective circadian time (SCT). Pavlidis (1973) defined circadian time as the phase difference, measured in hours, between the current phase of the system and its phase at the time of the last dark-light change. Thus CT zero is 12 hours before the start of continuous dim light in the treatments described here. Pittendrigh and Minis (1964) scaled the circadian time to 24 hours and called it subjective circadian time. This also differs in the choice of zero. SCT zero is given as 12 hours after the last light dark change for an organism formerly subjected to a 12:12 light-dark regime. Thus SCT and CT are related by:  $SCT = (CT - 24) 24/T_c$  (hours) - where  $T_c$  is the period of the circadian rhythm. Thus 24 hours of SCT represents a complete cycle of the natural rhythm. Plotting phase shifts against SCT is obviously more useful if PRC's for different organisms with differing natural frequencies are to be compared. The results presented in this section are plotted with SCT, rather than CT, as abscissa.

The PRC determined for the above conditions is given in figure 6.16. The PRC indicates that the phase change produced by the pulse varies slowly with the phase of the oscillation except between SCT hours of 17 and 21. Over this narrow range the response changes from a 4 hour lag to a 4.5 hour phase advance. Reference to information pertaining to PRC's for simple linear systems (chapter 3.11) indicates that the clover leaf PRC may correspond to a system with a phase lag of approximately  $90^\circ$  between the signal at the comparator and the observed output. That is, the total phase contribution of elements lying between the comparator and the output

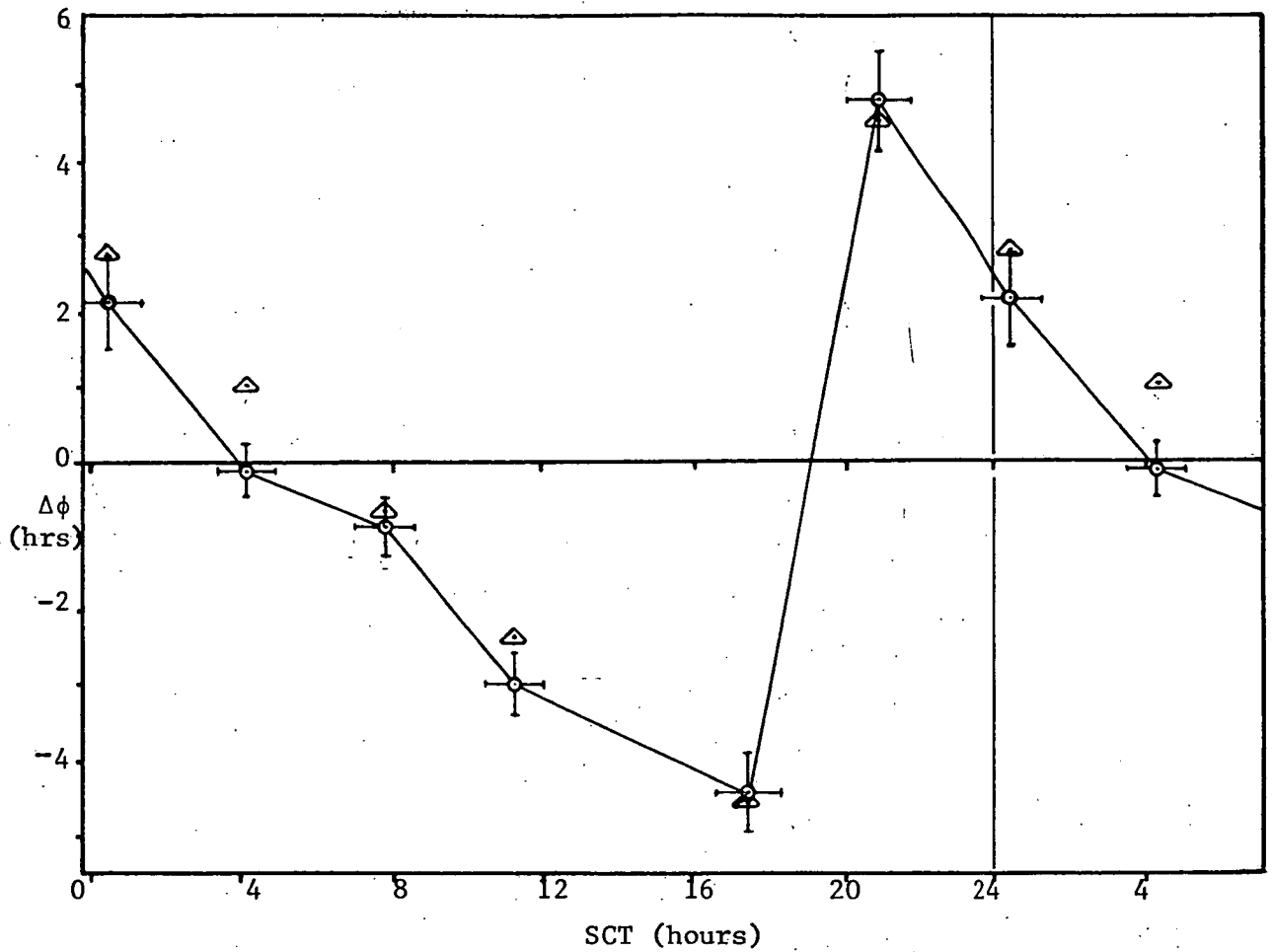


Fig. 6.16. PRC for 2 hour light pulses from 400 lux to 10,000 lux.

The first and second data points are repeated. Vertical bars are s.e. bars for the means of phase change estimates for from 4 to 6 leaves. Horizontal bars show the duration of each pulse. Points marked by triangles represent values for the PRC of best fit to the experimental data calculated for the model given in section 6.5.

is in the vicinity of  $-90^{\circ}$  for a signal at the natural frequency of the system. It may be observed that this is indeed the case for the model presented in section 6.5. The exponential lag of large time constant in the forward path of the feedback loop provides a phase lag approaching this figure, while the following secondary loop contributes a phase lead of  $10^{\circ}$  at the natural frequency.

The PRC for the model was calculated for a pulse duration of 2 hours and an R/h value of 0.50 (see section 3.11). The calculated points are included in figure 6.16. The PRC points for the model lie within the 95% confidence limits of the points in the clover leaf PRC. This provides strong support for the basic form of the model.

## 6.7 EXAMINATION OF SOME NONLINEAR FEATURES

### 6.7.1 Dependence of Response on Background Light Intensity

The frequency response presented in section 5 was determined by applying light variations superimposed on an 800 lux background intensity. It seems reasonable to suggest that this response may be dependent on the background light level itself. There may, for example, be a response threshold at low light levels, and light variations superimposed on high background intensities may have little effect due to saturation of the leaf receptors.

In order to examine these possibilities plants were treated with 10 c/d sinusoidal log-light variations superimposed on a range of background intensities. The leaf response was assumed to be logarithmically related to light intensity variations and for this reason the amplitudes of the applied variations were increased with

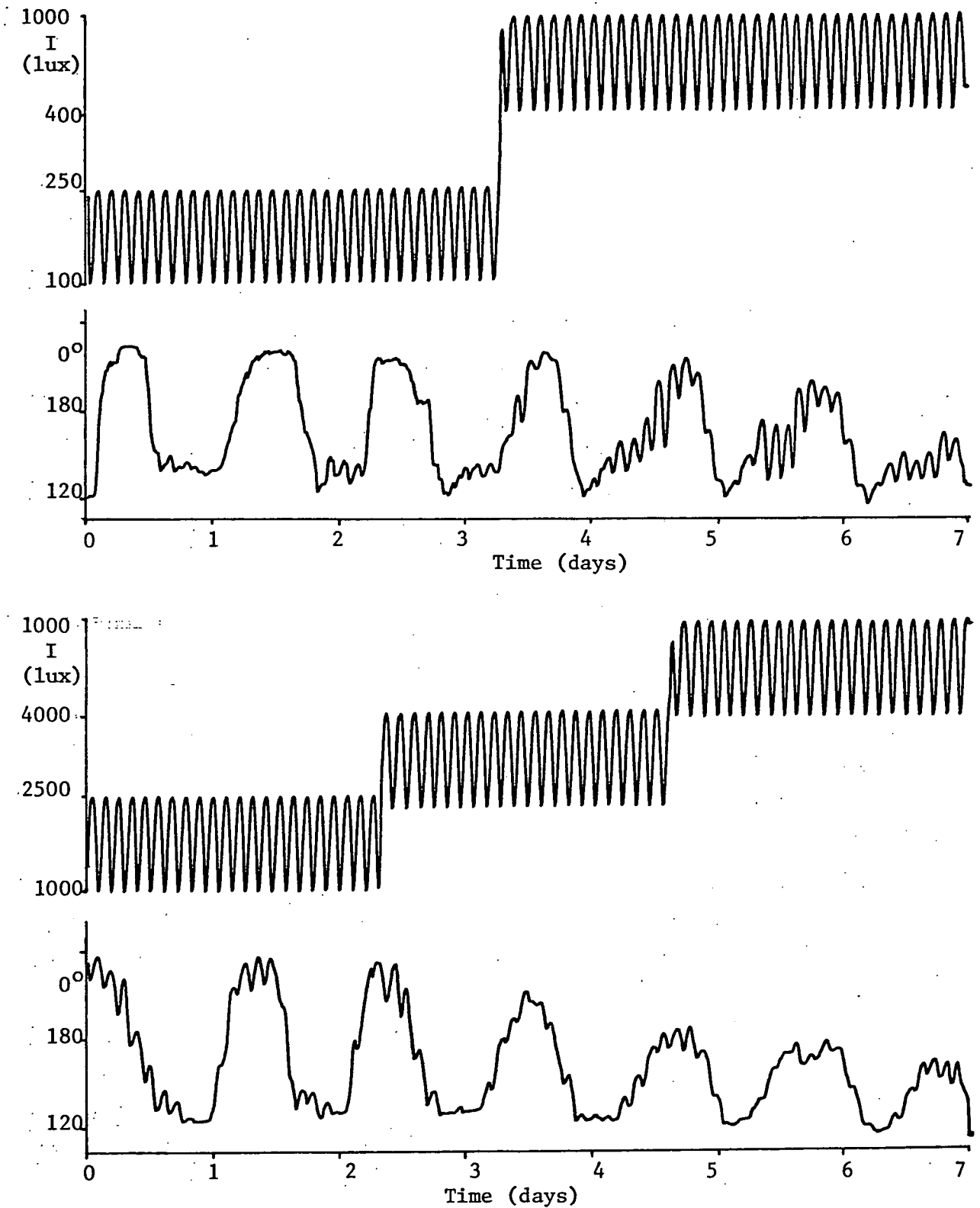


Fig. 6.17. Leaves were treated with a sinusoidal log-light variation superimposed on a range of background intensities. The light variation and examples of leaf movement are shown.

increasing background level so as to maintain the ratio of maximum to minimum light intensity in each cycle.

The two light regimes applied and typical leaf responses are shown in figure 6.17. Sections of leaf records corresponding to particular background light intensities were analysed (fig. 6.18) and the amplitudes of the spectral peaks at 10 c/d were averaged. Results for the 5 background intensities are plotted in figure 6.19. The graph shows a peak for a background intensity of 1000 lux, and also suggests that the clover leaves are most sensitive to light variations within the range 400 to 2500 lux.

#### 6.7.2 Dependence of Response on Leaf Position

It is conceivable that the response of a leaf to a small stimulus may vary with leaf angle. For example leaf motion may be more difficult if the leaf is approaching a limit to its normal range of movement. The frequency response records support this suggestion, the response to a rapid light oscillation being less marked for fully open leaves than for leaves in an intermediate or closed state (fig. 6.11e). This aspect was examined as follows.

Records for leaves subject to a 10 c/d variation (range 800-2800 lux) were Fourier transformed. Frequency components were identified from each amplitude spectrum (e.g. fig. 6.20b) and subtracted from the transform, by the method given in chapter 4, until all significant low frequency terms had been removed. The extracted components were then recombined to produce a record without high frequency terms (in this case without terms  $>5$  c/d). An example

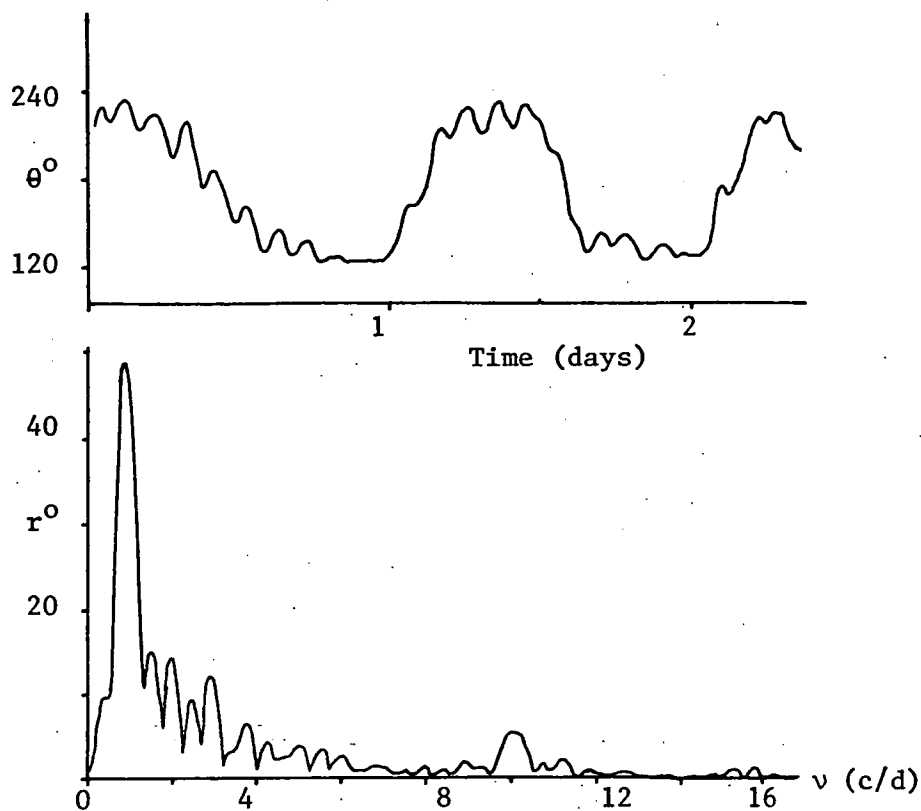


Fig. 6.18. First section from second leaf record in figure 6.17 and its transform.

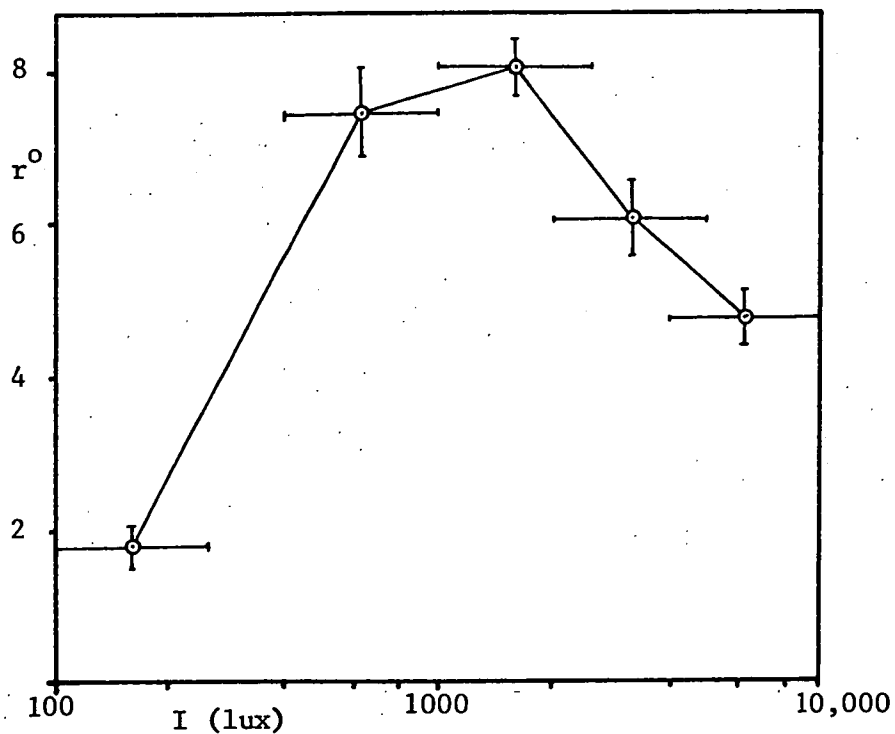


Fig. 6.19. Mean amplitude of oscillation at 10 c/d for 5 background light intensities. Vertical bars are s.e. bars for 5 or 6 leaves. Horizontal bars show the range of the light variations.

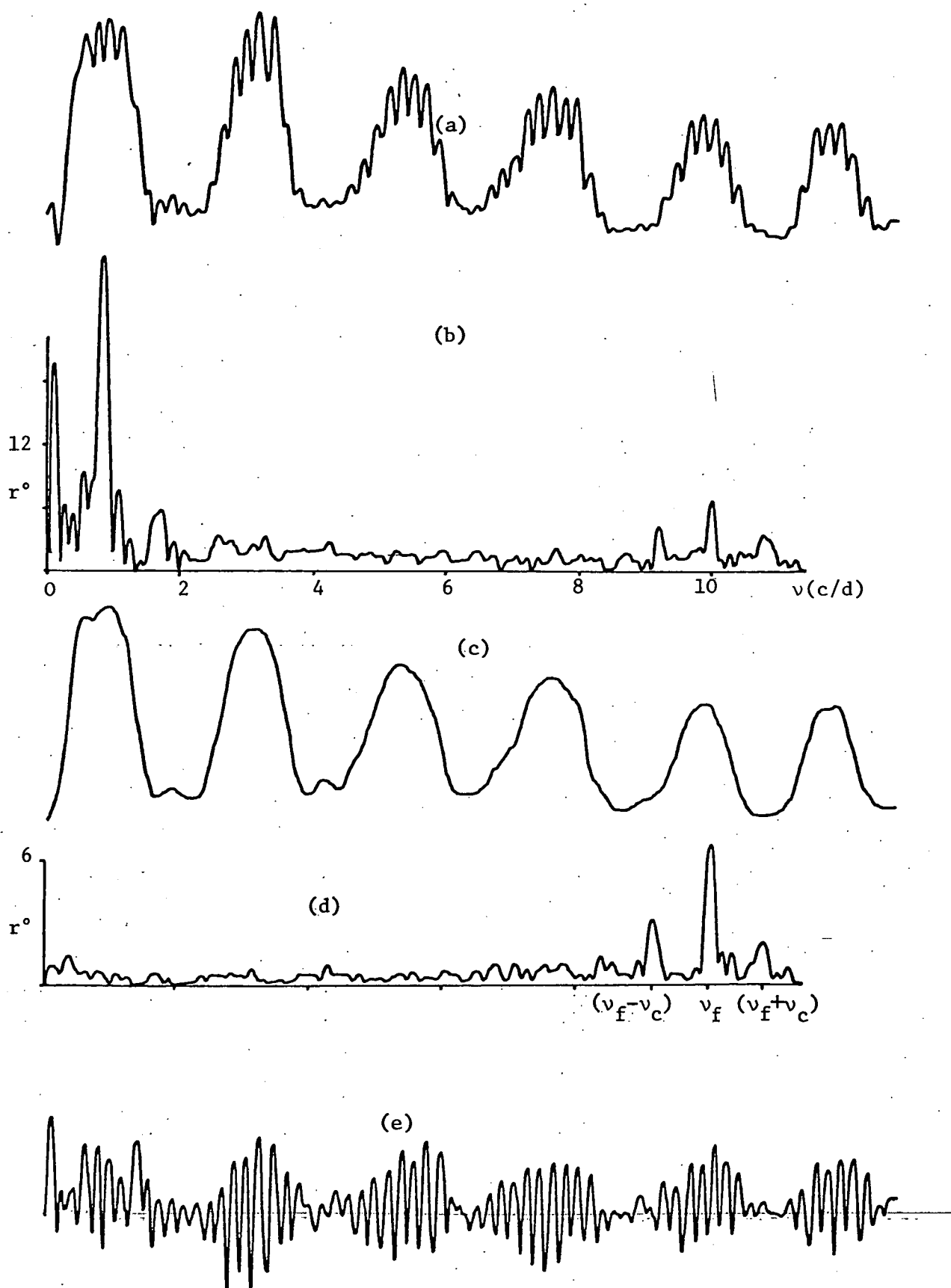


Fig. 6.20 (a) Leaf record for a 10 c/d light treatment. (b) is its amplitude spectrum and (c) is a signal constructed by identifying the low frequency components in the transform. (d) is the spectral residue with these components removed and (e) is the time series corresponding to this residue.



is given in fig. 6.20c along with the residual amplitude spectrum (fig. 6.20d). This 'smoothed' record was then subtracted from the original leaf record leaving the high frequency components (e). It may be noted that this procedure is actually equivalent to, but less time consuming than, performing a reverse Fourier transform on the residual transform. The amplitude of the high frequency oscillation is clearly varying periodically, being least when the leaf is fully open.

The range of movement given by the smoothed record for each leaf was then divided into  $15^\circ$  segments. By comparing the high frequency components (e) with the plot of leaf position (c) the mean amplitude of the response to the 10 c/d forcing oscillation for each segment was estimated. Estimates for equivalent range segments in leaf records were then averaged. The results are plotted in figure 6.21 as a graph of leaf position against amplitude of response. The graph indicates that there is a decrease in leaf response to the 10 c/d oscillation when the leaf angle becomes less than approximately  $165^\circ$ . For larger leaf angles the response is relatively constant, although there is some evidence for a peak in the response for leaf angles in the vicinity of  $195^\circ$ . The leaf response for mean leaf angles which are outside the range  $90^\circ$  to  $255^\circ$  could not be determined as this was the maximum range covered by leaf movements in the experiment.

It is now necessary to consider the effect that this nonlinear feature may have had on amplitude values estimated from each amplitude spectrum. Suppose the natural and forced oscillations in

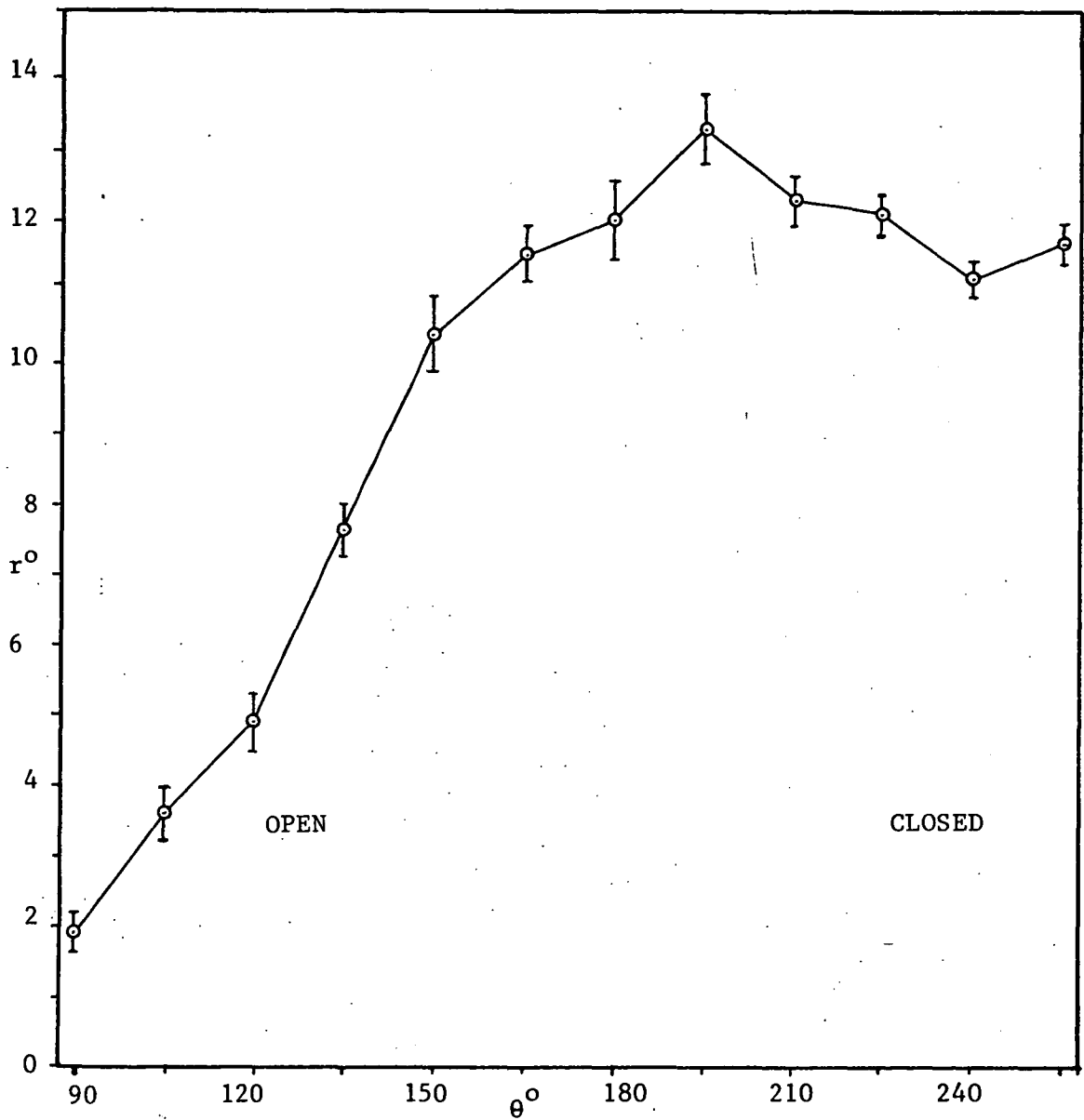


Fig. 6.21. Amplitude of 10 c/d component in leaf movement plotted against mean leaf angle. Vertical bars are s.e. bars for from 4 to 6 leaves.

figure 6.20a are approximated by their first harmonics (i.e. by sinusoids) and it is assumed that the amplitude of the forced oscillation is varying in a linear fashion with the natural oscillation. Then the leaf angle variation may be represented by  $\theta(t)$ , where:

$$\theta(t) = 180^\circ + R_c \sin(\omega_c t + \phi_c) + R_f \sin(\omega_f t + \phi_f) \{ 1 + (R_c/180^\circ) \sin(\omega_c t + \phi_c) \}$$

That is,  $\theta(t)$  contains a circadian component with parameters  $R_c$ ,  $\omega_c$  and  $\phi_c$ , and a forced component of frequency  $\omega_f$ , with amplitude varying between  $R_f (1 - R_c/180^\circ)$  and  $R_f (1 + R_c/180^\circ)$ . The forced component is being *amplitude modulated* at the frequency of the circadian component. Note that since the amplitude of the leaf oscillation is always less than  $180^\circ$ ,  $R_c/180^\circ < 1$ .

The third term on the right of the above equation can be expanded as:

$$R_f \sin(\omega_f t + \phi_f) + (R_f R_c / 180^\circ) \sin(\omega_f t + \phi_f) \sin(\omega_c t + \phi_c);$$

or:

$$R_f \sin(\omega_f t + \phi_f) + (R_f R_c / 360^\circ) \cos\{(\omega_f - \omega_c) t + \phi_f - \phi_c\} - (R_f R_c / 360^\circ) \cos\{(\omega_f + \omega_c) t + \phi_f + \phi_c\};$$

- i.e. three separate frequency components. Thus the amplitude spectrum for  $\theta(t)$  would contain peaks at the frequencies  $\omega_c$ ,  $\omega_f$  ( $\omega_f - \omega_c$ ) and ( $\omega_f + \omega_c$ ), with amplitudes  $R_c$ ,  $R_f$ ,  $R_f R_c / 360^\circ$  and  $R_f R_c / 360^\circ$  respectively. It may therefore be seen that in this case the amplitude of the forced oscillation, estimated from the spectrum, would be the *mean* amplitude of the response (i.e.  $R_f$ ).

The triple peak structure in the vicinity of  $\nu_f$  suggested by the above result is indeed observed in amplitude spectra (e.g. fig. 6.20d) although generally the peaks at the sum and difference frequencies are not of the same height. These results indicate that the value of the spectral peak corresponding to the forcing frequency may give an estimate of the average response of the system to the forcing frequency.

A function having the characteristic curve shown in figure 6.21 would, if placed after a linear system, introduce harmonics into the observed oscillation. For input signals composed of two separate frequencies sum and difference terms would also be created. It is thus possible that the circadian oscillator itself has only ~~minor nonlinear features and that the presence of harmonics in the~~ output for a sinusoidal input is largely due to the function relating circadian oscillator output to leaf position. This is discussed further in chapter 9.

---

## CHAPTER SEVEN

### EXPERIMENTAL RESULTS. B: CHEMICAL TREATMENTS

#### 7.1 INTRODUCTION

The apparatus and analytical techniques described in this thesis were applied to assess the effects of a number of chemical treatments on the clover leaf oscillation. Excised leaves were used in the experiments and these were mounted as described in section 5.5. Some preliminary experiments were performed to determine whether excision affected the behaviour of the leaves. These results are presented in section 7.2 and are compared with the results obtained for whole plants (i.e. unexcised leaves) presented in the previous chapter. The parameters for excised leaves (i.e. damping rate, frequency of oscillation etc.) were regarded as significantly different from these controls if the 95% confidence limits for their respective mean values did not overlap. The same criterion was applied to determine the effectiveness of chemical treatments though in these cases the means were compared with those for untreated excised leaves rather than for whole plants.

It is difficult to determine whether a negative result for a particular chemical treatment implies that the chemical has no effect on the system, or whether it simply has not reached a part of the plant where it has an effect on leaf movement - in this case the clover pulvinule cells. For this reason care must be taken in interpreting such results.

## 7.2 EFFECT OF EXCISION

Excised leaves with petioles immersed in either tap water or Hoagland's solution (see table 7.1) were treated with continuous bright light (10,000 lux), to dim light (25 lux), and to a 24 hour sinusoidal log-light variation over the range 800-2800 lux to determine the effect of excision on leaf movement. The treatments were conducted for a one week period and records for leaves in constant light were analysed as described in section 6.2.

Data resulting from these treatments is summarised in table 7.2. Leaves in tap water showed a damping of the natural oscillation, in both bright and dim light, that was more pronounced than for unexcised leaves. Calculation of damping coefficients as in section 6.2 revealed that these were significantly greater than those for the controls (i.e. leaves attached to plants). Leaves in Hoagland's solution also had larger damping coefficients than the controls, but in these cases the difference was not considered significant (see table 7.2).

Excised leaves in Hoagland's solution were treated with a sinusoidal log-light variation as described above. The resulting records were Fourier analysed to determine the mean amplitude and phase of the component corresponding to the forcing oscillation. These values were then compared with those for the controls. The differences between the mean amplitude and mean phases for the two cases was not significant (table 7.2).

Chemical	Concentration (mM)
$\text{Ca}(\text{NO}_3)_2 \cdot 4\text{H}_2\text{O}$	10
$\text{KNO}_3$	10
$\text{MgSO}_4 \cdot 7\text{H}_2\text{O}$	4
$\text{KH}_2\text{PO}_4$	2
EDTA	0.25
$\text{FeSO}_4 \cdot 7\text{H}_2\text{O}$	0.18
Micronutrients:	
$\text{H}_3\text{BO}_3$	0.09
$\text{MnCl}_2 \cdot 4\text{H}_2\text{O}$	0.018
$\text{ZnCl}_2$	0.0015
$\text{CuCl}_2 \cdot 2\text{H}_2\text{O}$	0.0005
$\text{NaMoO}_4 \cdot 2\text{H}_2\text{O}$	0.0002

Table 7.1. Composition of Hoagland's solution used in treatments described in this chapter.

	Controls (whole plants)	Leaves in Hoagland's	Leaves in tap water	Leaves in sucrose
Damping rate at 10,000 lux in d <sup>-1</sup>	.106	.138	.178	.128
s.e.	.011	.014	.016	.009
no.	5	6	5	3
Probability	-	.09	<.01	.4
- at 25 lux	.276	.316	.395	.245
s.e.	.037	.012	.009	.012
no.	5	3	3	5
Probability	-	.45	.05	<.01
Sinusoidal light Amplitude (°)	29.9	27.2	23.9	31.3
s.e.	4.1	2.5	3.4	3.3
no.	8	5	3	6
Probability	-	.65	.3	.3
Phase (°)	32	26	19	27
s.e.	6	5	3	4
Probability	-	.45	.15	.7

Table 7.2. Data arising from a study of the effects of excision and sucrose on leaf movement. In columns 2 and 3 the probabilities are that the controls and leaves in Hoagland's and tap water respectively are samples from the same population. For leaves in Hoagland's with sucrose, probabilities were calculated by comparing these results with those for leaves in Hoagland's solution only.



The above results seem to indicate that excision has little effect on clover leaf movement provided the leaf is not under osmotic stress and provided a sufficient quantity of nutrients is available to the leaf.

### 7.3 TREATMENT WITH SUCROSE

It has been shown for both whole plants and excised leaves that the damping rate for clover leaf oscillations is greater in dim than in bright light. Similar observations have been made with the legume *Samanea saman*, and it has been suggested (Simon et al, 1976) that the increased damping rate in dim light might be due to the depletion of a photosynthetic produce necessary for the maintenance of the oscillation. - Simon et al (1976) demonstrated that the damping rate for *Samanea* leaves in darkness could be decreased by the addition of sucrose to the medium bathing the stems of excised leaves. A similar result is described here for excised clover leaves.

Excised leaves were supplied with Hoagland's solution containing 20 mM sucrose and were subjected to light regimes identical to those described in the previous section. The presence of the sucrose had no significant effect on the leaf oscillations for constant bright light or for the 24 hour light variation. Analysis of the leaf records revealed that there was indeed no significant difference between the parameters for these oscillations and those for the controls. However, the mean damping rate for leaves in dim light was significantly less than that for untreated excised leaves and even somewhat less than the mean damping rate for unexcised leaves (see table 7.2).

Sucrose solution was also supplied to the soil of whole plants in dim light at concentrations of 20 mM and 50 mM. Neither treatments resulted in significant changes in damping rates in these cases. This absence of an effect with whole plants suggests that the sucrose is not reaching the clover pulvinule in sufficient concentration for its influence to be observable.

The sucrose experiments of Simon et al (1976) with *Samanea* involved a higher sucrose concentration (50 mM) than that used here. This was observed not only to decrease the damping rate for excised *Samanea* leaves in dim light, but also to partly inhibit leaf movement in bright light. A similar effect was not observed for clover at the lower concentration used.

#### 7.4 VARYING pH

It has been demonstrated (Hastings, 1960) that *Gonyaulax polyedra* cultures exposed to alternating light and dark periods (24 hour cycle) undergo cyclic variations in pH, the pH rising in the light and falling in the dark. If the darkness is continued this pH rhythm ceases immediately. This rhythm seems to be a purely light dependent rhythm, possibly caused by cyclic changes in CO<sub>2</sub> concentration in the medium due to photosynthesis and respiration.

Racusen and Galston (1977) treated excised *Samanea* pulvini in continuous darkness to 10 mM sucrose at various pH values. They observed that these caused a depolarization of the membrane potential in pulvinal cells if applied at particular times during the natural cycle, a lower pH causing a greater depolarization.

Little has been done to test the affect of external pH on the parameters of circadian rhythms (e.g. amplitude, frequency). It therefore seemed worthwhile to examine whether pH changes have some effect on the circadian leaf movement in clover. For this reason the petioles of excised clover leaves under continuous light (10,000 lux) were immersed in Hoagland's solutions with pH values ranging from 9 to 4.5 in successive experiments. The pH values were obtained using either a phosphate buffer or Tris buffer with hydrochloric acid. These values were measured with a Radiometer 22 pH meter immediately preceeding and following each 6 day treatment. In most cases the pH remained within 0.3 units of its initial value over the duration of the treatment.

Damping rates significantly greater than those for the controls of section 7.2 were observed for treatments outside of the pH range 6-8. A pH dependence of natural frequency was initially suggested by the results, the frequency apparently increasing with decreasing pH, but repetition of some treatments showed that the correlation between pH and natural frequency was not significant (correlation coefficient = 0.33, probability = 0.1). The results for these treatments are summarised in table 7.3.

The increased damping rate shows that the altered hydrogen ion concentration in the bathing medium had some effect at the clover pulvinules. However, the extent to which this might be due to an alteration in the pH at the pulvinule cells themselves is not known.

pH	$v_c$ (c/d)	s.e.	No.
4.5	.848	.004	3
5	.858	.004	3
6	.852	.003	5
7	.850	.002	4
8	.851	.003	6
9	.843	.002	3

Table 7.3. Mean frequency of the circadian rhythm for leaves treated with Hoagland's solution of pH within the range 4.5 to 9. The suggested downward trend in frequency with increasing pH does not appear to be significant. (Correlation coefficient = 0.33, probability of this occurring by chance - 0.1).

## 7.5 TREATMENTS WITH KCl AND NaCl

It has been shown that the potassium ion flux oscillates in a circadian fashion in clover pulvinule cells (Scott et al, 1976) and in pulvinule cells in *Samanea* (Satter et al, 1974a, 1974b). The circadian oscillation may also be reset by potassium ion pulses in *Phaseolus* (Bunning and Moser, 1972) and in *Aplysia* (Eskin, 1972). Njus et al (1974) have suggested that variations in potassium ion concentration may constitute part of the circadian oscillator. For these reasons excised clover leaves were treated with KCl of various concentrations and with KCl pulses to determine whether these affected circadian leaf movement. For purposes of comparison some leaves were treated in a similar fashion but with NaCl in place of KCl.

Groups of from 3 to 6 excised leaves under continuous bright light (10,000 lux) were treated with Hoagland's solution containing KCl or NaCl at concentrations of 10, 20, 50 or 100 mM for a six day period. Leaves in 50 and 100 mM KCl and 100 mM NaCl showed brown discolouration within two days, possibly due to a nutrient deficiency. The damping rates for these were significantly greater than those for the untreated leaves of section 7.2. By the completion of the treatments leaves in 20 mM KCl and in 50 mM NaCl were showing similar discolourations, though neither these, nor those leaves in 10 or 20 mM NaCl or 10 mM KCl had mean damping rates differing significantly from the controls. The frequency of the natural oscillation in each case was determined by spectral analysis. These were observed to be unaffected by the treatment (i.e. no significant change).

Two hour pulses of 20 mM KCl in Hoagland's solution were applied at 24 hour intervals to six excised leaves in bright light. This was continued for one week. The resulting leaf records were Fourier transformed and the amplitude spectra examined. These revealed that the leaves were still essentially oscillating at the circadian frequency (mean amplitude  $31^{\circ} \pm 3^{\circ}$  s.e.) although each spectrum did contain a peak at 1 c/d (amp.  $16^{\circ} \pm 2^{\circ}$  s.e.). However, the six leaves pulsed with 20 mM NaCl also revealed 1 c/d components in the leaf records, and of similar mean amplitude ( $11^{\circ} \pm 2^{\circ}$  s.e.) to that for KCl pulsed leaves. It therefore seems unlikely that the effect is due in this case to a response specific to the variation in the potassium ion concentration. The 1 c/d component may well be introduced by the osmotic changes caused by KCl and NaCl pulsing, or perhaps by a response to the variation in chloride ion concentration.

#### 7.6 EFFECT OF ETHANOL

Ethanol is one of the few chemicals known to alter the frequency of circadian oscillations in plants and in animals (see chapter 2.3). Experiments were therefore performed in which excised leaves under both continuous light and sinusoidally changing light were treated with ethanol in order to examine the effect of this substance on the clover leaf oscillation.

The movements of excised leaves under continuous bright light (10,000 lux) and in Hoagland's solution containing ethanol in proportions of 0.6%, 1%, 2%, 5% and 10% were recorded for a period of seven days. Records were Fourier transformed and the period of the natural oscillation estimated from the amplitude spectrum in each case. The results are plotted in Figure 7.1.

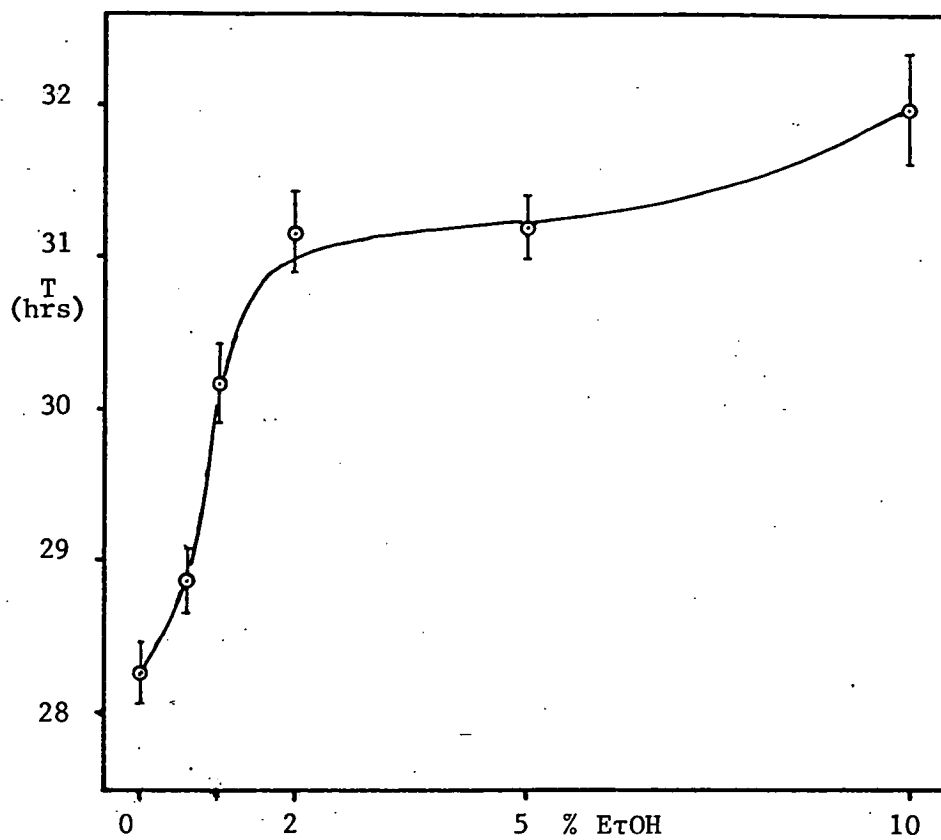


Fig. 7.1. Plot of period of natural oscillation in hours against percentage ethanol in the medium bathing the cut leaf petioles.

Leaves were in 10,000 lux continuous light. Bars are s.e.

bars for from 4 to 6 leaves.

Leaves in 10% ethanol ceased oscillating after just two cycles and perished before the completion of the experiment, so the frequency for these could not be estimated with any great degree of reliability. Nonetheless, the graph clearly shows an increase in period of oscillation with increasing ethanol concentration, although the rate of increase in period is less marked at above approximately 2% ethanol.

The following experiment was implemented to obtain an indication of the influence ethanol might have on the leaf frequency response. Leaves in Hoagland's solution with 2% ethanol were subjected to a 1 c/d sinusoidal light variation (range 800-2800 lux) for seven days. Leaf records were Fourier transformed and the amplitude and phase of the component in each transform corresponding to the forcing oscillation estimated. The results showed that the mean phase for five leaves lagged the light variation by  $8^{\circ}$  ( $\pm 6^{\circ}$  s.e.) and the mean amplitude was  $16.1^{\circ}$  ( $\pm 2.2^{\circ}$  s.e.). These figures may be compared with those for the controls (section 7.2) which showed a mean phase *advance* of  $26^{\circ}$  ( $\pm 5^{\circ}$  s.e.) and amplitude of  $27.2^{\circ}$  ( $\pm 2.5^{\circ}$  s.e.).

It appears from these data that the response of clover leaves in 2% ethanol to a 1 c/d light variation is similar to the response expected from the controls if they were to be subjected to a 1.2 c/d light variation. The ethanol appears to have moved at least part of the frequency response curves to lower frequencies. The ethanol truly seems to have altered the value of a parameter (gain term or time constant) which partly or wholly determines the frequency of the basic oscillator.



## 7.7 AZIDE

The azide ion is well known as a metabolic inhibitor: more specifically it acts as a respiratory poison by affecting electron transfer processes (Giese, 1968). It also inhibits CO<sub>2</sub> fixation in photosynthesis, but does not necessarily inhibit all photophosphorylation (Gingras et al, 1963). The effect of azide in relation to the *Gonyaulax* glow rhythm (Hastings, 1960) and the sporulation rhythm of *Oedogonium* (Buhnemann, 1955b) has been examined. Hastings reported that azide pulses (8 hours duration, 0.4 mM concentration) had no effect on the phase of the circadian rhythm in *Gonyaulax*, while Buhnemann demonstrated that although a continuous azide treatment decreased the *Oedogonium* rhythm markedly it had no apparent effect on the frequency of the rhythm. However, van Emmerik (1975) applied sodium azide at concentrations of 0.1, 1 and 10 mM to excised clover leaves in darkness and observed that at the lower concentrations leaf opening was advanced in phase. This result prompted the experiments described below.

Excised leaves under continuous bright light (10,000 lux) were treated with Hoagland's solution containing sodium azide in concentrations of 1 mM or 2.5 mM (3 leaves in each), the azide being added just prior to leaf closure. Leaf movement was then monitored for 4 days.

The 3 leaves in 2.5 mM azide ceased moving before the completion of one full cycle, halting in the open position. The leaves perished soon after. Leaves in 1 mM azide survived to complete two cycles before ceasing motion. No change in frequency due to the azide was apparent from the small amount of data available.

However, a phase delay in the first closure could be observed when the records were compared with those for untreated leaves. The following experiments were therefore performed.

Excised leaves in Hoagland's solution and under continuous light (10,000 lux) were treated with single azide pulses varying in duration from 1 to 4 hours and at concentrations of 1.0, 2.5, 5 and 10 mM. Pulses were applied 4 hours before leaf closure and leaf movements were then recorded for a 4 day period.

Pulses of 2 and 4 hours duration at 5 and 10 mM, and 4 hours at 2.5 mM proved lethal, the leaf petioles developing a withered appearance within one day and the leaves perishing shortly after. At the other extreme a one hour, 1.0 mM pulse had little observable effect on leaf movement or leaf appearance. However, other duration-concentration combinations caused readily observable phase shifts.

A pulse of 2.5 mM azide for 2 hours was chosen as optimum for obtaining an azide pulse phase response curve. Azide pulses were applied to 6 leaves in dim light (400 lux) at 6 different phases of the natural oscillation. The procedure was similar to that used to obtain the light pulse PRC in section 6.6. The results for the pulse treatment are plotted in figure 7.2.

The azide pulse PRC is similar in form to the light PRC, though of lesser amplitude and displaced toward an earlier phase (i.e. to the left) by about 3 hours. This displacement may possibly

indicate a different point of entry of the azide into the oscillatory system, or alternatively much of it might represent a time lag between application of the azide to the leaf petiole and its arrival at the site of the oscillator in sufficient concentration to have a significant effect.

The inhibitory action of azide seems to suggest that its effect would be to move the phase of the circadian rhythm to that of a lower energy. This could be achieved by, for example, inhibiting membrane ion pumps so that transmembrane ion concentration gradients are diminished. It has been suggested (Njus et al, 1974) that the effect of light might be to alter the configuration of membrane transport channels, leading to an ion gradient diminution similar to that suggested above as produced by azide. The observed resemblance between azide and light PRC's would then logically follow. This will be discussed further in Chapter 9.

---

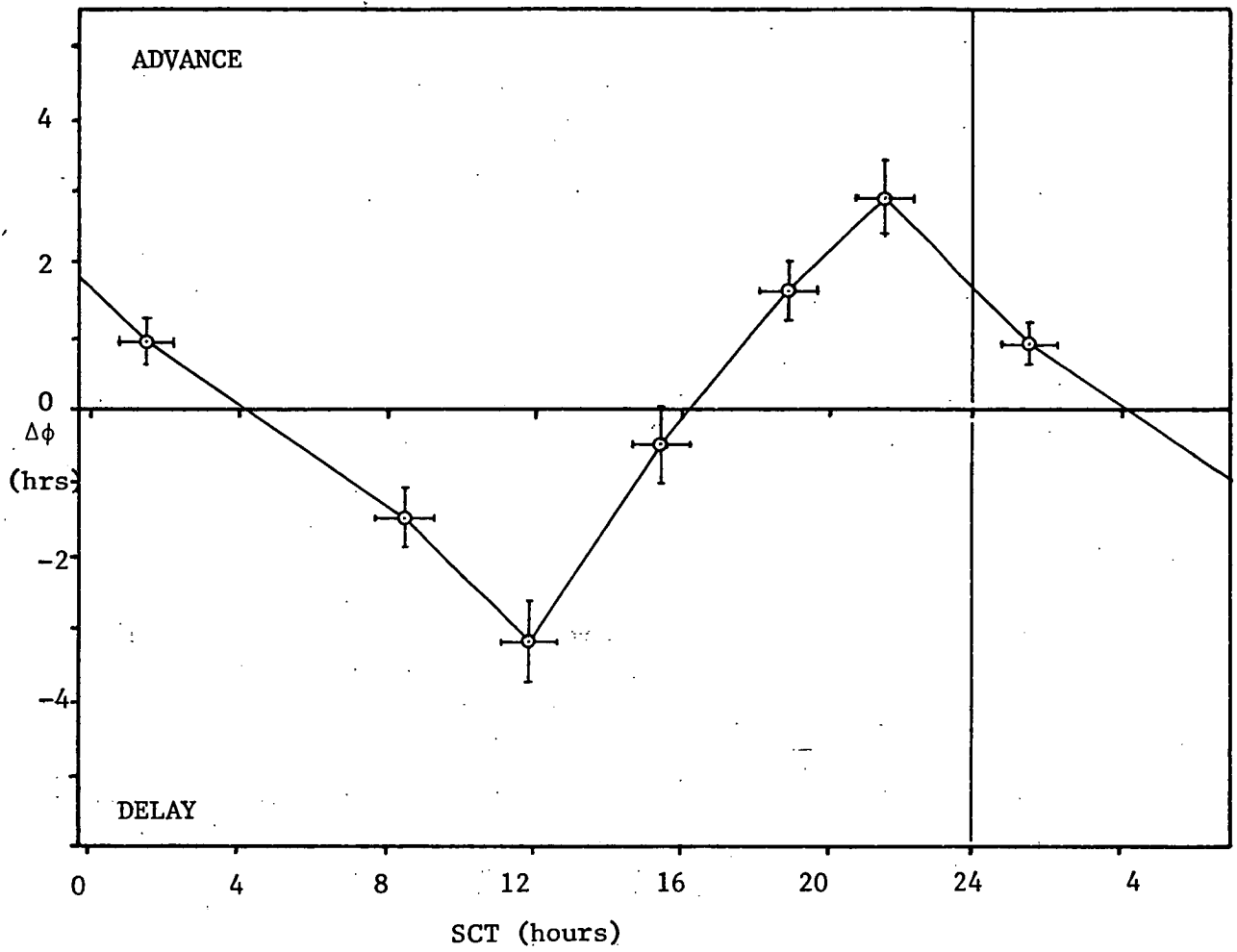


Fig. 7.2. PRC for 2 hour, 2.5 mM azide pulses. Vertical bars are s.e. bars for the means of phase change estimates for 5 or 6 leaves. Horizontal bars show the duration of each pulse.

## CHAPTER EIGHT

### EXPERIMENTAL RESULTS. C: PULVINULE CELL POTENTIAL CHANGES

#### 8.1 INTRODUCTION

The studies reported in Chapters 6 and 7 involved the measurement of a single output quantity, i.e. leaf position. It would be helpful if other quantities which also vary in a circadian fashion could be monitored. For example, a second monitored variable may be useful in distinguishing between those treatments which affect the circadian oscillator from those which merely alter the externally observed expression of the rhythm. If a particular treatment changes one observed rhythm but not another then it is obviously not the basic oscillator itself which is being affected (see section 2.3).

Racusen and Satter (1975) have shown that cells on opposite sides of the pulvini in *Samanea saman* undergo circadian variations in membrane electrical potential, and earlier work by Target (1973) as reported by Scott and Gulline (1975) suggested that similar oscillations occurred in cell membrane potential in *Trifolium pulvinules*. In this case it is not immediately obvious whether the membrane potential is merely driven through cyclic changes by the biological clock, as is leaf angle, or alternatively whether the membrane potential rhythm constitutes part of the basic oscillator itself. Circadian changes in membrane potential can, at least, mean that a second output may possibly be monitored; at best it may permit

a view into the operation of the clock itself. For these reasons a study of electrical changes occurring across the membranes of pulvinule cells in clover was undertaken.

Problems associated with the study of cell electrical potentials using glass pipette microelectrodes are well known and are well documented in the literature. Characteristics of such electrodes such as tip potential and electrical resistance and capacitance have been examined in depth by a number of authors (see Frank and Becker, 1964; Geddes, 1972). A particular problem that was examined prior to the studies reported in this chapter was that of tip potential.

Glass pipette microelectrode tips generally have associated with them an electrical potential difference, usually within the range  $\pm 20$  mV and probably due to the selective permeability to ions of the very thin glass wall in the proximity of the electrode tip. This potential also varies with the composition and concentration of ions in the medium bathing the electrode tip. Thus the tip potential is likely to change on insertion of the tip into a cell. This is likely to be a significant source of error in microelectrode measurements.

Agin and Holtzman (1966) reported that this problem could be largely overcome by the addition of small quantities ( $<10^{-4}$  M) of ions of the heavy metal Thorium to the medium bathing the electrode tip. For this reason a study of the effect of Thorium ions on microelectrode tip potential was conducted and is reported in Appendix 5. The results show that the effect of these ions is not

easily predicted and so they were not included in the bathing medium used in the following studies.

## 8.2 METHOD

### 8.2.1 Electrode Preparation and Potential Recording System

Glass pipette microelectrodes were pulled from glass tubing of 3 mm outside diameter on a vertical microelectrode forge. These were filled with 3 M KCl and tip diameters estimated by the method of Robinson and Scott (1973). The method involved inserting a fine pipette (20 mm tip diameter) into the barrel of the microelectrode. A syringe attached to the pipette was then depressed, causing KCl solution to flow into the electrode. The solution moved toward the tip by capillary action, its rate of advance providing a measure of the electrode's tip diameter. Microelectrodes with tip diameters greater than 0.5  $\mu\text{m}$  were discarded. Electrode resistance and tip potentials were measured as described below. Electrodes had resistances and tip potentials which were typically 8 to 15 megohms and 5 to 10 mV respectively. Those with resistances greater than 30 megohms and tip potentials larger than 20 mV were rejected.

The technique adopted for measuring potentials and monitoring resistance was that of Lassen and Sten-Knudsen (1968). The arrangement is shown schematically in figure 8.1. The medium bathing each excised pulvinule was grounded via a mercury calomel half cell and KCl agar bridge (1). Electrical connections were made to electrodes (2) in a similar fashion. Each electrode was connected to a preamplifier (3) provided with neutralization of input capacitance

(Geddes, 1971, p.178). The outputs of these preamplifiers were then fed to a differential input amplifier (4). Monitoring of resistance was accomplished as follows.

The output of a 1 KHz square wave generator was integrated and then rectified to produce an intermittent triangular voltage (5). This triangular voltage was applied to each preamplifier input via potential dividers (6) and small (1 pF) capacitors (7). This capacitance, coupled with the electrode resistance, differentiated the triangular voltage, producing biphasic rectangular voltage pulses (8) at each preamplifier input. The amplitudes of these signals were proportional to the resistance between each input and ground. A 10 megohm fixed resistance could also be joined between each input and ground to provide a means of calibrating these signals.

The magnitudes of the pulses were equalised by adjusting one or both of the potential dividers (6). With both electrodes in the bathing medium and the biphasic pulses optimally equalized the output from the differential amplifier consisted of only small, sharp spikes arising due to minor differences in the rise times of the two waveforms. An increase in resistance at either electrode caused by, for example, the penetration of a cell, resulted in the appearance of a biphasic signal at the differential amplifier output of an amplitude proportional to the increment in resistance. The concomittant potential change in the case of cell impalement resulted in a displacement of this signal. The amplifier output was monitored on a Solartron oscilloscope and recorded using a Rikadenki 'Tobshin Electron' chart recorder, the recorder having a sufficiently integrative behaviour to remove the relatively high frequency biphasic pulses.



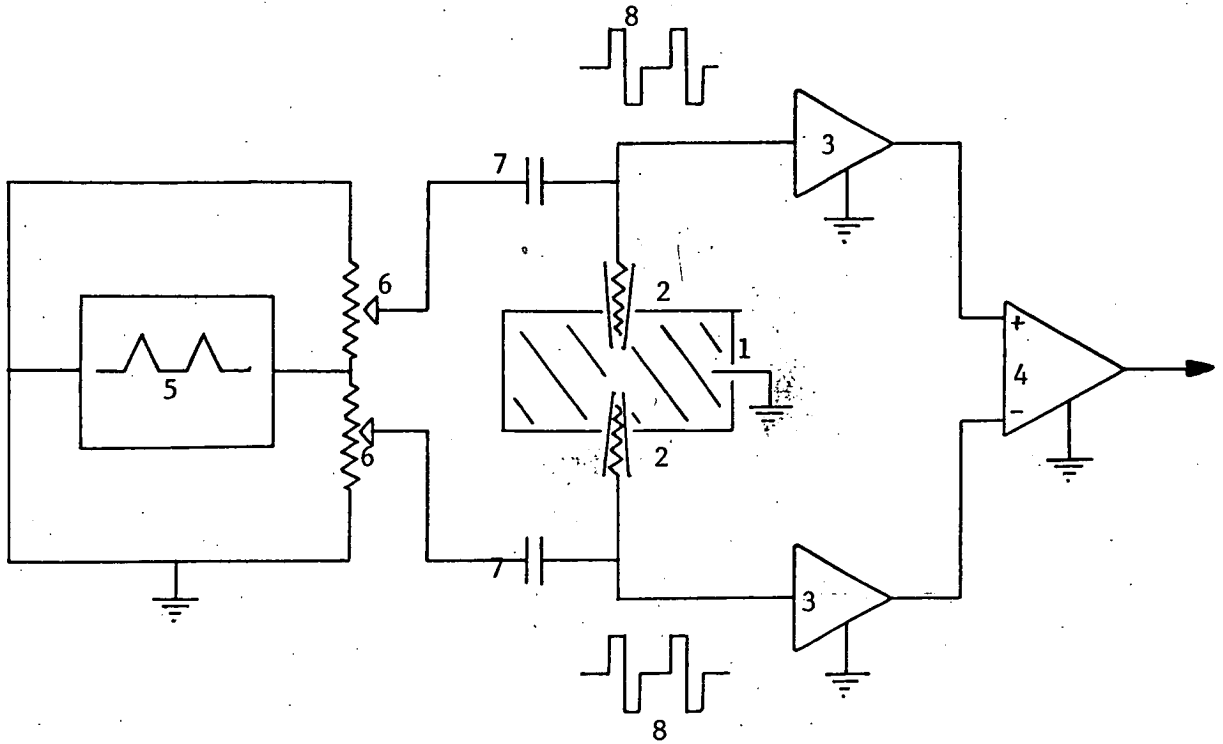


Fig. 8.1. Schematic diagram of the circuit used for measuring electrical potential differences and resistances. See text for a description.

### 8.2.2 Preparation and Mounting of Specimens

Plants were initially in a growth cabinet which was divided into two compartments, one of which was in darkness and the other illuminated by white fluorescent and incandescent lamps (intensity 2200 lux). The plants were spaced at regular intervals around a horizontal circular platform which was partly in each compartment and which rotated about a vertical axis. Rotation of the platform in  $15^{\circ}$  steps each hour resulted in each plant passing 12 hours in darkness and 12 hours in light. The phasing of the light-dark cycle for each plant depended on its position on the platform. Thus at any time a plant could be selected which was at any desired stage of its biological cycle. Immediately preceding each experiment plants were transferred from the growth cabinet to the room in which electrical measurements were performed. The pulvinule of the centre leaflet on the second fully opened leaf on each shoot was used in these studies. This was excised to approximately a 1 cm length and mounted on a perspex holder in a flowing solution of 1mM KCl. This holder could also be rotated so that the same electrode could be driven into either adaxial or abaxial tissue as desired. The excised pulvinule was viewed through a 100 x magnification binocular microscope and illuminated with a 30w Olympus microscope lamp equipped with a green filter (filter passband 5100 to 5900 Angstroms). For plants in the light part of their light-dark cycle, ambient fluorescent lighting of about 2000 lux was also supplied.

### 8.2.3 Observation of Potential Changes

Microelectrodes were driven approximately 50  $\mu\text{m}$  into the pulvinule tissue with the aid of a micromanipulator so that they passed through the epidermal cell layer into the cortex. Because of the density of the tissue it was not possible to visually control the position of the electrode tip and this had to be inferred from the potential and resistance readings. When a large negative potential was observed which was maintained to within 1 mV for more than two minutes it was taken to indicate that the electrode tip had made a satisfactory penetration of a cortical cell and the reading was assumed to be the transmembrane potential. In other locations of the electrode tip potentials 20 to 30 mV less negative were observed. These readings were assumed to be junction potentials produced at damaged cells and were discarded.

An increase in resistance of a few megohms was generally noted when a successful cell penetration occurred. In each case where a fall was observed it was taken to indicate that the probe tip had broken and the potential reading was disregarded. Large increases in electrode resistance were occasionally also observed and it was assumed that these were due to partial blockage of the electrode tip. Since such blockages can cause large changes in tip potential (see Appendix 5) and therefore large errors in potential measurements, potential readings corresponding to resistance changes in excess of 30 megohms were also rejected.

## 8.3 RESULTS

The electrical potentials (interior negative) for cortical cells on both adaxial and abaxial sides of the pulvinule are shown

in figure 8.2. Each point is the average of 5 to 11 readings on separate pulvinules. The average potential for a full cycle was -81.6 mV for adaxial and -86.4 mV for abaxial cells. In the swollen state both adaxial and abaxial cells were initially hyperpolarized but they depolarized subsequentially, the potential changing most rapidly about 3 hours after the cells expanded.

The resistance changes measured on cell penetration varied markedly, but were generally within the range 0.5 to 10 megohms. As was suggested in the previous section this was probably due in part to some blockage of electrode tips by cell debris. It is possible that the membranes of *Trifolium* pulvinule cells also undergo periodic changes in resistance. If such is the case these changes were effectively disguised by the large random variations in measured resistance.

Experiments were also performed in which the light period was extended for a further 12 hours. In these studies potential readings for adaxial and abaxial cells did not differ significantly from those in the 12 hours light, 12 dark cycle. Thus the observed potential changes are not merely a passive response to the light cycle, but appear to be circadian in nature.

#### 8.4 DISCUSSION

*Trifolium* pulvinules are not an ideal material for micro-electrode studies as they are capable of movement and the cells are thick walled. For these reasons there were difficulties firstly in

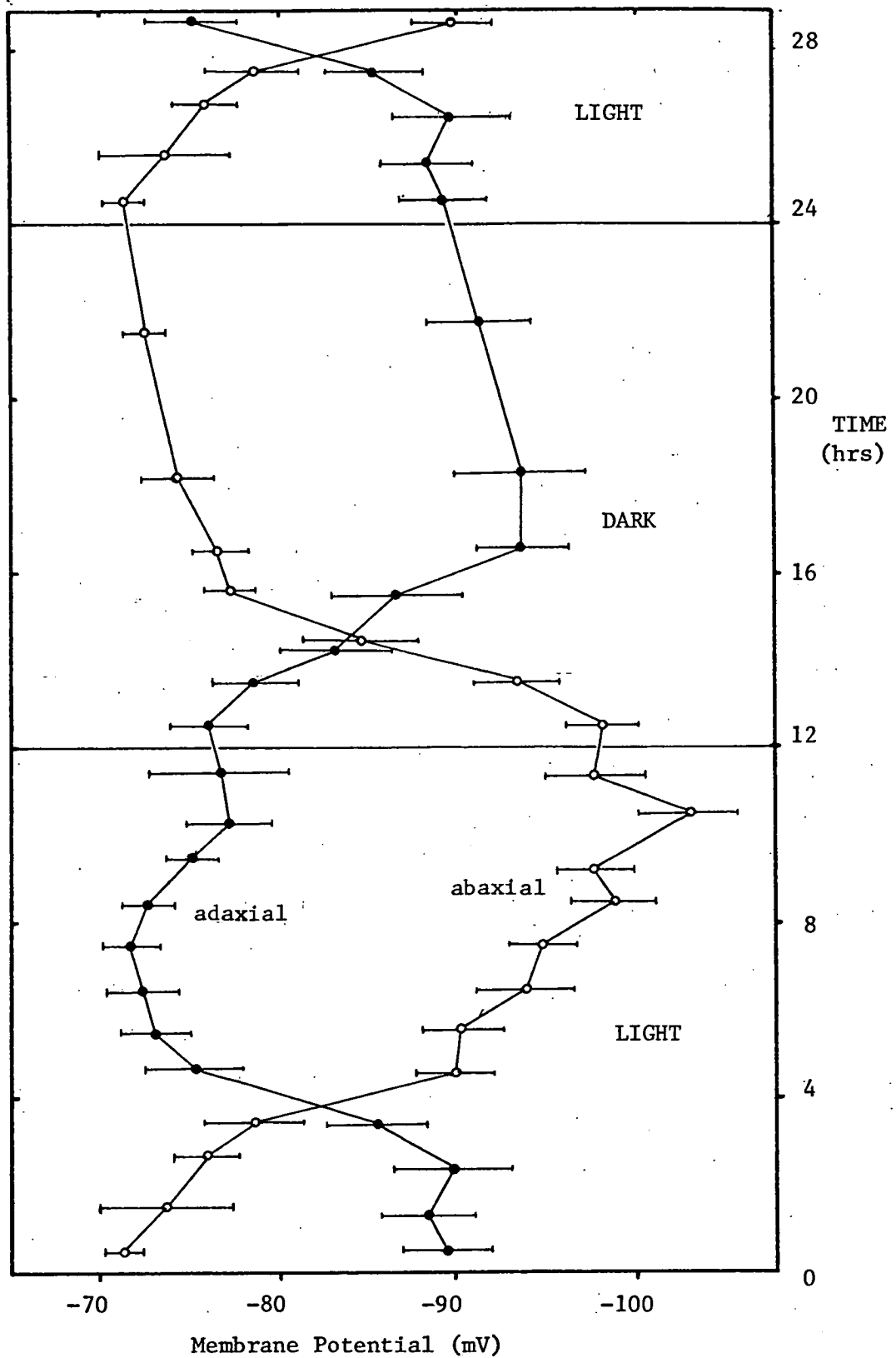


Fig. 8.2. Transmembrane potential (interior negative) for cortical cells in adaxial and abaxial pulvinule tissue in a 12 hours light, 12 dark cycle. Bars are s.e. bars for the means of from 5 to 11 measurements. Data for the first 5 hours are repeated.

impaling cells without breaking the electrodes, and secondly in maintaining a steady potential reading for longer than about 10 minutes. It would be useful to follow potential changes in one pulvinule through several circadian cycles, or through several cycles of a forced oscillation, but this does not seem possible using present microelectrode techniques.

Although pulvinule cell membrane potential changes proved unsuitable for routine monitoring in studies of the circadian oscillator, the results obtained are of considerable interest when combined with results for ion influx studies in *Trifolium* pulvinule tissue reported by Scott et al (1976). These studies, using  $^{42}\text{K}$  as a tracer for potassium show that the influx of this ion into *Trifolium* pulvinule cells has a strong circadian rhythm. The changes in the adaxial and abaxial components are similar but opposite in phase. In a 12 hours light, 12 dark cycle potassium influx changes were observed to precede leaf opening and closing by approximately two hours, the influx reaching a maximum just prior to cell expansion and a minimum prior to cell contraction.

Experiments using  $^{45}\text{Ca}$  and  $^{22}\text{Na}$  as tracers for the movement of calcium and sodium revealed that influxes for these ions did not vary significantly in the course of the light dark cycle. Later results obtained by Scott and Gulline (unpublished) using Bromine (82) as a tracer for the chloride ion indicate that chloride influx changes occur concomitantly with potassium influx changes.

It thus appears that the potential changes which occur approximately 3 hours after the change in light conditions are not directly due to changes in either potassium or chloride ion influx. Further experiments are therefore required to determine the immediate cause of these membrane potential changes.

---

## CHAPTER NINE

### DISCUSSION OF RESULTS

#### 9.1 INTRODUCTION

Some discussion of the experimental data concerning clover leaf movement and its relationship to light changes and chemical treatments was offered in conjunction with the presentation of these data. The current chapter is intended as a discussion of the general implications of these results in terms of the model proposed in section 6.5 and in relation to the mathematical and physical models for circadian oscillators which have been proposed by others (see section 2.4).

#### 9.2 LINEARITY OF THE SYSTEM

During the last three decades there has been considerable conjecture concerning the nature of circadian oscillators; in particular whether their conduct may be more readily approximated by simple harmonic (or pendulum) oscillators or alternatively by relaxation oscillators (see Winfree, 1975). Some investigators have favoured a relaxation oscillator model (e.g. Bunning, 1964), citing the behaviour of circadian systems at low temperatures as indicative of this type.

A relaxation oscillator moves through a tension phase, requiring the expenditure of metabolic energy, until a certain state is reached, whereupon a discharge or relaxation phase is initiated. The oscillator remains in the relaxation phase until the energy stored



in the tension phase has been exhausted, at which time a new tension phase commences.

On chilling, many circadian rhythms, including that of *Trifolium* (Yong, 1972) continue to a certain phase of the cycle, whereupon the observed quantity ceases to change. When returned to conditions favouring the utilization of metabolic energy these oscillations then continue from that final phase. This phase has been interpreted as the phase of the oscillation which involves the least energy, i.e. the terminal point for a relaxation phase in the oscillation. In addition at temperatures approaching that required for suppression of the rhythm rapid oscillations (5.5 hour period in clover) are sometimes observed. These have been interpreted as due to the aborting of tension phases in the rhythm resulting from the limited availability of metabolic energy.

Notwithstanding, the response of the clover leaf oscillator to sinusoidal log-light variations provides good evidence for a basic oscillator of the simple harmonic type. The Bode plots (fig. 6.13) indicate a continuous change in phase and amplitude of the response to a forcing oscillation with the frequency of that oscillation. Secondly the amplitude spectra for the leaf records generally show a peak corresponding to a damped oscillation at the natural frequency, concomittant with the response at the forcing frequency. These features are to be expected from a simple harmonic oscillator, but are unlikely to be produced by an oscillator of the relaxation type.

The circadian oscillator in the model presented here (fig. 9.1) is essentially a damped simple harmonic oscillator. The agreement between the predicted light pulse PRC for this and the experimentally obtained PRC for the clover leaf oscillator (see fig. 6.16) provides further support for the model.

Much of the harmonic content of the observed oscillation may arise due to such factors as the variation of the sensitivity of the system to light intensity changes with background light intensity, and to variation of the leaf response with leaf angle. These may be regarded as nonlinear features of the input and output stages of the model. The presence of these nonlinearities is indicated by the experimental data in section 6.7.

There is, however, some evidence that the circadian oscillator itself has some nonlinear properties. Firstly the damping of the natural oscillation is more severe in the presence of a large forcing signal than in its absence; i.e. the oscillator entrains more rapidly to a larger amplitude signal. Furthermore, the frequency characteristics suggest an oscillatory system with an even greater damping coefficient, namely  $0.67 \text{ (days)}^{-1}$ , compared with a typical experimental result of about  $0.2 \text{ (days)}^{-1}$  under the conditions for which the frequency characteristics were obtained.

A final point concerns the small (yet significant) change in the natural frequency which occurred when the forcing frequency was in the proximity of a natural frequency harmonic. As is reported in section 6.4 and listed in table 6.4, the natural frequency, typically

0.855 c/d ( $\pm$  0.015 s.e.), was actually about 0.833 c/d for forcing frequencies of 1.67, 2.5 and 3.33 c/d. No separate circadian component was detected when the forcing frequency was 0.833 c/d, nor when the input was a large amplitude sinusoid at 1 c/d (see section 6.3).

This shift in the frequency of the natural oscillation and suppression of its appearance when the input is large may result from the presence of a nonlinear element of the form described in section 6.2 within the feedback loop representing the oscillator. Such an element is also required to generate the observed changes in frequency and waveform with background light intensity.

The feedback loop in the model which represents the circadian oscillator consists of two exponential lag elements. No more than two lags were required to provide agreement with the system Bode plots. This does not, however, preclude the possibility of more than two such elements existing in the loop. Only when a means is found for opening the loop so that its 'open loop' frequency response (section 3.8) may be determined will the actual number of lags in the loop become apparent.

### 9.3 THE SECONDARY LOOP

The frequent presence of rapid oscillations (9-10 c/d) in leaf records necessitated the inclusion in the model of some mechanism for their production. Hence a secondary feedback loop, arranged to produce damped oscillations at 9.5 c/d, was incorporated in the model.

It was considered that this secondary loop might represent an interaction between cells on the adaxial and abaxial sides of each clover pulvinule. To test this possibility longitudinal incisions were made through the stele of some leaf pulvinules in an attempt to physically separate adaxial and abaxial tissue. This experiment proved unsuccessful in that the leaf pulvinules are very small (typically 1 mm diameter) and it was extremely difficult to incise each stele longitudinally without severing it. Leaves treated in this fashion invariably perished.

As an alternative experiments were conducted in which either adaxial or abaxial tissue was removed from clover pulvinules. Such removal of tissue considerably weakens a pulvinule, so to avoid further damage due to handling the excisions were performed with each leaf mounted in an anglemeter. For this reason the depth and extent of each excision could not be determined until the completion of the experiment.

These leaves were treated with a small amplitude rectangular wave light variation (as in section 6.3) in an effort to initiate rapid leaf oscillations, or with a 10 c/d sinusoidal log-light variation in order to determine whether any alteration in the high frequency response had occurred as a result of the excisions. The results were as follows.

The leaf oscillation, for both abaxial and adaxial excisions, was approximately in phase with the rectangular wave light variation. Rapid oscillations were not apparent. Leaves with abaxial tissue

removed oscillated about a mean leaf angle of  $130^{\circ}$  ( $\pm 4^{\circ}$  s.e. for 3 leaves). The amplitude of this oscillation was small ( $11^{\circ} \pm 2^{\circ}$  s.e.). In contrast leaves with adaxial tissue removed oscillated about a mean angle of  $185^{\circ}$  ( $\pm 5^{\circ}$  s.e. for 5 leaves) with considerably larger amplitude ( $31^{\circ} \pm 4^{\circ}$  s.e.).

Important results arising from this experiment are firstly that apart from the absence of high frequency oscillations, the leaf response appears to be affected little by the removal of adaxial tissue, and secondly that adaxial and abaxial tissue respond in converse fashion to changes in light intensity. That is, light causes cells on one side to contract and those in the other to expand. However, since rhythmic movement of leaves with most abaxial tissue removed was of very small amplitude the possibility that the phasing of the oscillations is controlled by the abaxial tissue alone cannot be rejected.

For the 10 c/d treatment leaves with adaxial tissue removed responded to the light variation, the leaf record spectra showing a 10 c/d component of mean amplitude  $7^{\circ}$  ( $\pm 1^{\circ}$  s.e. for 4 leaves) and with a mean phase of  $-97^{\circ}$  ( $\pm 6^{\circ}$  s.e.). These results are not significantly different from the results obtained for whole pulvinules (section 6.4). In contrast three leaves with abaxial tissue removed showed no significant response to the light variation. Since the mean leaf angle for these was  $126^{\circ}$ , this negative result might be due to the decreased sensitivity of the leaf to light changes when in the open position (see section 6.7.2).

While not proving that the secondary loop is due to an interaction between cells on the adaxial and abaxial sides of each pulvinule, the above results do lend support to the suggestion. Spontaneous rapid oscillations commonly observed in records for leaves treated with a 1 c/d rectangular wave light variation did not occur when one or other side of the pulvinule had been excised. Furthermore the mean response to the 10 c/d signal with adaxial tissue removed was similar to that for leaves with undamaged pulvinules. Thus the absence of spontaneous high frequency oscillatory behaviour is not due to the inability of excised leaves to oscillate at these frequencies, since they can still be forced to do so.

#### 9.4 INTERPRETATION OF THE MODEL

The model proposed in section 6.4 as a linear approximation to the system relating light changes to leaf movement may be divided into three sections. These are:

- (a) a *light input stage* containing two or three phase advance elements,
- (b) the *circadian oscillator* itself, and
- (c) an *output stage* containing the secondary loop (see fig. 9.1).

As has been indicated the results suggest that a more complete model would require some modification to account for the nonlinear behaviour displayed by each of these sections.

At this point it must be emphasised that the model represents the behaviour of a typical clover pulvinule, not of an individual cell in that pulvinule. Each cell may contain a system relating light variations to cell conformational changes, so the model must

be regarded as representing the behaviour of a large number of these systems functioning in a coupled or integrated fashion.

Bearing in mind the above note, questions may still be asked as to whether the elements in the model may be identified with particular stages or processes in a physical system. Light entering each system presumably affects it via photosensitive pigments. Adaptation of photoreceptors to light changes is commonplace in biology. For example, the output of retinal neurons increases markedly with a large increase in incident light, but then decreases toward a level in the vicinity of the original value as the light converts the photosensitive pigment rhodopsin from an active to an inactive form. Such adaptive behaviour may be represented by phase advance elements (Milsum, 1966, p.226) and it is suggested that the phase advance elements in the input stage of the model correspond to the behaviour of the light sensitive system which couples the circadian oscillator to the external light conditions.

The circadian oscillator itself is shown as consisting of two exponential lag elements, the output of each affecting the input to the other. Specification of the phase of the oscillation at any instant requires knowledge of the values of two quantities. For example, for a pendulum oscillator these would be the position and velocity of the pendulum. The mathematical models of Pavlidis (1967) and others (e.g. Berde, 1975) have also involved two such 'state variables', although these are presented as interacting in a manner which is rather more complex than that which is suggested here.

A biological oscillator consisting of two lag elements might be interpreted in the following fashion. Suppose the input is the rate of accumulation ( $\dot{x}$ ) of some substance  $x$ , through either synthesis or a net influx. The output of the first lag then represents the concentration of the substance  $x$  and thus in turn is postulated to control the rate of accumulation of a second substance  $y$ . The concentration of  $y$  is related to its accumulation rate by the second lag element. The presence of  $y$  is then assumed to inhibit the accumulation of  $x$ , thus completing the feedback loop (see fig. 9.2). Since in practice it is unlikely that the effect of  $x$  on the accumulation of  $y$  would be directly proportional to the concentration of  $x$  (and visa versa), some nonlinear behaviour is to be expected from such a system.

The quantities  $x$  and  $y$  may represent enzyme and substrate in a purely biochemical oscillator as suggested by Pavlidis (1971) or alternatively may represent ions or molecules which are actively transported across biological membranes (see Njus et al, 1976). A biochemical model for the circadian oscillator suggested by Cummings (1975) may be arranged in the form of a feedback loop containing two lag elements, as shown in figure 9.2. Light is regarded as affecting the activity of the enzyme adenyl cyclase (through intermediaries) which converts ATP to cAMP (cyclic AMP). The cAMP is then converted to AMP by the enzyme phosphodiesterase (PDE). The AMP then inhibits the activity of adenyl cyclase, thus completing the feedback loop.

As indicated in chapter 2 the effects of ethanol, deuterium oxide and other chemicals on circadian rhythms seem to suggest the



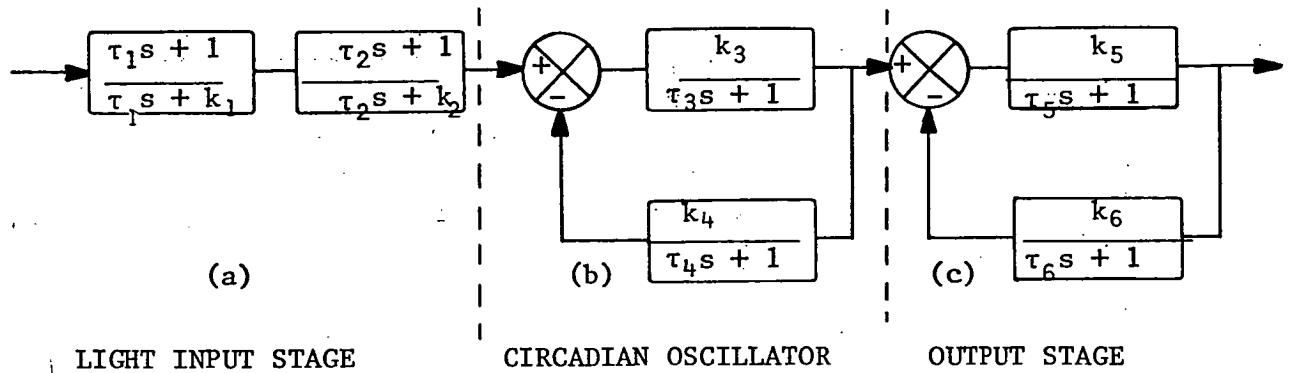


Fig. 9.1. The model proposed in section 6.5. The model may be divided into the above three parts as described in section 9.3.

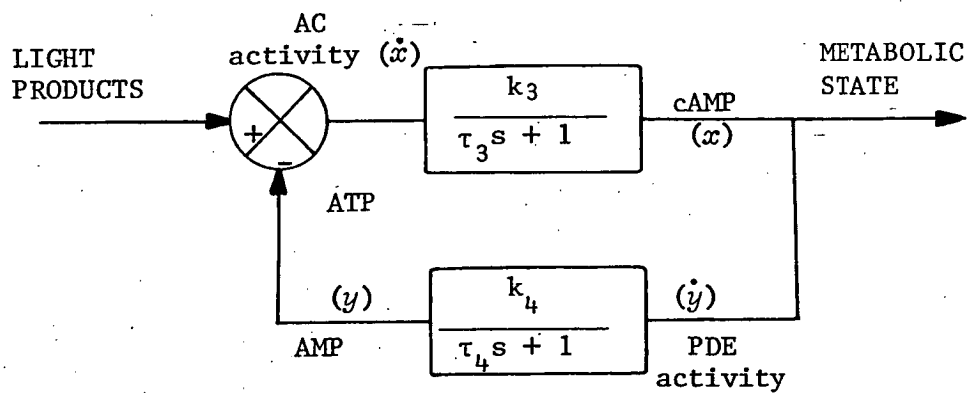


Fig. 9.2. Feedback loop representation of Cummings' biochemical model. AC = adenylyl cyclase. See text for a description.

participation of membranes in the circadian oscillator, but whether the membranes involved are the internal cell or organelle membranes (Sweeney, 1974) or the cell plasma membrane itself is not immediately apparent.

Njus et al (1976) considered evidence for the involvement of plasma and organelle membranes in the biological clock, and noted that if oscillating ion concentrations are generated by the plasma membrane as part of the time keeping process then fluctuations in external ion concentrations should affect this time keeping. Potassium (K) and chloride (Cl) ion influxes have been shown to vary in a circadian fashion in clover pulvinules (Scott et al, 1974) yet results presented in chapter 7 indicate that neither continuous KCl nor KCl pulses have a marked effect on the clover leaf rhythm when applied to excised leaf petioles. The available data, and in particular the *Acetabularia* rhythm paradoxes (see section 2.4) seem to suggest that internal cell membranes are more likely candidates for participants in the biological clock rather than the plasma membrane.

If ion fluxes across membranes are to be interpreted as part of the circadian oscillator then  $x$  and  $y$  of figure 9.2 may be regarded as ions or molecules whose respective fluxes ( $\dot{x}$  and  $\dot{y}$ ) are each controlled by the concentration of the other. Possible candidates for  $x$  and  $y$  are potassium, chloride and hydrogen ions and biochemicals such as the cAMP of Cumming's model.

The possibility that the distribution of membrane proteins and their lateral diffusion might constitute one of these state variables has been considered. However, such diffusion has been shown to be rapid (time constants of the order of minutes - Jain and White, 1977) and it therefore seems unlikely that such changing membrane properties could in themselves account for one lag element in the model. Nonetheless, presuming a two lag feedback loop is already present, a third, small lag due to changing membrane properties could play an important role in the biological clock. Simulation of such a system on an HP97 calculator indicates that small changes in the time constant for such an additional lag element results in large fluctuations in the damping rate for the oscillations generated by the system.

Finally, it has been suggested that the secondary loop corresponds to an interaction between cells comprising the adaxial and abaxial tissue of each pulvinule. If indeed the plasma membrane is not part of the biological clock, the first lag element in the secondary loop may possibly represent the relationship between a clock controlled trans-plasma membrane ion flux (input) and resulting ion concentration difference (output). This concentration difference would result in water movement due to osmosis and hence in changes in cell volume. Leaf movement would then automatically follow.

The feedback lag element in the secondary loop might then be interpreted as representing a feedback path which synchronizes changes occurring on the adaxial and abaxial sides of each pulvinule,

but which is also capable of producing spontaneous oscillations on occasion. Evidence for or against this tentative suggestion might be obtained from further studies of excised pulvinules.

---

## CHAPTER TEN

### CONCLUDING REMARKS

The results described in this thesis were obtained through the construction of a precise and efficient means for recording clover leaf angular changes and for controlling, recording and maintaining the environmental conditions surrounding each clover plant. The leaf records were examined and interpreted by applying the techniques of spectral analysis and of control theory. A model, which represented a linear approximation to the system relating light changes to clover leaf movement, was thereby developed. The frequency response and pulse phase response for this model were in substantial agreement with the response data for the clover leaf oscillator. The recording and analytical techniques described are not restricted in their application to the study of the system controlling leaf movement in clover but may be readily adapted for the investigation of a wide range of systems in other organisms.

Analysis of leaf records following chemical treatments showed that the clover leaf rhythm undergoes phase changes, both positive and negative, following the application of pulses of sodium azide. Frequency changes caused by the presence of ethanol were also recorded. Repeated KCl and NaCl pulses did not entrain the clover leaf oscillator, but did have some effect on leaf movement. Finally the damping of the circadian leaf rhythm in continuous light was shown to decrease markedly if the (excised) leaves were supplied with sucrose.

Attempts to continuously monitor pulvinule cell transmembrane potential changes proved unsuccessful. However, the potential for both abaxial and adaxial cells was shown to vary in a circadian fashion. It is suggested that studies involving the continuous monitoring of surface potential changes on each side of leaf pulvinules might be more readily performed, and could provide data concerning electrical changes occurring in individual pulvinules during both natural and forced leaf oscillations.

The experiments described in chapter 9, involving the light treatment of clover pulvinules following the surgical removal of tissue segments, were chronologically the last performed in these studies. They provided some worthwhile results and further work in this area could supply important information pertaining to the nature of the clover leaf oscillator.

The cabinet control circuitry described in this thesis permitted the varying of both light intensity and temperature. Only light was varied in the studies described, temperature being maintained at 20°C. Future studies might involve the varying of temperature, or of both light and temperature simultaneously. For example an analysis of the frequency response of the clover leaf system to sinusoidal temperature changes would be a worthwhile undertaking, since temperature changes provide a different input to the clover leaf system.

Finally the linearized model might be extended to encompass the nonlinear features of the clover leaf system indicated in chapter 9. Computer simulation of such a model should permit the prediction of clover leaf movements in response to a wide range of light inputs.

- 0 - 0 - 0 - 0 - 0 - 0 - 0 - 0 - 0 - 0 -

APPENDIX 1

The residual variance  $V(\hat{A}, \hat{B}, \omega)$  is required for each least squares estimate of A and B at each  $\omega$  (see section 4.3.1).

$$\begin{aligned} \text{Now } V(\hat{A}, \hat{B}, \omega) &= (1/n) \sum_{t/T=0}^{n-1} (f_t - \hat{A} \cos \omega t - \hat{B} \sin \omega t)^2 \\ &= (1/n) \{ \sum (f_t)^2 + \hat{A}^2 \sum (\cos \omega t)^2 + \hat{B}^2 \sum (\sin \omega t)^2 \\ &\quad + 2\hat{A}\hat{B} \sum \cos \omega t \sin \omega t - 2\hat{A} \sum f_t \cos \omega t - 2\hat{B} \sum f_t \sin \omega t \}. \end{aligned}$$

Using  $a = (2/n) \sum f_t \cos \omega t$  and  $b = (2/n) \sum f_t \sin \omega t$  and defining  $\alpha = (\sin 2 \omega T)/2\omega T$  and  $\beta = (\sin \omega T)^2/\omega T$

then for  $n \gg \omega T$ ,

$$\begin{aligned} V(\hat{A}, \hat{B}, \omega) &= (1/n) \sum (f_t)^2 + \hat{A}^2 (1 + \alpha)/2 + \hat{B}^2 (1 - \alpha)/2 \\ &\quad + \hat{A}\hat{B}\beta - \hat{A}a - \hat{B}b \end{aligned} \quad \dots\dots\dots (A1)$$

Also from section 4.3.1,

$$\hat{A} = p\{a(1 - \alpha) - b\beta\}$$

$$\text{and } \hat{B} = p\{b(1 + \alpha) - a\beta\}$$

Rearranging gives:

$$a = \hat{A} (1 + \alpha) + \hat{B}\beta$$

$$\text{and } b = \hat{B} (1 - \alpha) + \hat{A}\beta,$$

and substituting for a and b in equation (A1);

$$V(\hat{A}, \hat{B}, \omega) = (1/n) \sum (f_t)^2 - \hat{A}^2 (1 + \alpha)/2 - \hat{B}^2 (1 - \alpha)/2 - \hat{A}\hat{B}\beta$$

Defining:  $\hat{R} \cos \hat{\phi} = \hat{A}$  and  $\hat{R} \sin \hat{\phi} = \hat{B}$  gives:



$$V(\hat{A}, \hat{B}, \omega) = (1/n) \Sigma (f_t)^2 - \hat{R}^2 (1 + \alpha \cos 2\hat{\phi} + \beta \sin 2\hat{\phi})/2$$

$$\begin{aligned} \text{Now } \alpha \cos 2\hat{\phi} + \beta \sin 2\hat{\phi} &= \{\sin 2\omega T \cos 2\hat{\phi} + 2(\sin \omega T)^2 \sin 2\hat{\phi}\}/2\omega T \\ &= (\sin 2\omega T \cos 2\hat{\phi} - \cos 2\omega T \sin 2\hat{\phi} + \sin 2\hat{\phi})/2\omega T \\ &= \{\sin 2(\omega T - \hat{\phi}) + \sin 2\hat{\phi}\}/2\omega T \\ &= \{\sin \omega T \cos (\omega T - 2\hat{\phi})\} / \omega T \end{aligned}$$

Thus:

$$V(\hat{A}, \hat{B}, \omega) = (1/n) \Sigma (f_t)^2 - (\hat{R}^2/2) \{ 1 + \sin \omega T \cos(\omega T - 2\hat{\phi}) / \omega T \}$$

Similarly, by substituting for  $\hat{A}$  and  $\hat{B}$  rather than for  $a$  and  $b$  in equation (A1) and defining:  $a = r \cos \bar{\phi}$  and  $b = r \sin \bar{\phi}$  the following result follows:

$$V(\hat{A}, \hat{B}, \omega) = (1/n) \Sigma (f_t)^2 - (r^2/2) \{ 1 - \sin \omega t \cos(\omega t - 2\bar{\phi}) / \omega T \}$$


---

APPENDIX 2

Suppose the quantity  $y$  depends on several observed variables  $x_1, x_2, \dots, x_n$

$$\text{i.e. } y = f(x_1, x_2, \dots, x_n)$$

The error  $\Delta y_i = y_i - \bar{y}$  resulting from errors  $x_{1i}, x_{2i}, \dots, x_{ni}$  in the  $i$ 'th measurement of the  $n$  values may be represented by:

$$\Delta y_i = (\partial y / \partial x_1) \Delta x_{1i} + (\partial y / \partial x_2) \Delta x_{2i} + \dots + (\partial y / \partial x_n) \Delta x_{ni}.$$

If the variance of  $y$  estimated from  $m$  measurements of  $y$  is defined

$$\text{as: } \text{var } y = (1/m) \sum_{i=1}^m (\Delta y_i)^2,$$

$$\text{then } \text{var } y = (1/m) \sum_{i=1}^m \{ (\partial y / \partial x_1) \Delta x_{1i} + \dots + (\partial y / \partial x_n) \Delta x_{ni} \}^2$$

Squaring gives:

$$\begin{aligned} \text{var } y &= (\partial y / \partial x_1)^2 \text{var } x_1 + (\partial y / \partial x_2)^2 \text{var } x_2 + \dots + (\partial y / \partial x_n)^2 \text{var } x_n \\ &+ 2(\partial y / \partial x_1)(\partial y / \partial x_2) \text{cov}(x_1, x_2) + \dots + 2(\partial y / \partial x_1)(\partial y / \partial x_n) \text{cov}(x_1, x_n) \\ &+ 2(\partial y / \partial x_2)(\partial y / \partial x_3) \text{cov}(x_2, x_3) + \dots \text{etc.}, \end{aligned}$$

$$\text{where } \text{var } x_j = (1/m) \sum_{i=1}^m (\Delta x_{ij})^2$$

$$\text{and } \text{cov}(x_j, x_k) = (1/m) \sum_{i=1}^m \Delta x_{ij} \Delta x_{ik}, \quad j, k \text{ integers}$$

Now using the notation in chapter 4,

$$r = (a^2 + b^2)^{1/2}$$

$$\begin{aligned}
 \text{Thus var } r &= (\partial r / \partial a)^2 \text{ var } a + (\partial r / \partial b)^2 \text{ var } b \\
 &\quad + 2(r \partial / \partial a)(\partial r / \partial b) \text{ cov } (a, b). \\
 &= (a/r)^2 \text{ var } a + (b/r)^2 \text{ var } b + (2 a b / r^2) \text{ cov } (a, b).
 \end{aligned}$$

From section 4.5.2

$$\text{var } a = (2\sigma^2/n)(1 + 3 B^2/r^2)$$

$$\text{var } b = (2\sigma^2/n)(1 + 3 A^2/R^2)$$

$$\text{and cov } (a, b) = (-6\sigma^2/n)(AB/r^2)$$

For  $n > \omega T \gg 1$ , A and B are approximately given by a and b.

Furthermore as  $\omega T$  becomes larger a tends to A and b to B. Therefore, it seems reasonable to replace A, B and R in the above expressions with a, b and r.

Thus:

$$\begin{aligned}
 \text{var } r &= (a/r)^2 (2\sigma^2/n)(1 + 3b^2/r^2) + (b/r)^2 (2\sigma^2/n)(1 + 3a^2/r^2) \\
 &\quad - (2ab/r^2)(6\sigma^2/n)(ab/r^2), \text{ provided } n > \omega t \gg 1 \\
 &= (2\sigma^2/nr^2)\{a^2 + 3(ab/r)^2 + b^2 + 3(ab/r)^2 - 6(ab/r)^2\}
 \end{aligned}$$

$$\therefore \text{var } r = 2\sigma^2/n$$

Similarly, for  $\bar{\phi} = \text{artan } b/a$ ,  $\partial \bar{\phi} / \partial a = -b/r^2$  and  $\partial \bar{\phi} / \partial b = a/r^2$ .

$$\begin{aligned}
 \therefore \text{var } \bar{\phi} &= (2\sigma^2/nr^4)\{b^2(1 + 3b^2/r^2) + a^2(1 + 3a^2/r^2) + 6a^2b^2/r^2\} \\
 &= (2\sigma^2/nr^4)\{b^2 + a^2 + 3(a^4 + 2a^2b^2 + b^4)/r^2\} \\
 &= (2\sigma^2/nr^4)(r^2 + 3r^2)
 \end{aligned}$$

$$\text{Thus var } \bar{\phi} = 8\sigma^2/nr^2.$$


---

APPENDIX 3

The estimates of frequency, amplitude and phase of one sinusoid are affected by the presence of a second sinusoid in the data. This effect may be assessed as follows:-

If the single sinusoid:  $f_1(t) = R_1 \cos(2\pi v_1 t - \phi_1)$  is observed in the interval  $0 \leq t \leq T$ , its Fourier transform is

$$F_1(\omega) = R_1 \text{sinc}(\omega - \omega_1) \{ \cos(\omega - \omega_1 + \phi_1) - j \sin(\omega - \omega_1 + \phi_1) \} + \\ + R_1 \text{sinc}(\omega + \omega_1) \{ \cos(\omega + \omega_1 - \phi_1) - j \sin(\omega + \omega_1 - \phi_1) \}$$

where  $\omega = \pi T v$  and  $\text{sinc}(\omega - \omega_1) = \sin(\omega - \omega_1) / (\omega - \omega_1)$

The two terms in the expression for  $F_1(\omega)$  represent spectral peaks at  $+\omega_1$  and  $-\omega_1$  respectively. Provided there are several cycles of  $f_1(t)$  within the interval  $T$ , the contribution of the second term is small in the vicinity of  $\omega_1$  and initially it will be ignored.

Now suppose a second sinusoid  $(v_2, R_2, \phi_2)$  is added to the first  $(v_1, R_1, \phi_1)$ . The transform becomes

$$F(\omega) = R_1 \text{sinc}(\omega - \omega_1) \cos(\omega - \omega_1 + \phi_1) + R_2 \text{sinc}(\omega - \omega_2) \cos(\omega - \omega_2 + \phi_2) - \\ - j \{ R_1 \text{sinc}(\omega - \omega_1) \sin(\omega - \omega_1 + \phi_1) + R_2 \text{sinc}(\omega - \omega_2) \sin(\omega - \omega_2 + \phi_2) \}$$

and when  $\omega = \omega_1$ , the magnitude of  $F(\omega_1)$  is

$$|F(\omega_1)| = \{ R_1^2 + R_2^2 \sin^2 \Delta\omega + 2R_1 R_2 \sin \Delta\omega \cos(\Delta\omega - \Delta\phi) \}^{1/2}$$

where  $\Delta\omega = \omega_1 - \omega_2$  and  $\Delta\phi = \phi_1 - \phi_2$

In general, the peak that was at  $\omega_1$  will now be shifted from this position. Consider the magnitude of the transform at a small departure  $\partial\omega$  from  $\omega_1$ . That is,

$$|F(\omega_1 + \partial\omega)| = \{(R_1 \text{sinc } \partial\omega)^2 + (R_2 \text{sinc}(\Delta\omega + \partial\omega))^2 + 2R_1R_2 \text{sinc } \partial\omega \text{sinc}(\Delta\omega + \partial\omega) \cos(\Delta\omega + \partial\omega - \Delta\phi)\}^{1/2}$$

It is necessary to find  $\partial\omega$  such that  $|F(\omega_1 + \partial\omega)|$  is maximized. This gives the error in the estimate of frequency for the first component due to the presence of the corrupting component. The amplitude and phase of the combined signal in the position of the displaced peak can now also be determined. These departures from the uncorrupted values (i.e.  $\nu_1$ ,  $R_1$  and  $\phi_1$ ) depend on the relative amplitudes and phases of the two sinusoids, and on the difference in the number of cycles of each within the data window (i.e.  $T\Delta\nu$ ).

Estimates of the shift in peak frequency due to corruption were made by an iterative procedure using an HP97 calculator. For particular values of  $T\Delta\nu$  and  $R_2/R_1$ , these errors in  $\nu_1$ ,  $R_1$  and  $\phi_1$  are functions of  $\Delta\phi$ . The upper and lower limits of the errors are plotted against  $T\Delta\nu$  in Figures A1, A2 and A3 respectively. Since the error in frequency,  $\partial\nu_1$ , is also inversely proportional to  $T$ , the product  $T\partial\nu_1$  is plotted as ordinate in Figure A1.  $T\partial\nu_1$  always lies between +1 and -1 and is the difference in the numbers of cycles of the observed and correct frequencies that would occupy the data

window. Thus if the circadian component (0.85 c/d) in, for example, figure 6.10c has amplitude half that of the forced oscillation (1 c/d) and the combined oscillation is observed for seven days, then  $T\Delta v = 7 \times (1 - .85) = 1.05$ . From Figure A1 the error in  $T\Delta v_1$  lies between 0.10 and -0.20 (depending on the phase relationship of the two sinusoids), so that the frequency error lies between 0.014 c/d and -0.029 c/d. The corresponding error in relative amplitude lies between 0.05 and 0 (Figure A2) and for phase between  $18^\circ$  and  $-35^\circ$  (Figure A3). The limiting errors for phase and amplitude shown in Figures A1 and A2 occur when  $(\Delta\omega - \Delta\phi)$  is a multiple of  $180^\circ$ . The limiting errors in phase (Figure A3) are generally found to occur when  $\Delta\phi$  is close to  $0^\circ$  or  $180^\circ$ .

These graphs show that the ranges of possible errors vary markedly with  $T\Delta v$ , the lobes having the same spacing as the side lobes of the corrupting component. The errors are least for values of  $T\Delta v = 1.5, 2.5, 3.5, \dots$  for both frequency and phase, and for near integral values in the case of amplitude. For all values of  $T\Delta v$  the error increases approximately in proportion to the relative amplitude of the corrupting signal.

It was shown earlier that the full Fourier transform of a sinusoid contains a term centred on  $-\omega_1$  (as well as one at  $+\omega_1$ ), so that its side lobes will have some effect on the estimation of  $\omega_1$ , particularly if the number of cycles in the data window is small. This term may be treated as a second frequency component by the methods discussed in this Appendix. Jackson (1967) showed that if

the data window contains exactly one cycle of a sinusoid, the fractional error in frequency lies between the extremes of .12 and -.16, depending on the phase of the sinusoid. These estimates can be confirmed in Figure A1, where  $T\Delta\nu = 2$  and  $R_2/R_1 = 1$ . It may be noted that for the Maximum Entropy Method the negative frequency term has a similar corrupting influence on frequency estimation (Chen and Stegen, 1974).

The error introduced by this negative frequency component rapidly diminishes as the number of cycles in the data window is increased. For example, for three cycles (i.e.  $T\Delta\nu = 6$ ) an extrapolation of Figure A1 would show that the fractional error in frequency lies between .013 and -.015. As shown in Section 4.3, the Fourier transform may be regarded as an approximation to a least squares approach for the estimation of  $\nu$ ,  $R$  and  $\phi$ . Since the errors due to the negative frequency component do not arise in a complete least squares estimation, they may be regarded as caused by the approximations that are made in deriving the Fourier transform equations from the least squares approach.

---

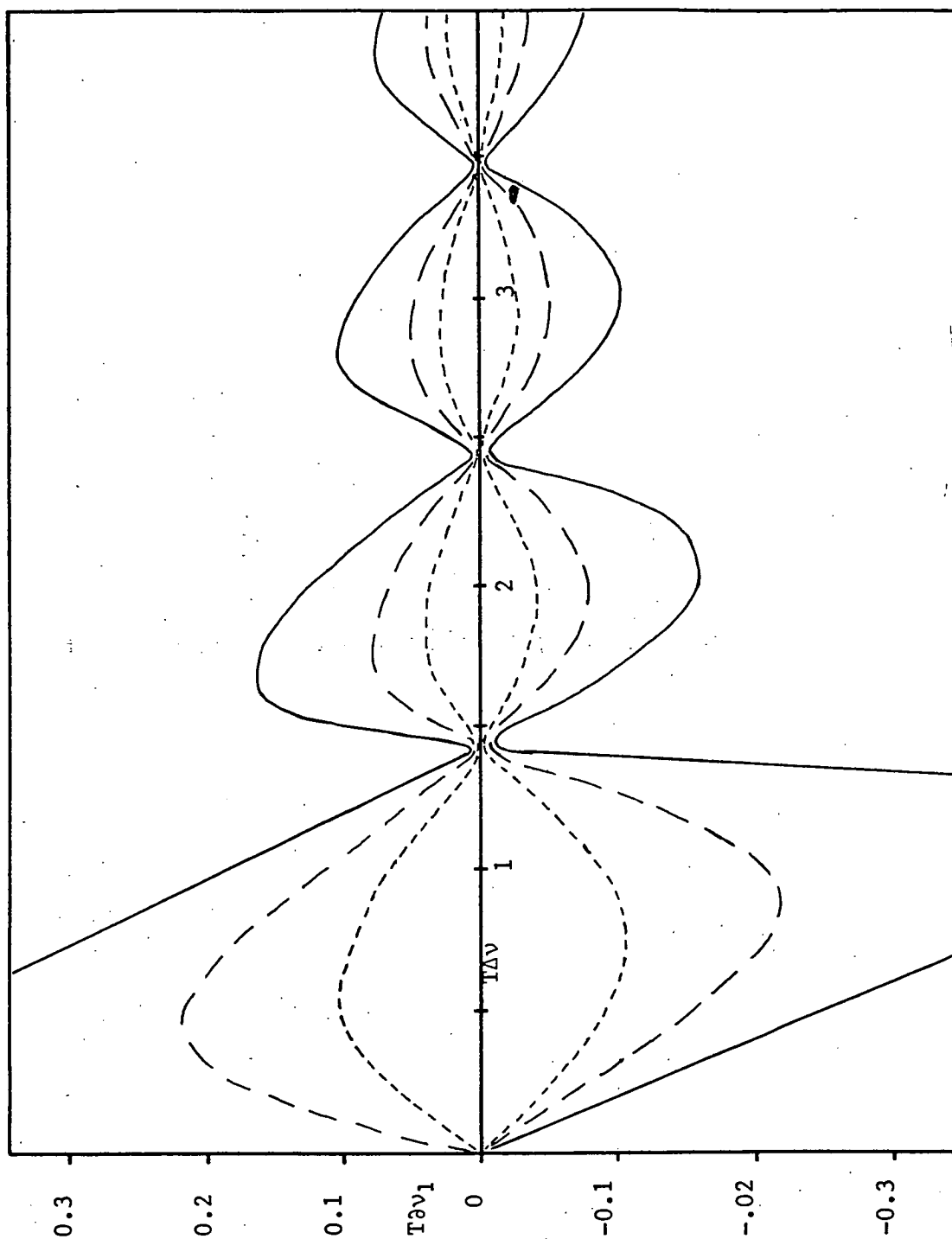


Fig. A1. Error in the estimate of the number of cycles at frequency  $\nu_1$  in the data window due to corruption by a neighbouring peak at frequency  $\nu_2 = \nu_1 + \Delta\nu$ .  $T\Delta\nu$  is the difference in the number of cycles at the two frequencies within the data window. Errors lie between the limits shown, for amplitude ratios:  $R_2/R_1 = 0.25$  (---),  $0.5$  (— —) and  $1.0$  (—).



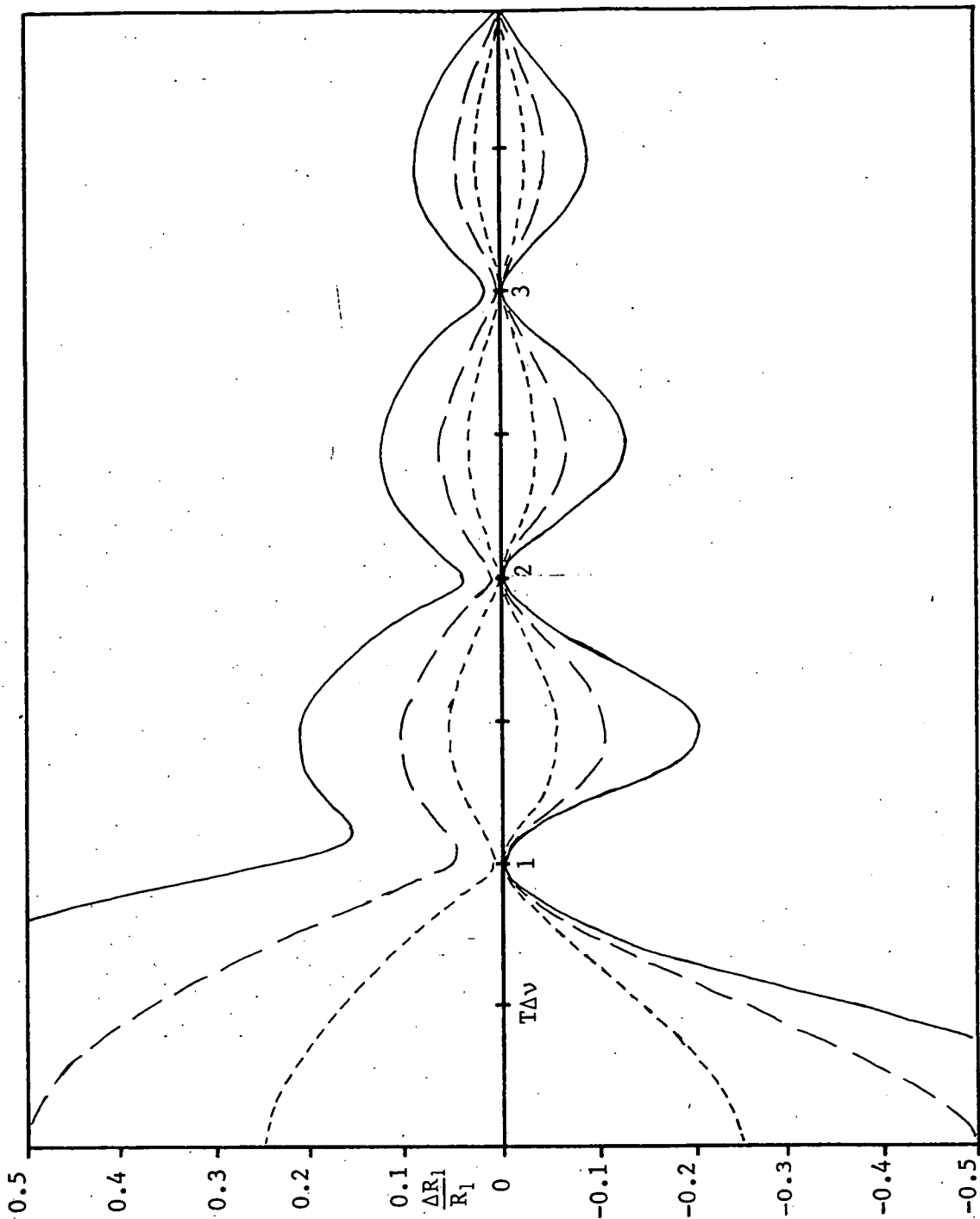


Fig. A2. Relative error in the estimate of amplitude due to corruption. Conditions are as for figure A1.

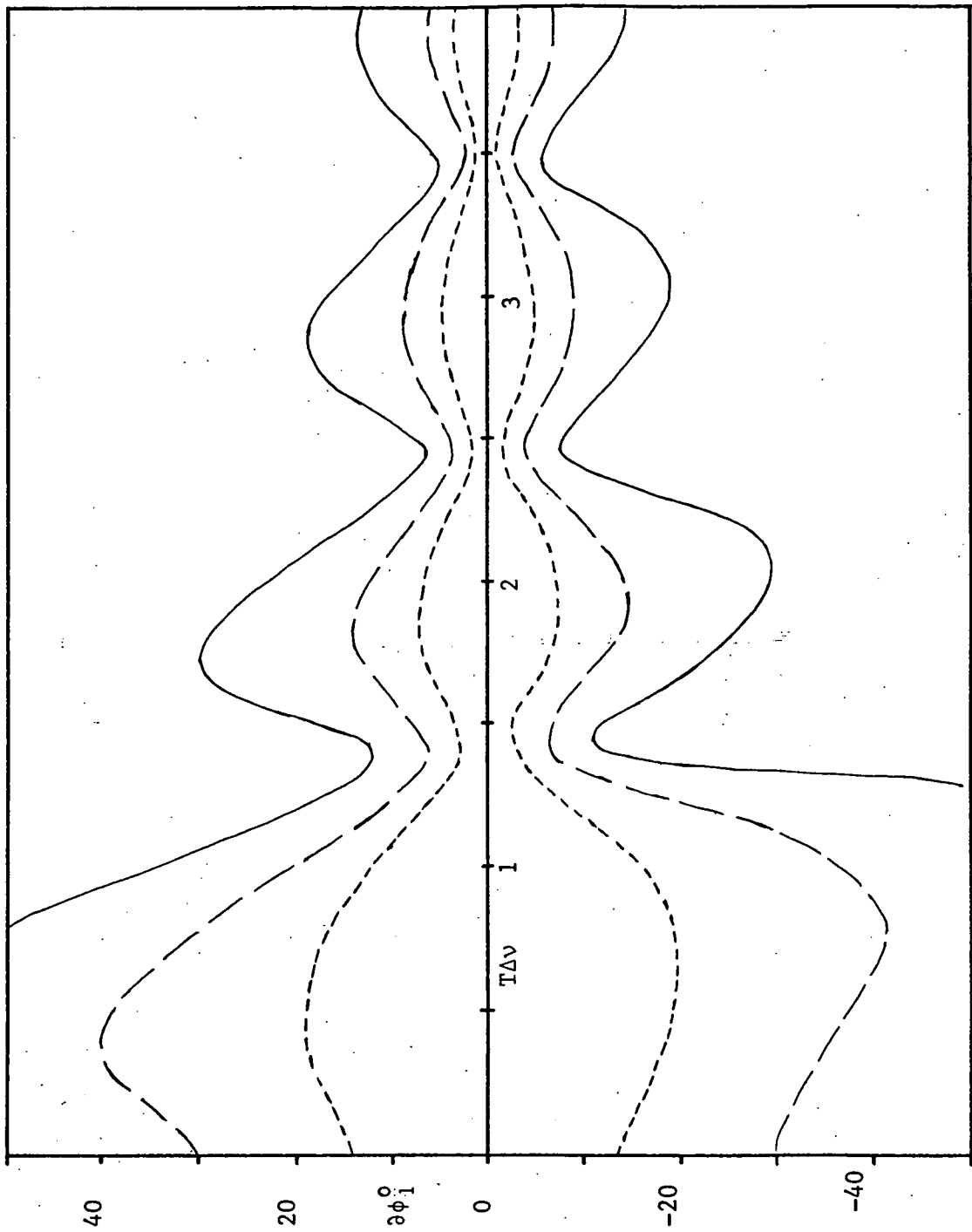


Fig. A3. Error in the estimate of phase due to corruption.

Conditions are as for figure A1.

APPENDIX 4A4.1 LEAF ANGLEMETERS

The electronic circuitry which formed part of each leaf anglemeter is shown in figure A4. That part in A4(a) was in close proximity to the rotating arm (i.e. inside the cabinet) while A4(b) was connected to the recording apparatus. Each leaf anglemeter functioned as follows.

In touching the fine wire attached to the leaf the rotating arm grounded the base of a PNP transistor (BC 177). This triggered an LM 3905 pulse generator which was set to produce a 10 second pulse. In this interval the rotating arm would break contact with the fine wire and thus retriggering of the LM 3905 could not occur.

The rising edge of the 10 second pulse activated a monostable flip-flop (DM74121) which supplied a 15  $\mu$ sec load signal to a parallel in - serial out 8-bit shift register (DM 8590). The register was thereby loaded with the current value of an 8-bit counter. The rotating arm and the 8-bit counter were synchronized so that this 8-bit number represented the angular position of the rotating arm at the moment of contact with the fine wire. Since the fine wire was attached to the centre rib of a clover leaflet this was also a measure of the angular position of the leaflet itself. At the end of a period of usually 10 minutes duration the contents of this register and of others were transmitted in serial fashion to a cassette recorder by the application of a series of pulses to each register clock input (fig. A4).

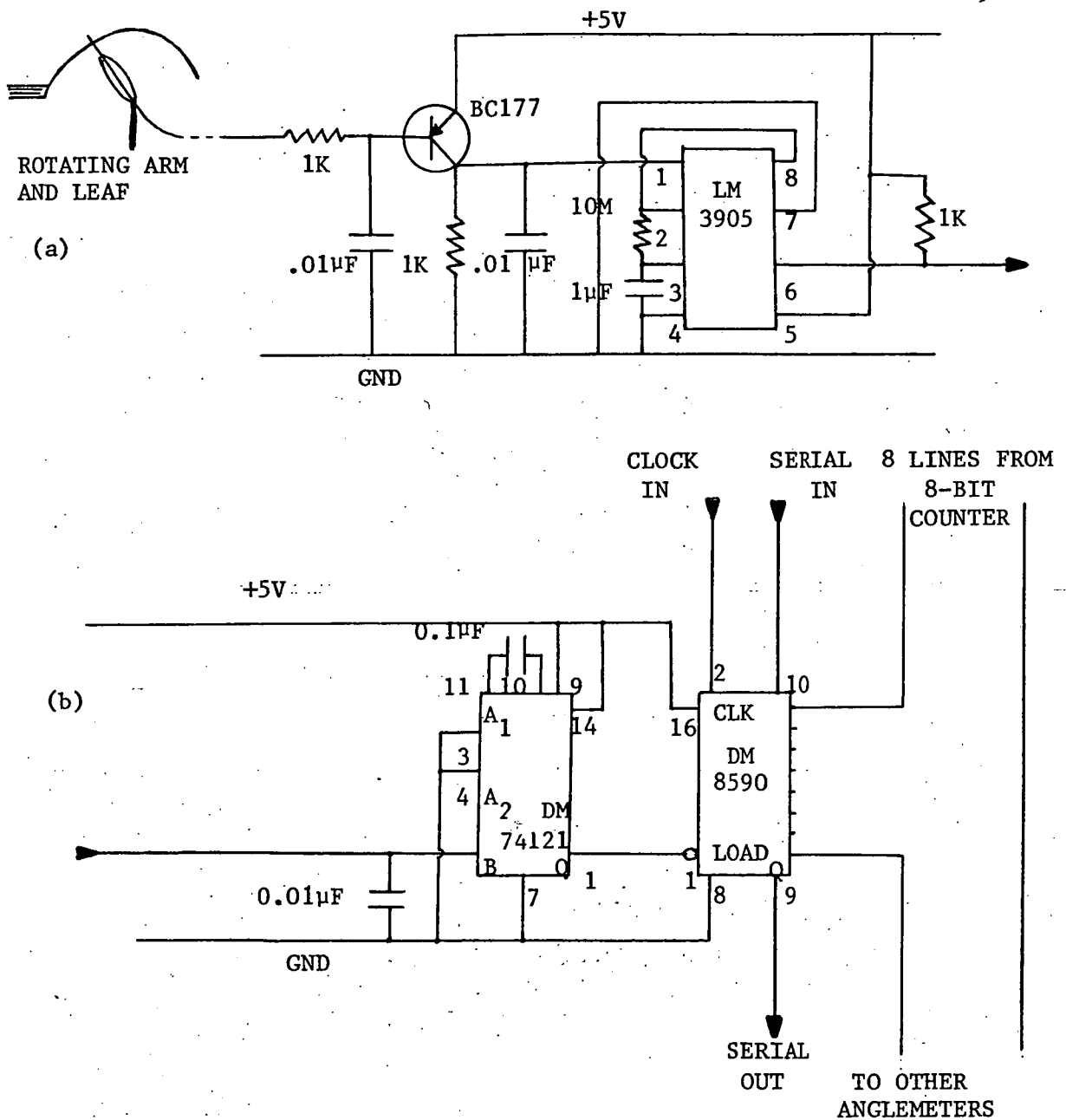


Fig. A4. Circuitry used in each leaf anglemeter. Part (a) is in close proximity to the leaf anglemeter apparatus while part (b) is attached to the recording equipment. See text for description.

#### A4.2 MONITORING AND CONTROL OF CABINET CONDITIONS

The light and temperature monitoring and control circuitry is shown in figures A5(a) and (b). The outputs from these determined the fraction of each 240 V AC cycle for which the fluorescent tubes were struck, and for which power was dissipated in the heating elements. This was accomplished via a modified version of a control for fluorescent lamp installations by Laletin and Erdman (1964), shown in figure A5(c). The humidity monitoring apparatus is given in figure A6.

Light intensity could be varied from approximately zero lux to 10,000 lux by varying the potential difference applied to the input of the control circuitry over the range of zero to 5 volts. A calibration curve for one cabinet is shown in figure A7(a). It can be observed that there is an approximately linear relationship between the logarithm of light intensity and the control voltage for the range 600 lux to 3500 lux.

Temperature could be varied over the range  $12^{\circ}\text{C}$  to  $32^{\circ}\text{C}$  in a similar fashion. A temperature-control voltage calibration curve is shown in figure A7(b).

---

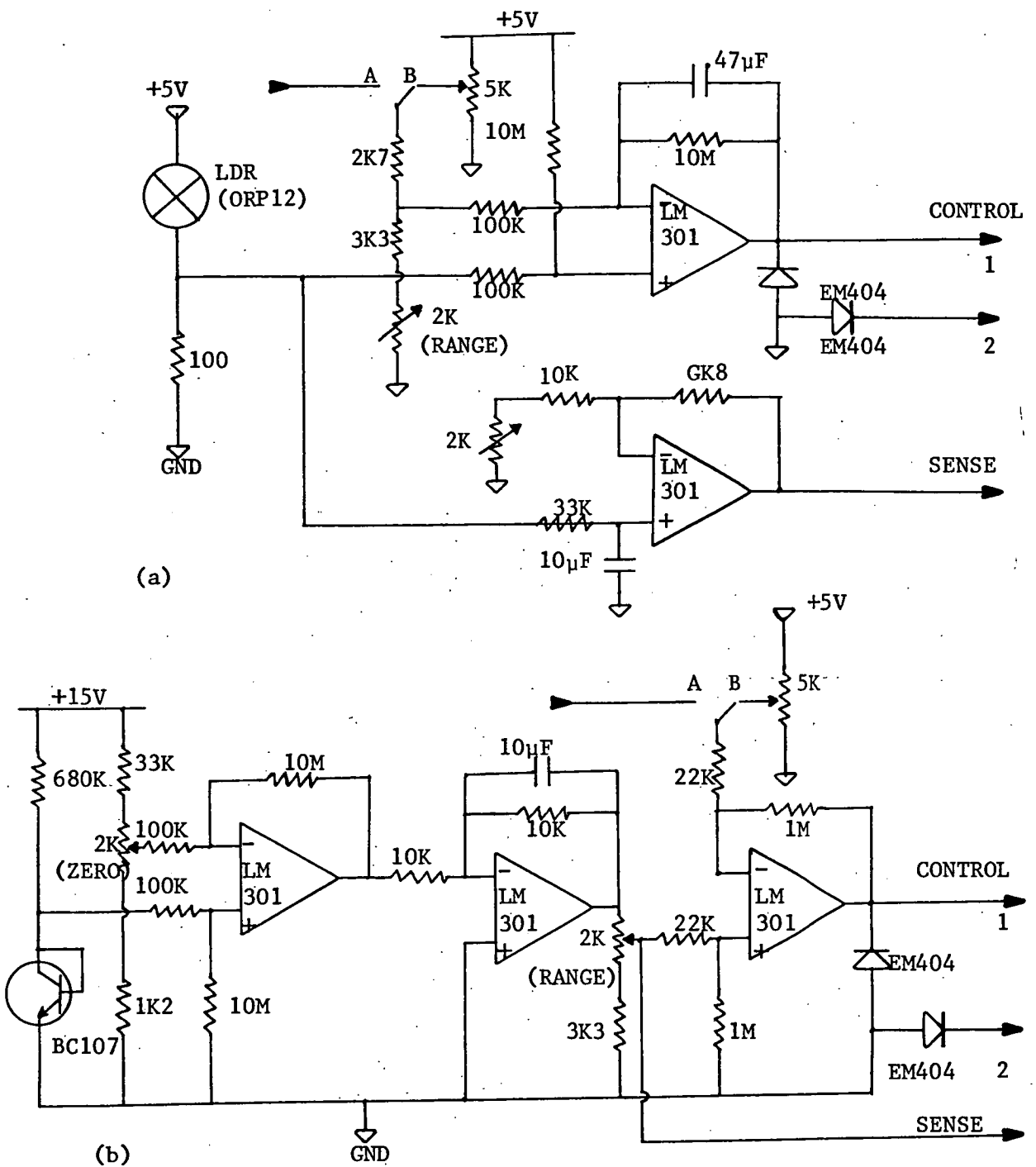


Fig. A5. Circuitry for monitoring and controlling light intensity (a) and temperature (b). These could be either manually set (switch in B position), or controlled by a minicomputer via a digital to analog converter (A position). A light dependent resistor (LDR) and a BC107 transistor were used as light and temperature sensors respectively.

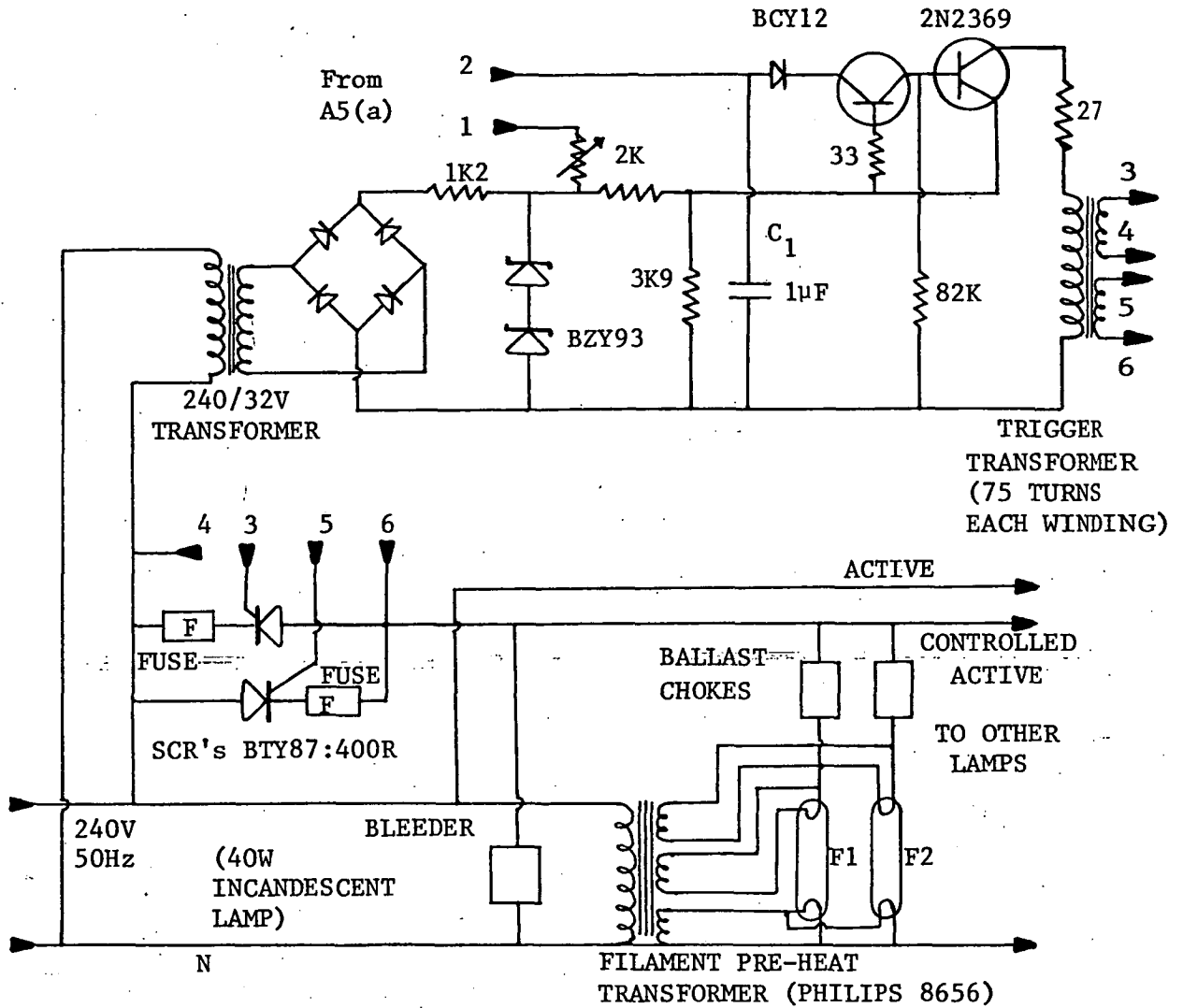


Fig. A5(c) 240V AC control circuit for determining light intensity.

The charging rate for capacitor  $C_1$  determines the point in each AC half-cycle at which the SCR's become conducting - i.e. the point at which the fluorescent lamps are struck. Temperature was controlled with a similar circuit, the fluorescent lamps being replaced by heating elements.

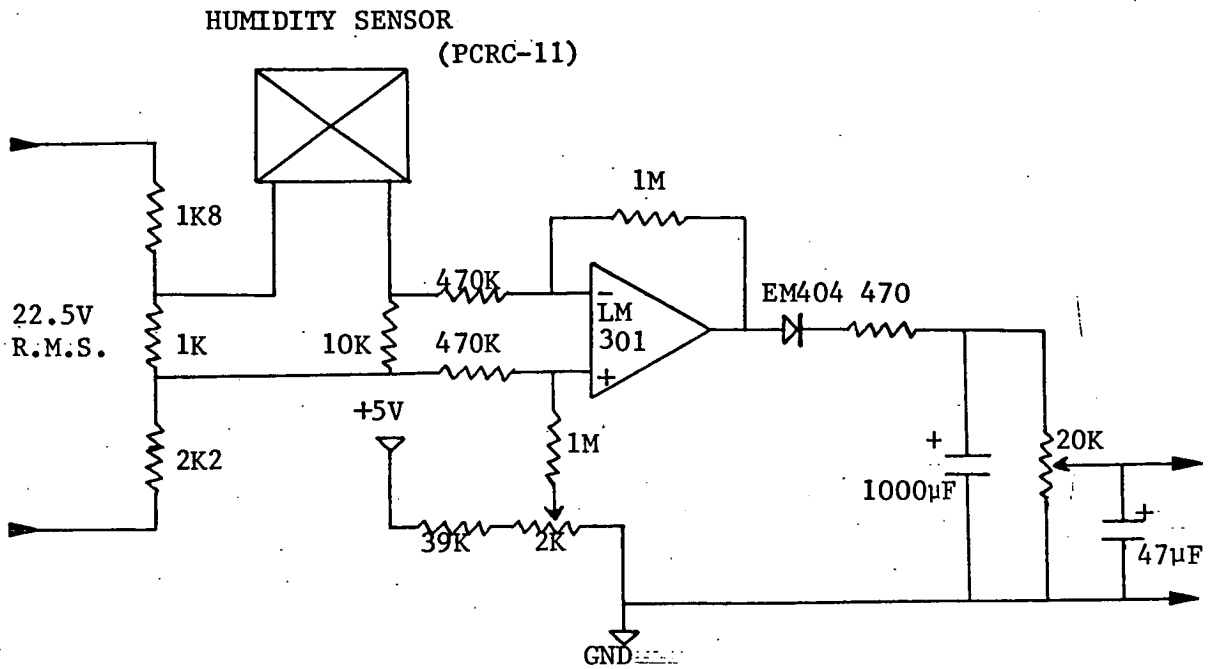


Fig. A6. Circuit for monitoring relative humidity. The resistance of the humidity sensor varies over the range 1K3 (100% humidity) to 4M (10% humidity).



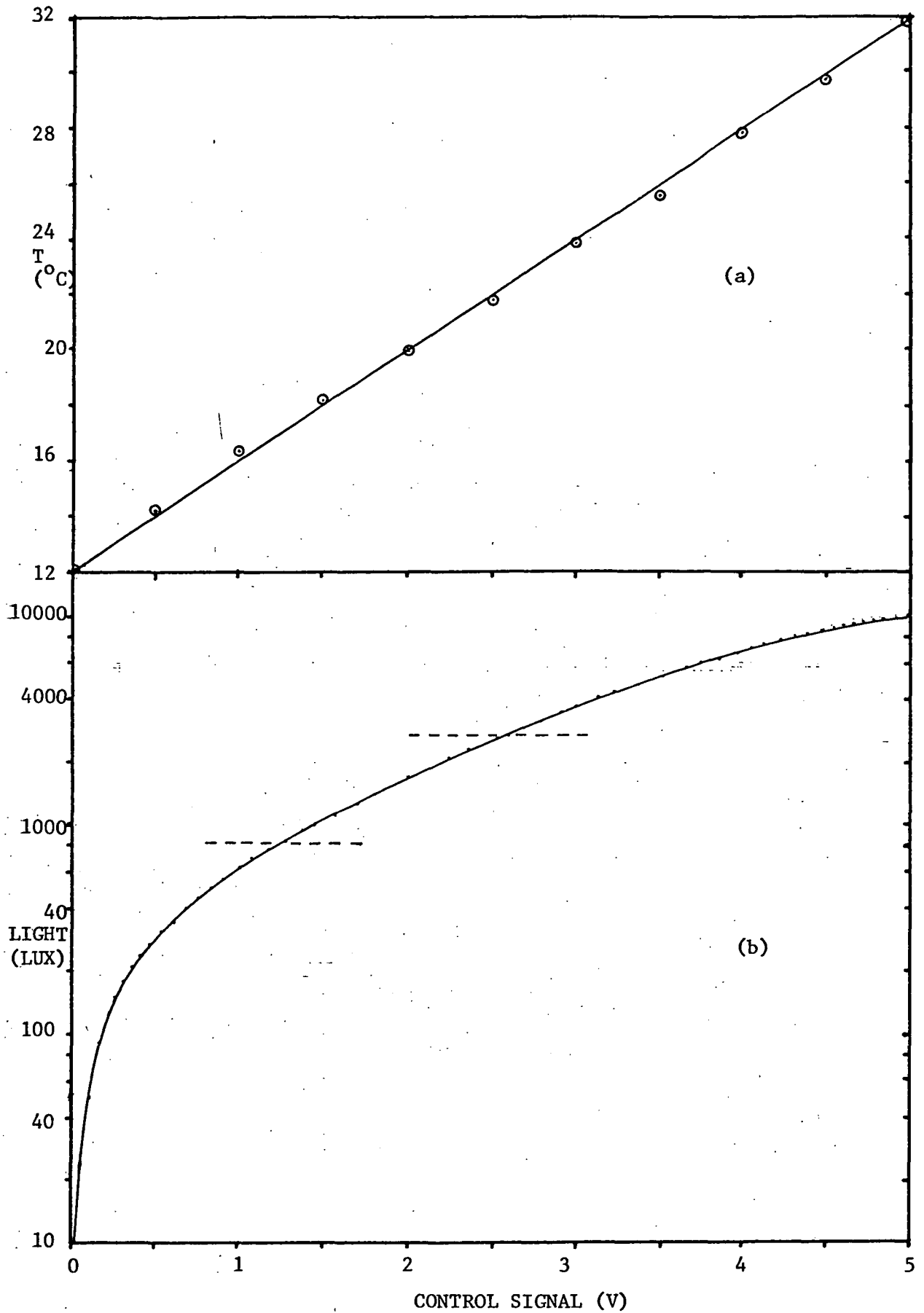


Fig. A7. Calibration curves for temperature control (a) and light intensity control (b). The range 800-2800 lux has been marked on the light curve.

APPENDIX 5

## INFLUENCE OF THORIUM IONS ON MICROELECTRODE TIP POTENTIALS

Agin and Holtzman (1966) reported that glass pipette microelectrode tip potentials could be largely overcome by the addition of compounds of thorium or of other heavy metals to the medium bathing the electrode tip. Their results indicate that tip potentials are decreased markedly by very low concentrations ( $<10^{-4}$  M) of thorium ions. Since tip potentials can be an important source of error in microelectrode measurements experiments were performed to ascertain the value of using thorium in the microelectrode studies reported in this thesis.

The tips of microelectrodes (see section 8.2) with resistance in the range 8 megohms to 30 megohms were successively immersed in 10 mM KCl followed by 10 mM KCl containing  $2.5 \mu\text{M ThCl}_4$  and  $10 \mu\text{M ThCl}_4$ , or in 10 mM NaCl followed by 10 mM NaCl containing  $10 \mu\text{M ThCl}_4$ . Tip potentials were measured for each solution some 5 minutes after the electrode had been transferred to that solution. It was observed that such an interval was required for the tip potential to stabilize. Electrodes were then returned to the original solution and the first measurement repeated. The results are summarized in table A1.

It can be noted from these results that although the presence of thorium caused a more positive tip potential which

Solution	$V_T$ (mV)	s.e.	no.
10mMKCl (initial)	-8.83	0.63	55
10mMKCl +2.5 $\mu$ MTh	-1.90	1.32	55
10mMKCl +10 $\mu$ MTh	5.74	1.99	55
10mMKCl (final)	-7.85	2.17	45
10mMNaCl (initial)	-10.89	1.56	28
10mMNaCl +10 $\mu$ MTh	3.61	2.99	28
10mMNaCl (final)	-9.90	2.85	28

Table A1. Mean tip potentials for glass pipette microelectrodes. Potentials were measured with the electrode tips immersed in the solutions listed.

generally moved the value of this potential nearer to zero, the amount by which the tip potential changed varied markedly between electrodes. That is, the scatter in the tip potential values was much larger for electrodes in the solutions containing thorium. Furthermore, returning each electrode to the original 10 mM solution caused the tip potential to alter again, so that the new reading approached or even exceeded the original value in magnitude. These results suggest that although a particular concentration of thorium ions might move the mean tip potential toward zero, once the electrode enters a relatively thorium free environment, such as living tissue, a tip potential in the vicinity of the original value will be reinstated. Thus at this stage it appears that little is to be gained from diminishing tip potentials with low thorium ion concentrations.

- 0 - 0 - 0 - 0 - 0 - 0 - 0 - 0 -

# REFERENCES

- ABLES, J.G. (1974). Maximum entropy spectral analysis. *Astron. Astrophys. Suppl.* 15, 383-393.
- ADAMICH, M., LARIS, P.C. & SWEENEY, B.M. (1976). In vivo evidence for a circadian rhythm in membranes of *Gonyaulax*. *Nature* 261, 583-585.
- AGIN, D. & HOLTZMAN, D. (1966). Glass microelectrodes: the origin and elimination of tip potentials. *Nature* 221, 1194-1195.
- AIMI, R. & SHIBASAKI, S. (1975). Diurnal change in bioelectric potential of *Phaseolus* plant in relation to the leaf movement and light condition. *Plant & Cell Physiol.* 16, 1157-1162.
- ASCHOFF, J. (1960). Exogenous and endogenous components in circadian rhythms. *Cold Spring Harb. Symp. Quant. Biol.* 25, 11-28.
- ASCHOFF, J. (1963). Diurnal rhythms. *Ann. Rev. Physiol.* 25, 581-600.
- ASCHOFF, J. (1965). *Circadian clocks*. North Holland Publishing, Amsterdam, 479pp.
- ASCHOFF, J. & WEVER, R. (1962). Spontanperiodik des Menschen bei ausschluss aller zeitgeber. *Naturwiss.* 49, 337-342.
- BALL, J.A. (1975). Computations in radio-frequency spectroscopy. *Meth. Comp. Phys.* 14, 177-219.
- BASAR, E. (1976). *Biophysical and physiological systems analysis*. Addison-Wesley, Lond. 429pp.
- BERDE, C. (1976). Nonmonotonic transients and some mathematical models of circadian rhythms. *J. Theor. Biol.* 56, 435-441.

- BERGLAND, G.D. (1969). A guided tour of the fast Fourier transform.  
IEEE Spectrum 6, 41-52.
- BLACKMAN, R.B. & TUKEY, J.W. (1958). The measurement of power  
spectra. Dover Publications Inc., N.Y. 190pp.
- BLISS, C.I. (1970). Statistics in Biology. McGraw-Hill Book Co.,  
N.Y. & Lond. 639pp.
- BLOOMFIELD, P. (1976). Fourier analysis of time series: an  
introduction. John Wiley & Sons, N.Y. 258pp.
- BRACEWELL, R. (1965). The Fourier transform and its applications.  
McGraw-Hill Co., N.Y. 381pp.
- BRIGHAM, E.O. (1974). The Fast Fourier Transform. Prentice-Hall  
Inc., New Jersey. 252pp.
- BRINKMANN, K. (1967). The influence of alcohols on the circadian  
rhythm and metabolism of *Euglena gracilis*. J. Interdispl.  
Cycle Res. 7(2), 149-170.
- BROWN, F.A. (Jr.) & WEBB, H.M. (1948). Temperature relations of an  
endogenous daily rhythmicity in the fiddler crab *Uca*.  
Physiol. Zool. 21, 371-381.
- BROWN, F.A. (Jr.), HASTINGS, J.W. & PALMER, J.D. (1970). The  
Biological Clock, two views. Academic Press, Lond.  
94pp.
- BRUCE, V.G. & PITTENDRIGH, C.S. (1956). Temperature independence in  
a unicellular 'clock'. Proc. Natn. Acad. Sci. U.S.A.  
42, 676-682.
- BRUCE, V.G. & PITTENDRIGH, C.S. (1957). Endogenous rhythms in  
insects and micro-organisms. Amer. Naturalist 91,  
179-195.

- BRUCE, V.G., WEIGHT, F. & PITTENDRIGH, C.S. (1960). Resetting the sporulation rhythm in *Pilobolus* with short light flashes of high intensity. *Science*, N.Y. 131, 728-729.
- BUCHNEMANN, F. (1955a). Das endodiurnale system der Oedogonium - Zelle. III. Über den Temperatureinfluss *Z. Naturforsch.* 10B, 305-310.
- BUHNEMANN, F. (1955b). Das endodiurnale system der Oedogonium - Zelle. II. Der Einfluss von stoffwechselgiften und arderen wirkstoffen. *Biol. Zbl.* 74, 691-705.
- BUNNING, E. (1931). Untersuchungen über die autonomen tagesperiodischen bewegungen der primarblätter von *Phaseolus multiflorus*. *Jb. Wiss. Bot.* 25, 439-480.
- BUNNING, E. (1964). *The Physiological Clock*. Springer-Verlag, Berlin, 145pp.
- BUNNING, E. & BÄLTES, J. (1963). Zur Wirkung von schweren wasser die endogene tagesrhythmic. *Naturwiss.* 50, 622.
- BUNNING, E. & MOSER, I. (1972). Influence of Valinomycin on circadian leaf movements of *Phaseolus*. *Proc. Nat. Acad. Sci. U.S.A.* 69(9), 2732-2733.
- BUNNING, E. & TAZAWA, M. (1957). Über den Temperatureinfluss auf die endogene tagesrhythmic bei *Phaseolus*. *Planta* 50, 107-121.
- BUNSOW, R.C. (1960). The circadian rhythm of photoperiodic responsiveness in *Kalanchoe*. *Cold Spring Harb. Symp. Quant. Biol.* 25, 149-158.
- BURG, J.P. (1967). Maximum entropy spectral analysis. Presented at the 37th Annual International S.E.G. Meeting, Oklahoma City, Oct. 31.

- BURG, J.P. (1972). The relationship between maximum entropy spectra and maximum likelihood spectra. *Geophys.* 37(2), 375-376.
- CAPON, J. (1969). High-resolution frequency - wavenumber spectrum analysis. *Proc. IEEE.* 57(8), 1408-1418.
- CHADFIELD, C. (1975). The analysis of time series: theory and practice. Chapman & Hall, Lond. 263pp.
- CHAPMAN, K.M. & SMITH, R.S. (1963). A linear transfer function underlying impulse frequency modulation in a cockroach mechanoreceptor. *Nature* 197, 699-700.
- CHEN, W.Y. & STEGEN, G.R. (1974). Experiments with maximum entropy power spectra of sinusoids. *J. Geophys. Res.* 79(20), 3019-3022.
- CLOUDSLEY-THOMPSON, J.L. (1974). Rhythmic activity in animal physiology and behaviour. Academic Press, N.Y. & Lond. 236pp.
- CLYNES, M.E. (1960). Biology: application of control system theory. pp72-80: *Medical Physics* 3, ed. Otto Glasser, Year Book Publishers, Chicago.
- COLD SPRING HARBOR SYMPOSIA ON QUANTITATIVE BIOLOGY, XXV: BIOLOGICAL CLOCKS (1960). The Biological Laboratory, Cold Spring Harbor, L.I., N.Y. 524pp.
- CONROY, R.T.W.L. & MILLS, J.N. (1970). Human circadian rhythms. J.A. Churchill, Lond. 236pp.
- COOLEY, J.W., LEWIS, P.A.W. & WELSH, P.D. (1969). The fast Fourier transform. *IEEE Trans. Audio. Electroacoust.* AU-17, 77-85.
- COOLEY, J.W. & TUKEY, J.W. (1965). An algorithm for the machine calculation of complex Fourier series. *Math. of Comput.* 19, 297-301.



CUMMING, B.G. & WAGNER, E. (1968). Rhythmic processes in plants.

Ann. Rev. Plant Physiol. 19, 381-416.

CUMMINGS, F.W. (1975). A biochemical model of the circadian clock.

J. Theor. Biol. 55, 455-470.

DECOURSEY, P.J. (1960). Phase control of activity in a rodent.

Cold Spring Harb. Symp. Quant. Biol. 25, 49-55.

DE MAIRAN (1729). Observation botanique Histoire de l'Academie

Royale des Sciences, Paris. p35.

EHRET, C.F. & TRUCCO, E. (1967). Molecular model for the circadian

clock. I: the chronon concept. J. Theor. Biol. 15,  
240-262.

ENGLEMANN, W. (1960). Endogene Rhythmik und photoperiodische

bluhinduktion bei Kalanchoe. Planta 55, 496-511.

ENGLEMANN, W. (1972). Lithium slows down the Kalanchoe petal rhythm.

Z. Naturforsch. 27B, 477.

ENGLEMANN, W. (1973). A slowing down of circadian rhythms by

Lithium ions. Z. Naturforsch. 28C, 733-736.

ENGLEMANN, W., KARLSSON, H.G. & JOHNSON, A. (1973). Phase shifts

in the Kalanchoe petal rhythm, caused by light pulses of  
different duration. Int. J. Chronobiol. 1, 147-156.

ENRIGHT, J.T. (1971a). The internal clock of drunken isopods.

Z. Vergl. Physiol. 75, 332-346.

ENRIGHT, J.T. (1971b). Heavy water slows biological timing processes.

Z. Vergl. Physiol. 72, 1-16.

ESKIN, A. (1972). Phase shifting a circadian rhythm in the eye of

Aplysia by high potassium pulses. J. Comp. Physiol.  
80, 353-376.

FELDMAN, J.F. (1967). Lengthening the period of a biological clock

in Euglena by cycloheximide, an inhibitor of protein  
synthesis. Proc. Natn. Acad. Sci. U.S.A. 57, 1080-1087.

FISHER, R.A. (1929). Tests of significance in harmonic analysis.

Proc. Roy. Soc. A. 125, 54-59.

FRANK, K. & BECKER, M.C. (1964). Microelectrodes for recording and stimulation. Pp23-84 in: Physical techniques in biological research. 5(A). ed. Nastuk, W.L. Academic Press, N.Y. & Lond.

GEDDES, L.A. (1972). Electrodes and the measurement of bioelectric events. Wiley-Interscience, N.Y. 364pp.

GIESE, A.C. (1968). Cell Physiology. Saunders, Philadelphia. 534pp.

GINGRAS, G., LEMASSON, C. & FORK, D.C. (1963). A study of the action of 3-(4-chlorophenyl)1, 1 dimethylurea on photosynthesis. Biochim. Biophys. Acta 69, 438-440.

GORDON, R.D., SPINKS, J., DULMANIS, A., HUDSON, B., HALBERG, F. & BARTTER, F.C. (1968). Amplitude and phase relations of several circadian rhythms in human plasma and urine. Demonstration of a rhythm for tetrahydrocortisol and tetrahydrocorticosterone. Clin. Sci. 35, 307-324.

GRAY, D.F. & DESIKACHARY, K. (1973). A new approach to periodogram analysis. Astrophys. J. 181, 523-530.

HALBERG, F. (1959). Physiologic 24-hour periodicity in human beings and mice, the lighting regime and daily routine. Pp803-878 in: Photoperiodism and related phenomena in plants and animals, ed. Withrow. Washington, A.A.A.S.

HALBERG, F. (1969). Chronobiology. Ann. Rev. Physiol. 31, 675-725.

HALBERG, F., TONG, Y.L. & JOHNSON, E.A. (1967). Circadian system phase - an aspect of temporal morphology: - procedures and illustrative examples. Pp20-48 in: The cellular aspects of biorhythms. Springer-Verlag, Berlin.

- HARKER, J.E. (1956). Factors controlling the diurnal rhythm of activity of *Periplaneta Americana* L. *J. Exp. Biol.* 33, 224-234.
- HARKER, J.E. (1958). Diurnal rhythms in the animal kingdom. *Biol. Rev.* 33, 1-52.
- HARRIS, P.J.C. & WILKINS, M. (1976). Light-induced changes in the period of the circadian rhythm of carbon dioxide output in *Bryophyllum* leaves. *Planta* 129, 253-258.
- HARTLEY, H.O. (1949). Tests of significance in harmonic analysis. *Biometrika* 36, 194-201.
- HASTINGS, J.W. (1960). Biochemical aspects of rhythms: phase shifting by chemicals. *Cold Spring Harb. Symp. Quant. Biol.* 25, 131-143.
- HASTINGS, J.W., ASTRACHAN, L. & SWEENEY, B.M. (1960). A persistent daily rhythm in photosynthesis. *J. Gen. Physiol.* 45, 69-76.
- HASTINGS, J.W. & BODE, V.C. (1962). Biochemistry of rhythmic systems. *Ann. N.Y. Acad. Sci.* 98, 876-889.
- HASTINGS, J.W. & SWEENEY, B.M. (1957). On the mechanism of temperature independence in a biological clock. *Proc. Natn. Acad. Sci. U.S.A.* 43, 804-811.
- HERMAN, H.T. & STARK, L. (1963). Photoreceptor unit transfer characteristics. *J. Neurophysiol.* 26, 215-228.
- HESS, B. & BOITEUX, A. (1971). Oscillatory phenomena in biochemistry. *Ann. Rev. Biochem.* 40, 237-258.
- HIGGINS, R.J. (1976). Fast Fourier transform: an introduction with some minicomputer experiments. *Amer. J. Phys.* 44(8), 766-773.
- HILLMAN, W.S. (1976). Biological rhythms and physiological timing. *Ann. Rev. Plant Physiol.* 25, 159-179.

- HILLMAN, W.S. & KOUKHARI, W.L. (1967). Phytochrome effects in the nyctinastic leaf movements of *Albizzia julibrissin* and some other legumes. *Plant Physiol.* 42, 1413-1418.
- HOFFMAN, K. (1957). Ueber den einfluss der temperatur auf die tagesperiodik bei einem Poikilothermen. *Naturwiss.* 44, 358-359.
- HOFFMAN, K. (1960). Experimental manipulation of the orientational clock in birds. *Cold Spring Harb. Symp. Quant. Biol.* 25, 379-387.
- HOSHIZAKI, T. & HAMNER, K.C. (1964). Circadian leaf movements: persistence in bean plants grown in high intensity light. *Science* 144, 1240-1241.
- HOSHIZAKI, T. & HAMNER, K.C. (1969). Computer analysis of the leaf movements of Pinto beans. *Plant Physiol.* 44, 1045-1050.
- IBERALL, A.S. & CARDON, S.Z. (1964). Control in biological systems - a physical review. *Ann. N.Y. Acad. Sci.* 117, 445-515.
- JACKLET, J.W. & GERONIMO, J. (1971). Circadian rhythm in a population of interacting neurons. *Science* 174, 299-302.
- JACKSON, P.L. (1967). Truncations and phase relationships of sinusoids. *J. Geophys. Res.* 72(4), 1400-1403.
- JAFFE, J.J. & GALSTON, A.W. (1967). Phytochrome control of rapid nyctinastic movements and membrane permeability in *Albizzia julibrissin*. *Planta* 77, 135-141.
- JAIN, M.K. & WHITE, H.B. (1977). Long-range order in biomembranes. *Adv. Lipid Res.* 15, 1-60.
- JENKINS, G.M. & PRIESTLEY, M.B. (1957). The spectral analysis of time series. *J. Roy. Stat. Soc. B.* 19(1), 1-12.
- JENKINS, G.M. & WATTS, D.G. (1968). Spectral analysis and its application. Holden-Day, N.Y. 525pp.

- JOHNSSON, A. & KARLSSON, H.G. (1972). A feedback model for biological rhythms. I: Mathematical description and basic properties of the model. *J. Theor. Biol.* 36, 153-174.
- KALMUS, H. (1966). Regulation and control in living systems. John Wiley & Sons, Lond. 468pp.
- KARAKASHIAN, M.W. & HASTINGS, J.W. (1963). The effect of inhibitors of macromolecular synthesis upon the persistent rhythm of luminescence in *Gonyaulax*. *J. Gen. Physiol.* 47, 1-12.
- KARLSSON, H.G. & JOHNSSON, A. (1972). A feedback model for biological rhythms. II: Comparisons with experimental results, especially on the petal rhythm of *Kalanchoe*. *J. Theor. Biol.* 36, 175-194.
- KENDALL, M.G. (1946). The advanced theory of statistics, Vol. II. Charles Griffin & Co., Lond. 521pp.
- KINARIWALA, B.K., KUO, F.F. & TSAO, N. (1973). Linear circuits and computation. Wiley, N.Y. 598pp.
- KLEITMAN, N. (1949). Biological rhythms and cycles. *Physiol. Rev.* 29, 1-30.
- KOUKHARI, W.L., HALBERG, F. & GORDON, S.A. (1973). Quantifying rhythmic movements of *Albizia julibrissin* pinnules. *Plant Physiol.* 51, 1084-1088.
- LACOSS, R.T. (1971). Data adaptive spectral analysis methods. *Geophysics* 36(4), 661-675.
- LASSEN, U.V. & STEN-KNÜDSEN, O. (1968). Direct measurement of potential difference across the human red blood cell membrane. *Biophys. J.* 9, 115-121.
- LALETIN, N. & ERDMAN, A.J. (1964). Thyristor control of fluorescent lamp installations. *Miniwatt Digest*, April, 106-111.

- LUCE, G.C. (1971). Biological rhythms in human and animal physiology. Dover Publications Inc., N.Y. 183pp.
- MACDOWALL, F.D.H. (1964). Reversible effects of chemical treatments on the rhythmic exudation of sap by tobacco roots. Can. J. Bot. 42, 115-122.
- MACHIN, K.E. (1964). Feedback theory and its application to biological systems. S.E.B. Symposia 18, 421-445.
- MILHORN, H.T. (1966). The application of control theory to physiological systems. W.B. Saunders Co., Lond. 386pp.
- MILSUM, J.H. (1966). Biological control systems analysis. McGraw-Hill, N.Y. & Lond. 466p.
- MURDOCK, J.B. (1970). Network Theory. McGraw-Hill, N.Y. & Lond. 525pp.
- NJUS, D., GOOCH, V.D., MERGENHAGEN, D., SULZMAN, F & HASTINGS, J.W. (1976). Membranes and molecules in circadian systems. Fed. Proc. 35(12), 2353-2357.
- NJUS, D., SULZMAN, F.M. & HASTINGS, J.W. (1974). Membrane model for the circadian clock. Nature 248, 116-120.
- NOZAWA, Y., IIDA, H., FUKUSHIMA, H., OHKI, K. & OHNISHI, S. (1974). Studies on Tetrahymena membranes: temperature-induced alterations in fatty acid composition of various membrane fractions in Tetrahymena pyriformis and its effect on membrane fluidity as inferred by spin-label study. Biochim. Biophys. Acta 367, 134-147.
- OTNESS, R.K. & ENOCHSON, L. (1972). Digital time series analysis. Wiley, Lond. 467pp.
- PALMER, J.D. (1976). An introduction to biological rhythms. Academic Press, N.Y. & Lond. 375pp.

- PALMER, J.H. & ASPREY, G.F. (1958). Studies in the nyctinastic movement of the leaf pinnae of *Samanea saman* (Jacq.) Merril. I: A general description of the effect of light on the rhythm. *Planta* 51, 757-769.
- PAVLIDIS, T. (1967a). A mathematical model for the light effected system in the *Drosophila* eclosion rhythm. *Bull. Math. Biophys.* 29, 291-310.
- PAVLIDIS, T. (1967b). A model for circadian clocks. *Bull. Math. Biophys.* 29, 781-791.
- PAVLIDIS, T. (1969). Populations of interacting oscillators and circadian rhythms. *J. Theor. Biol.* 22, 418-436.
- PAVLIDIS, T. (1971). Populations of biochemical oscillators as circadian clocks. *J. Theor. Biol.* 33, 319-338.
- PAVLIDIS, T. (1973). Biological oscillators; their mathematical analysis. Academic Press, N.Y. & Lond. 207pp.
- PAVLIDIS, T., ZIMMERMAN, W.F. & OSBORN, J. (1968). A mathematical model for the temperature effects on circadian rhythms. *J. Theor. Biol.* 18, 210-221.
- PITTENDRIGH, C.S. (1960). Circadian rhythms and the circadian organization of living systems. Cold Spring Harb. Symp. Quant. Biol. 25, 159-184.
- PITTENDRIGH, C.S. & MINIS, D.H. (1964). The entrainment of circadian oscillations by light and their role as photoperiodic clocks. *Amer. Naturalist.* 98 (902), 261-293.
- PRINGLE, J.S.W. & WILSON, V.J. (1952). The response of a sense organ to a harmonic stimulus. *J. Exp. Biol.* 29, 220-234.
- PYE, E.K. (1969). Biochemical mechanisms underlying the metabolic oscillations in yeast. *Can. J. Bot.* 47, 271-285.
- QUEIROZ, O. (1974). Circadian rhythms and metabolic patterns. *Ann. Rev. Plant Physiol.* 25, 115-134.

- RACUSEN, R.H. & GALSTON, A.W. (1977). Electrical evidence for rhythmic changes in the cotransport of sucrose and hydrogen ions in *Samanea pulvini*. *Planta* 135, 57-62.
- RACUSEN, R.H. & SATTER, R.L. (1975). Rhythmic and phytochrome-regulated changes in transmembrane potential in *Samanea pulvini*. *Nature* 255, 408-510.
- RIGGS, D.S. (1970). Control theory and physiological feedback mechanisms. Williams & Wilkins, Baltimore, U.S.A. 599pp.
- ROBINSON, G.R. (1976). A high redundancy method for recording digital data on commercially available cassettes. *J. Phys. E: Sci. Inst.* 9, 110-111.
- ROBINSON, G.R. & SCOTT, B.I.H. (1973). A new method of estimating micropipette tip diameter. *Experientia* 29, 1033-1034.
- RUST, T.S.O. (1974). Frequency components in the leaf oscillations of *Trifolium repens*. B.Sc. (Hons.) thesis, University of Tasmania. 110pp.
- SAGAWA, K., ROSS, J.M. & GUYTON, A.C. (1961a). Quantization of the cerebral ischemic pressor response in dogs. *Am. J. Physiol.* 200, 1164-1168.
- SAGAWA, K., TAYLOR, A.E. & GUYTON, A.C. (1961b). Dynamic performance and stability of the cerebral ischemic pressor response. *Am. J. Physiol.* 201, 1164-1172.
- SAGAWA, K., CARRIER, O. & GUYTON, A.C. (1962). Elicitation of the theoretically predicted feedback oscillation in arterial pressure. *Am. J. Physiol.* 203, 141-150.
- SATTER, R.L., APPLEWHITE, P.B. & GALSTON, A.W. (1974b). Rhythmic potassium flux in *Albizia*. *Plant Physiol.* 54, 280-285.
- SATTER, R.L., GEBALLE, G.T., APPLEWHITE, P.B. & GALSTON, A.W. (1974a). Potassium flux and leaf movement in *Samanea saman*. I: Rhythmic movement. *J. Gen. Physiol.* 64, 413-430.
- SAUNDERS, D.S. (1976). Insect clocks. Pergamon Press, Oxford & N.Y. 280pp.



- SCHMIDLE, A. (1951). Die tagesperiodizitat der asexuellen reproduktion von *Pilobolus sphaerosporus*. Arch. Mikrobiol. 16, 80-100.
- SCHUSTER, SIR A. (1898). On the investigation of hidden periodicities with application to a supposed 26-day period of meteorological phenomena. Terr. Mag. 3, 13.
- SCHWEIGER, E., WALLRAFF, H.G. & SCHWEIGER, H.G. (1964). Endogenous circadian rhythms in cytoplasm of *Acetabularia*: influence of the nucleus. Science 146, 658-659.
- SCOTT, B.I.H. & GULLINE, H.F. (1972). Natural and forced circadian oscillations in the leaf of *Trifolium repens*. Aust. J. Biol. Sci. 25, 61-76.
- SCOTT, B.I.H. & GULLINE, H.F. (1975). Membrane changes in a circadian system. Nature 254, 69-70.
- SCOTT, B.I.H., GULLINE, H.F. & ROBINSON, G.R. (1977). Circadian electrochemical changes in the pulvinules of *Trifolium repens* L. Aust. J. Plant Physiol. 4, 193-206.
- SIMON, E., SATTER, R.L. & GALSTON, A.W. (1976). Circadian rhythmicity in excised *Samanea pulvini*. I: Sucrose-white light interactions. Plant Physiol. 58, 417-420.
- SIMON, E., SATTER, R.L. & GALSTON, A.W. (1976). Circadian rhythmicity in excised *Samanea pulvini*. II: Resetting the clock by phytochrome conversion. Plant Physiol. 58, 421-425.
- SOLLBERGER, A. (1962). General properties of biological rhythms. Ann. N.Y. Acad. Sci. 98(4), 757-774.
- SOLLBERGER, A. (1965). Biological rhythm research. Elsevier, Amsterdam, 461pp.
- SOUCEK, B. (1976). Microprocessors and microcomputers. Wiley - Interscience, N.Y. 607pp.

- STARK, L.R. & SHERMAN, P.M. (1957). A servoanalytical study of consensual pupil reflex to light. *J. Neurophysiol.* 20, 17-26.
- STARK, L. & YOUNG, L.R. (1964). Defining biological feedback control systems. *Ann. N.Y. Acad. Sci.* 117, 427-444.
- STRUMWASSER, F. (1965). The demonstration and manipulation of a circadian rhythm in a single neuron. Pp442-462 in: *Circadian clocks*, ed. Aschoff, J., North Holland Publishing, Amsterdam.
- SUTER, R.B. & RAWSON, K.S. (1968). Circadian activity rhythm of the deer mouse, *Peromyscus*: effect of deuterium oxide. *Science* 160, 1011-1014.
- SWADE, R.H. & PITTENDRIGH, G.S. (1967). Circadian locomotor rhythms of rodents in the arctic. *Amer. Natur.* 101(922), 431-466.
- SWEENEY, B.M. (1969). Rhythmic phenomena in plants. Academic Press. N.Y. & Lond. 147pp.
- SWEENEY, B.M. (1974). The potassium content of *Gonyaulax polyedra* and phase changes in the circadian rhythm of stimulated bioluminescence by short exposures to ethanol and Valinomycin. *Plant Physiol.* 53, 337-342.
- SWEENEY, B.M. (1974). A physiological model for circadian rhythms derived from the *Acetabularia* rhythm paradoxes. *Int. J. Chronobiol.* 2, 25-33.
- SWEENEY, B.M. & HASTINGS, J.W. (1958). Characteristics of the diurnal rhythm of luminescence in *Gonyaulax polyedra*. *J. Cell Comp. Physiol.* 49, 115-128.
- SWEENEY, B.M. & HAXO, F.T. (1961). Persistence of a photosynthetic rhythm in enucleated *Acetabularia*. *Science* 134, 1361-1363.

- TARGET, P.S. (1973). Membrane potentials of a clover pilvinus.  
B. Sc. (Hons.) thesis, University of Tasmania, 41pp.
- ULRYCH, T. (1972). Maximum entropy power spectrum of long period  
geomagnetic reversals. *Nature* 235, 218-219.
- ULRYCH, T.J., SMYLIE, D.E., JENSEN, O.G. & CLARKE, G.K.C. (1973).  
Predictive filtering and smoothing of short records by  
using maximum entropy. *J. Geophys. Res.* 78, 4959-4964.
- VAADIA, Y. (1960). Autonomic diurnal fluctuations in rate of  
exudation and root pressure of decapitated sunflower  
plants. *Physiol. Plantarum* 13, 701-717.
- VANDEN DRIESSCHE, T. (1966). The role of the nucleus in the  
circadian rhythm of *Acetabularia mediterranea*. *Biochim.  
Biophys. Acta* 126, 456-470.
- VAN EMMERIK, E.F. (1975). Effects of external solutions of ionic  
salts and metabolic inhibitors on clover leaf movement.  
B. Sc. (Hons.) thesis, University of Tasmania, 49pp.
- WALKER, A.M. (1971). On the estimation of a harmonic component in  
a time series with stationary independent residuals.  
*Biometrika* 58(1), 21-36.
- WALKER, SIR G. (1914). On the criterion for the reality of  
relationships or periodicities. *Calcutta Ind. Med. Mems.*  
21, 9.
- WEST, J.C. (1960). Analytical techniques for non-linear control  
systems. English Universities Press. 223pp.
- WEVER, R. (1965). Pendulum versus relaxation oscillation. Pp74-83  
in: *Circadian clocks*, ed. Aschoff, J., North Holland  
Publishing, Amsterdam.
- WHITTLE, P. (1952). The simultaneous estimation of a time series  
harmonic components and covariance structure. *Trab.  
Estad.* 3, 43-57.

- WILKINS, M.B. (1960). An endogenous rhythm in the rate of carbon dioxide output of Bryophyllum. II: The effect of light and darkness on the phase and period of the rhythm. J. Expl. Bot. 11, 269-288.
- WINFREE, A.T. (1970). Integrated view of resetting a circadian clock. J. Theor. Biol. 28, 327-374.
- WINFREE, A.T. (1975). Unclocklike behaviour of biological clocks. Nature 253, 315-319.
- YONG, S.H. (1972). Transient behaviour of the leaf oscillator in Trifolium repens. B.Sc. (Hons.) thesis, University of Tasmania. 67pp.
- ZIMMER, R. (1962). Phasenverschiebung und andere storlichtwirkungen auf die endogen tagesperiodischen blutenblattbewegungen von Kalanchoe blossfeldiana. Planta 58, 283-300.
- ZINN, J.G. (1759). Von dem schlafe der pflanzen. Hamburgisches Magazin 22(1), 49-50.

- 0 - 0 - 0 - 0 - 0 - 0 - 0 - 0 - 0 -